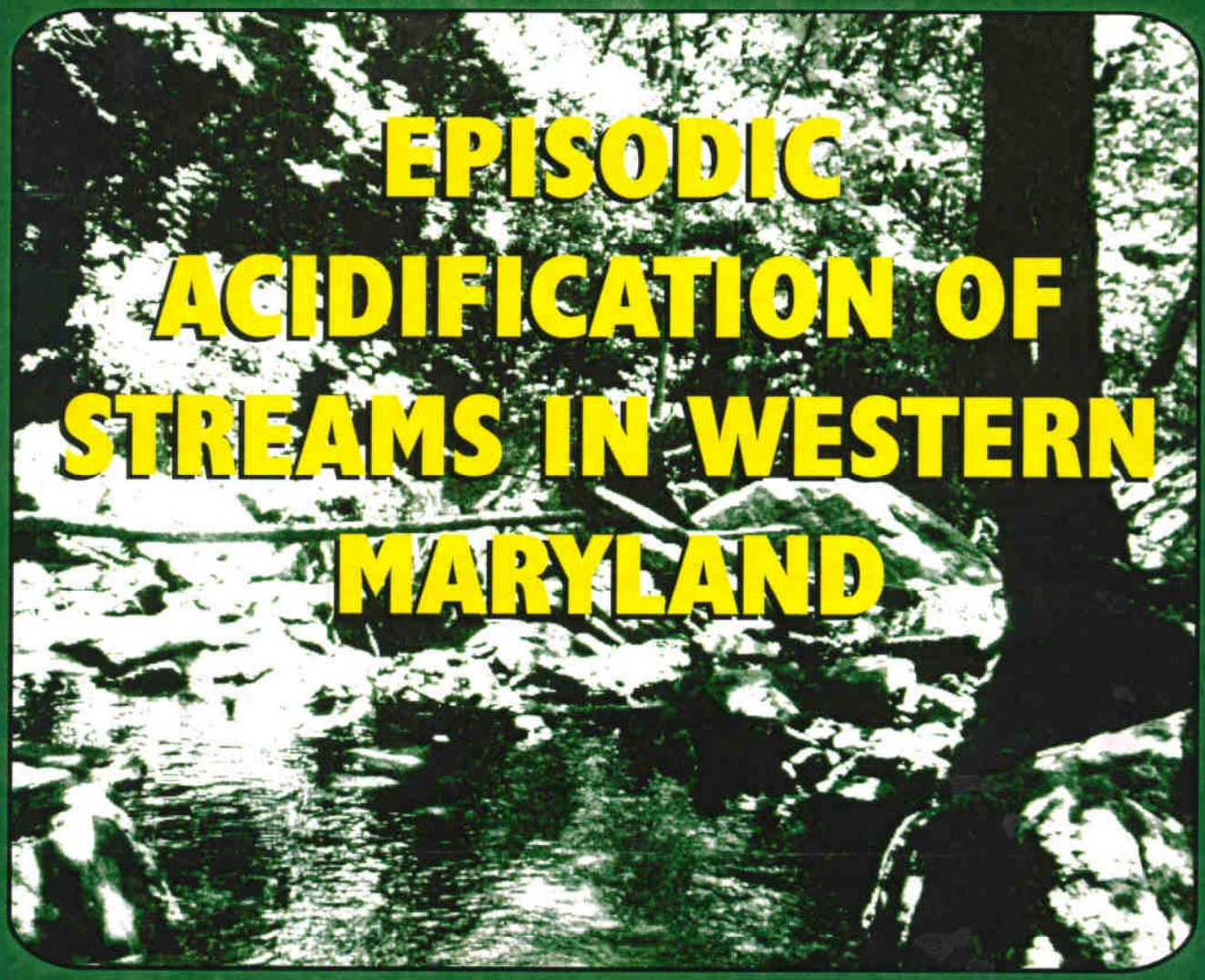

EPISODIC ACIDIFICATION OF STREAMS IN WESTERN MARYLAND

A FIELD & MODELING STUDY FOR QUANTIFYING AND PREDICTING REGIONAL ACID DEPOSITION IMPACTS

CHESAPEAKE BAY AND WATERSHED PROGRAMS
MONITORING AND NON-TIDAL ASSESSMENT

CBWP-MANTA- AD-00-1

Episodic Acidification of Streams in Western Maryland: A Field & Modeling Study for Quantifying and Predicting Regional Acid Deposition Impacts

FINAL REPORT

Submitted to:
Maryland Department of Natural Resources
Chesapeake & Watershed Assessment Administration
Annapolis, MD 21401

Contract No. CB95-009-002

Keith N. Eshleman[1], Raymond P. Morgan II[1], Nancy M. Castro[1], and Kathleen M. Kline[1]

[1]Appalachian Laboratory, University of Maryland Center for Environmental Science, Frostburg, MD 21532

Table of Contents

	Page No.
Title Page	i
Table of Contents	ii
List of Tables	iii
List of Figures	iv
Foreword	x
Executive Summary	1
1. Introduction	5
2. Study Sites	9
3. Methods	15
A. Field Methods	15
B. Laboratory Methods	19
4. Results and Discussion	23
A. Surface Water Gaging/Watershed Water Balances	23
B. Temporal Variations in Streamwater Acid-Base Composition	31
C. Analysis of Episodic Chemical Data	53
D. Temporal Variations in Low-Level Dissolved Metals in Streamwater	84
E. Temporal Variations in Trace Metals in Streamwater	118
F. Extensive Stream Sampling	138
G. Hydrochemical Modeling of Episodic Acidification	142
H. Analysis of Long-Term Changes in Streamwater	149
5. Conclusions	162
6. Acknowledgements	165
7. References Cited	166
Appendix A. Absolute Ion Changes and Ion Contribution Ratios	171
Appendix B. Laboratory Analysis: Quality Assurance/Quality Control (QA/QC)	177

List of Tables

		Page no.
Table 2.1.	Descriptions of five stream sampling sites in western Maryland and their watersheds	10
Table 2.2	Land use/land cover in five western Maryland watersheds (as a percentage of total land area	11
Table 3.1	Summary of discharge (Q) and gage height (G) data for five gaging stations	17
Table 3.2	Number of grab, sequential, and other samples collected and analyzed during the project	22
Table 4.1	Annual water balances for the five gaged watersheds	29
Table 4.2	Episodes sampled at five sites during the period 1995 –1998	49
Table 4.3	Median values of ion changes and ion contribution ratios for episodes sampled at the five sites	78
Table 4.4	Correlation matrix for all low-level metals, discharge, ANC, and pH data	111
Table 4.5	Comparison of Cd, Pb, As, and Se among Bear Branch, Herrington Creek tributary (HRTB), and Black Lick Run (BLAC) for maximum levels observed during events	138
Table 4.6	Predicted percentages of affected Appalachian Plateau cumulative stream length in western Maryland under current and future conditions	150

List of Figures

		Page no.
Figure 2.1	Location of episodic monitoring sites and watersheds in Garrett County, Maryland	12
Figure 2.2	Land use/land cover distribution within the five study watersheds based on 1997 imagery	13
Figure 2.3	Topographic relief within the five study watersheds based on published digital elevation model (DEM) data	14
Figure 3.1	Relative recoveries of dissolved nitrogen (N) for five N-containing substances (normalized to nitrate-N)	21
Figure 4.1	Stage/discharge data and rating curves for the five streamwater monitoring sites	24
Figure 4.2	Annual hydrographs for the five streamwater monitoring sites for the 1996 water year (October, 1995 through September, 1996	25
Figure 4.3	Annual hydrographs for the five streamwater monitoring sites for the 1997 water year (October, 1996 through September, 1997)	26
Figure 4.4	Annual hydrographs for the five streamwater monitoring sites for the 1998 water year (October, 1997 through September, 1998)	27
Figure 4.5	Comparison of annual runoff hydrographs (mean daily runoff) for the Upper Big Run (BIGR) and Savage River near Barton, MD (SAVR) stations for the 1996, 1997, and 1998 water years	30
Figure 4.6	Temporal variations in ANC, NO_3^- and SO_4^{2-}, DOC, sum of base cations, pH, exchangeable reactive Al, and runoff at the Upper Big Run (BIGR) site during the three year project	32-34
Figure 4.7	Temporal variations in ANC, NO_3^- and SO_4^{2-}, DOC, sum of base cations, pH, exchangeable reactive Al, and runoff at the Black Lick Run (BLAC) site during the three year project	35-37
Figure 4.8	Temporal variations in ANC, NO_3^- and SO_4^{2-}, DOC, sum of base cations, pH, exchangeable reactive Al, and runoff at the Herrington Creek tributary (HRTB) site during the three year project	38-40
Figure 4.9	Temporal variations in ANC, NO_3^- and SO_4^{2-}, DOC, sum of base cations, pH, exchangeable reactive Al, and runoff at the North Prong LostlandRun (NPLR) site during the three year project	41-43
Figure 4.10	Temporal variations in ANC, NO_3^- and SO_4^{2-}, DOC, sum of base cations, pH, exchangeable reactive Al, and runoff at the Upper Poplar Lick tributary (UPTB) site during the three year project	44-46

Page no.

Figure 4.11 Annual discharge hydrographs (1996 water year) for the five study sites indicating periods of high frequency streamwater sampling during episodes 50

Figure 4.12 Annual discharge hydrographs (1997 water year) for the five study sites indicating periods of high frequency streamwater sampling during episodes 51

Figure 4.13 Annual discharge hydrographs (1998 water year) for the five study sites indicating periods of high frequency streamwater sampling during episodes 52

Figure 4.14 Temporal variations in ANC, NO_3^- and SO_4^{2-}, pH, exchangeable reactive Al, and stream discharge at the Upper Big Run (BIGR) site during the period January 15-30, 1996 54-55

Figure 4.15 Temporal variations in ANC, NO_3^- and SO_4^{2-}, pH, exchangeable reactive Al, and stream discharge at the Upper Big Run (BIGR) site during the period September 5-11, 1996 56-57

Figure 4.16 Temporal variations in ANC, NO_3^- and SO_4^{2-}, pH, exchangeable reactive Al, and stream discharge at the Black Lick Run (BLAC) site during the period September 5-11, 1996 58-59

Figure 4.17 Temporal variations in ANC, NO_3^- and SO_4^{2-}, pH, exchangeable reactive Al, and stream discharge at the Herrington Creek tributary (HRTB) during the period September 5-11, 1996 60-61

Figure 4.18 Temporal variations in ANC, NO_3^- and SO_4^{2-}, pH, exchangeable reactive Al, and stream discharge at the North Prong Lostland Run (NPLR) during the period September 5-11, 1996 62-63

Figure 4.19 Temporal variations in ANC, NO_3^- and SO_4^{2-}, pH, exchangeable reactive Al, and stream discharge at the Upper Poplar Lick tributary (UPTB) during the period September 5-11, 1996 64-65

Figure 4.20 Relationship between ΔANC and ΔSBC – ΔSAA for all episodes sampled at the BIGR site 68

Figure 4.21 Relationship between ΔANC and ΔSBC – ΔSAA for all episodes sampled at the BLAC site 69

Figure 4.22 Relationship between ΔANC and ΔSBC – ΔSAA for all episodes sampled at the HRTB site 70

Figure 4.23 Relationship between ΔANC and ΔSBC – ΔSAA for all episodes sampled at the NPLR site 71

Figure 4.24 Relationship between ΔANC and ΔSBC – ΔSAA for all episodes sampled at the UPTB site 72

Figure 4.25 Relationship between ΔANC and ΔSBC – ΔSAA for all episodes sampled at all sites during the project 73

Page no.

Figure 4.26 Graph of dimensionless ion contribution ratio for SBC for all episodes sampled at all sites during the project 74

Figure 4.27 Graph of dimensionless ion contribution ratio for SO_4^{2-} for all episodes sampled at all sites during the project 75

Figure 4.28 Graph of dimensionless ion contribution ratio for NO_3^- for all episodes sampled at all sites during the project 76

Figure 4.29 Graph of dimensionless ion contribution ratio for OA^- for all episodes sampled at all sites during the project 77

Figure 4.30 Graph of median ion contribution ratios for all ions for all episodes sampled at each of the sites during the project vs. ANC_{index} 79

Figure 4.31 Graph of ΔSBC vs. $\Delta SO_4^{2-} + \Delta NO_3^- + \Delta OA^-$ for all episodes sampled during the project 81

Figure 4.32 Relationship between ANC_{min} measured during episodes at BIGR vs. log peak daily discharge measured at the SAVR (Savage River near Barton) station 82

Figure 4.33 Relationships between ΔANC and ANC_{min} vs. ANC_{pre} for all episodes sampled at all sites during the project 83

Figure 4.34 Relationships between ΔANC and ANC_{min} vs. ANC_{index} for the five study sites 85

Figure 4.35 Mean low-level dissolved metal concentrations at the five sites during the study 86

Figure 4.36 Temporal variations in Zn, Fe, Mn, ANC, pH, and discharge at BIGR during the project 88

Figure 4.37 Temporal variations in Zn, Fe, Mn, ANC, pH, and discharge at BLAC during the project 89

Figure 4.38 Temporal variations in Zn, Fe, Mn, ANC, pH, and discharge at HRTB during the project 90

Figure 4.39 Temporal variations in Zn, Fe, Mn, ANC, pH, and discharge at NPLR during the project 91

Figure 4.40 Temporal variations in Zn, Fe, Mn, ANC, pH, and discharge at UPTB during the project 92

Figure 4.41 Temporal variation in dissolved low-level metals, ANC, pH, and discharge at HRTB during the period November 6-10, 1997 93

Figure 4.42 Temporal variation in dissolved low-level metals, ANC, pH, and discharge at BLAC during the period November 6-10, 1997 94

Figure 4.43 Temporal variation in dissolved low-level metals, ANC, pH, and discharge at BLAC during the period February 10-15, 1998 95

Figure 4.44 Temporal variation in dissolved low-level metals, ANC, pH, and discharge at HRTB during the period February 10-15, 1998 96

Page no.

Figure 4.45 Temporal variation in dissolved low-level metals, ANC, pH, and discharge at HRTB during the period February 16-21, 1998 97
Figure 4.46 Temporal variation in dissolved low-level metals, ANC, pH, and discharge at BLAC during the period February 16-21, 1998 98
Figure 4.47 Temporal variation in dissolved low-level metals, ANC, pH, and discharge at BIGR during the period February 16-21, 1998 100
Figure 4.48 Temporal variation in dissolved low-level metals, ANC, pH, and discharge at UPTB during the period February 16-21, 1998 101
Figure 4.49 Temporal variation in dissolved low-level metals, ANC, pH, and discharge at NPLR during the period February 16-21, 1998 102
Figure 4.50 Temporal variation in dissolved low-level metals, ANC, pH, and discharge at HRTB during the period April 18-22, 1998 103
Figure 4.51 Temporal variation in dissolved low-level metals, ANC, pH, and discharge at BLAC during the period April 18-22, 1998 105
Figure 4.52 Temporal variation in dissolved low-level metals, ANC, pH, and discharge at BIGR during the period April 18-22, 1998 106
Figure 4.53 Temporal variation in dissolved low-level metals, ANC, pH, and discharge at UPTB during the period April 18-22, 1998 107
Figure 4.54 Temporal variation in dissolved low-level metals, ANC, pH, and discharge at NPLR during the period April 18-22, 1998 108
Figure 4.55 Relationship between measured dissolved manganese concentration and discharge, pH, and ANC at the five sites 109
Figure 4.56 Relationship between manganese concentration and discharge at each sampling site 110
Figure 4.57 Relationship between manganese concentration and pH at each sampling site 113
Figure 4.58 Relationship between manganese concentration and ANC at each sampling site 114
Figure 4.59 Relationship between zinc concentration and discharge at each sampling site 115
Figure 4.60 Relationship between iron concentration and discharge at each sampling site 116
Figure 4.61 Relationship between iron concentration and pH at each sampling site 117
Figure 4.62 Relationship between iron concentration and ANC at each sampling site 119
Figure 4.63 Monthly mercury levels for BLAC and HRTB, including total and particulate levels 120

Page no.

Figure 4.64. Monthly cadmium, lead, arsenic and selenium levels for BLAC and HRTB, including total and particulate levels 121
Figure 4.65 Total mercury and methyl mercury concentrations for the 11/6-10/97 episode at BLAC and HRTB 122
Figure 4.66 Cadmium, lead, arsenic and selenium concentrations for the 11/6-10/97 episode at BLAC and HRTB 124
Figure 4.67 Total mercury and methyl mercury concentrations for the 1/8-10/98 episode at BLAC and HRTB 125
Figure 4.68 Cadmium, lead, arsenic and selenium concentrations for the 1/8-10/98 episode at BLAC and HRTB 126
Figure 4.69 Total mercury and methyl mercury concentrations for the 2/10-15/98 episode at BLAC and HRTB 128
Figure 4.70 Cadmium, lead, arsenic and selenium concentrations for the 2/10-15/98 episode at BLAC and HRTB 129
Figure 4.71 Total mercury and methyl mercury concentrations for the 2/17-21/98 episode at BLAC and HRTB 130
Figure 4.72 Cadmium, lead, arsenic and selenium concentrations for the 2/17-21/98 episode at BLAC and HRTB 131
Figure 4.73 Mercury and trace metal levels for all episodes as a function of pH 132
Figure 4.74 Total mercury and methyl mercury as a function of flow for all episodes 134
Figure 4.75 Total cadmium concentration as a function of flow for both sites for all episodes 135
Figure 4.76 Frequency distribution of the difference between a) spring episode ANC and spring baseflow ANC and b) spring episode ANC and fall baseflow ANC for the 33 synoptic Savage River sampling sites 139
Figure 4.77 Observed statistical relationship between spring episode ANC and spring baseflow ANC for the 33 synoptic Savage River sampling sites 140
Figure 4.78 Observed statistical relationship between spring episode ANC and fall baseflow ANC for the 33 synoptic Savage River sampling sites 141
Figure 4.79 Cumulative proportion of stream reach length as a function of measured baseflow ANC measured in Appalachian Plateau (AP) streams in western Maryland during the 1987 Maryland Synoptic Stream Chemistry Survey 143
Figure 4.80 Relationship between ANC_{min} and ANC_{index} for the five study streams 145
Figure 4.81 Relationship between ANC_{min} and ANC_{index} for 11 streams on the Appalachian Plateau in Pennsylvania and Maryland 146
Figure 4.82. Ion contribution ratios for BIGR, BLAC, and HRTB for the 9/5/96 episode 147
Figure 4.83 Ion contribution ratios for BIGR, BLAC, and HRTB for the 2/18/98 episode 148

Page no.

Figure 4.84 Temporal sequence of observed values of ANC_{min} measured at BIGR during episodes as part of this study and as part of a previous study 151

Figure 4.85 Graph of (approximately) bi-weekly measurements SO_4^{2-} concentration in streamwater measured at BIGR as part of this study and as part of a previous study 153

Figure 4.86 Graph of (approximately) bi-weekly measurements NO_3^- concentration in streamwater measured at BIGR as part of this study and as part of a previous study 154

Figure 4.87 Computed monthly streamwater fluxes of SO_4^{2-} at BIGR based on discharge and concentration data collected during this study and as part of a previous study 155

Figure 4.88 Computed monthly streamwater fluxes of NO_3^- at BIGR based on discharge and concentration data collected during this study and as part of a previous study 156

Figure 4.89 Computed annual fluxes of NO_3^- at BIGR (water years 1990-98) based on discharge and concentration data collected during this study and as part of a previous study 157

Figure 4.90 Computed annual discharge-weighted streamwater concentrations of NO_3^- at BIGR (water years 1990-98) based on discharge and concentration data collected during this study and as part of a previous study 158

Figure 4.91 Computed annual runoff of water at BIGR (water years 1990-98) based on discharge data collected during this study (and using long-term discharge records from the SAVR site) 159

Figure 4.92 Computed annual streamwater fluxes of SO_4^{2-} at BIGR (water years 1990-98) based on discharge and concentration data collected during this study and as part of a previous study 160

Figure 4.93 Computed annual discharge-weighted streamwater concentrations of SO_4^{2-} at BIGR (water years 1990-98) based on discharge and concentration data collected during this study and as part of a previous study 161

Foreword

This report describes research and monitoring that were conducted under the auspices of the Maryland Department of Natural Resources. Funding for the project was provided by the Power Plant Research Program under the direction of Dr. Paul E. Miller through contract no. CB95-009-002 to the principal investigator, Dr. Keith N. Eshleman, University of Maryland Center for Environmental Science.

Executive Summary

The regional extent to which atmospheric deposition has contributed to the long-term, chronic acidification of surface waters in the United States was one of the most scientifically and politically controversial environmental issues of the 1980's (Schindler, 1988). Within the last fifteen years, both federal and state agencies have used synoptic surveys to estimate the extent to which lakes and streams are either affected by or at risk from acidification (Linthurst *et al.*, 1986; Landers *et al.*, 1987; Kaufmann *et al.*, 1988; Knapp *et al.*, 1988; Webb *et al.*, 1989). The randomized systematic sampling design used in the National Surface Water Survey (NSWS) conducted during the mid-1980s by the U.S. Environmental Protection Agency (USEPA) produced statistically unbiased estimates of the numbers and proportions of surface waters within a region (or subregion or stratum) that are adversely affected by acidification, assuming some chemical sensitivity criterion.

A major uncertainty of the regional surface water surveys was the extent to which a process known as *episodic acidification*—the transient depression in acid neutralizing capacity (ANC) and changes in other water chemistry parameters—could also be affecting streams or lakes that were not chronically acidified. Previous field studies have confirmed that episodic acidification is a ubiquitous hydrochemical process, having been observed in the United States, Canada, and Europe (Wigington *et al.*, 1990). Periodic sampling at short time intervals during periods of high discharge suggests that many water chemistry variables (e.g., ANC, pH, NO_3^-, SO_4^{2-}, and Al) exhibit complex temporal and spatial patterns. Depressions of pH and increases in the concentration of inorganic aluminum (Al) are particularly important because field and laboratory toxicological evidence suggests that these conditions can kill fish (Haines, 1981; Wigington *et al.*, 1990; Baker *et al.*, 1990; Carline *et al.*, 1992). Although many studies of episodic acidification have been performed to date, significant gaps in the understanding of the extent and severity of the problem still remain (Wigington *et al.*, 1993). Previous field studies have documented that some streams in western Maryland experience transient short-term declines in ANC and changes in other water chemistry variables (e.g., pH and Al concentrations) during periods of high discharge (Morgan *et al.*, 1994). However, due to a lack of field data from this geologically and hydrologically diverse region, it has not been possible to predict with certainty the proportion of western Maryland streams that are episodically acidified nor the proportion that will be acidic in the future given reductions in sulfur deposition brought about by the 1990 Federal Clean Air Act Amendments. The research summarized in this final report was conducted to address the problem of episodic acidification in western Maryland and to reduce the uncertainties associated with estimating the numbers of streams affected.

The integrated approach to the problem involved the detailed characterization of hydrological and hydrochemical changes in five small streams (Upper Big Run, Black Lick Run, Herrington Creek unnamed tributary, North Prong Lostland Run, and Upper Poplar Lick unnamed tributary) draining predominantly forested watersheds in western Maryland over a period of three years (October 1995 through September 1998). All streams were gaged using standard protocols.

Over the course of the study, both baseflow and stormflow chemical conditions were characterized using a combined "grab" and automated sampling design; nearly 1500 streamwater samples collected bi-weekly and during major stormflow events were analyzed for a complete suite of analytes including ANC, pH, conductivity, exchangeable and nonexchangeable reactive Al, Na^+, K^+, NH_4^+, Mg^{2+}, Ca^{2+}, Cl^-, NO_3^-, SO_4^{2-}, dissolved organic carbon, and Si.

Trace metal levels during baseflow conditions and during selected episodes were monitored at both Black Lick Run and at the Herrington Creek unnamed tributary. Western Maryland falls within a high acidic deposition zone, with elevated trace metals from power plant emissions. A limited number of samples were collected and analyzed for low-level dissolved and trace metals (Be, Cd, Co, Cr, Fe, Mn, Si, Vn, Zn, Hg, CH_3Hg, Pb, As, and Se) in order to screen for potential metal effects on the aquatic biota during baseflow and episodes.

The results of the study clearly demonstrated that episodic acidification of surface waters—the transient loss of ANC that accompanies rainfall and snowmelt events—is ubiquitous in western Maryland watersheds. All five study streams experienced dramatic depressions in ANC, especially during or immediately following high stream discharge conditions caused by intense rainfall, rapidly melting snow, or a combination of rain-on-snow. In particular, data associated with two major floods in 1996—one in mid-January due to rain-on-snow and a second in September due to the remnants of Hurricane Fran—illustrate the magnitude of ANC decline. ANC in three of the five streams was "over-titrated" to negative values during one of more of these two episodes, causing major depressions in pH (to values less than 5.0) and increases in exchangeable reactive Al concentrations (to levels exceeding 50 μg/L). These levels are clearly within the range of conditions that should be considered deleterious to populations of fish and other aquatic biota.

While the conditions measured during the two "Floods of 1996" are illustrative of the most extreme hydrological and hydrochemical conditions observed during the study, data from these and many other episodes conform to a predictable pattern that provides evidence for the underlying causes of episodic acidification in western Maryland streams, as well as in streamwaters in general. Minimum values of ANC (ANC_{min}) and changes in ANC (ΔANC) based on 75 discrete episode-stream observations were found to be predictable, varying linearly with the antecedent (i.e., pre-event) value of ANC (ANC_{pre}); ANC_{min} at our long-term monitoring site (Upper Big Run) was also found to vary as a linear function of the log of peak daily discharge. All of these results strongly support the previous conclusion based on data from a variety of watersheds in the eastern U.S. that episodic acidification is inherently a hydrological mixing process that can usually be described by a simple two-component mixing model (Eshleman, 1988; Eshleman *et al.*, 1995).

Using this rather robust modeling approach, the episodic response of an entire population of streams within a region could be estimated using calibration data from a small number of streams such as was obtained in the current study. For streams draining the Appalachian Plateau in western Maryland, the combined field/modeling study suggested that about 20% (95% confidence

limits = 8%, 35%) of the cumulative length of streams in the region is either *episodically* or *chronically* acidic, based on an ANC_{min} criterion of 25 μeq/L. Compared to an estimate (based on the 1997 MSSCS reported by Knapp *et al.*, 1988) that 12% of the combined stream length is *chronically* acidic, episodic acidification may currently be causing deleterious impacts on fish populations in approximately the same number and length of streams in the region as is chronic acidification.

While the estimates of current regional acidification are based on a robust model that is also verifiable using data obtained from other watersheds draining the Appalachian Plateau (both in Maryland and Pennsylvania), determining the specific role of atmospheric deposition of sulfuric and nitric acids (as well as the role of natural strong organic acids) in the episodic acidification process is far more difficult. In general, our data support the conclusion that hydrological dilution of base cations during stormflow events was the primary cause of ANC depression in the five study streams; this interpretation is further supported by the fact that dilution of base cations is more important in the higher ANC streams, a result that is also consistent with the conceptual acidification model employed. In the average episode observed, base cation dilution was just about equal (on an equivalent basis) to the depression in ANC, with nitric acid and organic acid concentrations increasing very slightly; the median change in sulfuric acid concentration was actually found to be negligible—a quite interesting result not necessarily inconsistent with an "acid rain" interpretation.

In fact, a conceptual model known as REALSM could be calibrated using data from two episodes that were particularly well-characterized. Results from application of the calibrated model to the regional stream population suggest that abatement of episodic acidification should occur in western Maryland once sulfuric acid concentrations are reduced by 40% from current levels (consistent with the 1990 Federal Clean Air Act Amendments [CAAA] and subsequent atmospheric emission controls), although there is substantial uncertainty associated with these predictions. In particular, the current model is quite sensitive to the value of the regional "F-factor", which is very difficult to estimate. One interesting result of the modeling study is that reductions in nitric acid concentrations—even by dramatic percentages—do not cause a significant abatement of episodic acidification at the regional scale, despite the fact that nitric acid is a more consistent contributor to episodic acidification than is sulfuric acid. This result is consistent with a previous finding of Eshleman *et al.* (1995) for episodic acidification of Adirondack lakes associated with spring snowmelt.

Monthly total and particulate levels of Hg, Cd, Pb, As and Se were low, as were levels of total and particulate CH_3Hg. Monthly mean baseflow levels for total Hg were 1.7 ng/L at Black Lick Run and 2.1 ng/L at Herrington Creek unnamed tributary. Cd, Pb, As, and Se all had mean monthly averages below 0.7 μg/L at both sites. Particulate Hg was found to be a significant component of total Hg, but the particulate phases were not significant for Cd, Pb, As, and Se. However, western Maryland streams have higher trace metal concentrations than central and

eastern Maryland streams during episodes, reflecting higher deposition rates in the area. Elevated levels of As, Pb and Se may also be of concern during episodes.

Finally, data collected as part of this project and a previous field study at the Upper Big Run site provide little evidence of any long-term decline in sulfate concentrations in streamwater during the period 1990-98, while the data clearly demonstrate an exponential decline in nitrate concentrations during the same period. Additional research is needed to explain why sulfate concentrations are not declining in this system, despite the known reduction in acid deposition of sulfur brought about by the CAAA. In contrast, we propose that the decline in rather high nitrate concentrations in this system can be explained by recovery of the forest from disturbances during the late 1980's and early 1990's that was caused by gypsy moth defoliation, rather than by a watershed response to deposition of atmospheric nitrogen. On-going analyses of these data—as well as data collected in other forested watersheds in the mid-Atlantic region—should provide a particularly significant test of the competing "nitrogen saturation" and "forest disturbance" hypotheses.

1. Introduction

The regional extent to which atmospheric deposition has contributed to the long-term, chronic acidification of surface waters in the United States was one of the most scientifically and politically controversial environmental issues of the 1980's (Schindler, 1988). Within the last fifteen years, both federal and state agencies have used synoptic surveys to estimate the extent to which lakes and streams are either affected by or at risk from acidification (Linthurst *et al.*, 1986; Landers *et al.*, 1987; Kaufmann *et al.*, 1988; Knapp *et al.*, 1988; Webb *et al.*, 1989). The randomized systematic sampling design used in the National Surface Water Survey (NSWS) conducted during the mid-1980s by the U.S. Environmental Protection Agency (USEPA) produced statistically unbiased estimates of the numbers and proportions of surface waters within a region (or subregion or stratum) that are adversely affected by acidification, assuming some chemical sensitivity criterion. For example, the National Stream Survey (NSS) conducted in the mid-Atlantic and southeastern regions of the United States during the spring of 1986 indicated that approximately 5500 ($\pm$ 1600) km of stream reaches within this area were acidic during the survey, as evidenced by acid neutralizing capacity (ANC) values less than 0 μeq/l (Kaufmann *et al.*, 1991). Most of these reaches were within the Northern Appalachian Plateau (1500 $\pm$ 780 km) and the Mid-Atlantic Coastal Plain (2600 $\pm$ 1300 km); the remaining acidic reaches were in the Pocono and Catskill mountains, the Valley and Ridge Province, the Southern Appalachian Mountains, and Florida (Kaufmann *et al.*, 1991).

Although such regional and statewide surveys have provided useful information about the extent of acidification of streams, resource managers and researchers have paid little attention to the uncertainty caused by using only a single water sample (or in some cases two samples) to determine the chemical characteristics of the sampled population. To attempt to reduce the uncertainty associated with the single-sample approach, researchers tried to select suitable sampling times so that the resultant data would provide a reasonable "index" of acidification potential. For example, the National Lake Survey (NLS) sampled during fall overturn, when lakes were isothermally mixed, and the NSS sampled during spring baseflow (March 15 to May 15), excluding periods of high flow that could have been associated with storm-induced depressions of ANC and pH.

Episodic acidification of surface waters, often defined as the transient loss of acid neutralizing capacity (ANC) associated with rainfall and snowmelt runoff events, has usually been considered to be distinguishable from long-term chronic acidification due to the relatively brief response time of the former process (hours to a few weeks; Wigington *et al.*, 1990) relative to the latter (years to centuries; e.g., Cosby *et al.*, 1985). Notwithstanding the greater focus on chronic acidification, previous field studies have confirmed that episodic acidification is a ubiquitous hydrochemical process, having been observed in the United States, Canada, and Europe (Wigington *et al.*, 1990). Periodic sampling at short time intervals during periods of high discharge suggests that many water chemistry variables (e.g., ANC, pH, NO_3^-, SO_4^{2-}, and Al)

exhibit complex temporal and spatial patterns. Depressions of pH and increases in the concentration of inorganic aluminum (Al) are particularly important because field and laboratory toxicological evidence suggests that these conditions can kill fish (Haines, 1981; Wigington *et al.*, 1990; Baker *et al.*, 1990; Carline *et al.*, 1992). Although many studies of episodic acidification have been performed to date, significant gaps in the understanding of the extent and severity of the problem still remain (Wigington *et al.*, 1993).

The severity of episodes varies tremendously throughout geographic regions (Wigington *et al.*, 1992; Tranter *et al.*, 1994) and the processes controlling the increases in acidity are not fully understood (Potter *et al.*, 1988). Typically there is no direct link between the incoming precipitation and the observed streamwater chemistry (Neal *et al.*, 1990; Davies *et al.*, 1992), indicating that the rain or snowmelt is significantly altered by the watershed before it enters a stream or lake. Episodic acidification can occur both naturally and through anthropogenic additions of acidity. Natural mechanisms that can cause an ANC loss are: (1) production of organic acids, (2) nitrification, (3) sea-salt additions, and (4) dilution of base cations.

Episodic acidification has been at least partially attributed to anthropogenic sources of sulfur and nitrogen from atmospheric deposition when increases in strong acid anion concentrations during stormflow periods have been observed (Tranter *et al.*, 1994). In colder regions where atmospheric pollutants accumulate in deep snowpacks and are released relatively quickly during snowmelt periods, there is some evidence that the magnitude of episodic acidification during snowmelt is dependent upon the accumulated amount of deposition (Wigington *et al.*, 1990). Eshleman *et al.* (1995) also used a two-component mixing model to show that the concentration of major ions in early snowpack leachates in the Adirondacks is large enough to account for the ion changes observed in surface waters during snowmelt. However, it is now known that the effects of atmospheric deposition during the episodic acidification process are substantially more complex: Eshleman *et al.* (1995), again using the two-component mixing model, showed that sulfuric acid deposition is an important contributor to the episodic response of Adirondack surface waters during snowmelt periods, despite that fact that sulfate concentrations are actually "diluted". In regions where annual runoff is dominated by responses to rainfall events, there has been little study of the role of atmospheric deposition on the severity of episodic hydrochemical responses of surface waters. It has also been shown that the natural and anthropogenic mechanisms of episodic acidification may occur singularly or act in concert depending on the site. While far too many studies exist to adequately review them here, comprehensive reviews do exist on the mechanisms causing ANC loss in Europe (Davies *et al.*, 1992), Canada (Tranter *et al.*, 1994), and the United States (Wigington *et al.*, 1992).

In theory, the sensitivity of a particular stream to episodic acidification depends greatly on the watershed and on the reactions that occur between the event water and the soils and rocks within the watershed (Cosby *et al.*, 1985; Hendershot *et al.*, 1992). The reactions that can occur in the watershed are also thought to be controlled by the hydrological flowpaths during the event, and consequently the flowpaths drive the stream chemistry as well (Wigington *et al.*, 1990).

Generally, shallow flow through organic horizons produces more acidic waters, while deeper flow through the mineral horizons and bedrock produces a more alkaline water source (Chen *et al.*, 1984; Neal *et al.*, 1990). The flowpaths are undoubtedly changing throughout the course of a hydrologic event, further altering the contribution of different source regions (Robson and Neal, 1990) and making the net water flux an important consideration in either the accumulation or loss of certain constituents of interest (Christopherson and Wright, 1981). However, due in part to an inability of hydrologists to quantify watershed-scale hydrological flowpaths during stormflow events, a broadly-applicable mechanistic hydrochemical theory of episodic acidification—including its relationship to watershed and atmospheric deposition processes and to chronic acidification—remains elusive (Wigington *et al.*, 1990; Tranter *et al.*, 1994; Davies *et al.*, 1992; Eshleman *et al.*, 1992).

One recently-published regional acidification model utilizes a two-component mixing model that treats episodic acidification as superimposed on chronic acidification; the model effectively mixes acidic stormflow with more alkaline baseflow (representing annual average chemical conditions) to describe the most extreme conditions during peak stormflow conditions (Eshleman *et al.*, 1995). While conceptual models of this form are easily proposed, there has been to our knowledge no evaluation of this type of model using long-term surface water hydrochemical data bases. Models such as the two-component mixing model use ANC, the equivalent ability of a sample to neutralize additions of strong acids, as the primary response variable that describes the acidification process; an acidic episode is one in which the ANC is depressed to a value at or below zero (Wigington *et al.*, 1993). The decrease in ANC from positive to negative values is typically accompanied by significant pH declines and increases in monomeric aluminum concentrations (Reuss *et al.*, 1987) and these changes in hydrogen ion and aluminum concentrations are thought to be the direct cause of fish mortality during stormflow conditions. Bricker and Rice (1989) noted that any stream having a baseflow ANC less than 100 μeq/L is considered sensitive to acidification (Wigington *et al.*, 1993).

Previous field studies have documented that some streams in western Maryland experience transient short-term declines in ANC and changes in other water chemistry variables (e.g., pH and Al concentrations) during periods of high discharge (Morgan *et al.*, 1994). However, due to a lack of field data from this geologically and hydrologically diverse region, it has not been possible to estimate with certainty the proportion of western Maryland streams that are episodically-acidic (ANC < 0) nor the proportion that will be acidic in the future given reductions in sulfur deposition brought about by the 1990 Federal Clean Air Act Amendments. The research summarized in this final report was conducted to address the problem of episodic acidification in western Maryland and to reduce the uncertainties associated with estimating the numbers of streams affected. Specifically, the objectives of this three-year research project were to:

(1) establish a network of regionally-representative stream/watershed monitoring sites in western Maryland for quantifying the episodic acidification of streams which are

representative of the most critical (acid-sensitive) systems;

(2) verify an empirical episodic acidification model previously developed for acid-sensitive streams on the Appalachian Plateau (Eshleman, 1995);

(3) estimate with improved precision the current number of streams in western Maryland that are episodically-acidified during hydrological events, using the verified model;

(4) determine the among-year variability of the empirical episodic acidification model, using data collected over several years from the monitoring network;

(5) calibrate a regional episodic acidification model (REALSM: Regional Episodic Acidification of Lakes and Streams Model; Eshleman *et al.*, 1995) for western Maryland streams which can be linked to one or more chronic acidification models for predicting episodic chemical conditions in streams in western Maryland;

(6) quantify the sensitivity of REALSM predictions to assumptions about long-term changes in nitric and sulfuric acid concentrations; and

(7) examine low-level dissolved and trace metals during baseflow and episodic conditions in order to assess potential effects on aquatic biota.

2. Study Sites

Five small, acid sensitive watersheds located on the Appalachian Plateau in western Maryland were selected as stream hydrochemical monitoring sites for the project based on a review of site selection criteria (and field reconnoitoring) from several dozen candidate sites. The site selection criteria included: (1) stream water ANC and major ion (especially chloride) concentrations; (2) suitability for surface water gaging (i.e., presence of stable channel controls); (3) relative ease of gaining convenient, legal access to a gaging location; (4) degree of public land protection; and (5) absence of disturbances and confounding land use factors (e.g. mining, acid mine drainage, agriculture, non-point source pollution, etc.). A primary consideration in site selection was to identify a set of watershed sites that spanned a spring baseflow ANC range from about 0 to 100 μeq/L—a range that would allow the model for western Maryland to be properly calibrated and verified. This set of criteria provides our working definition of the term "regionally-representative" that was referred to in the list of project objectives.

As expected, it was impossible to identify sites which strictly met all of these criteria. However, it was possible to select five sampling sites that spanned the necessary range in ANC, are minimally influenced by road salting, are suitable for gaging, are located on state lands, and are thus legally accessible (Table 2.1). All of the study sites (and much or all of their watersheds) are located within Maryland State Forest boundaries in Garrett County and are conveniently accessible by car from the Appalachian Laboratory (AL) in Frostburg (Figure 2.1). A color map (Figure 2.2) and tabular summary (Table 2.2) of the land use/land cover information for each of the five watersheds was produced using ArcView software and digital data for Garrett County (based on 1997 SPOT satellite imagery) obtained from the Maryland Office of Planning. A color map depicting topographic relief of the watersheds (Figure 2.3) was produced using ArcView software and digital elevation model (DEM) data for the entire Chesapeake Bay watershed obtained from USEPA (Region 3, ReVA-MAIA 30-m DEM data).

Although the watersheds were found to be predominantly forested (66 – 97%), the land use disturbance criterion was the most difficult to achieve. In fact, all of the sites are apparently influenced to some degree by one or more potentially confounding land use activities. The most problematic site from this perspective is the North Prong of Lostland Run (NPLR), which will be shown to be chemically affected by acid mine drainage, despite the fact that no acid mine seeps have been located within the watershed (although Table 2.2 shows that mining comprises 5.4% of the land area of NPLR). The sites that are least affected by human land use activities are the Herrington Creek (unnamed) tributary (HRTB) and Black Lick (BLAC); Upper Big Run (BIGR) and the the tributary to Upper Poplar Lick (UPTB) are modestly affected (Table 2.1).

Table 2.1. Descriptions of five stream sampling sites in western Maryland and their watersheds.

Feature	Upper Big Run (BIGR)	Black Lick (BLAC)	Herrington Creek Trib. (HRTB)	North Prong Lostland Run (NPLR)	Upper Poplar Lick Tributary (UPTB)
Area (hectares)	162	558	255	1275	53
Stream Gage Location					
Latitude (N)	39 35'46"	39 36'34"	39 27'55"	39 22'21"	39 38'33"
Longitude (W)	79 10'33"	79 04'56"	79 25'55"	79 15'19"	79 06'40"
Elevation (m)					
Maximum	878	835	786	981	835
Minimum	750	570	744	689	777
USGS Topographic Quads	Bittinger	Avilton Barton	Oakland	Mt. Storm Gorman Kitzmiller Deer Park	Avilton
Geologic Formations	Pocono Greenbrier Mauch Chunk Allegheny/Pottsville	Jennings Hampshire Pocono	Conemaugh	Conemaugh Allegheny/Pottsville	Pocono Greenbrier Mauch Chunk
State Forest	Savage River	Savage River	Potomac-Garrett	Potomac-Garrett	Savage River
Site Installation Completed	Sep95	May96	Jan96	Jan96	May96
Spring Baseflow Chemistry (May96)					
ANC (ueq/L)	30	77	-1	32	13
Chloride (ueq/l)	20	34	22	22	55
Confounding Land Use Activities	Road Drainage Transmission Corridor	Light Residential	Agriculture Beavers	Acid Mine Drainage Light Residential Road Drainage	Timber Harvest.

Table 2.2. Land use/land cover in five western Maryland watersheds (as a percentage of total land area).

Land Use/Land Cover	Upper Big Run (BIGR)	Black Lick (BLAC)	Herrington Creek Tributary (HRTB)	North Prong Lostland Run (NPLR)	Upper Poplar Lick Tributary (UPTB)
Total land area (hectares)	162	558	255	1275	53
Mining	0.0	0.0	0.0	5.4	0.0
Cropland	0.0	14.7	3.4	4.8	33.7
Pasture	0.2	5.0	0.0	4.9	0.0
Deciduous forest	96.8	60.6	88.5	81.2	7.4
Evergreen forest	0.0	4.5	8.1	1.3	0.0
Mixed forest	0.0	15.2	0.0	0.0	58.9
Brush	3.1	0.0	0.0	2.4	0.0
TOTAL	100.0	100.0	100.0	100.0	100.0

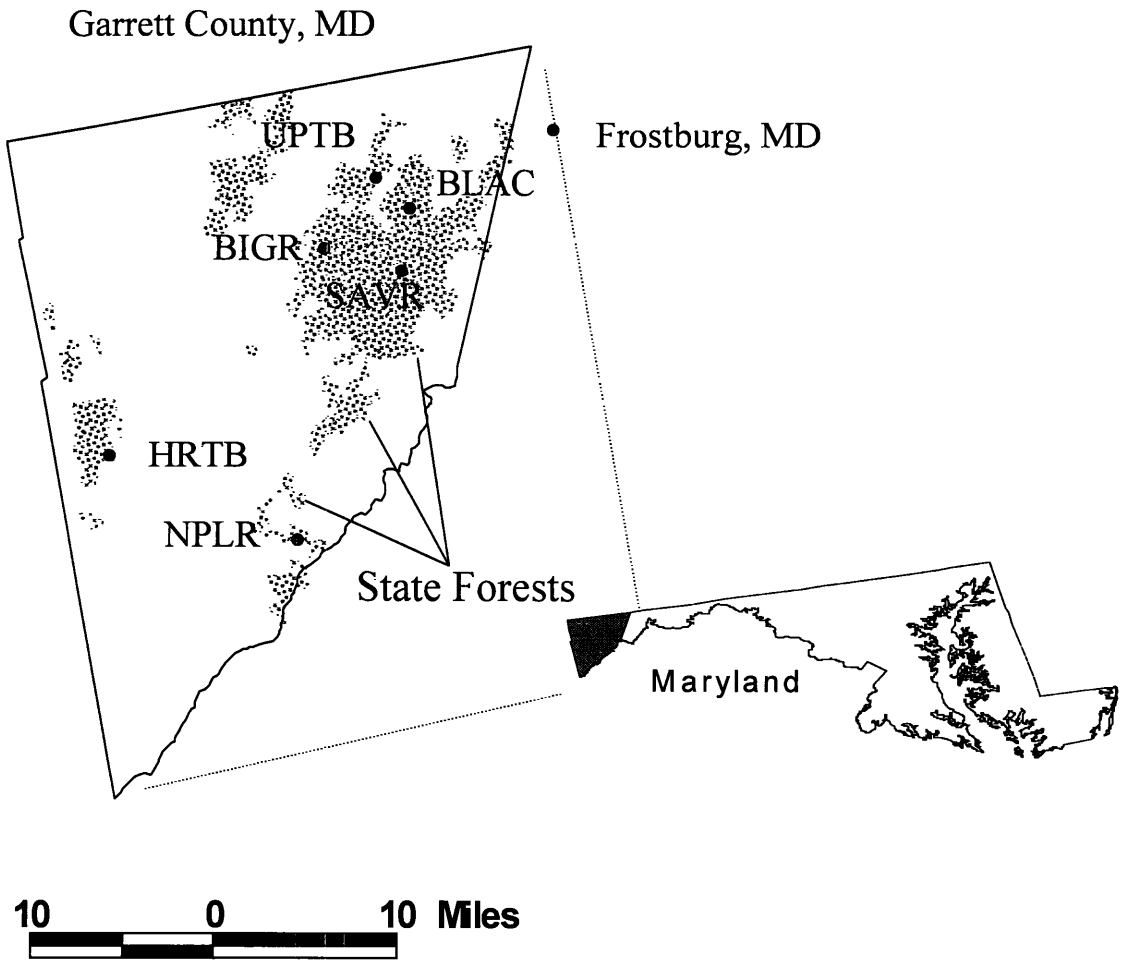

Figure 2.1. Location of episodic monitoring sites and watersheds in Garrett County, Maryland (BIGR=Upper Big Run, BLAC=Black Lick, HRTB=Herrington Creek tributary, NPLR=North Prong Lostland Run, and UPTB=Upper Poplar Lick).

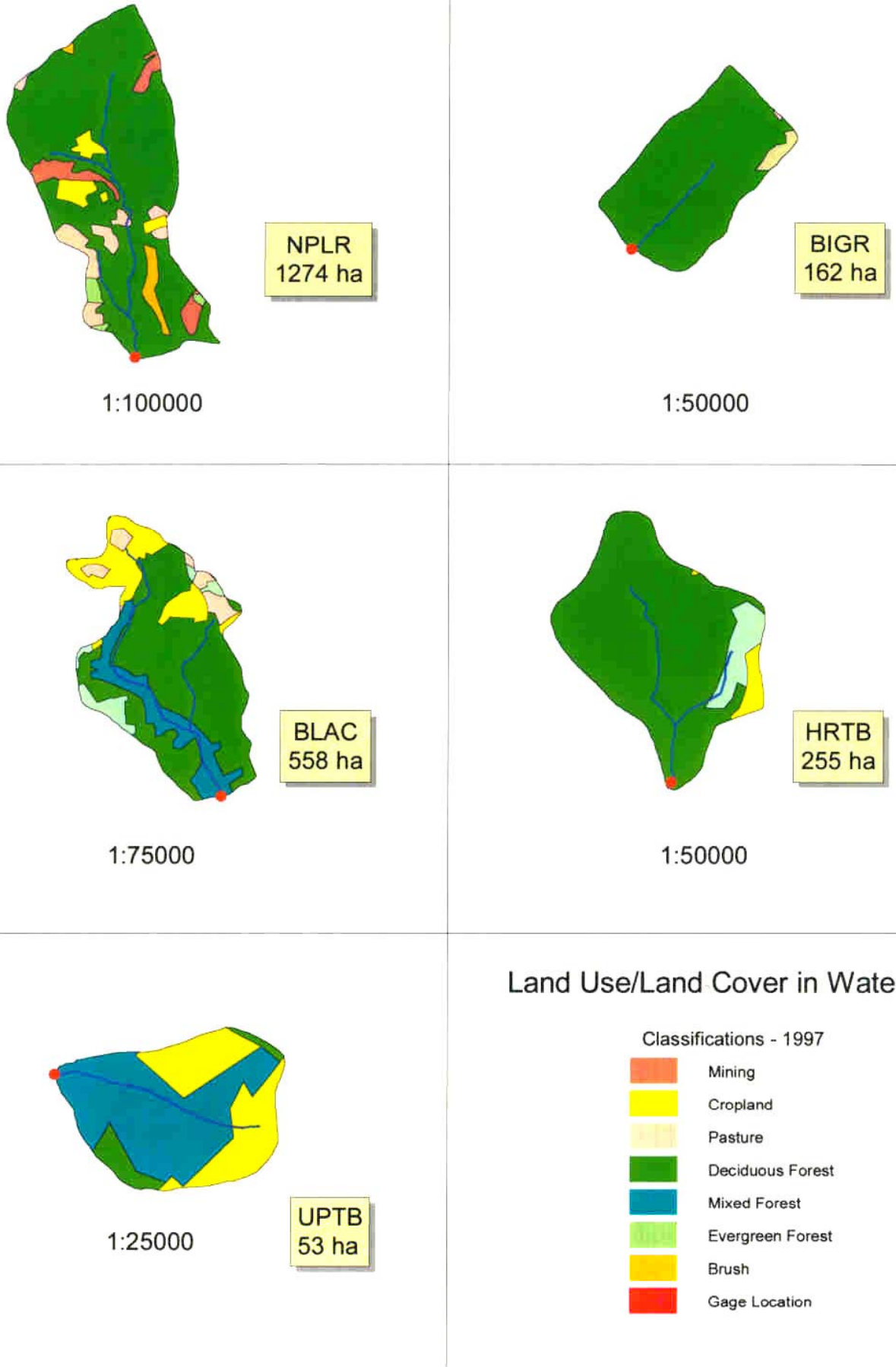

Figure 2.2. Land use/land cover distributions within the five study watersheds based on 1997 imagery.

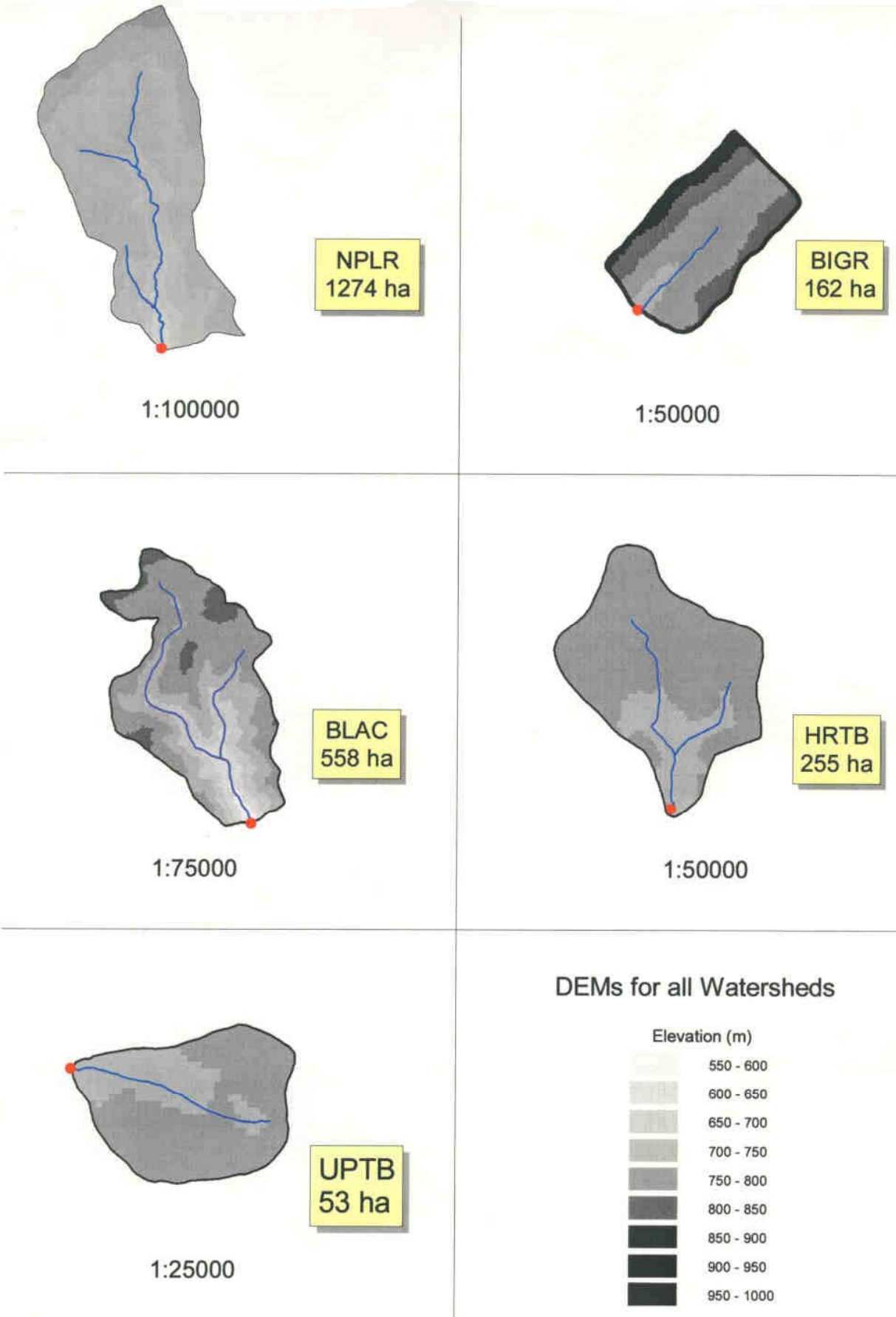

Figure 2.3. Topographic relief within the five study watersheds based on published digital elevation model (DEM) data.

3. Methods

A. Field Methods

Installation of stream gaging and surface water sampling equipment commenced in September of 1995 following the detailed field reconnoitering of the selected sites and the fabrication of stilling wells and instrument shelters. Stilling wells were constructed from 18" steel culvert pipe and sheet metal (for the bottom of the well) by a local welding shop; plywood instrument shelters (approx. dimensions of 18"H x 30"W x 36"D) were built to sit atop the stilling wells and house water level recorders. Five CCA-treated plywood boxes (approx. dimensions of 30"H x 30"W x 48"D) with foam-insulated lids were built to house portable sequential water samplers. Installation at each site involved manual excavation of a large hole and trench to a depth below the elevation (e) associated with zero channel flow to receive the stilling well and its intake pipe (2" dia. PVC). The shelter for the water sampler was sited adjacent to the stilling well at a depth in the soil that would allow access through the lid, but which provided significant insulation from freezing during cold weather; a PVC sleeve (1.5" dia.) for the sampler tubing was sited in the same trench that contained the stilling well intake pipe. The entire site was backfilled and the instrument shelter for the water level recorder was bolted onto the stilling well. Finally, a non-recording (staff) gage was installed within the gaging pool at each site to provide a quick visual check of the recorder readings.

Each site was equipped with a Stevens Type A analog water level recorder (10" float), although a backup Stevens Type F analog recorder was used temporarily when a Type A recorder was either "on order" or "out of service". Each site was also equipped with an ISCO Model 3700 (or American Sigma Model 800 SL) portable, programmable, sequential water sampler; each sampler was configured for 24, 1L bottles and was powered by a 12V "rechargeable" lead/acid car battery; batteries were swapped and trickle-charged regularly to minimize permanent loss of power. Three of the five sites were fully operational according to the proposed project schedule: BIGR (9/95), NPLR (1/96), and HRTB (1/96). However, owing to an unusually severe winter in the area which began in early November and lasted through mid-April, it was not possible to get the last two sites—UPTB and BLAC—fully operational until May 1996.

Following installation of the stream gaging equipment during the first year of the project, each of the five stream sites was continuously gaged at appropriate natural control sites using conventional, established methods of the USGS (Rantz *et al.*, 1982a, b). Each site, equipped with both a non-recording staff gage and a recording gage, provided virtually continuous gage height (G) data throughout the project (except for brief periods when a recorder malfunctioned or the water in the stilling well froze during an extended period of extremely low air temperatures). The analog stage records were returned regularly to the Appalachian Laboratory (AL) where they were digitized using ArcInfo software and incorporated into a continuous data base. Field personnel were generally able to keep channel control features clear of ice and debris during the project, thus minimizing temporary shifts in rating curves. Discharge (Q) measurements (Table 3.1) using the standard "mid-section" method (Rantz *et al.*, 1982a) were made periodically by

field personnel at appropriate cross-sections using a Marsh-McBirney Model 200 Flo-mate electromagnetic current meter attached to a top-setting wading rod; eight discharge measurements made at BIGR during a previous project were provided by R.P. Morgan II (AL) to extend the gaging record at that site. Each set of measurements was used to define the define rating curve (i.e., log Q vs. log[G-e] relationship) for each gaging station. A customized program (coded in FORTRAN) was used to automatically compute a continuous hourly discharge record (units of m^3/sec or cms) from the continuous digital stage record (units of cm) and the rating curve for a particular station for the period of record; each continuous hourly record was then time-integrated over daily intevals to provide a continuous record of mean daily discharge for each site.

As checks on the accuracy of the gaging effort, annual water balances were computed for one watershed (BIGR) for the 1996 water year (October 1, 1996—September 30, 1997) and for all five watersheds for the 1997 and 1998 water years. The water balances are based on the continuous records of mean daily discharge (cms) from each site and precipitation data from the Savage River Reservoir dam, located 3.5 miles southeast of BIGR; precipitation data were provided courtesy of the Maryland State Climatology office. Discharge records were converted to depth units (mm/day) by dividing each discharge value by the specific watershed area. Both the precipitation data and discharge data were time-integrated over monthly intervals and summed for each of the three water years.

Streamwater sampling to characterize seasonal and episodic changes in acid/base composition of the five streams commenced according to plan in January 1996 at three of the sites, but due to the unusual severity of the winter, sampling at the other two sites (UPTB and BLAC) was delayed until field equipment was made fully operational in May 1996; biweekly "grab" sampling at UPTB began in January 1996, however. All field sampling was consistent with standard USEPA protocols for monitoring surface water quality for acid deposition studies (USEPA, 1989). Laboratory quality assurance/quality control (QA/QC), data and sample tracking, and data management protocols conformed to procedures utilized in similar recent projects (USEPA, 1987; 1991). Bi-weekly sampling was used to characterize antecedent baseflow chemical conditions in each stream, as most "grab" samples were not collected during major events. In addition, the bi-weekly sampling provided an excellent data base for computing fluxes and for characterizing seasonal variability in acid-base composition of streamwater.

Grab sampling for ANC and conductivity required manually filling a 1L cubitainer (that had been rinsed several times in the laboratory with deionized (DI) water) in the field; the cubitainer was carefully "burped" to remove head space. Other streamwater aliquots were taken at the same time for: (1) major ions (Na^+, K^+, NH_4^+, Mg^{2-}, Ca^{2+}, Cl^-, NO_3^- and SO_4^{2-}); (2) dissolved organic carbon (DOC) and dissolved Si; and (3) total dissolved nitrogen (TDN) using 50-ml syringes (filled and refilled manually); aliquots were filtered (0.45 μm) in the field into pre-cleaned aliquot bottles. Two 50-mL syringes were then used for obtaining aliquots for pH and Al determinations. All syringes and aliquot bottles were rinsed at least three times with streamwater

Table 3.1. Summary of discharge (Q) and gage height (G) data for the five gaging stations.

Date of Measurement	BIGR G (cm)	BIGR Q (cms)	UPTB G (cm)	UPTB Q (cms)	NPLR G (cm)	NPLR Q (cms)	HRTB G (cm)	HRTB Q (cms)	BLAC G (cm)	BLAC Q (cms)
unknown	28.5	0.017								
unknown	29.5	0.032								
unknown	30.0	0.035								
unknown	32.0	0.053								
unknown	32.5	0.050								
unknown	34.0	0.071								
unknown	34.0	0.066								
unknown	44.0	0.203								
24-Jan-96	46.0	0.303	18.0	0.045			44.0	0.922		
29-Jan-96	33.5	0.053	16.0	0.020			34.5	0.149		
22-Feb-96	34.5	0.077	15.5	0.030			34.0	0.153		
07-Mar-96	37.0	0.112	18.5	0.055						
11-Apr-96	29.0	0.010	11.5	0.004	35.5	0.282	30.5	0.055		
21-May-96			12.0	0.010	38.5	0.174	32.0	0.107	28.0	0.096
06-Sep-96	77.1	1.462	47.9	0.890	68.5	2.685	38.5	0.422		
20-Feb-97									35.0	0.776
16-Apr-97	28.0	0.007	8.0	0.003	25.5	0.108			14.0	0.030
15-May-97	29.5	0.015	7.5	0.003	32.0	0.296			18.5	0.063
21-May-97			10.0	0.007	31.5	0.260			24.0	0.170
07-Aug-97					16.5	0.022	19.5	0.003		

prior to filling and all samples were kept on ice in a cooler for transport to AL. Each DOC/Si aliquot was preserved with one drop of concentrated H_3PO_4. For QA/QC purposes, a duplicate ("blind" or "phantom") sample was taken bi-weekly from one of the five streams and used to quantify total precision; field blanks (DI water samples filtered and aliquotted in the field) were used to routinely assess field contamination.

Portable ISCO (or Sigma) sequential water samplers were used for automatically collecting streamwater samples during major hydrological (both rainstorm and snowmelt) events; our stated goal was to sample approximately 3 or 4 of the most significant stormflow events (or "episodes") each year of the project (total of 9-12 events per site over the entire study). All polyethylene sample bottles were pre-leached with dilute HCl and soaked/rinsed for several days with DI water prior to sampler activation. Samplers were ordinarily programmed to sample at 6-hour intervals to allow samples to be collected over a complete 6-day period and were manually activated prior to anticipated major stormflow events. Samples were retrieved within 48 hours of final collection and were returned to the laboratory. Unlike the grab samples, filtering of the episodic samples was performed in the laboratory within 24 hours of final collection using a vacuum pump and an array of glass filter holder assemblies. Aliquotting and preservation were similar to the methods used in the field, except that syringe aliquots for pH and Al were not drawn from the ISCO bottle.

Beginning in July of 1997, streamwater samples were also collected for analysis of the following low-level dissolved metals at AL by inductively-coupled plasma atomic emission spectroscopy (ICP-AES): beryllium (Be), cadmium (Cd), chromium (Cr), cobalt (Co), iron (Fe), manganese (Mn), vanadium (Vn), and zinc (Zn). Bi-weekly grab samples were collected by filtering the samples through 0.45 μm filters in the field into acid-washed, pre-leached polyethylene bottles. The samples were then preserved in the laboratory with Ultrex-grade HNO_3. Low-level metals samples were also collected during high flow storm events at selected points on the storm hydrograph. All event samples were filtered in the laboratory following the same protocol as for the other dissolved analytes.

In October 1997, the scope of the project was expanded and additional samples were collected at two of the sampling sites for the analysis of trace metals/metalloids by the analytical laboratory at Chesapeake Biological Laboratory (CBL); field sampling methods required strict adherence to standard protocols for sampling ambient water for trace metals analysis (method 1669; USEPA, 1995). Monthly baseflow grabs were collected at BLAC and HRTB, while four stormflow events were also sampled over the next year at the two sites using reconfigured automated samplers. These ISCO samplers were modifed by using acid-washed, teflon-coated inlet tubing and silicone pump head tubing and acid-washed sampling bottles appropriate for the specified analytes (glass for mercury analysis and polyethylene for trace metal/metalloid analyses). Because sample bottles that would fit into the base of the ISCO sampler were not suitable for shipping and long term storage, at the end of an event (and while still in the field) the trace metal samples were transferred into acid-washed polyethylene bottles with securely locking

tops and the mercury samples were transferred into teflon bottles. Back at the lab, the samples were frozen and shipped to Dr. Rob Mason at CBL for chemical analysis.

In order to test the general validity of a regional empirical acidification model, we conducted a synoptic streamwater survey by sampling 33 stream locations on all major tributaries to the Savage River Reservoir (and its outlet) during (a) fall baseflow conditions (November 18, 1996), (b) spring baseflow conditions (April 4, 1997) and (c) spring stormflow conditions (June 2, 1997). Stream locations were identified from a comprehensive list of tributary nodes generated from USGS topographic quadrangles for the watershed; the 33 stream nodes sampled were all readily accessible locations (at most a short walk from a paved road), which enabled all water samples to be collected within several hours of peak flow during the June event by two, two-person sampling crews. Sampling proceeded from the lowest order nodes to the higher order nodes during the event (which approximated a LaGrangian sampling scheme where the teams were moving with the flood wave). All water samples ("grabs") were returned to the AL water chemistry laboratory and processed in the normal manner.

B. Laboratory Methods

All streamwater samples were analyzed according to standard EPA laboratory methods appropriate for monitoring surface water quality in acid deposition studies (USEPA, 1987) as follows:

(1) Grab sample pH was measured using the "closed system" method on syringe samples to minimize changes due to equilibration with atmospheric CO_2.

(2) During the first two years of the project, ANC was measured on 40 mL unfiltered samples using manual acidimetric Gran titration with dilute HCl (standardized against a primary standard solution of Na_2CO_3) with electrometric pH detection, following measurement of ambient pH (open system) prior to the first addition of strong acid; only those titration points (typically 6-8 points) taken in the range 4.7 to 3.5 were used to compute the Gran function and ANC. During the third year of the project, a Brinkmann-Metrohm autotitrator was used to perform the same method automatically; an intercomparison study indicated excellent agreement between the two methods.

(3) Conductivity was measured using a conductivity cell and Yellow Springs conductivity meter with manual temperature correction to 25 deg C.

(4) Dissolved organic carbon (DOC) was measured by infrared detection following UV-assisted persulfate oxidation on a Dohrmann DC-80 analyzer.

(5) Major cation (including NH_4^+) and anion concentrations were determined using a Dionex DX-500 ion chromatography system, equipped with electronic conductivity suppressors, autosampler, and a computer-based data acquisition/controller system.

(6) Total exchangeable and nonexchangeable reactive Al concentrations were measured using an automated fractionation/pyrocatechol violet (PCV) flow injection technique on a Lachet (Quikchem) automated analyzer.

(7) Dissolved Be, Cd, Co, Cr, Fe, Mn, Si, Vn, and Zn concentrations were determined by ICP-AES.

(8) The suite of total and particulate trace metal/metalloid analyses performed at CBL during the third year of the project included: mercury (Hg), methyl mercury (CH_3Hg), Cd, lead (Pb), arsenic (As), and selenium (Se). Mercury was measured using cold vapor atomic fluorescence spectrometry (CVAFS), while As, Se, Cd, and Pb were measured via inductively-coupled plasma mass spectrometry (ICP-MS).

(9) In the first year of the project, TDN concentrations were measured on selected samples collected during significant hydrological events using an Antek Model 7000 Nitrogen analyzer (loaned by Antek Instruments, Inc.); dissolved organic N (DON) concentrations were computed by subtracting NO_3^- and NH_4^+ concentrations from TDN concentrations. Prior to using this experimental "difference" method for quantifying DON concentrations in water samples, a laboratory experiment was performed in which recoveries of five known N-containing compounds (potassium nitrate, ammonium chloride, pyridine, alanine, and diaminobenzene) were compared; this group includes compounds with the N atom in a variety of oxidation states. Overall, actual mean N recoveries (of five replicates) from 250 μg/L solutions were excellent, ranging from 86% for alanine to 95% for diaminobenzene. When normalized to the nitrate-N recovery (assumed 100%), relative mean recoveries ranged from 95% for alanine to 105% for diaminobenzene and were not statistically ($p = 0.05$) different (Figure 3.1).

Over the course of the entire study, 1,477 regular streamwater samples (338 grab samples and 1,139 ISCO sequential samples) from the five intensive sites were collected and analyzed (Table 3.2); in addition, we collected and analyzed 59 field duplicate (PHAN) samples, 19 field blanks (XBLK), and 40 samples (ENVC) from Environment Canada's National Water Research Institute (NWRI) Ecosystem Interlaboratory Quality Assurance Program as part of our rigorous quality assurance (QA) and quality control (QC) programs. A summary of the results of our laboratory QA/QC and data verification programs (as well as a detailed description of the laboratory methods) can be found in Appendix B.

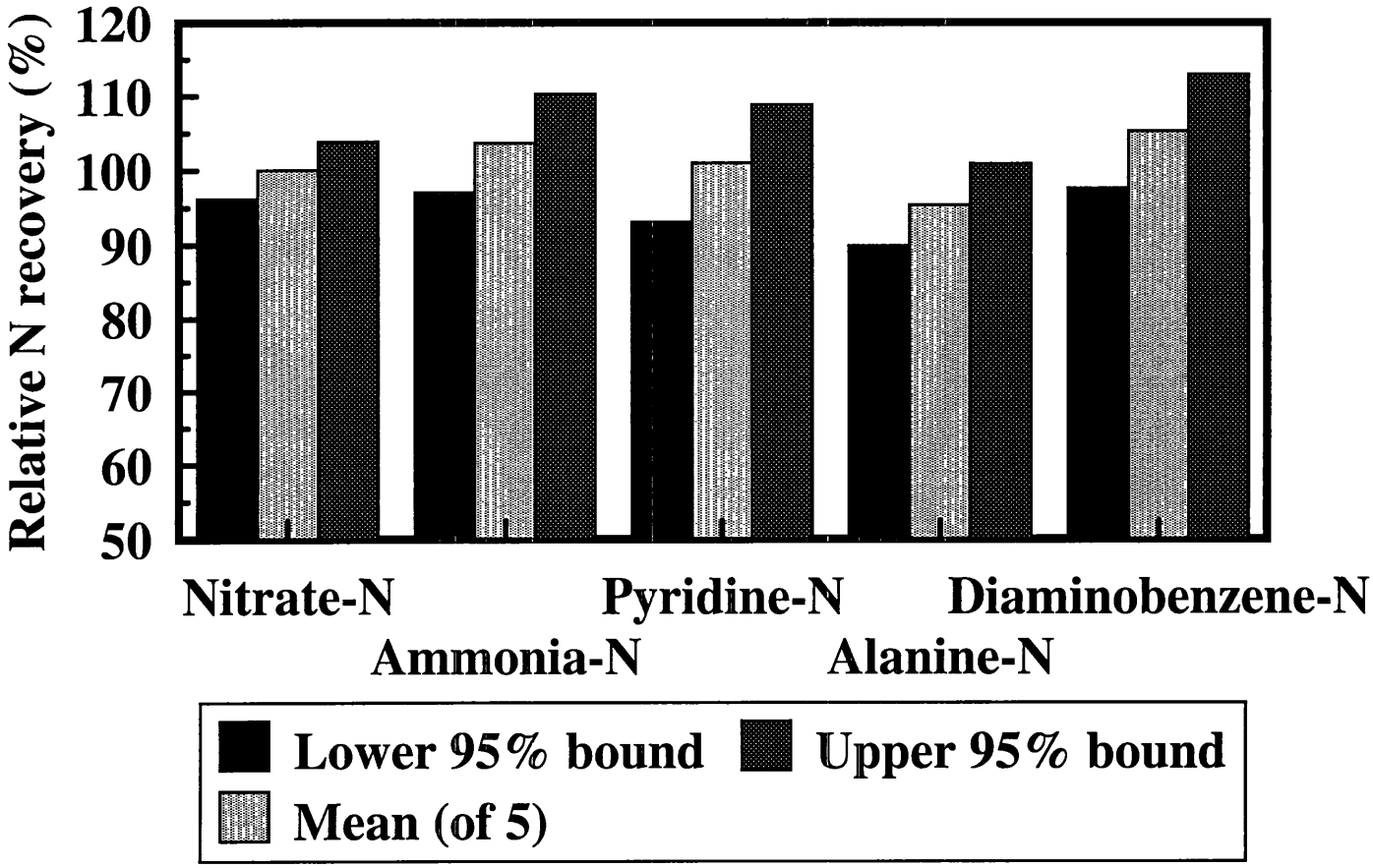

Figure 3.1. Relative recoveries of dissolved nitrogen (N) for five synthetic N-containing compounds (normalized to nitrate-N). Mean, upper and lower confidence bounds shown.

Table 3.2. Number of grab, sequential, and other samples collected and analyzed during the project. PHAN indicates a field duplicate from one of the intensive sites, XBLK indicates a field blank, and ENVC indicates an Environment Canada interlaboratory comparison sample.

	Sample Types			
Stream	**Grab**	**Sequential**	**Other**	**Total**
Intensive Sites				
BIGR	72	315	0	387
BLAC	57	175	0	232
HRTB	69	260	0	329
NPLR	70	252	0	322
UPTB	70	137	0	207
Subtotal	338	1139	0	1477
QA Samples				
PHAN	59	0	0	59
XBLK	19	0	0	19
ENVC	0	0	40	40
Subtotal	78	0	40	118
Extensive Sites				
Savage River watershed	105	0	0	105
Subtotal	105	0	0	105
TOTAL	**521**	**1139**	**40**	**1700**

4. Results and Discussion

Project results are presented in the following six subsections of the chapter: (A) surface water gaging/watershed water balances, (B) temporal variations in streamwater acid-base composition, (C) analysis of episodic chemical data, (D) temporal variations in low-level dissolved metals in streamwater, (E) temporal variations in trace metals in streamwater, (F) extensive stream sampling, (G) hydrochemical modeling of episodic acidification, and (H) analysis of long-term changes in streamwater.

A. Surface Water Gaging/Watershed Water Balances

The gaging stations became fully operational within the first six months of the project: BIGR was on line in October 1995, NPLR and HRTB began gathering data in January 1996, and UPTB and BLAC were fully operational in May 1996. Discharge measurements made at each of the gaging stations were used to define a "rating curve" that could be applied to the continuous stage record for computation of discharge. Linear rating curves were developed by linear regression of the logarithm of measured discharge (log Q) on the logarithm of gage height corrected by subtraction of the elevation of zero flow (log[G-e]); e was optimized by trial and error, but generally agreed closely with field estimates (Figure 4.1). Each linear rating curve explained at least 95% of the total variation in discharge and enabled computation of discharge over the full range of conditions, although some extrapolation was necessary for peak values at several of the sites. Continuous hourly discharge records were constructed using the digital records of hourly gage heights at each site and the rating curve. Daily average discharge records were also compiled for the length of the field study (10/1/95-9/30/98). Hydrographs (discharge vs. time) for individual water years (October 1—September 30) illustrate that the discharge peaks generally occurred concurrently at all sites and that the relative magnitudes of the peaks ordinarily varied in the same order as the respective watershed areas (i.e., NPLR > BLAC > HRTB > BIGR > UPTB; Figures 4.2, 4.3, 4.4). However, due to the spatial variability in precipitation, there were a few storms each year during which the southern watersheds (NPLR and HRTB) experienced a rise in flow while the northern watersheds (BLAC, BIGR and UPTB) did not.

In 1996, two extreme flood events occurred—one in January 1996 and a second in September 1996; the January event was a rain-on-snow event following an early January blizzard that dumped 2-3 feet of snow on western Maryland. During September, the remnants of Hurricane Fran dumped almost 11 inches of precipitation at the Savage River Reservoir as the storm moved north over inland areas of the east coast, making water year 1996 the wettest year on record. Discharge values measured at all sites for this event are the highest of the three-year study period (Figure 4.2). Changes in streamwater chemical composition associated with both of these extreme events are presented and discussed in latter sections of the chapter.

Average monthly precipitation during the 1997 and 1998 water years was approximately 3 and 4 inches/month, respectively. Even with these differences, however, storms of

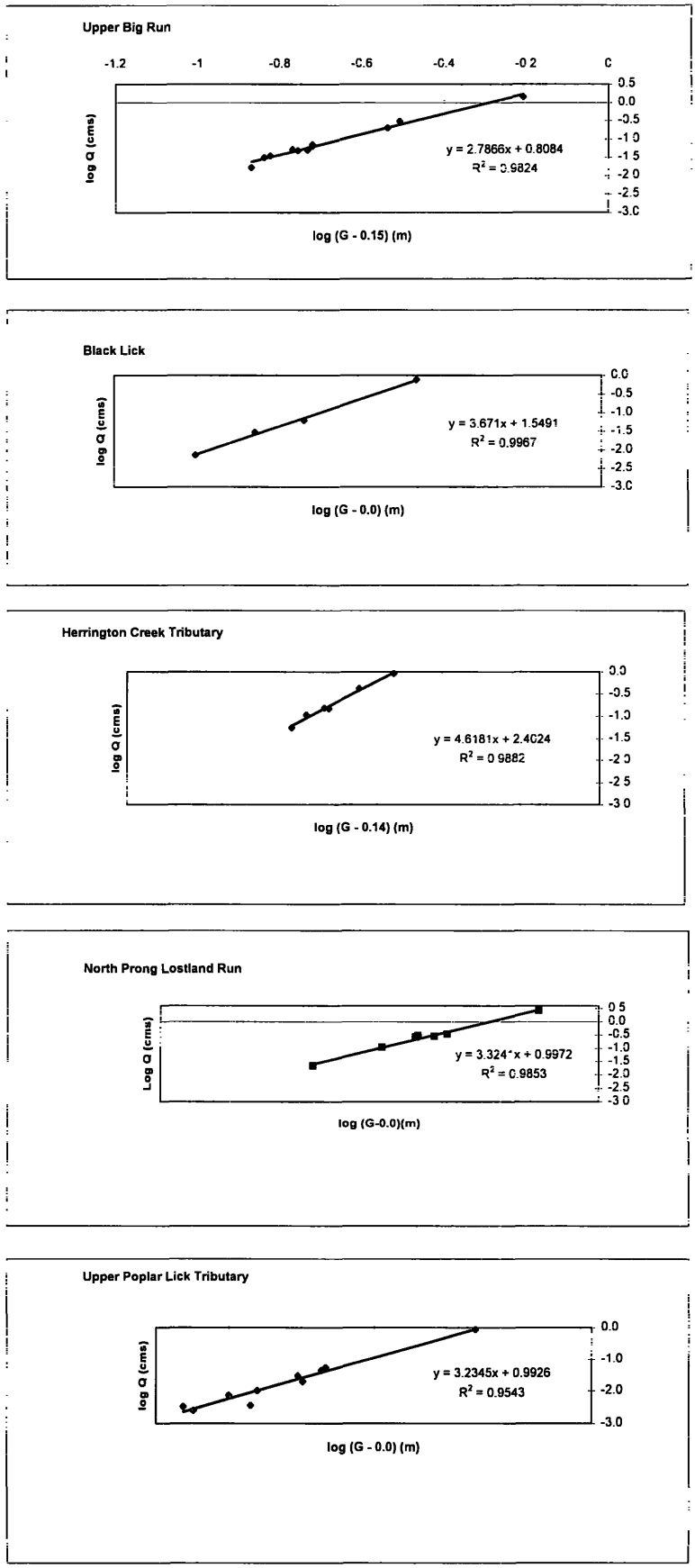

Figure 4.1. Stage/discharge data and rating curves for the five streamwater monitoring sites.

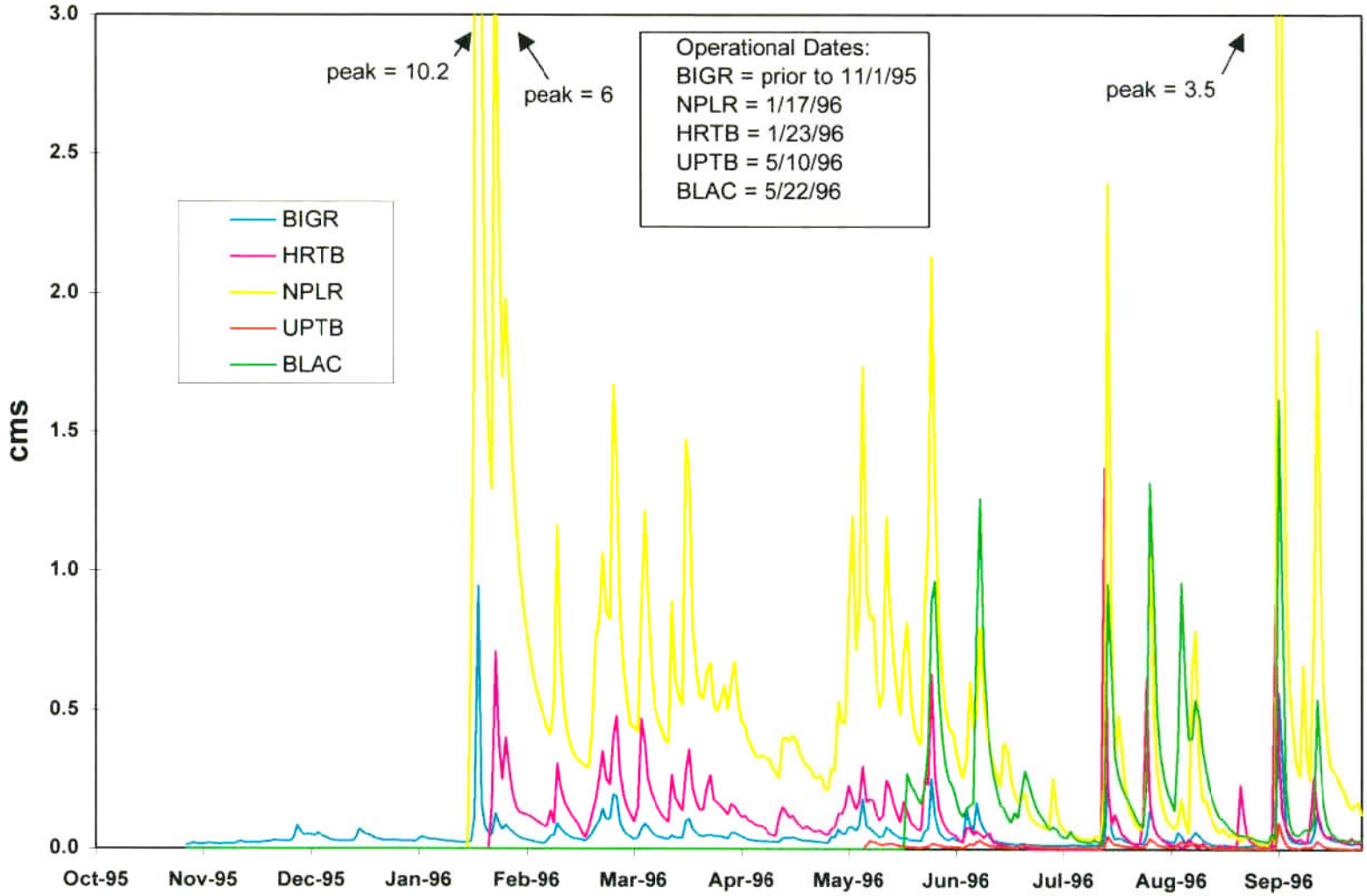

Figure 4.2. Annual hydrographs (mean daily discharge values) for the five streamwater monitoring sites for the 1996 water year (October, 1995 through September, 1996).

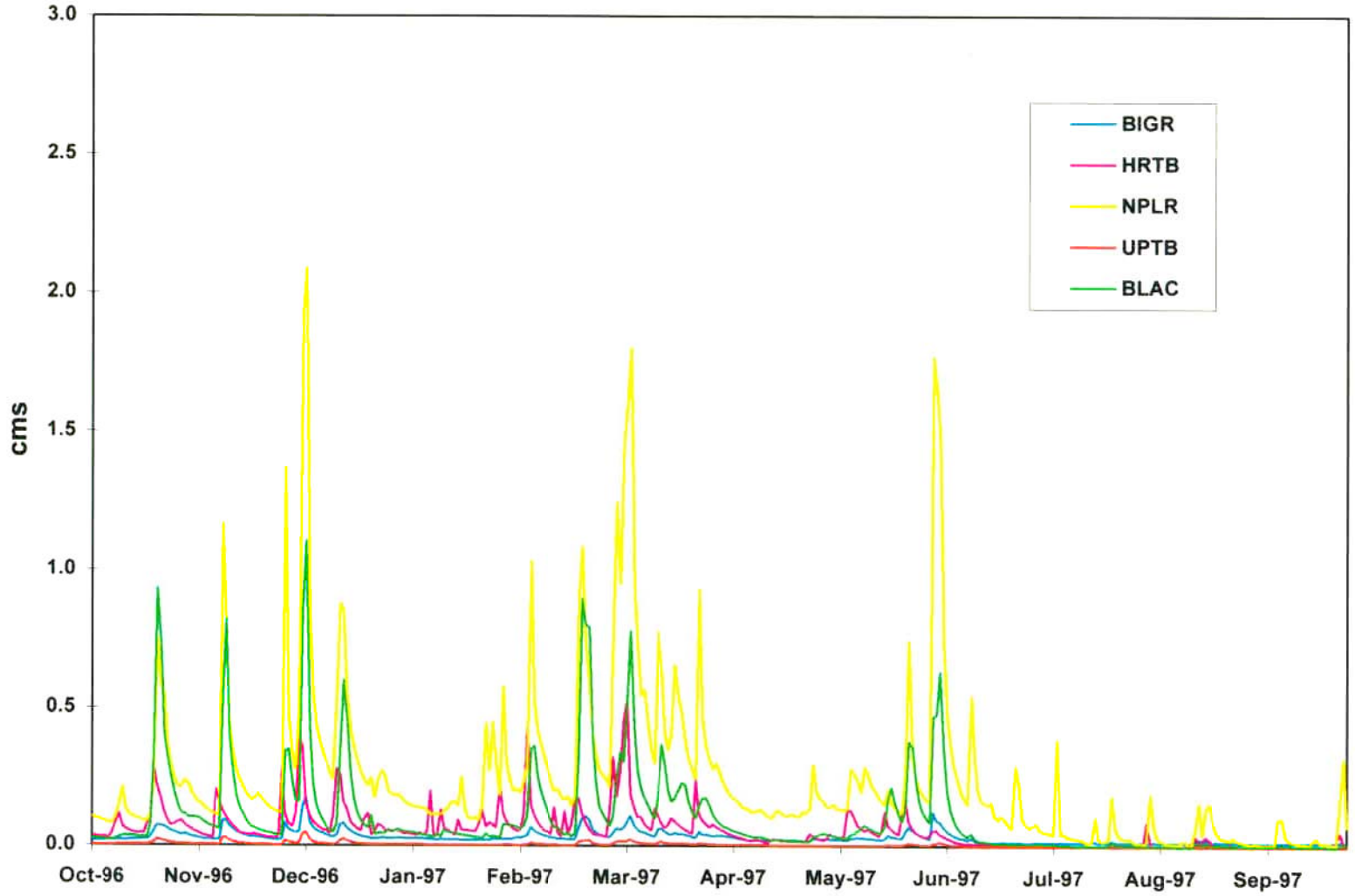

Figure 4.3. Annual hydrographs (mean daily discharge values) for the five streamwater monitoring sites for the 1997 water year (October, 1996 through September, 1997).

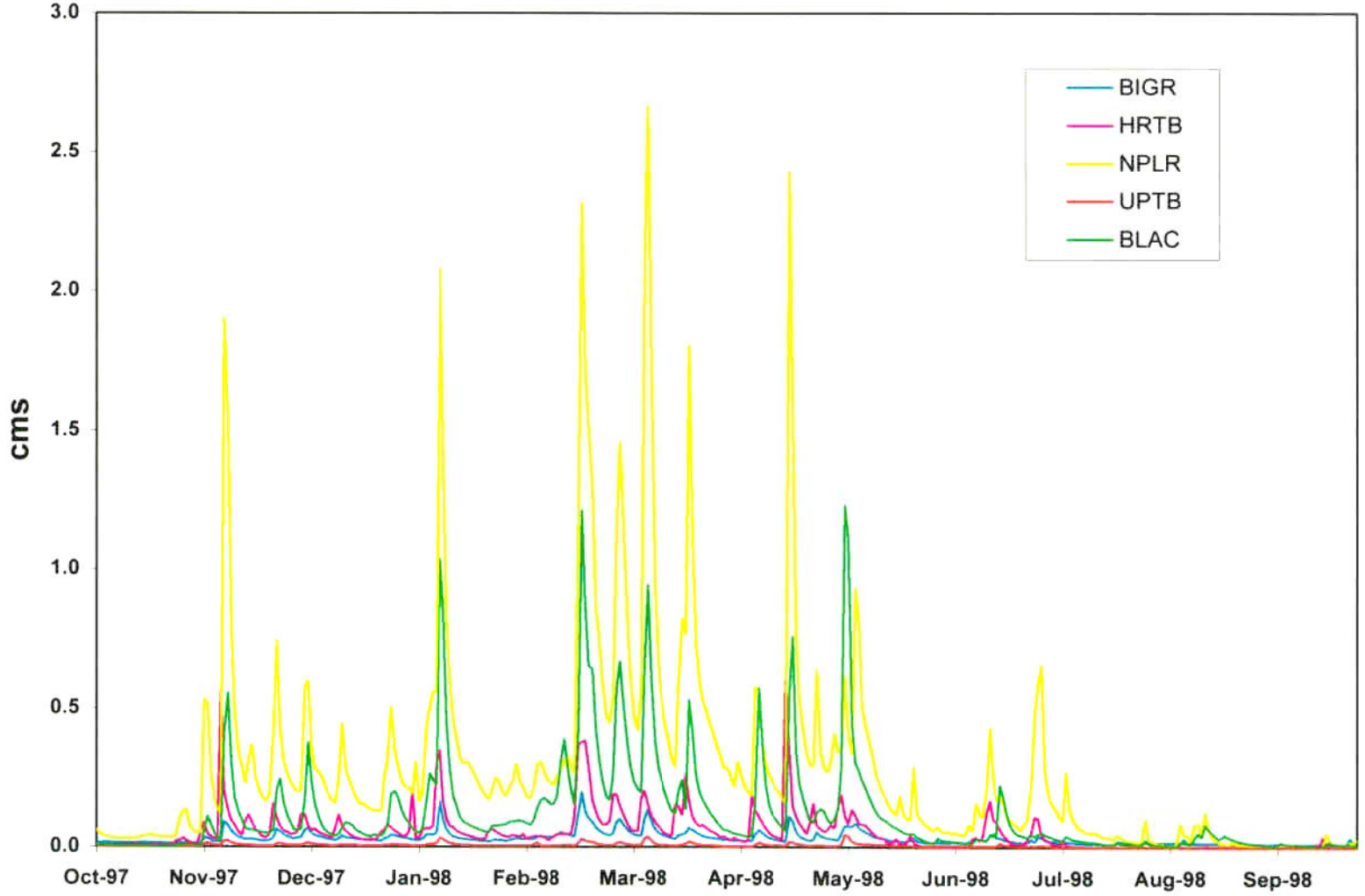

Figure 4.4. Annual hydrographs (mean daily discharge values) for the five streamwater monitoring sites for the 1998 water year (October, 1997 through September, 1998).

approximately equal magnitude occurred throughout the fall and spring of both years as evidenced by discharge peaks of comparable magnitude (Figures 4.3, 4.4). The summer of 1997 was punctuated by brief thunderstorms (approximately three per month from June through August), while in 1998 after a brief wet period in June, drought conditions were experienced over the study area.

The water balance calculations give us confidence that our gaging efforts are consistent with accepted field hydrological methods. With the exception of UPTB (discussed below), water yield and computed evapotranspiration (ET) for all watersheds are reasonable for the humid, mid-Atlantic region. As validation of our methods, we compared our results with both contemporaneous (1995-1998) and long term (50^{+} years) mean daily discharge data for the Savage River near Barton MD gaging station (SAVR) that we downloaded from the USGS world wide web site (http://water.usgs.gov/public/data.html). These data were time-integrated (water year basis) and normalized accordingly. Precipitation, runoff and estimates of ET for the three water years of the study are presented in Table 4.1.

During the 1996 water year, the timing and magnitude of most runoff peaks were consistent between BIGR and SAVR (Figure 4.5); however, beginning in 1997, it appears that the runoff peaks are consistently higher at SAVR than at BIGR (perhaps due to a shifted rating curve at the former station that has not been properly taken account of). Total computed annual runoff for BIGR and SAVR for 1996, 1997 and 1998 water years are also very similar, differing by 4%, 7%, and 16%, respectively. These two facts alone give us confidence that our gaging methods are consistent with those of the USGS and are being conducted with normal accuracy associated with such field hydrological studies. The long term averages for precipitation, water yield, runoff and ET for SAVR are 1150 mm/yr, 46%, 530 mm/yr and 620 mm/yr, respectively. Annual precipitation varied from 902 mm/yr in 1997 to 1489 mm/yr in 1996 (long-term normal of 1150 mm/yr) and water yields at SAVR and BIGR over the three-year study (60-67%) are consistently higher than the long-term average (46%). Correspondingly, the estimated rates of ET (295 – 595 mm/yr) are substantially lower than the long-term average (620 mm/yr). ET rates estimated for the study are also substantially lower than estimated annual normal lake evaporation rates for the regions (30 in/yr or 762 mm/yr; Table 4.1).

In 1996, BIGR was the only site that was operational for the entire water year; therefore it is the only site with a complete water balance. Total annual precipitation for 1996 was 1489 mm, substantially higher than 1997 (902 mm) and 1998 (1199 mm). Correspondingly, runoff at BIGR for 1996 was highest of all sites over the three-year period. In both 1997 and 1998, estimated ET (194-595 mm/year) for all sites except UPTB (discussed below) were lower than the SAVR long term average (620 mm/year). In both years, the ranges of water yield (50-78%) and runoff (580-724 mm/yr) were greater than the SAVR long-term averages. These results suggest that the three years of the study were much wetter than three average years in western Maryland (Table 4.1).

Table 4.1. Annual water balances for the five gaged watersheds.

Site	1996 Water Year					1997 Water Year					1998 Water Year				
	PPT (mm/yr)	Runoff (mm/yr)	ET (mm/yr)	ET (%)	Yield (%)	PPT (mm/yr)	Runoff (mm/yr)	ET (mm/yr)	ET (%)	Yield (%)	PPT (mm/yr)	Runoff (mm/yr)	ET (mm/yr)	ET (%)	Yield (%)
SR Long Term	1150	530	620	54	46	1150	530	620	54	46	1150	530	620	54	46
SAVR	1489	972	517	35	65	902	564	338	37	63	1199	719	480	40	60
BIGR	1489	933	556	37	63	902	607	295	33	67	1199	604	595	50	50
HRTB						902	708	194	22	78	1199	649	550	46	54
NPLR						902	621	281	31	69	1199	724	475	40	60
BLAC						902	580	322	36	64	1199	685	514	43	57
UPTB						902	286	616	68	32	1199	338	861	72	28

Water Year = October 1 to September 30.
PPT = Precipitation. Data from Savage River Reservoir dam station.
ET = Evapotranspiration, calculated by difference.
SR Long Term = Savage River long term (50+ years record) annual normal.

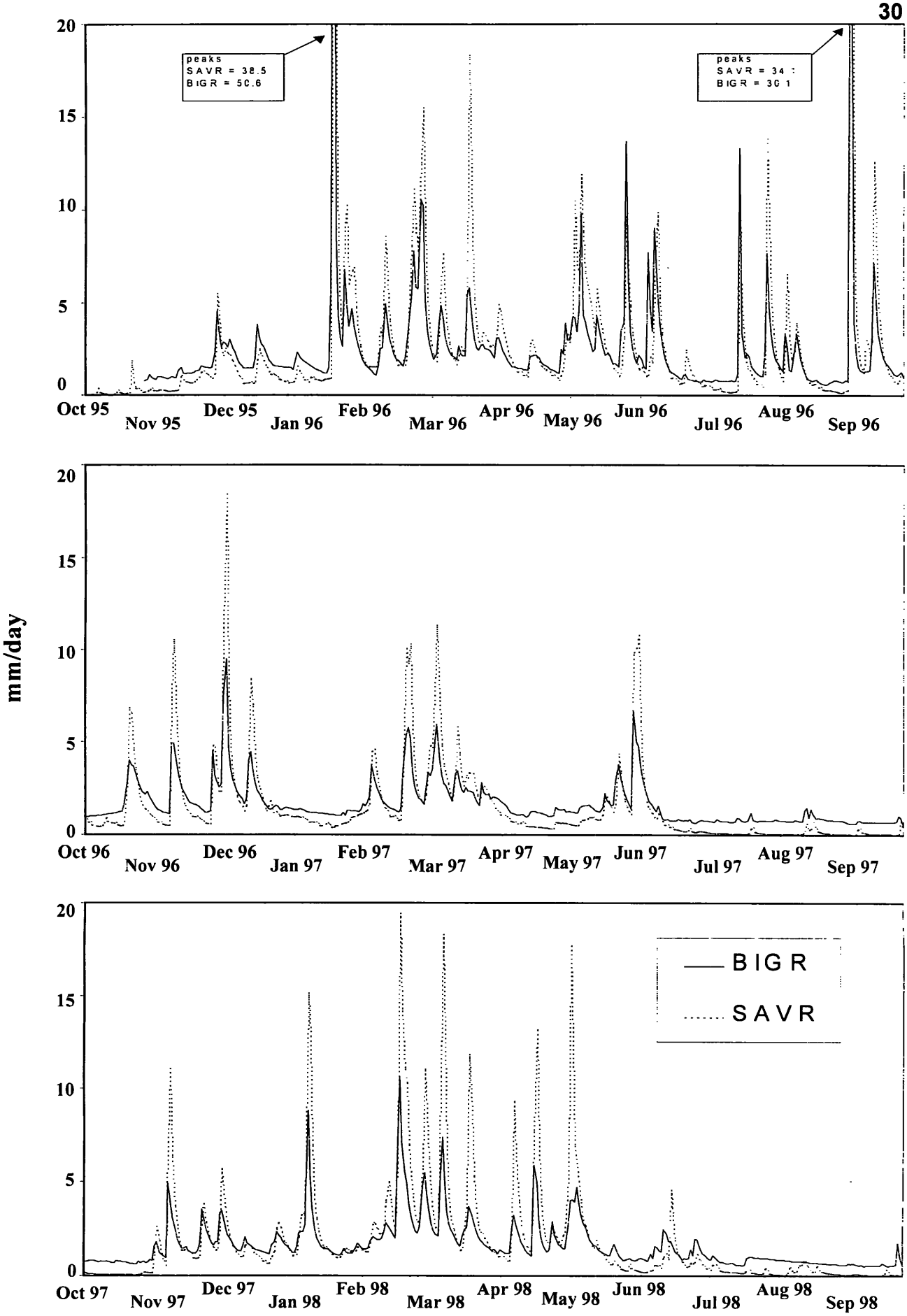

Figure 4.5. Comparison of annual runoff hydrographs (mean daily runoff) for the Upper Big Run (BIGR) and Savage River near Barton, MD (SAVR) stations for the 1996, 1997, and 1998 water years.

Although precipitation measured at the Savage River Reservoir dam was almost 25% lower in 1997 (902 mm) than in 1998 (1199 mm), the range of water yield across all sites except UPTB (see below) was lower in 1998 (50-60%) than in 1997 (64-78%). Correspondingly, estimated ET was greater in the wetter year (604-724 mm in 1998 vs. 194-322 mm in 1997). This would suggest that climatological conditions in the area allowed for greater ET in the presence of more water. Another explanation could be that a portion of the water accounted for in the 1998 estimate of ET is not going into the atmosphere, but is actually leaving the surface channel to recharge the groundwater during the very dry summer months experienced that year (Table 4.1).

Although site installation and gaging techniques used were identical to those at the other four sites, results at UPTB do not seem reasonable. For all three years, estimated ET greatly exceeds runoff in UPTB. For the 1997 and 1998 water years, ET and runoff at UPTB were the highest and lowest values, respectively, measured at all five of the study watersheds (Table 4.1). Low runoff values might be attributed to errors inherent in making flow measurements in such a small stream; over the study period, depth at baseflow was typically less than 5 cm (and reached only 20 cm during high flow of Hurricane Fran) and stormflow did not exceed 0.05 cms (with the exception of Hurricane Fran when peak flow reached approximately 0.1 cms). In addition, it is possible that a portion of our estimate of ET represents water leaving the watershed via groundwater or subsurface stream flow. The watershed of UPTB is the smallest in our study (53 ha), with the lowest relief (< 100 m). The land cover is 33% cropland and approximately 67% forested (although a small portion of this area was selectively logged just prior to the beginning of this project). Since we are unaware of any consumptive agricultural water uses in the watershed and believe that we have drawn accurate watershed divides, it is presumed that rainfall infiltrating the cleared land may exit the watershed via ungaged subsurface flow or may be contributing to basin-wide deep groundwater recharge.

B. Temporal Variations in Streamwater Acid-Base Composition

Temporal variations in the acid-base composition of streamwater at the five sampling stations was quantified first by inspection of time plots of concentrations of key chemical constituents: ANC, NO_3^-, SO_4^{2-}, DOC, sum of base cations (SBC), pH, and exchangeable reactive Al (hereafter referred to simply as Al); plots of daily runoff (mm/day) for each station were also developed for interpretive purposes (Figures 4.6 – 4.10). Of the chemical constituents displayed, pH and ANC display the most consistent and greatest seasonal and interannual variability. At all of the sites, pH and ANC are normally lowest during the first quarter of the year (winter), increase gradually during the second (spring) and third (summer) quarters, and peak near the beginning of the fourth quarter (autumn); the fourth quarter peaks appear to vary as a function of seasonal runoff, with higher values of pH and ANC corresponding to lower runoff amounts. Seasonal variations in other chemical constituents are more difficult to discern, although it appears that at some of the sites (e.g., BIGR and HRTB), NO_3^- and SO_4^{2-} concentrations peak during the first quarter and reach a minimum during the third or fourth

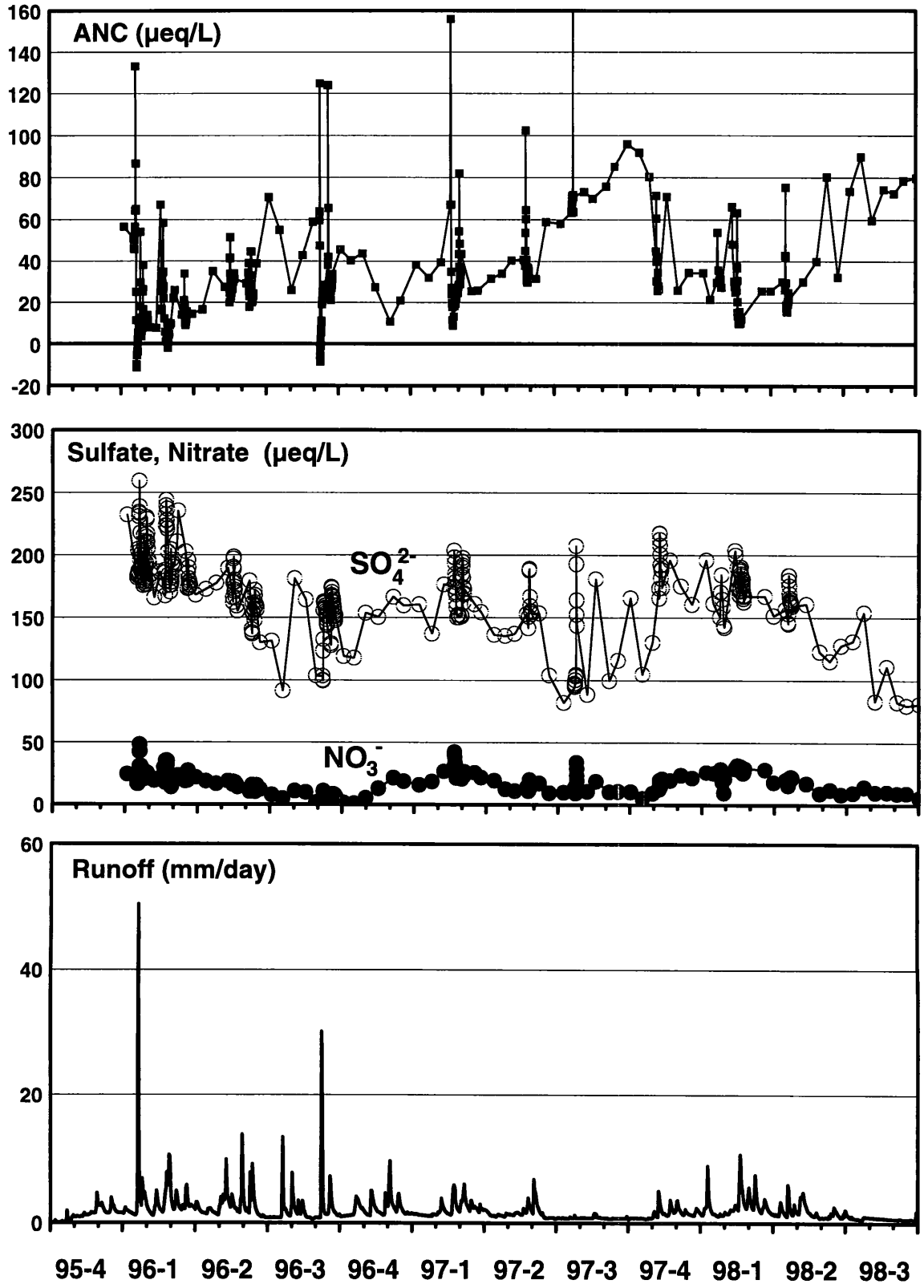

Figure 4.6. Temporal variations in a) ANC, b) NO_3^- and SO_4^{2-}, and c) runoff at the Upper Big Run (BIGR) site during the three year project (October, 1995 through September, 1998).

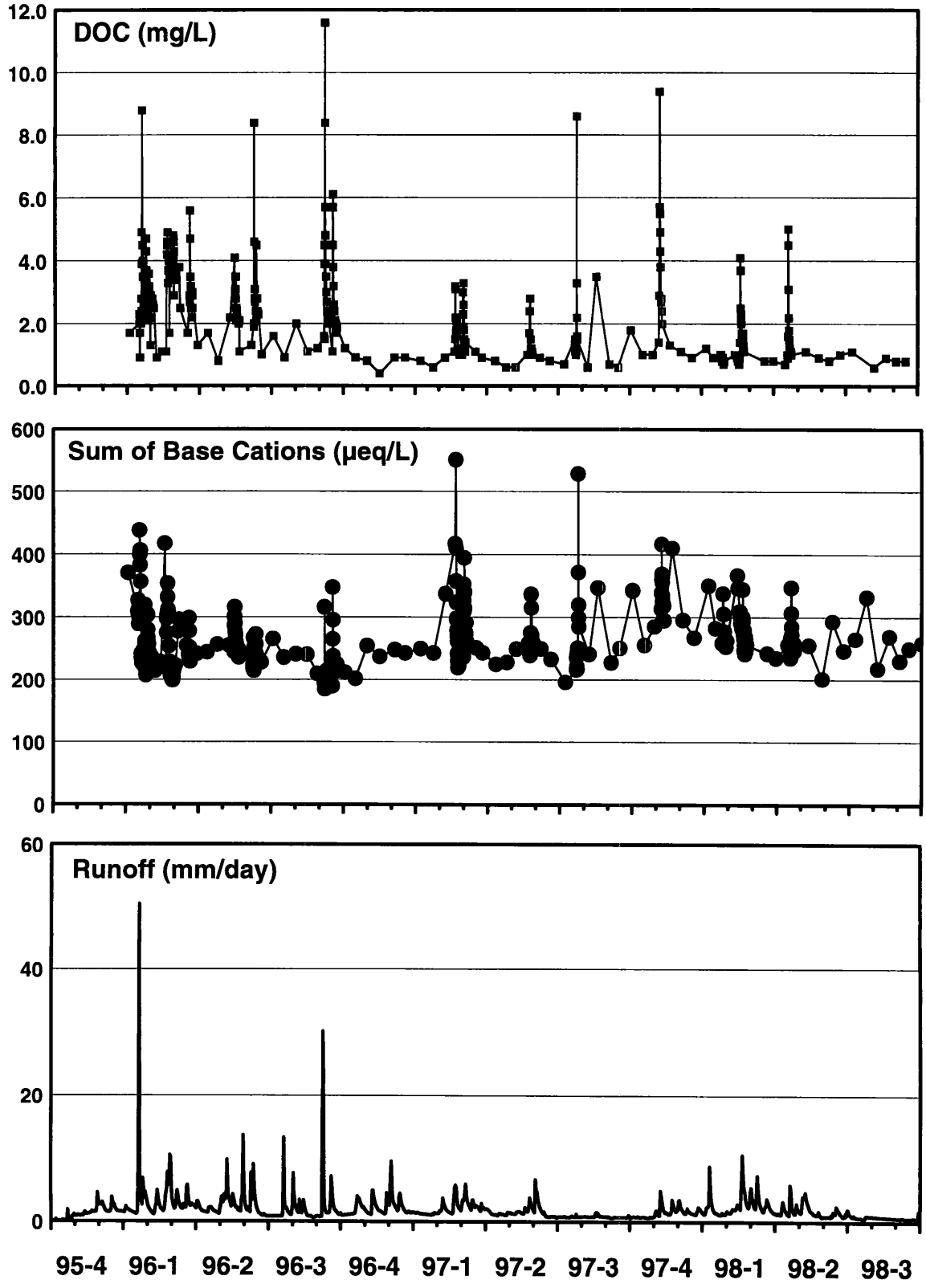

Figure 4.6 (continued). Temporal variations in d) DOC, e) sum of base cations (SBC), and f) runoff at the Upper Big Run (BIGR) site during the three year project (October, 1995 through September, 1998).

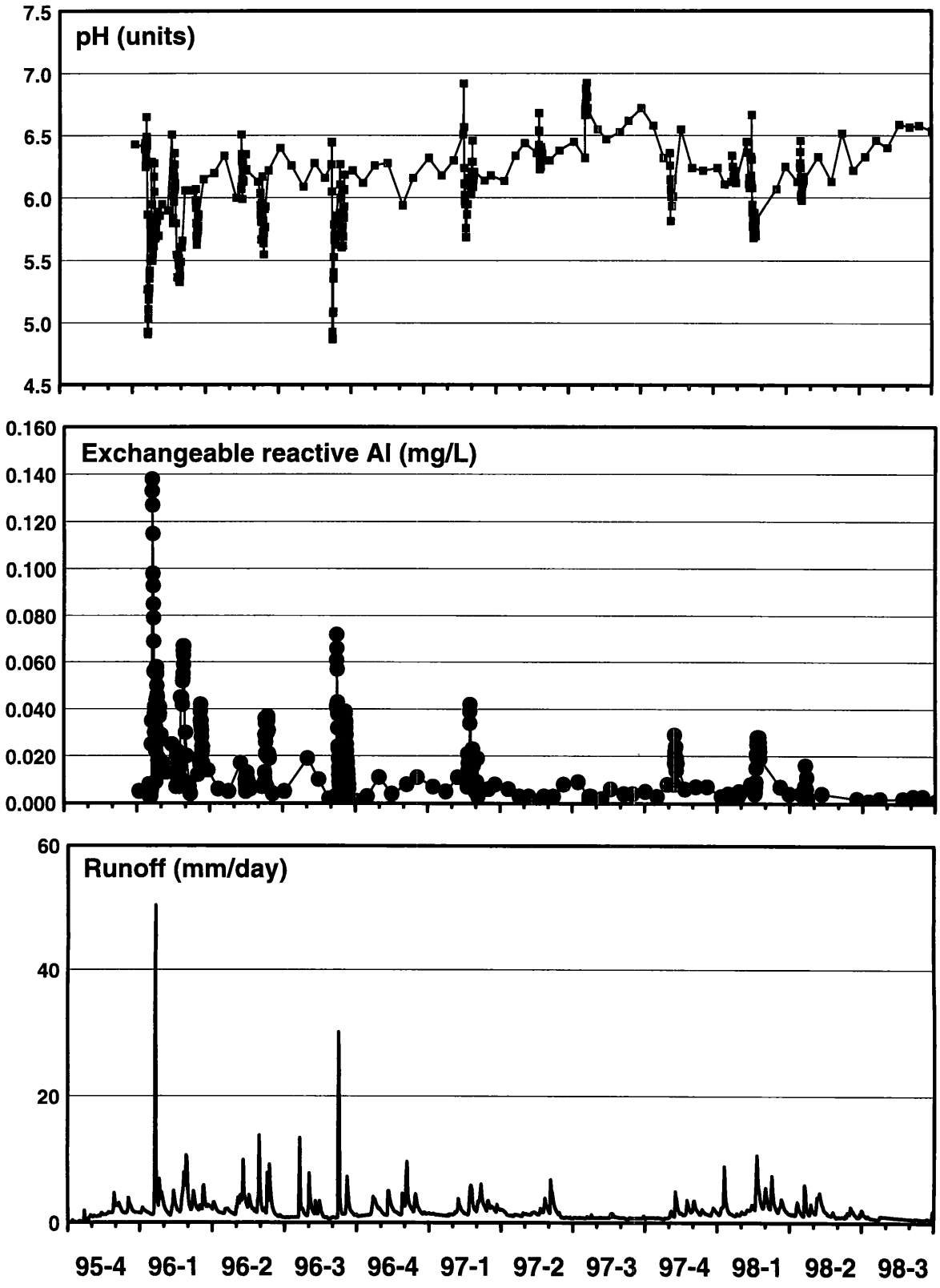

Figure 4.6 (continued). Temporal variations in g) pH, h) exchangeable reactive Al, and i) runoff at the Upper Big Run (BIGR) site during the three year project (October, 1995 through September, 1998).

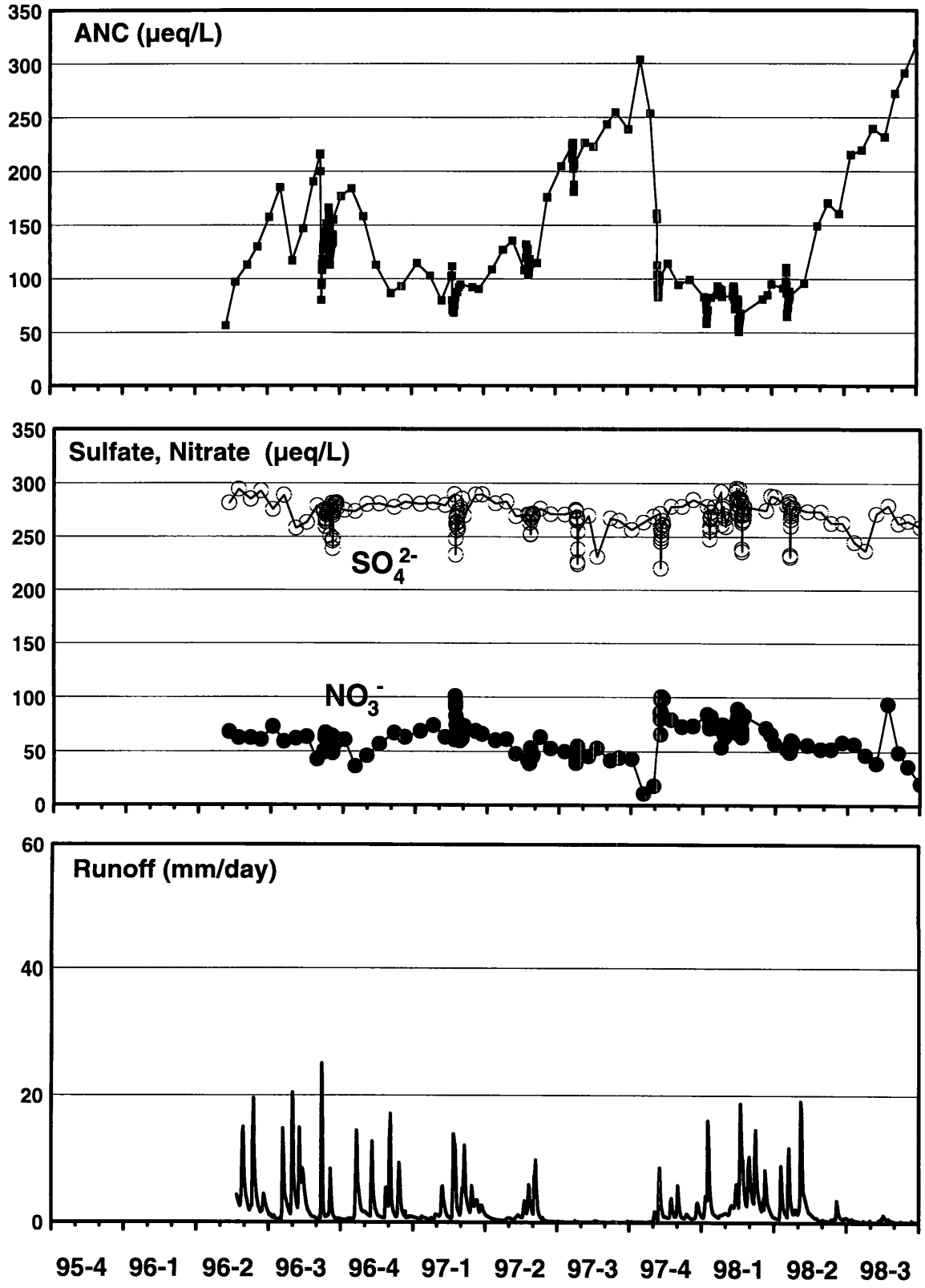

Figure 4.7. Temporal variations in a) ANC, b) NO_3^- and SO_4^{2-}, and c) runoff at the Black Lick (BLAC)site during the three year project (October, 1995 through September, 1998).

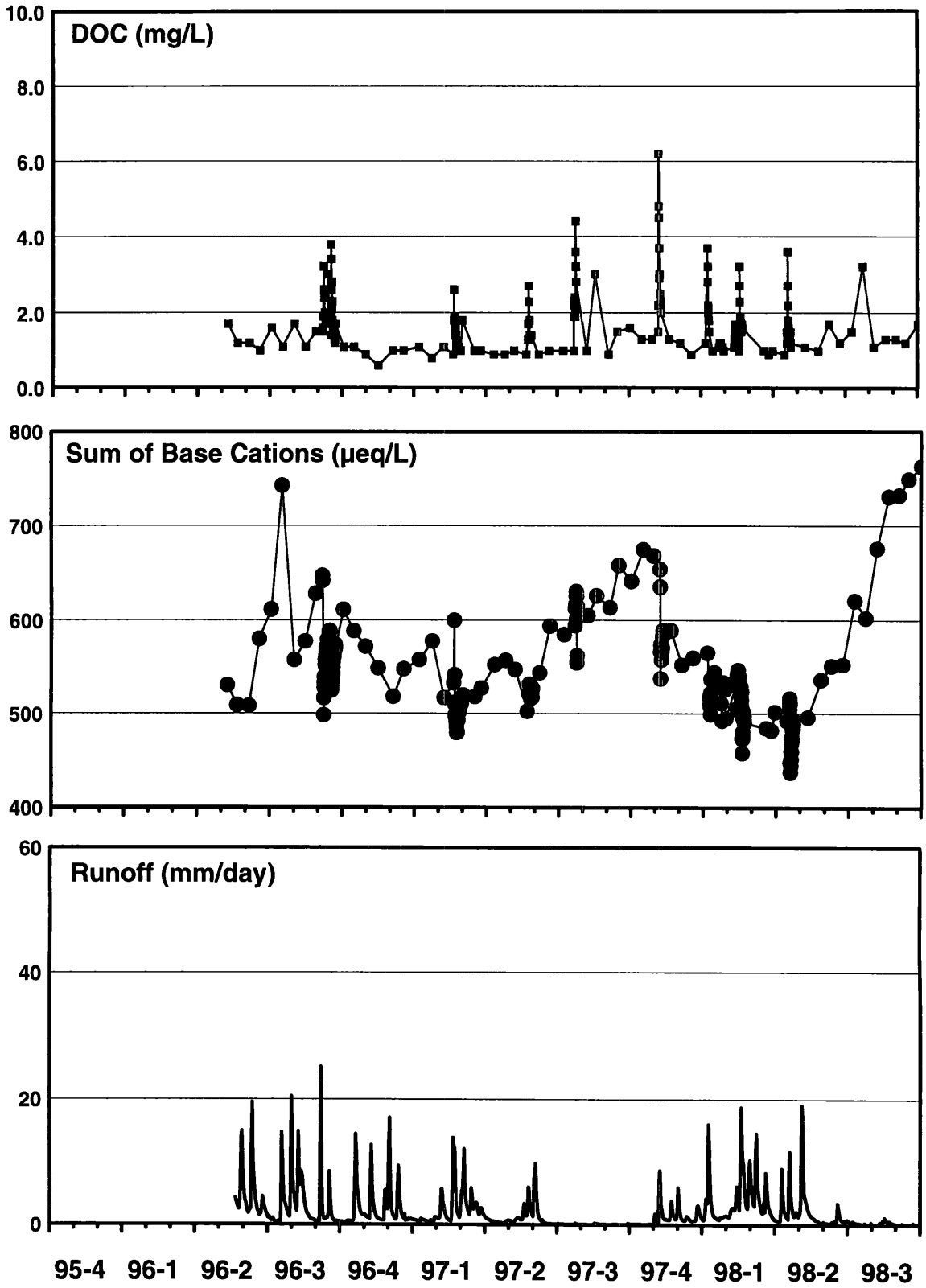

Figure 4.7 (continued). Temporal variations in d) DOC, e) sum of base cations (SBC), and f) discharge at the Black Lick (BLAC) site during the three year project (October, 1995 through September, 1998).

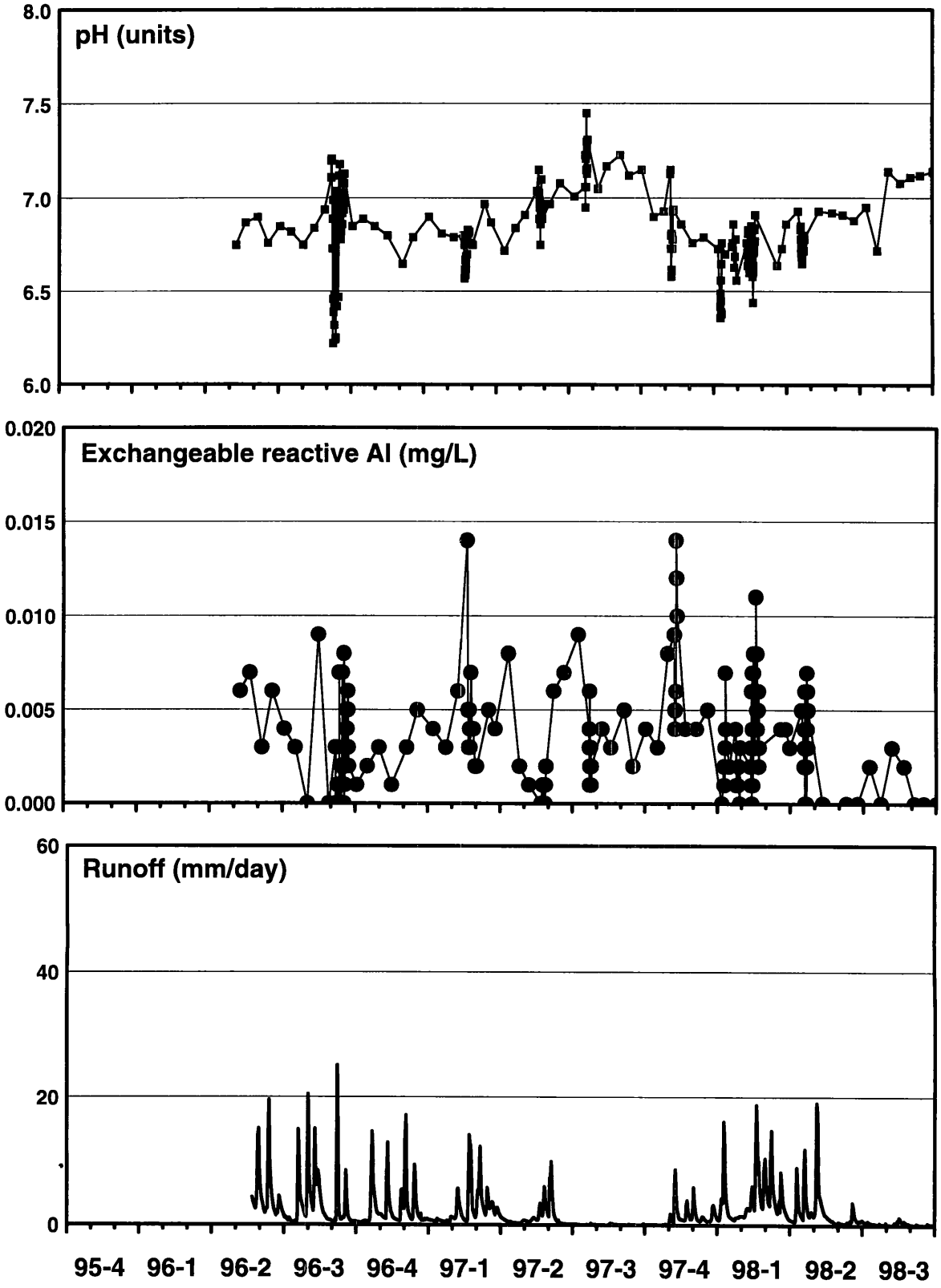

Figure 4.7 (continued). Temporal variations in g) pH, h) exchangeable reactive Al, and i) runoff at the Black Lick (BLAC) site during the three year project (October, 1995 through September, 1998).

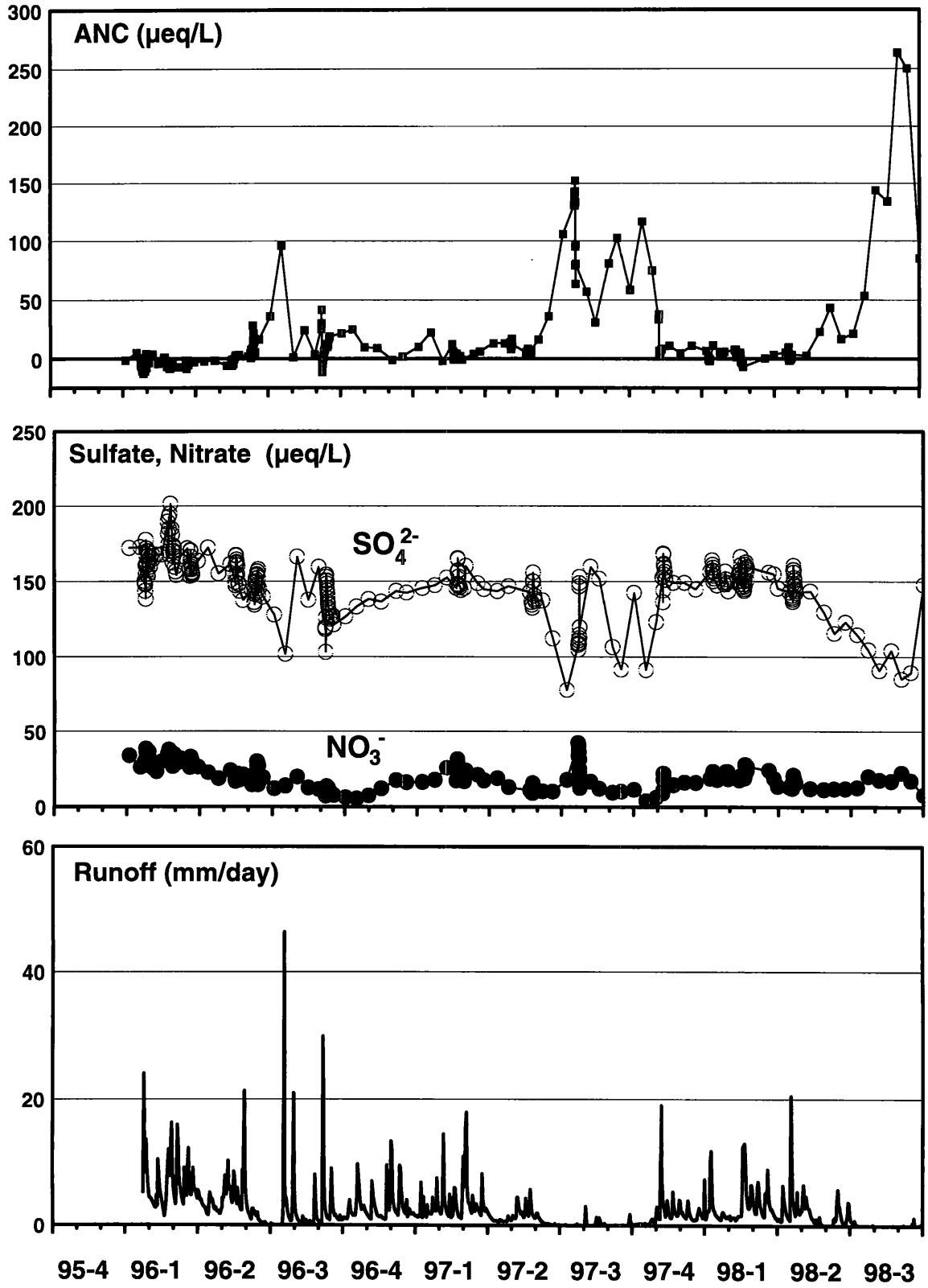

Figure 4.8. Temporal variations in a) ANC, b) NO_3^- and SO_4^{2-}, and c) runoff at the Herrington Creek tributary (HRTB) site during the three year project (October, 1995 through September, 1998).

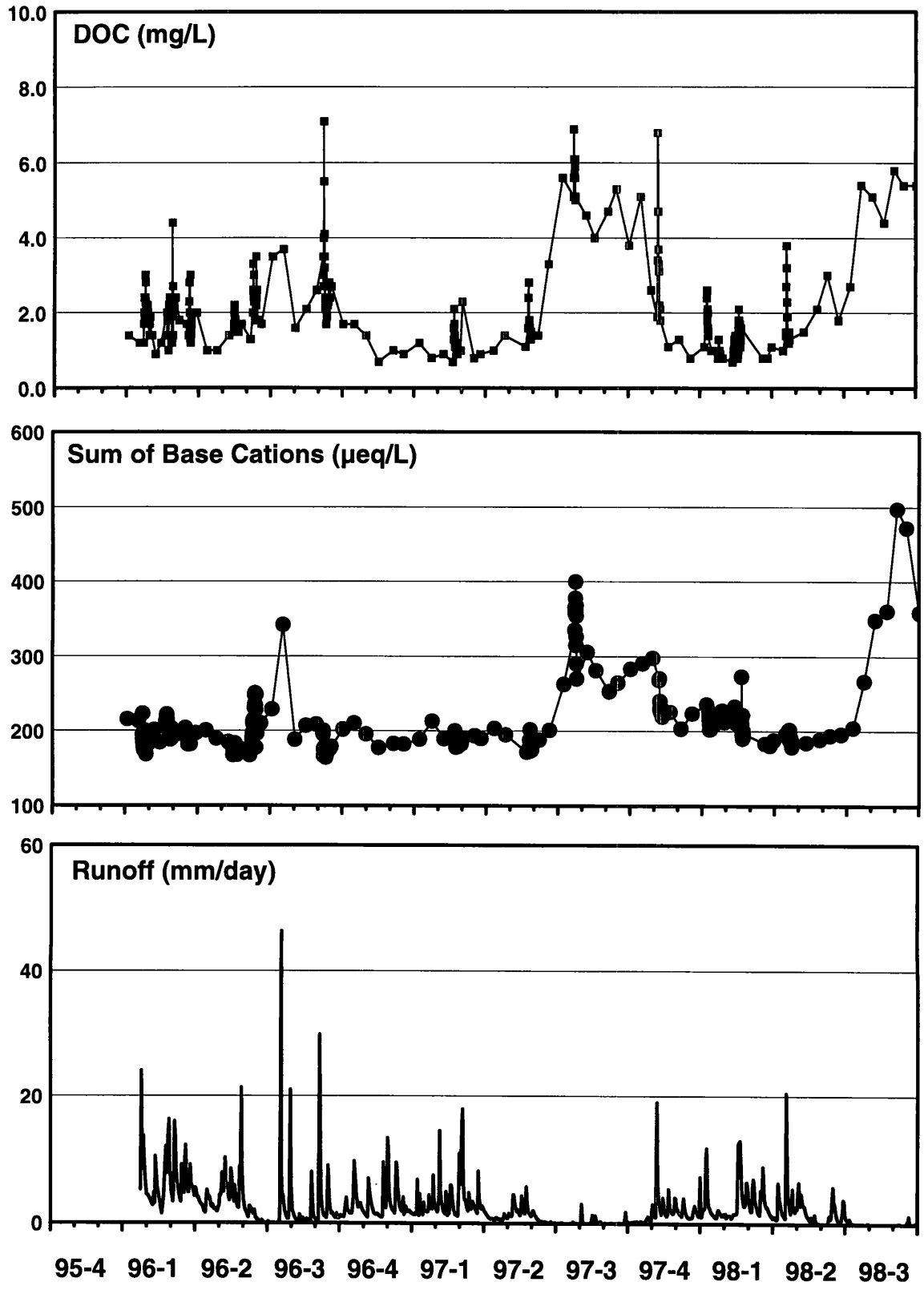

Figure 4.8 (continued). Temporal variations in d) DOC, e) sum of base cations (SBC), and f) discharge at the Herrington Creek tributary (HRTB) site during the three year project (October, 1995 through September, 1998).

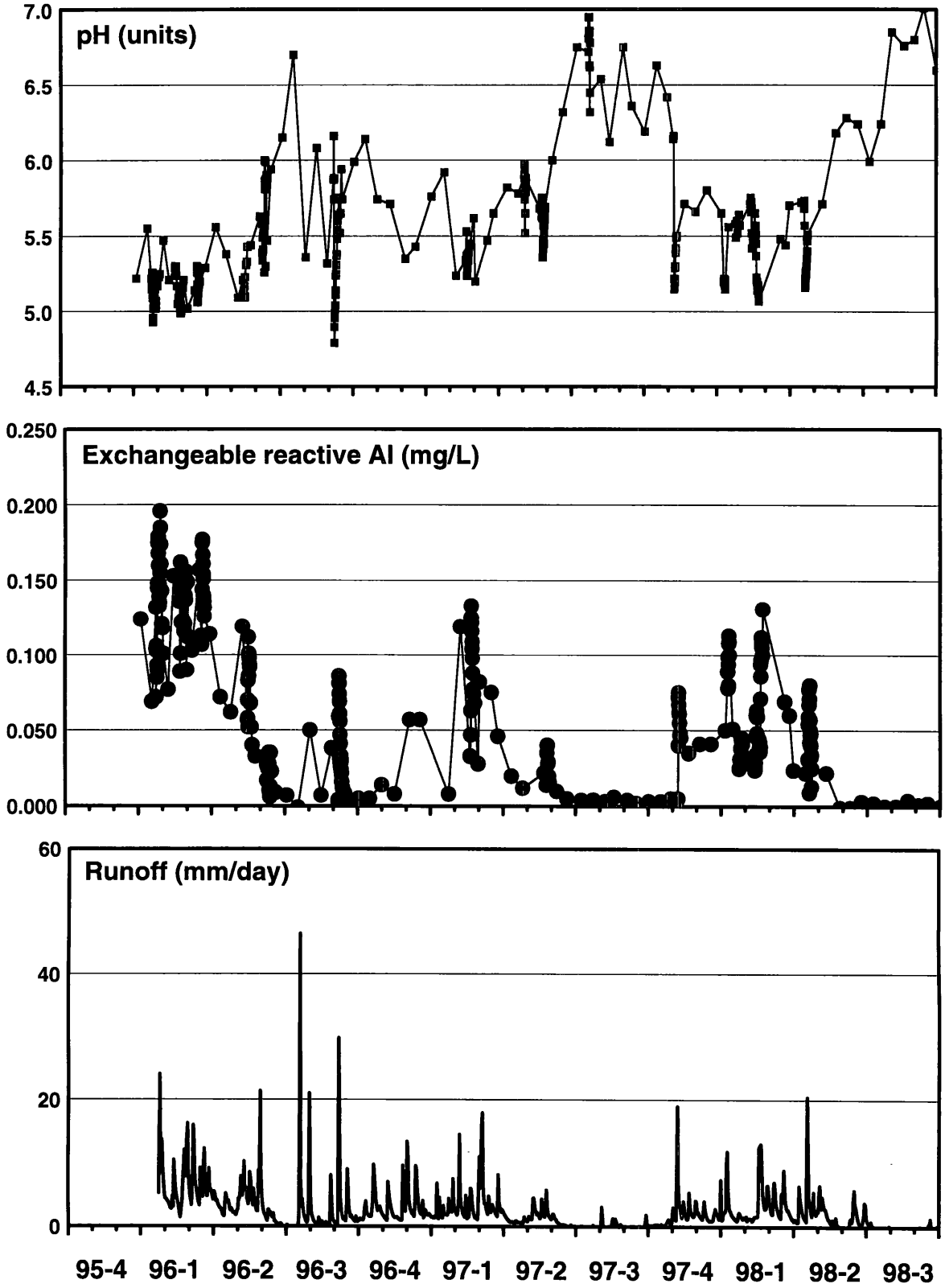

Figure 4.8 (continued). Temporal variations in g) pH, h) exchangeable reactive Al, and i) runoff at the Herrington Creek tributary (HRTB) site during the three year project (October, 1995 through September, 1998).

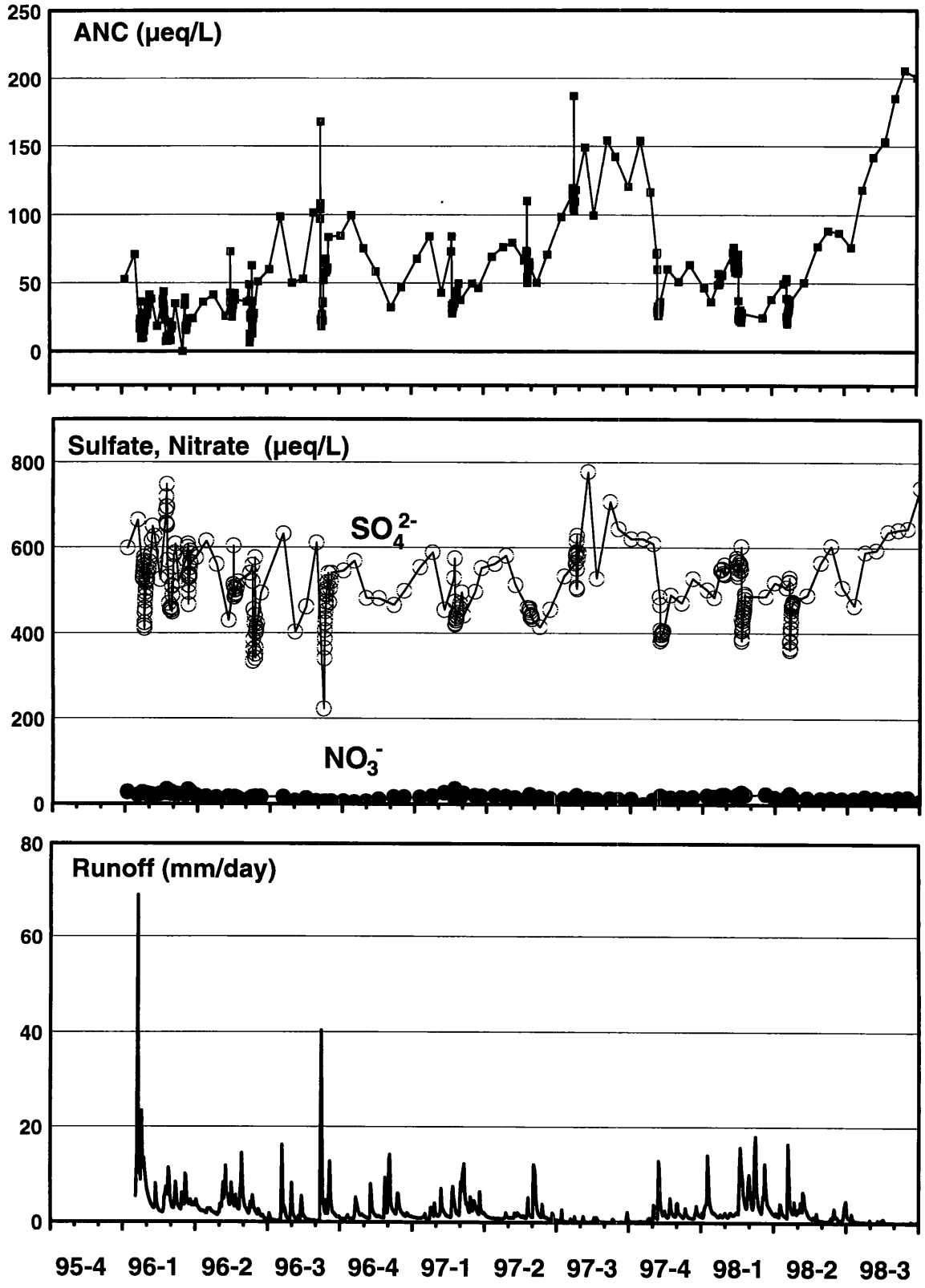

Figure 4.9. Temporal variations in a) ANC, b) NO_3^- and SO_4^{2-}, and c) runoff at the North Prong Lostland Run (NPLR) site during the three year project (October, 1995 through September, 1998).

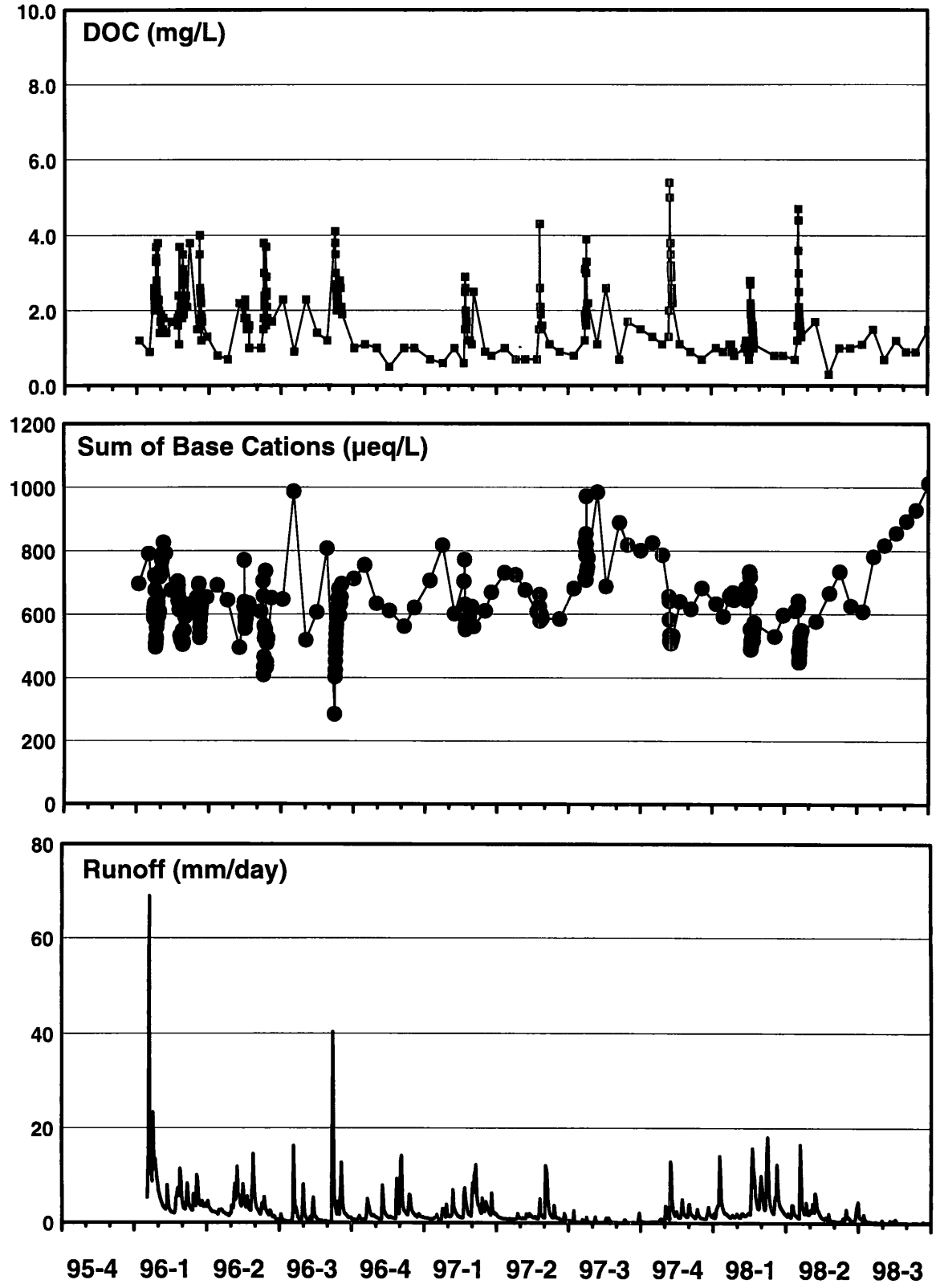

Figure 4.9 (continued). Temporal variations in d) DOC, e) sum of base cations (SBC), and f) discharge at the North Prong Lostland Run (NPLR) site during the three year project (October, 1995 through September, 1998).

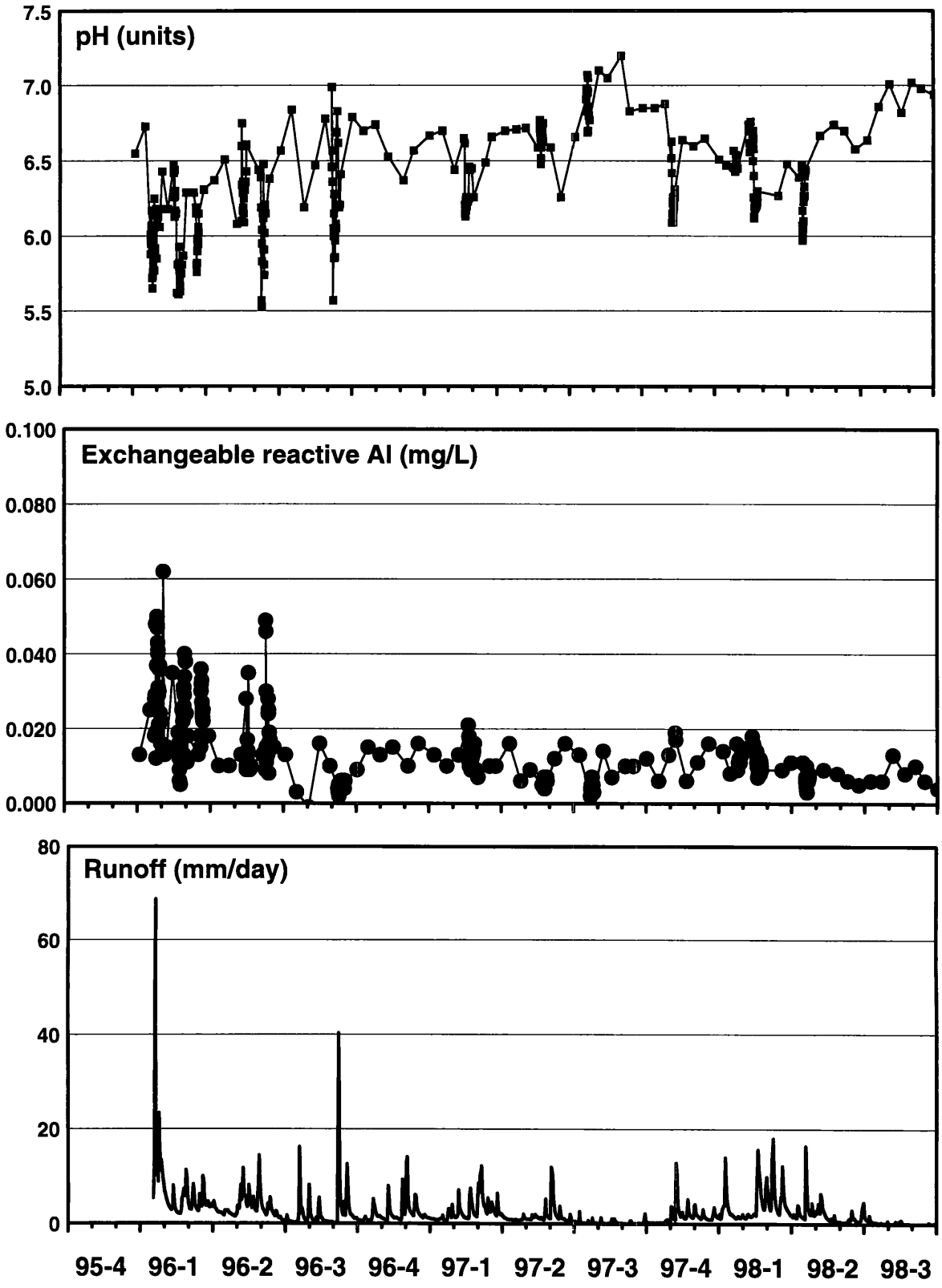

Figure 4.9 (continued). Temporal variations in g) pH, h) exchangeable reactive Al, and i) runoff at the North Prong Lostland Run (NPLR) site during the three year project (October, 1995 through September, 1998).

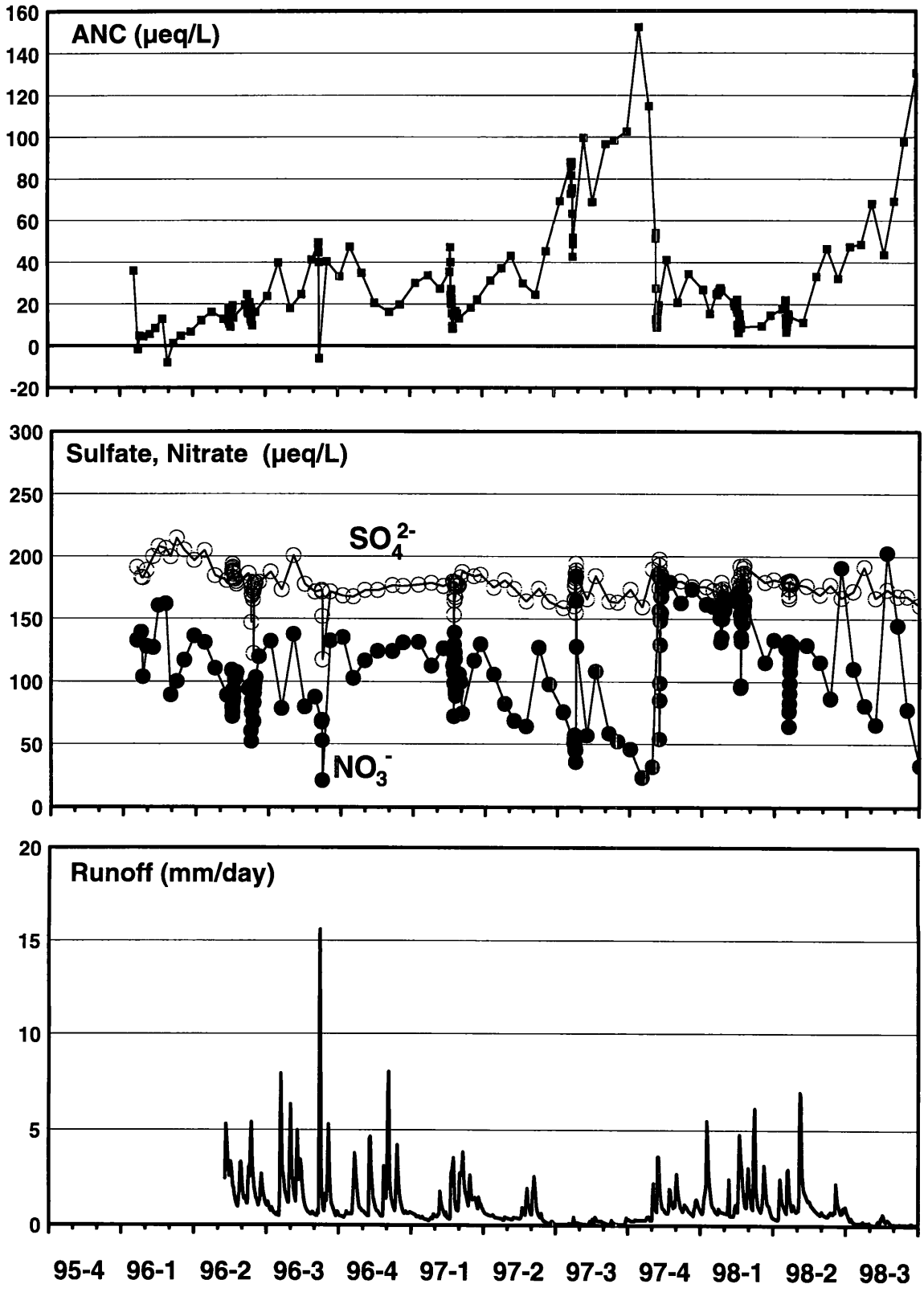

Figure 4.10. Temporal variations in a) ANC, b) NO_3^- and SO_4^{2-}, and c) runoff at the Upper Poplar Lick tributary (UPTB) site during the three year project (October, 1995 through September, 1998).

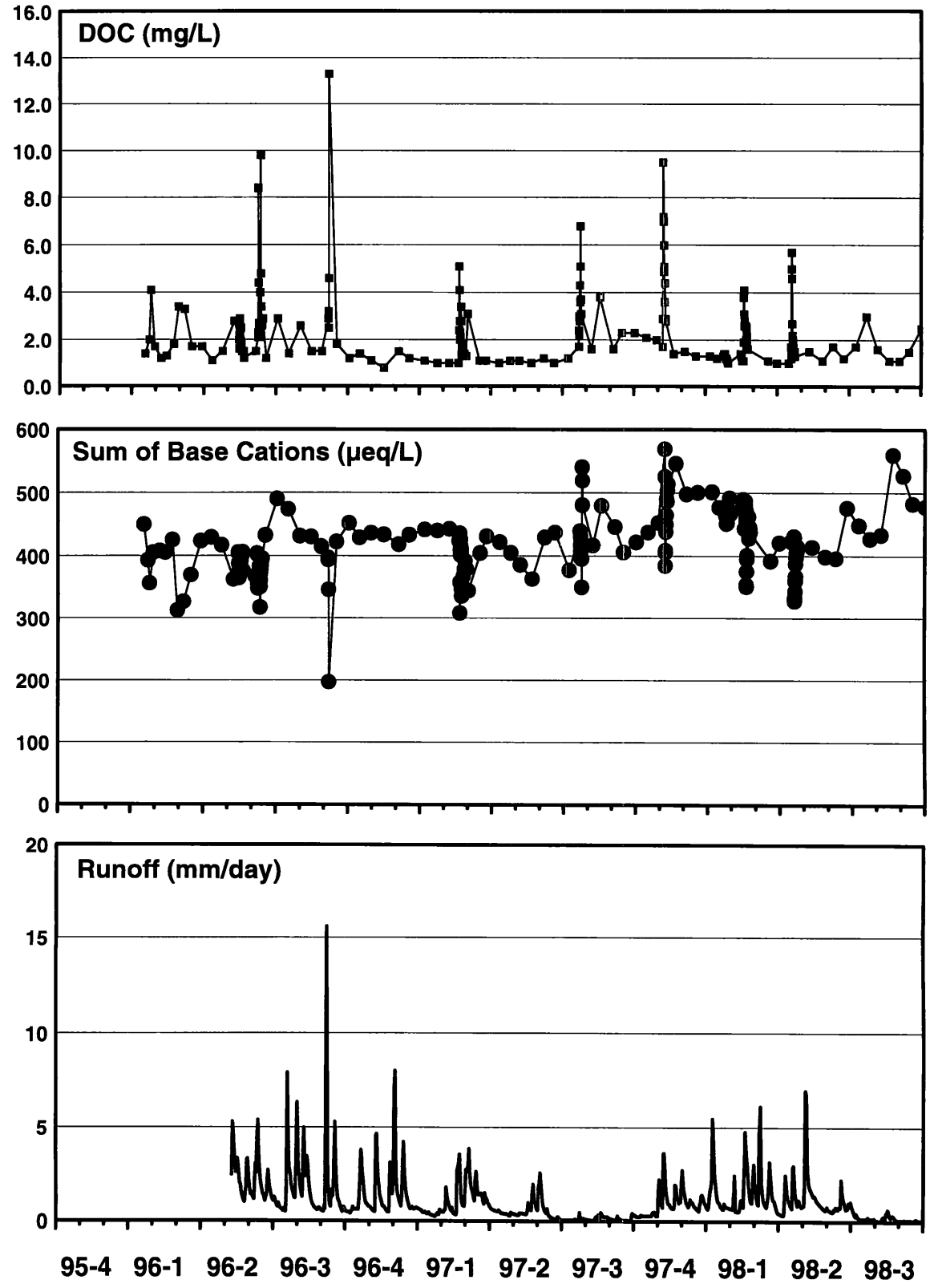

Figure 4.10 (continued). Temporal variations in d) DOC, e) sum of base cations (SBC), and f) discharge at the Upper Poplar Lick tributary (UPTB) site during the three year project (October, 1995 through September, 1998).

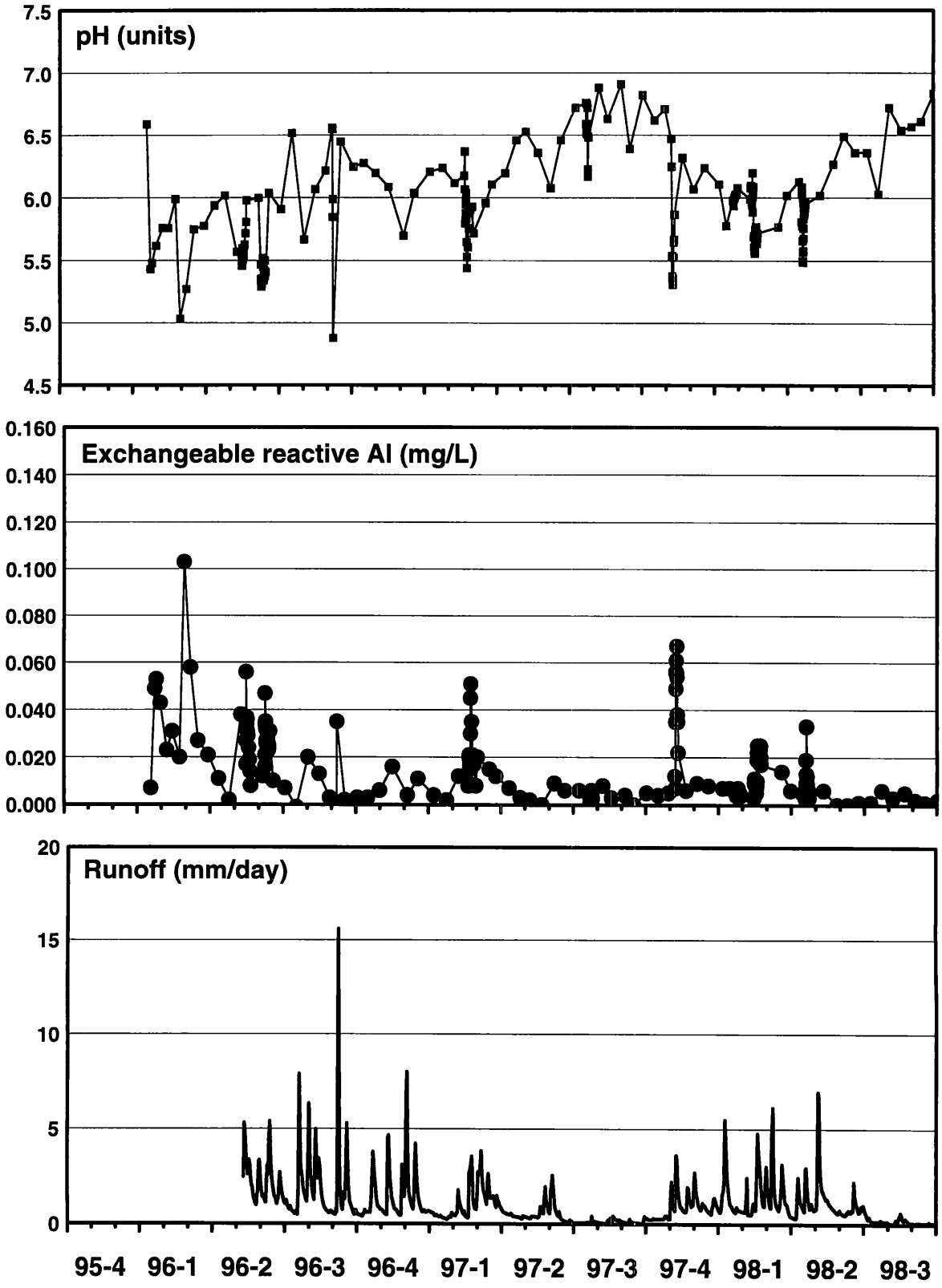

Figure 4.10 (continued). Temporal variations in g) pH, h) exchangeable reactive Al, and i) runoff at the Upper Poplar Lick tributary (UPTB) site during the three year project (October, 1995 through September, 1998).

quarters (Figures 4.6, 4.8). SBC concentrations exhibited clear seasonal variability at two of the sites (BLAC and HRTB), reaching highest levels during the third or fourth quarters when ANC was also peaking.

For many of the graphed chemical constituents, seasonal variations in concentrations are actually quite modest compared to the temporal component of variability associated with stormflow conditions (henceforth referred to as "episodes"). For example at BIGR, ANC varied from about -10 to 140 μeq/L during a 24-hour period during the January 1996 flood—which is not much smaller than the absolute range in ANC over the entire study; a similar result is shown for pH, exchangeable reactive Al, and DOC at BIGR also (Figure 4.6). While not unexpected, the results illustrate that at three of the four other study sites (but not HRTB), a domination of "episodic" or stormflow-induced variation on stream chemical composition was also observed for pH, ANC, Al, and DOC concentrations (Figures 4.7, 4.9, 4.10). A presentation of our characterization of temporal changes in chemical conditions during stormflow events is the subject of the following sections of the chapter.

Episodic and antecedent streamwater acid-base chemical composition (selected constituents only) can be discerned from the time plots of chemical composition at the five sites (Figures 4.6 – 4.10). During each of the many stormflow periods sampled at BIGR, ANC initially *rose* on the rising limb of the hydrograph and then *decreased* dramatically on the falling limb to levels much lower than those measured during antecedent baseflow conditions. The lowest ANC value measured during the study was -15 μeq/L, with negative ANC values reported for both rain-on-snow, snowmelt, and rain events. Episodic changes in BIGR streamwater composition were characterized by increases in NO_3^- and SO_4^{2-} concentrations, pH depressions (by as much as 1.7 units), and increases in Al (by as much as 130 μg/L). Most episodes are characterized by dilution of SBC concentrations, and DOC increases were the highest of any of the study streams (Figure 4.6). It should be noted that minimum ANC values, minimum pH values, and maximum Al concentrations associated with episodes monitored during the study exceeded the extreme values reported by Morgan *et al.* (1994) for a previous study of BIGR, although the general temporal variations were quite similar.

Episodic changes in ANC were found to be largest at BLAC—the least acid-sensitive of the five study streams. For example, during the September 1996 event, ANC declined by nearly 125 μeq/L, largely in response to dilution of SBC. While NO_3^- concentrations often increased during episodes at BLAC, SO_4^{2-} concentrations almost always decreased. Changes in pH and Al concentrations during episodes were usually quite modest, although the September 1996 event caused a pH decline of nearly a full pH unit (Figure 4.7).

Episodic streamwater changes at HRTB are very similar to the patterns observed at BIGR, except that HRTB must be considered a chronically acidic (ANC < 0) stream. Minimum ANC values during stormflow periods were commonly 5-10 μeq/L lower, Al concentrations are usually about a factor of two higher, and NO_3^- and SO_4^{2-} concentrations are of comparable magnitude. Changes in NO_3^- and SO_4^{2-} concentrations during episodes were nearly always positive at HRTB, while SBC dilution was again the rule. Episodic changes in DOC were more

modest, however (Figure 4.8).

Episodic changes in streamwater composition at NPLR were unique among the five study sites. While ANC and pH were both significantly depressed and both Al and DOC concentrations increased during episodes as at the other sites, changes in SO_4^{2-} and SBC concentrations at NPLR were almost always negative; it was not uncommon to observe these chemical constituents to be diluted by several hundred μeq/L. Changes in NO_3^- concentrations were insignificant relative to these other constituents (Figure 4.9).

Finally, episodic dynamics observed at UPTB were found to be similar to changes observed at nearby BIGR for most chemical constituents with the exception of NO_3^-. Nitrate concentrations at UPTB were the highest of any of the five sites and often were diluted during episodes. In particular, pH and ANC depressions and increases in Al concentrations were very similar to changes observed at BIGR (Figure 4.10).

As discussed previously, stormflow conditions ("episodes") were sampled at all five sampling stations throughout the three-year study. The timing of the collection of samples taken during episodes is presented in both tabular and graphical form (Table 4.2; Figures 4.11 – 4.13). Not including events for which samples were only analyzed for ANC and trace metals, Table 4.2 shows that 18 episodes were sampled at BIGR, 12 at BLAC, 17 at HRTB, 16 at NPLR, and 12 at UPTB (total of 75 site-episode combinations) during the three-year study. It should be pointed out that many of the episodes are comprised of multiple stormflow peaks, while in a few cases sampled episodes are based on only one sample obtained near the time of peak flow. In particular, four of the five sites were sampled during the January 1996 event (two with only single samples due to flooding of the instrument shelters, however), while four were sampled during the September 1996 event also (unfortunately the sampler at UPTB failed during this period and some peak runoff samples for BLAC were lost when they accidentally spilled in the field technician's pack). Since a total of 1139 sequential samples were analyzed, on average each site-episode characterized was based on a pre-event sample and more than 15 samples taken over the course of the event.

Some of the most extreme chemical responses at the study sites were observed during two extreme hydrological events that occurred during the 1996 water year: (1) the period from January 18-24, 1996 corresponding to the first "Flood of '96", and (2) the period from September 6-8, 1996 affected by the remnants of Hurricane Fran. On January 7, 1996, a major blizzard struck the entire east coast of the United States, dumping 2-3 feet of snow in the mountains of western Maryland. During the period January 7-16, the snowpack in the region had gradually ripened until on January 17, a warm rainfall began to fall on the area. By mid-day on January 18, 2-4 in of rain had fallen in the area, causing widespread snowmelt and subsequent flooding of small streams and larger rivers; flood crests on major rivers in the Potomac and Susquehanna River basins exceeded those that occurred during Hurricane Agnes and in many cases set all-time records (USGS, personal communication). These flooding conditions severely tested our

Table 4.2. Episodes sampled at five sites during the period 1995 - 1998.

Sampling Period	Hydrograph Peak(s)	Upper Big Run (BIGR)	Black Lick (BLAC)	Herrington Creek Tributary (HRTB)	North Prong Lostland Run (NPLR)	Upper Poplar Lick Tributary (UPTB)
16Jan-22Jan96	21-Jan	X		X [1]	X [1]	X [1]
22Jan-6Feb96	24,27 Jan	X		X	X	
19Feb-2Mar96 (*)	24,27,28 Feb	X		X	X	X [1]
17Mar-22Mar96	19-Mar	X		X	X	
15May-21May96	16,17 May	X		X	X	X
7Jun-14Jun96	8,9,10,11,12 Jun	X		X	X	X
5Sep-16Sep96	6-Sep	X	X	X	X	X
16Sep-22Sep96	16-Sep	X	X			
19Feb-26Feb97 (*)	20-Feb	X	X	X	X	X
27Feb-4Mar97 (*)	1,2,3 Mar	X	X	X	X	X
3May-6May97	4-May			X [3]		
24May-30May97	25-May	X	X	X	X	
22Jul-26Jul97	24-Jul	X	X	X	X	X
6Nov-10Nov97	7-Nov	X	X [2]	X [2]	X	X
8Jan-10Jan98	8,9 Jan		X [2]	X [2]		
22Jan-28Jan98	24-Jan	X	X	X	X	X
11Feb-16Feb98 (*)	12-Feb	X	X [2]	X [2]	X	
16Feb-21Feb98 (*)	18-Feb	X	X [2]	X [2]	X	X
18Apr-23Apr98	20-Apr	X	X	X	X	X

X[1] = One sample taken near peak flow only.

X[2] = Samples taken for mercury and trace metal analyses, in addition to the "regular" suite of analyses.

X[3] = Samples taken for mercury, trace metals and ANC analyses only.

* Snow melt combined with rain or rain-on-snow occurred during this period.

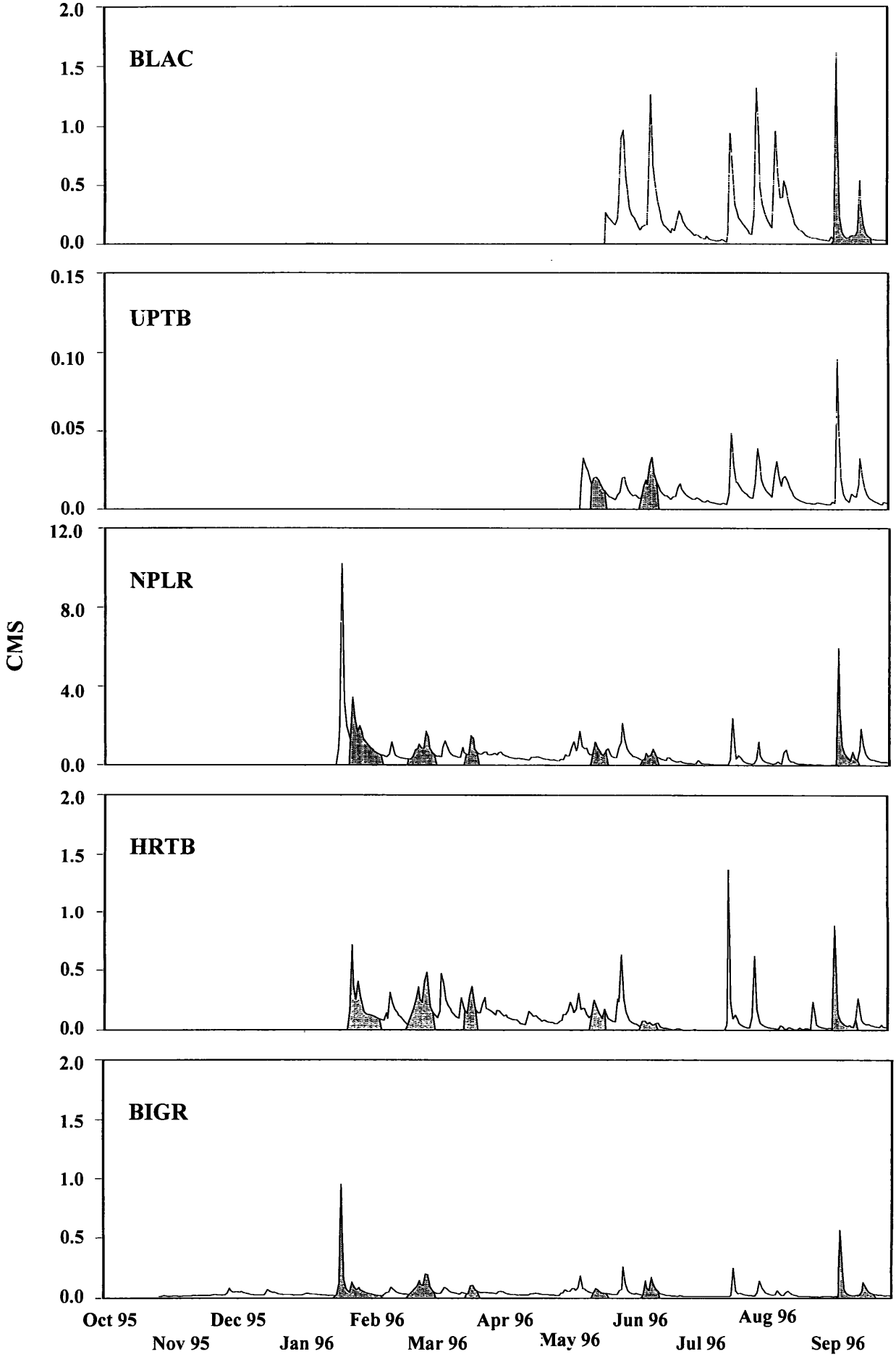

Figure 4.11. Annual discharge hydrographs (1996 water year) for the five study sites indicating periods of high frequency streamwater sampling during episodes (gray shaded areas).

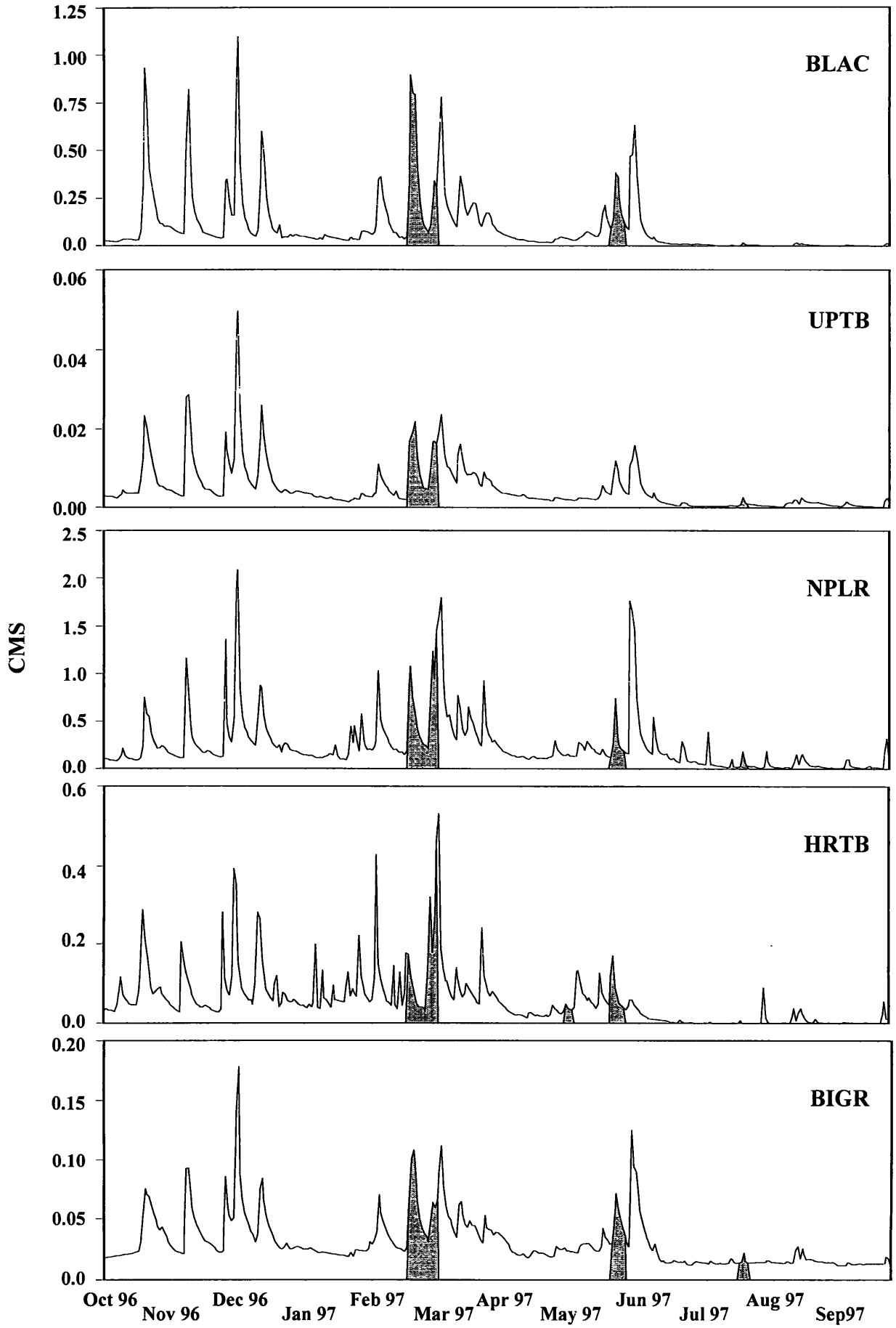

Figure 4.12. Annual discharge hydrographs (1997 water year) for the five study sites indicating periods of high frequency streamwater sampling during episodes (gray shaded areas).

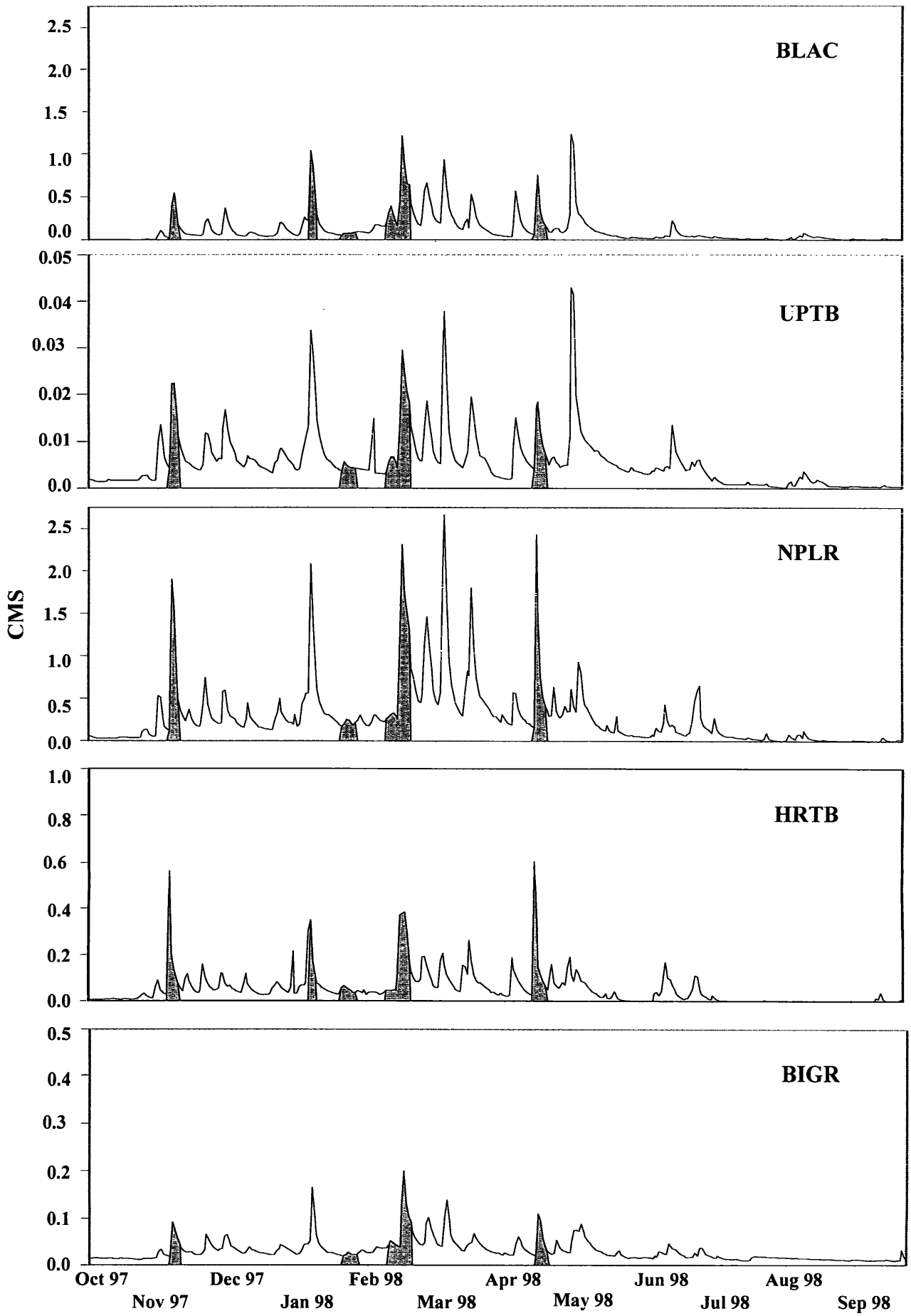

Figure 4.13. Annual discharge hydrographs (1998 water year) for the five study sites indicating periods of high frequency streamwater sampling during episodes (gray shaded areas).

recently-installed equipment and, unfortunately, resulted in samples being contaminated at two of the sampling sites. However, samples obtained during this period at the BIGR site could be analyzed. At this site, a peak discharge of 3.06 cms was measured at noon on January 18, which was accompanied by dramatic changes in ANC, pH, Al, and major ion concentrations (Figure 4.14). Interestingly, the most dramatic changes in acid-base conditions actually lagged the flood peak by 12-36 hours, suggesting that the flushing of the soil water reservoir may be the dominant physical mechanism by which the chemical composition of the stream is most perturbed. During this extreme event, ANC was depressed to negative values for a duration of nearly two days, pH remained below 5.5 for three days, and the exchangeable reactive Al concentration exceeded 100 μg/L for an entire 24-hour period (Figure 4.14).

To our complete surprise, the first "Flood of '96" was followed by the second "Flood of '96" on September 6th as the remnants of Hurricane Fran made their way up the east coast, dumping 5-10 in of rain on the area in a period of about 12 hours. Fortunately for us (but unfortunately for many others living in low-lying areas of western Maryland!), our sequential sampling equipment functioned perfectly at four of the five sites (failing only at POPL), although some key samples from BLAC were also accidentally spilled in transit from the field. Fortunately, some samples were also collected at POPL during the first part of the flood which can be used to interpret the changes in water chemistry. The results from this extreme stormflow event represent our best regional characterization of the effects of extreme episodic events on the acid-base chemistry of streams draining the Appalachian Plateau (Figures 4.15 – 4.19). At BIGR, ANC and pH were depressed to levels observed earlier in January 1996, although the peak Al concentration was only about half as large as the January peak value. ANC was observed to decline at all other study sites and was depressed to negative values in three of the five streams (BIGR, HRTB, and POPL), with each stream showing commensurate depressions in pH and increases in Al concentrations (Figures 4.15, 4.17, 4.19).

C. Analysis of Episodic Chemical Data

The relative contribution of each ion to the loss in ANC was determined using a modified version of the analysis done by Molot *et al.* (1989), a technique that allows a quantitative assessment of the relative contribution of each ion by normalizing the change in each ion by the overall ΔANC during that event. For our western Maryland streams, ANC can be defined in equivalent units (e.g., μeq/L) as:

$$ANC = [SBC] - [SO_4^{2-}] - [NO_3^-] - [Cl^-] - [OA^-] \quad (4.1)$$

where [OA-] is the concentration of dissolved strong organic acids estimated using the model of Oliver *et al.* (1983). Therefore, for each episode sampled, the change (Δ) in acid-base chemical composition could be evaluated using the measurements of streamwater concentrations immediately before the event (ANC_{pre} or *pre-event* value) and at the time of the transient condition of *minimum* ANC (ANC_{min}). These two samples for each event were thus selected in order to quantify the relative importance of both natural and anthropogenic sources of strong

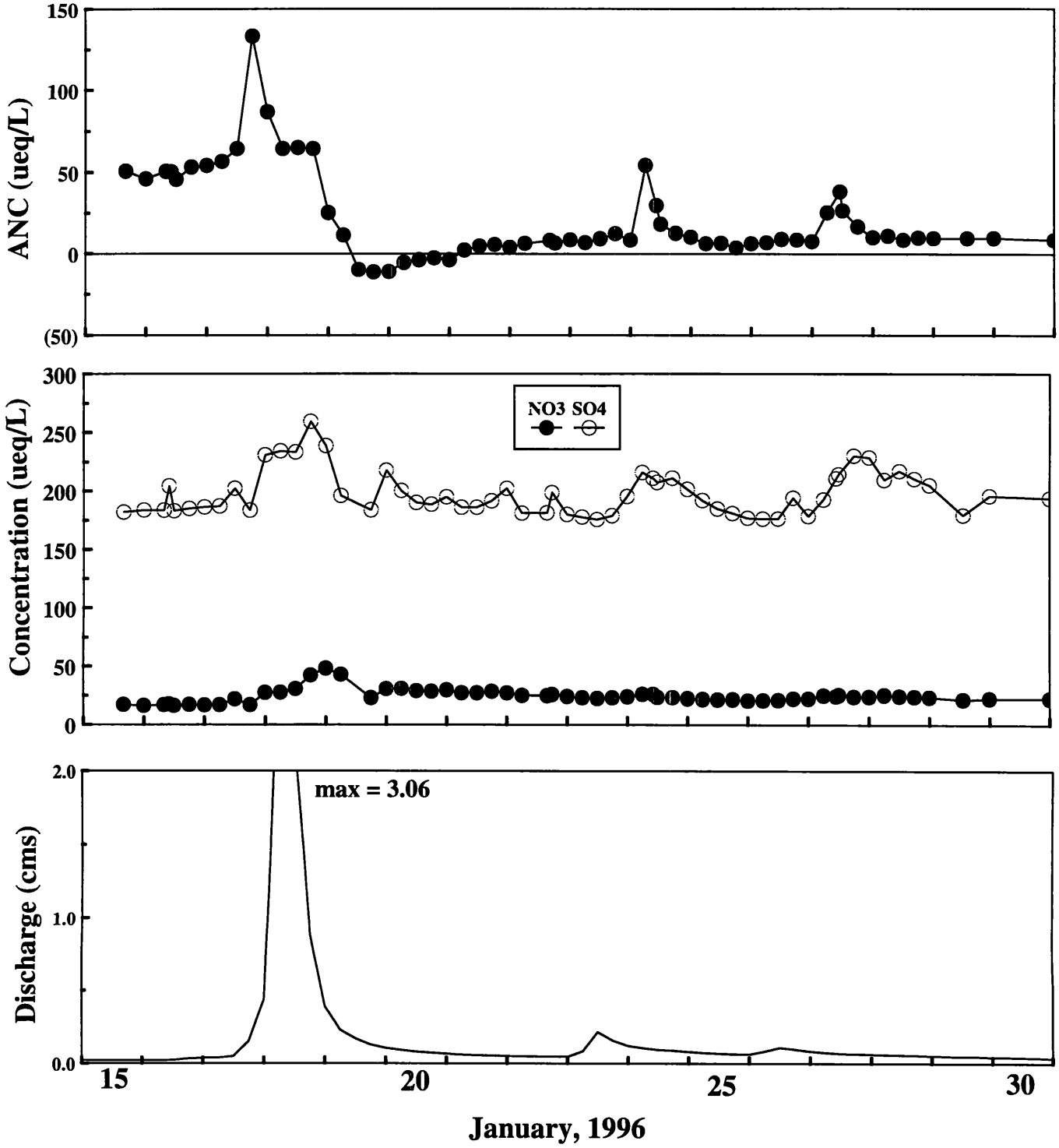

Figure 4.14. Temporal variations in a) ANC, b) NO_3^- and SO_4^{2-}, and c) discharge at the Upper Big Run (BIGR) site during the period January 15-30, 1996.

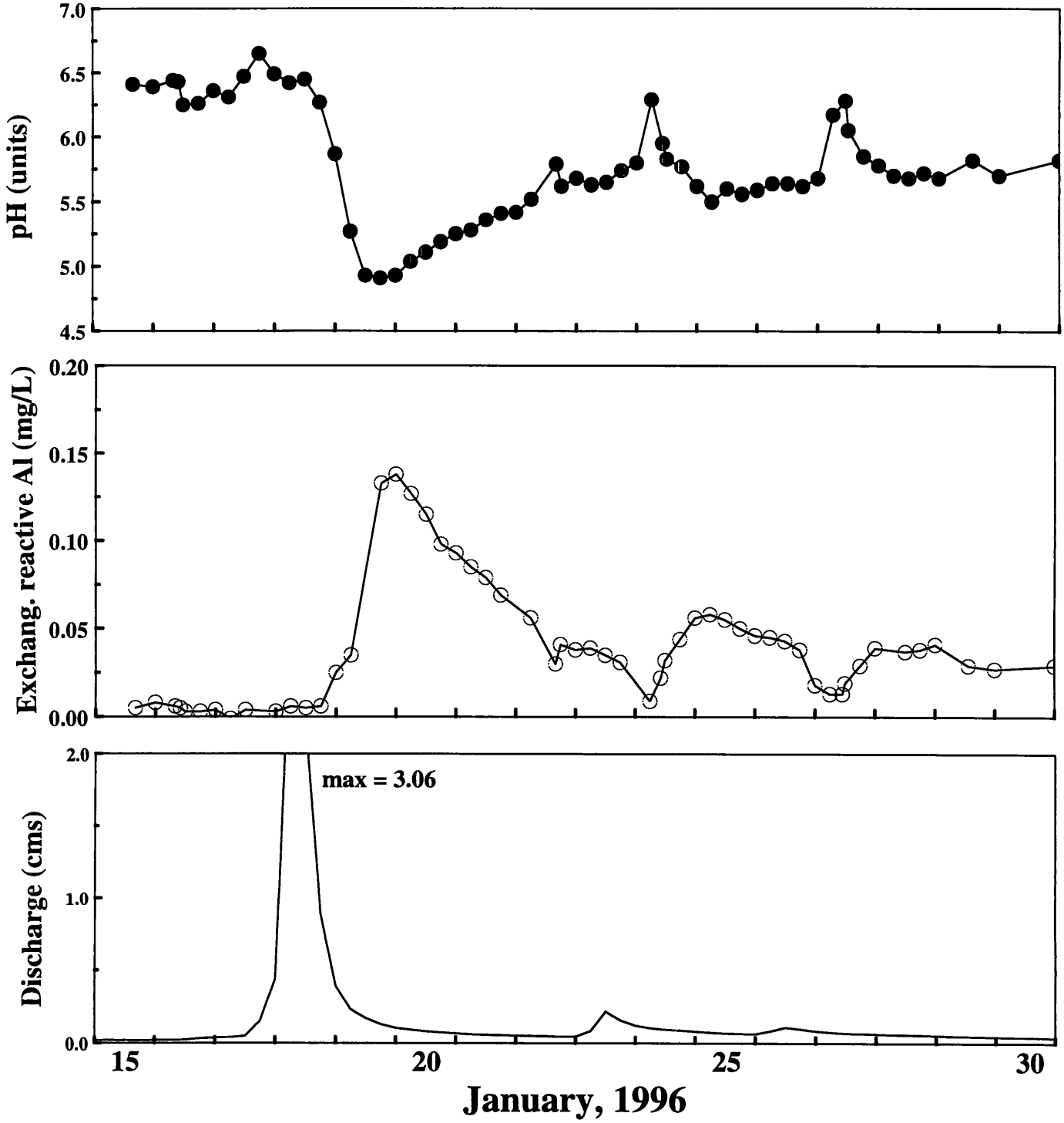

Figure 4.14 (continued). Temporal variations in d) pH, e) exchangeable reactive Al, and f) discharge at the Upper Big Run (BIGR) site during the period January 15-30, 1996.

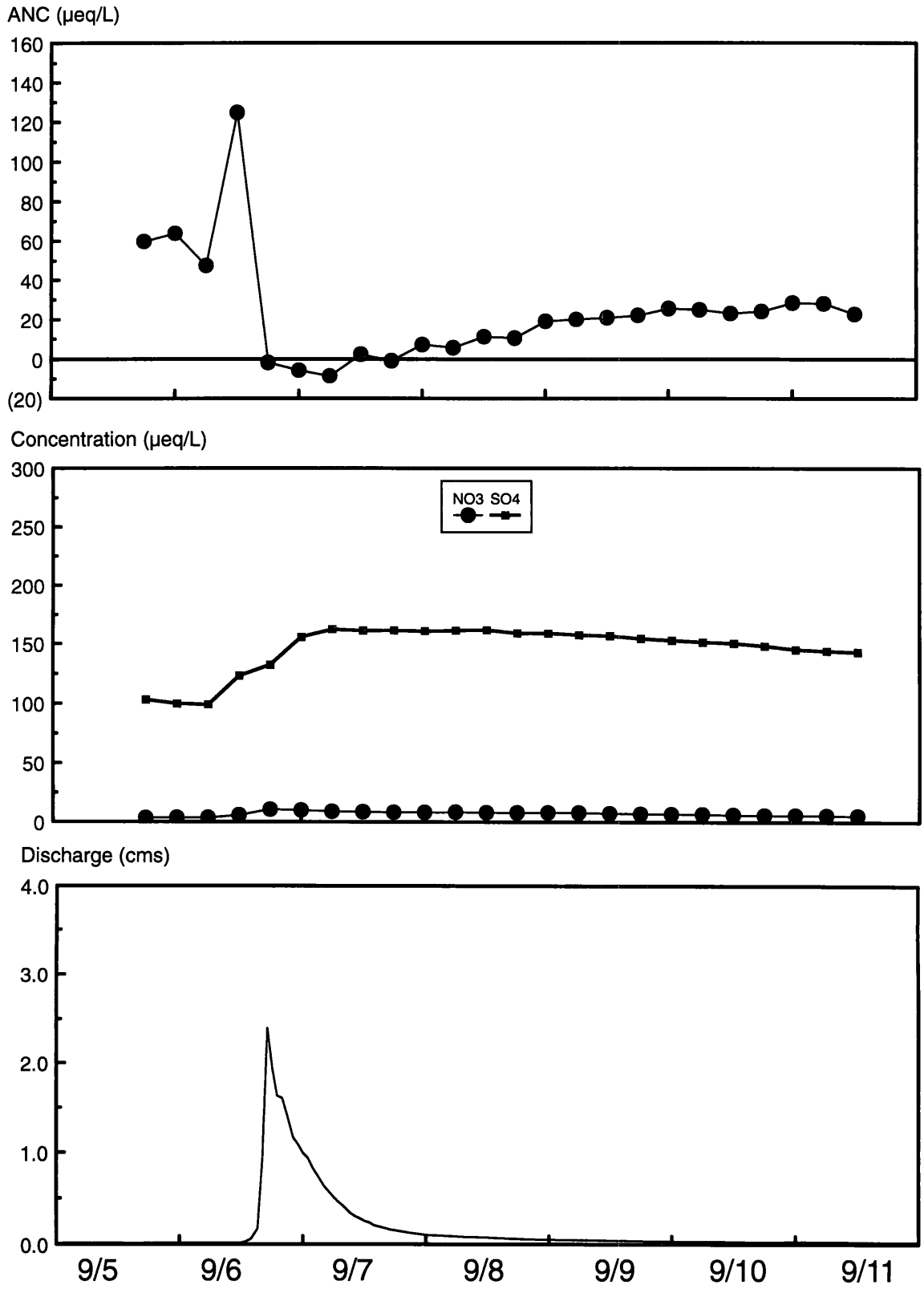

Figure 4.15. Temporal variations in a) ANC, b) NO_3^- and SO_4^{2-}, and c) discharge at the Upper Big Run (BIGR) site during the period September 5-11, 1996.

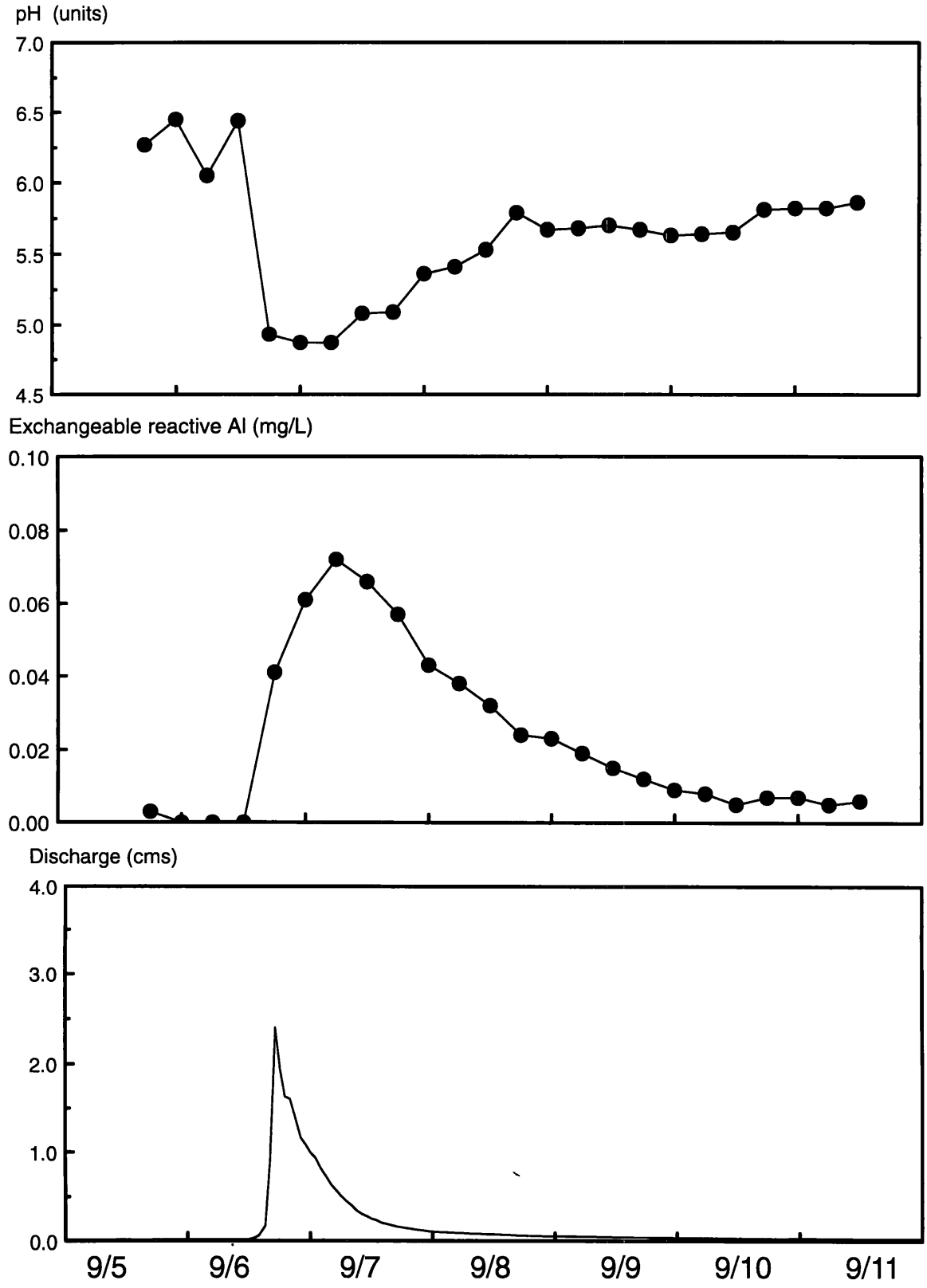

Figure 4.15 (continued). Temporal variations in d) pH, e) exchangeable reactive Al, and f) discharge at the Upper Big Run (BIGR) site during the period September 5-11, 1996.

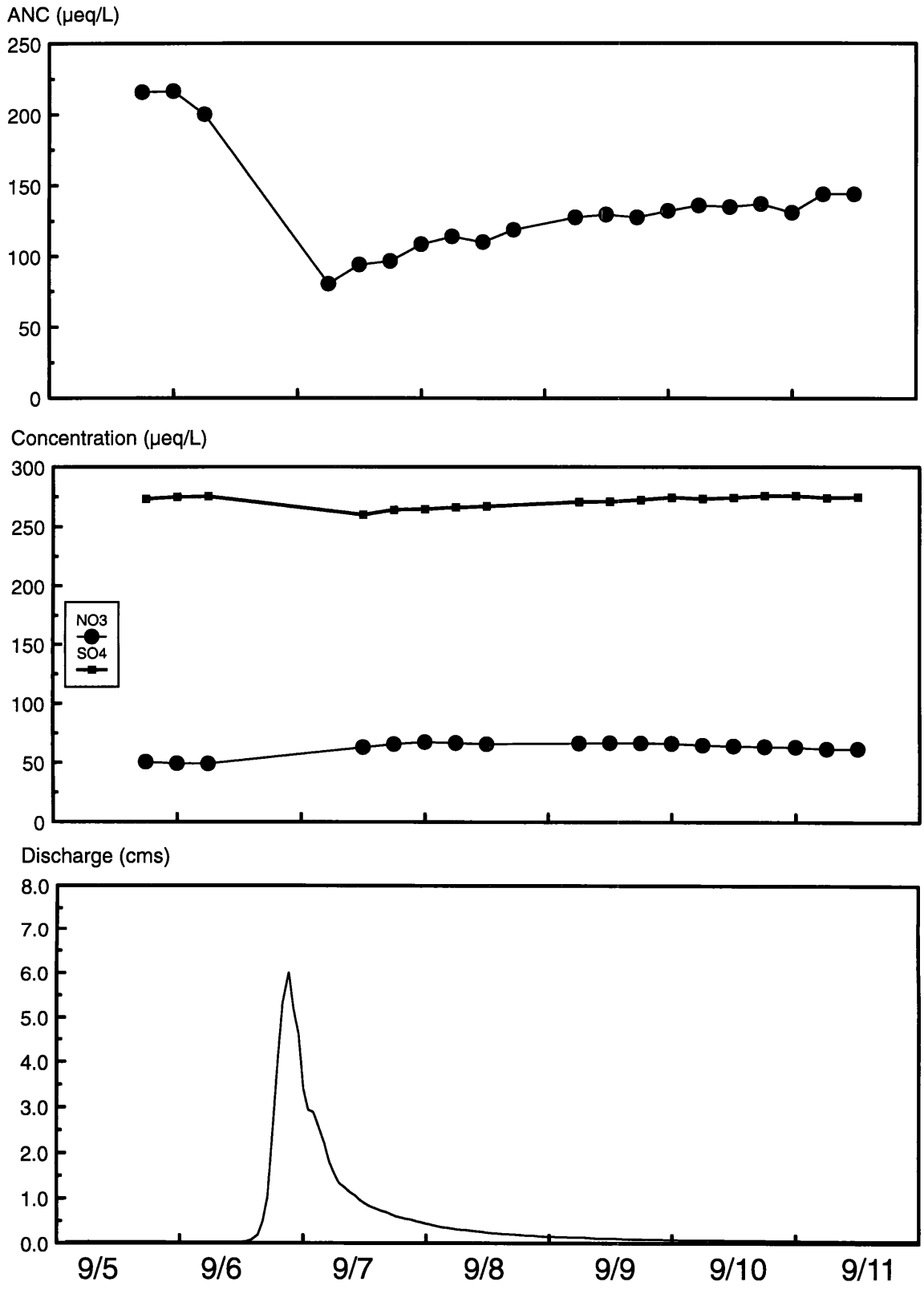

Figure 4.16. Temporal variations in a) ANC, b) NO_3^- and SO_4^{2-}, and c) discharge at the Black Lick (BLAC) site during the period September 5-11, 1996.

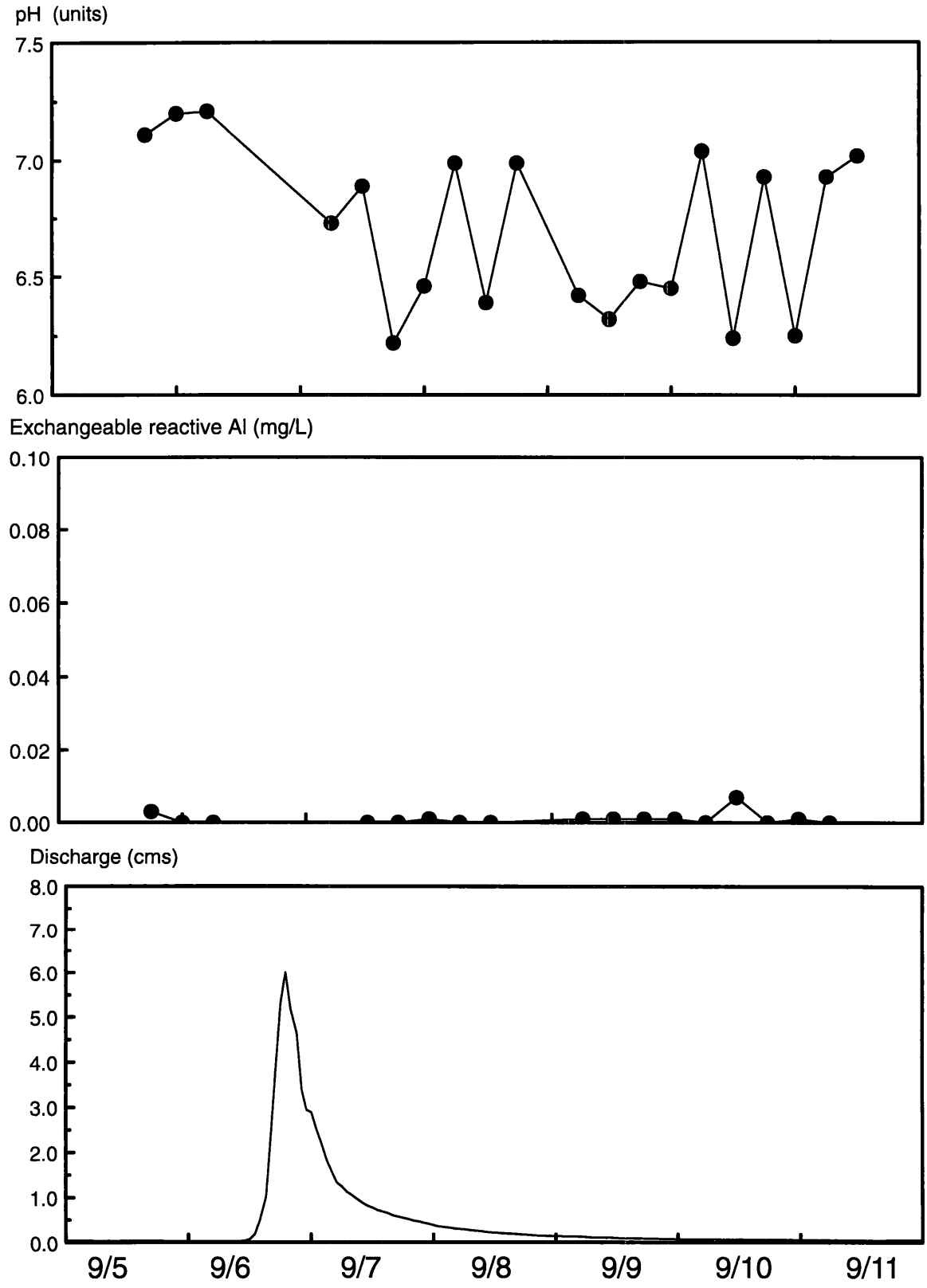

Figure 4.16 (continued). Temporal variations in d) pH, e) exchangeable reactive Al, and f) discharge at the Black Lick (BLAC) site during the period September 5-11, 1996.

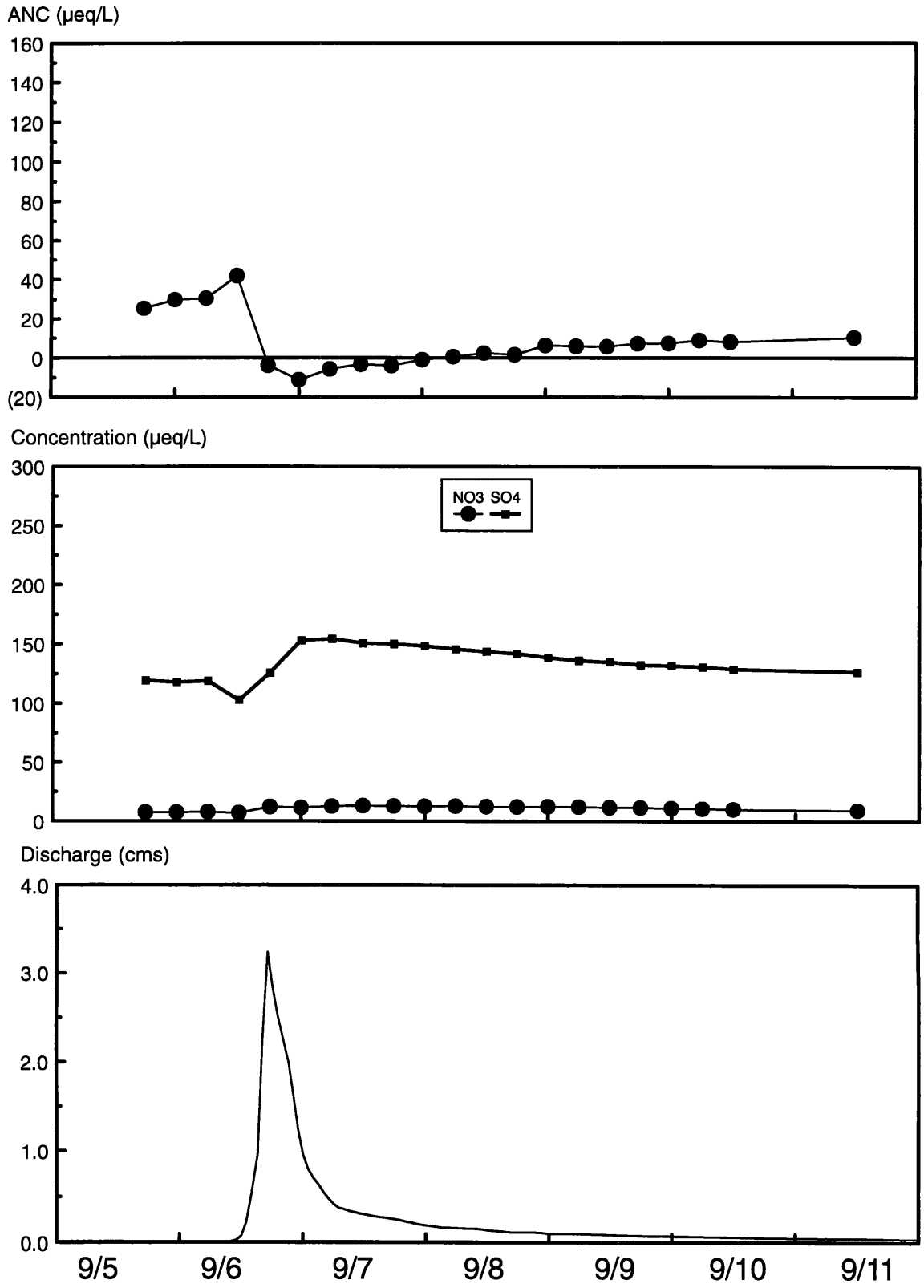

Figure 4.17. Temporal variations in a) ANC, b) NO_3^- and SO_4^{2-}, and c) discharge at the Herrington Creek tributary (HRTB) site during the period September 5-11, 1996.

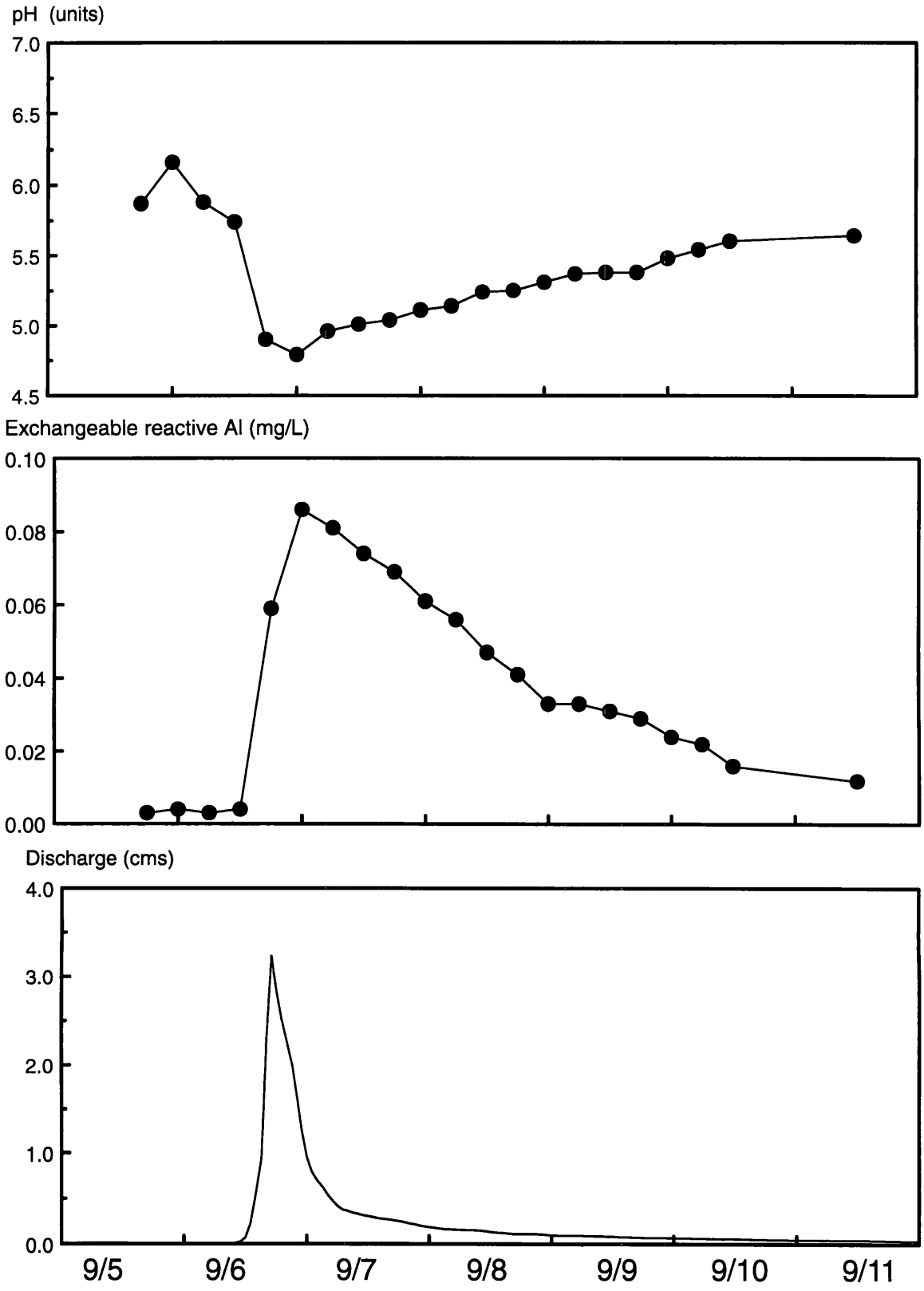

Figure 4.17 (continued). Temporal variations in d) pH, e) exchangeable reactive Al, and f) discharge at the Herrington Creek tributary (HRTB) during the period September 5-11, 1996.

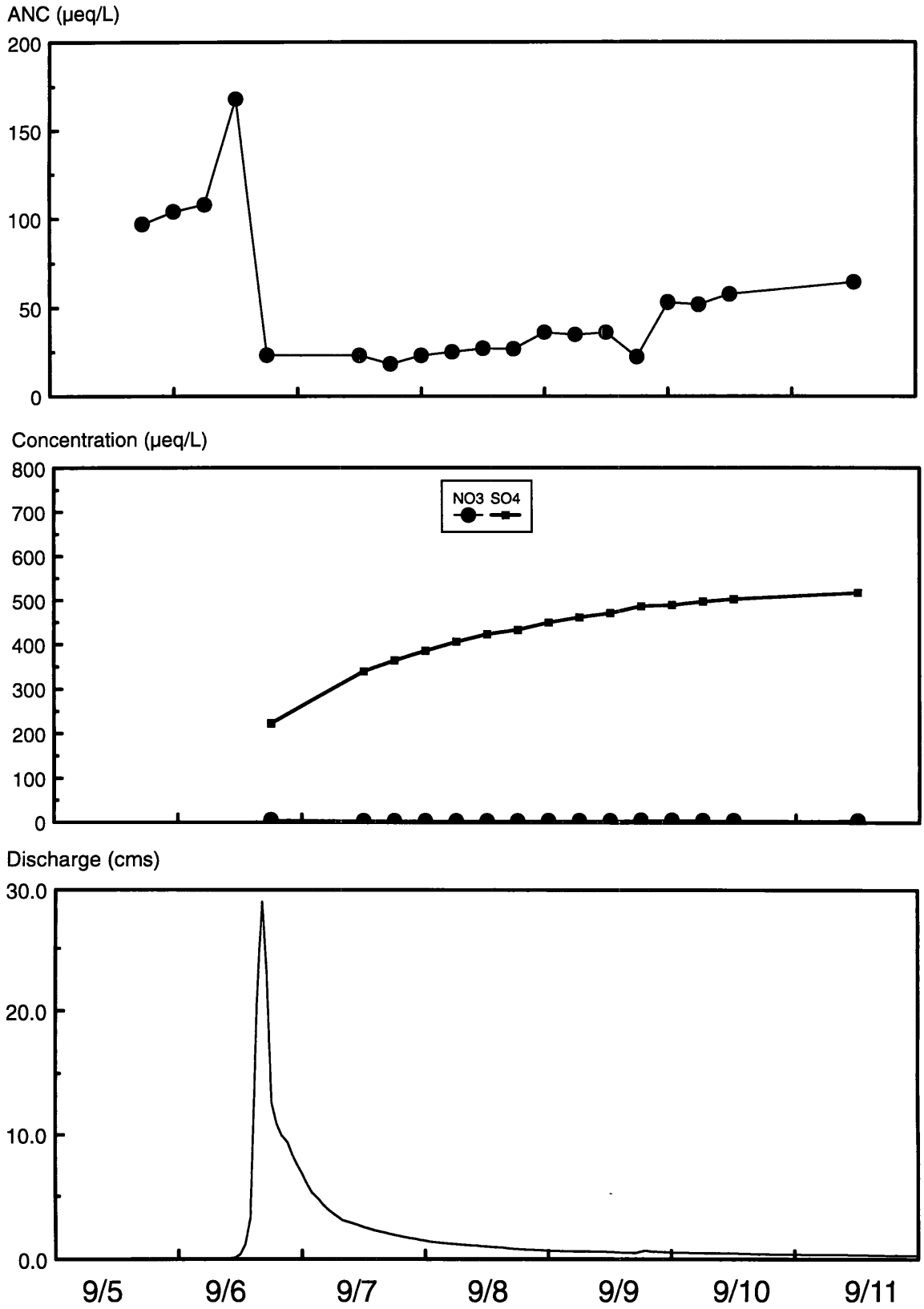

Figure 4.18. Temporal variations in a) ANC, b) NO_3^- and SO_4^{2-}, and c) discharge at the North Prong Lostland Run (NPLR) site during the period September 5-11, 1996.

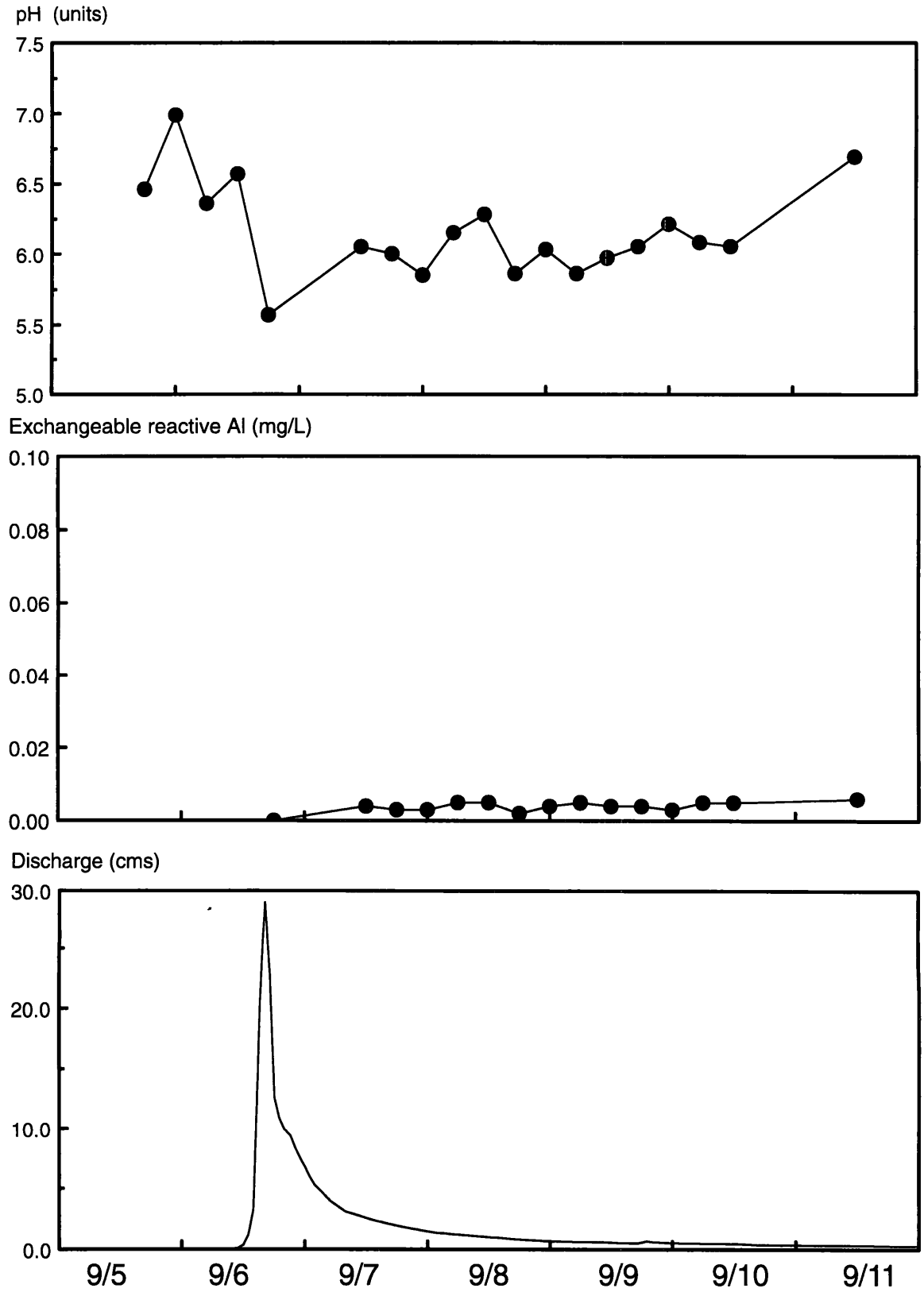

Figure 4.18 (continued). Temporal variations in d) pH, e) exchangeable reactive Al, and f) discharge at the North Prong Lostland Run (NPLR) during the period September 5-11, 1996.

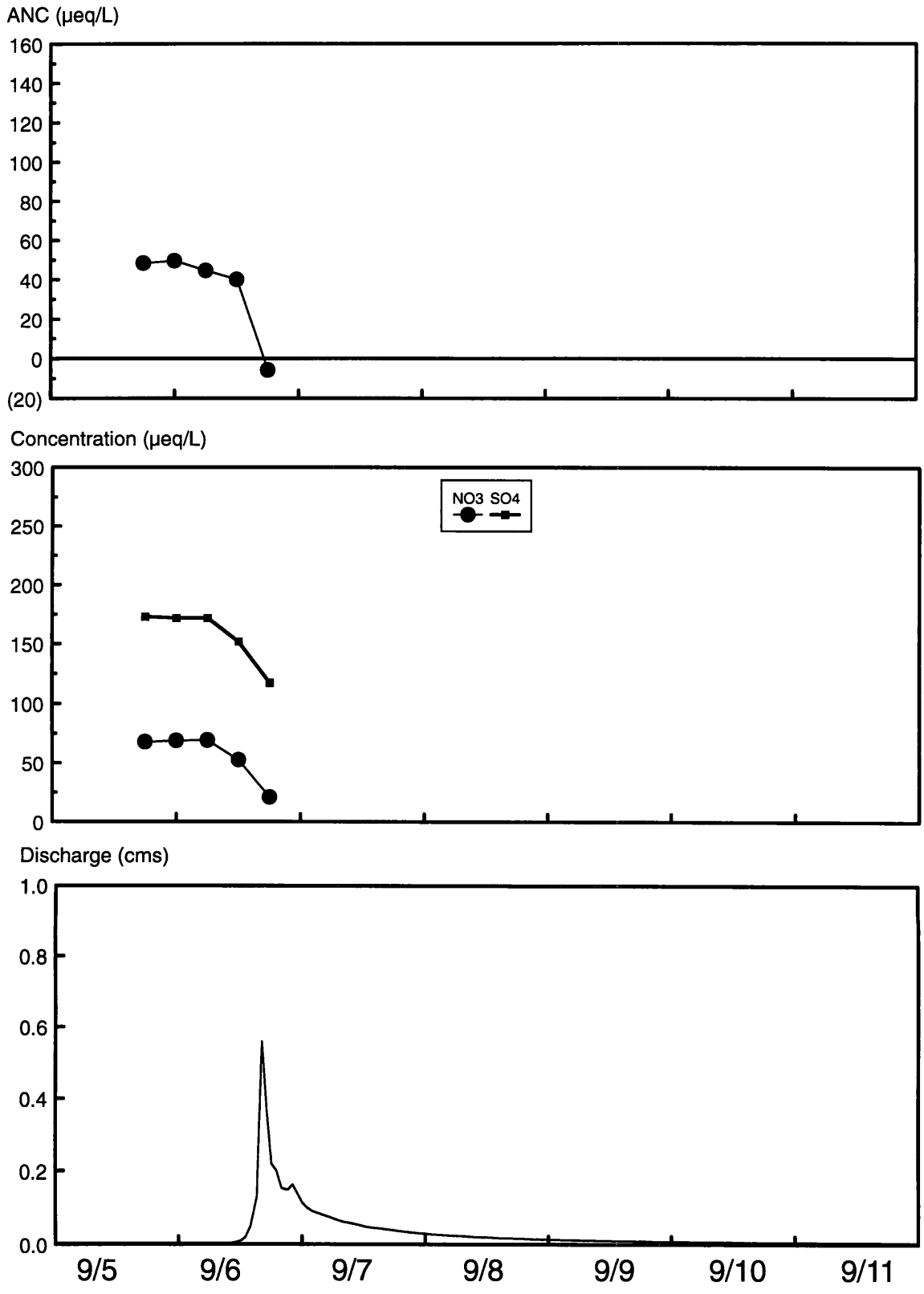

Figure 4.19. Temporal variations in a) ANC, b) NO_3^- and SO_4^{2-}, and c) discharge at the Upper Poplar Lick tributary (UPTB) site during the period September 5-11, 1996.

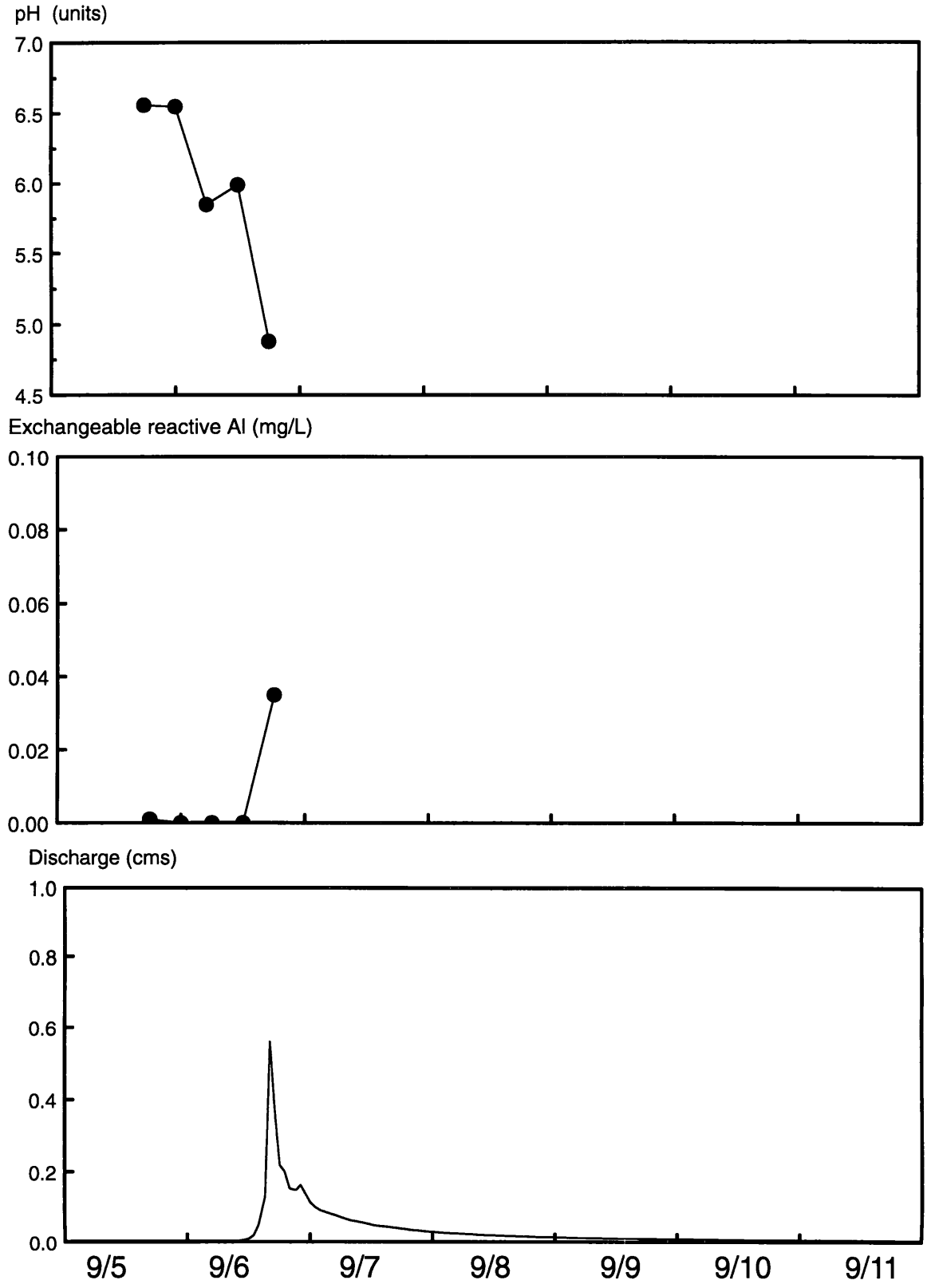

Figure 4.19 (continued). Temporal variations in d) pH, e) exchangeable reactive Al, and f) discharge at the Upper Poplar Lick tributary (UPTB) during the period September 5-11, 1996.

acidity (as well as base cation dilution) to the observed transient changes in streamwater ANC. Consistency was maintained in selecting the pre-event and minimum ANC samples. All pre-event samples were selected as close to the increase in discharge as possible without selecting a point on the rising limb of the hydrograph. Typically, the pre-event sample was collected only a few hours before the event began, but in some cases a sample collected as much as a week or two prior to an extended snowmelt episode was used as the antecedent sample. Therefore:

$$\Delta ANC = ANC_{min} - ANC_{pre} \quad (4.2)$$

$$\Delta SBC = SBC \text{ at } ANC_{min} - SBC_{pre} \quad (4.3)$$

$$\Delta SO_4^{2-} = SO_4^{2-} \text{ at } ANC_{min} - SO_4^{2-}{}_{pre} \quad (4.4)$$

$$\Delta NO_3^- = NO_3^- \text{ at } ANC_{min} - NO_3^-{}_{pre} \quad (4.5)$$

$$\Delta Cl^- = Cl^- \text{ at } ANC_{min} - Cl^-{}_{pre} \quad (4.6)$$

$$\Delta OA = OA \text{ at } ANC_{min} - OA_{pre} \quad (4.7)$$

To determine the relative contribution of each ion to the ANC loss, the change (Δ) in the ion concentration is divided by the value of ΔANC for that particular episode:

$$\text{Relative contribution ratio} = \Delta\text{ion}/\Delta ANC \quad (4.8)$$

A minor sign convention—reversing the sign of the ΔSBC term—allows the contribution of each ion change to ΔANC to be quantified. Using this convention, any positive value of the relative contribution ratio indicates a positive contribution to ANC loss, while a negative ratio indicates a contribution to an ANC increase during an episode. The more positive the value, the greater the contribution to the ANC loss. The ratios can be summed for each event and should in theory equal unity:

$$\Delta SO_4^{2-}/\Delta ANC + \Delta NO_3^-/\Delta ANC + \Delta Cl^-/\Delta ANC + \Delta OA^-/\Delta ANC + \Delta SBC/\Delta ANC = 1 \quad (4.9)$$

Any deviations from a sum of unity are attributable to either analytical error or unmeasured ion changes.

Finally, each of the ion ratios can be assigned a relative proportional contribution value (R_{ion}) by dividing each value by the sum of all values for a particular episode (Schaefer *et al.*, 1990; Eshleman *et al.*, 1995), such as for SBC:

$$R_{SBC} = \Delta SBC/(\Delta SBC - \Delta NO_3^- - \Delta SO_4^{2-} - \Delta OA^-) \quad (4.10)$$

Since these values are normalized, the sum of the R_{ion} values must also equal unity. Tables A.1 through A.5 in Appendix A provide a tabulation of the absolute changes in ion concentrations as well as the relative contribution values for each ion to the observed episodic ANC losses in the five streams. These data will provide the primary data base for testing and verification of various acidification models in subsequent sections of the chapter.

Consistent with our QA/QC results, the predicted values of ΔANC computed as the difference between the change in sum of base cations (ΔSBC) and the change in sum of acid anions (ΔSAA) agree closely with measured values of ΔANC. For four of the five study streams, X-Y graphs of these two variables indicate that the points generally fall fairly close to the 1:1 line (indicating perfect prediction of ΔANC), although occasional points deviate significantly from the line (Figure 4.20 – 4.24). Deviations of points at NPLR from the 1:1 line are due to the relatively large values in both ΔSBC and ΔSAA measured in this stream (Figure 4.23), which is

interpreted as dilution of acid mine drainage. Figure 4.25 suggests that only 6 of the 75 points fall outside a window of ± 50 μeq/L.

The ion contribution ratios (R_{ion}) can in fact be used to ascribe the causes of episodic changes in ANC that are observed during episodes in the five streams. We graphed the R_{ion} values vs. antecedent values of ANC (ANC_{pre}) as one way of examining this information: R_{SBC} (Figure 4.26), R_{SO4} (Figure 4.27), R_{NO3} (Figure 4.28), and R_{OA} (Figure 4.29). Variability of R_{SBC} values was quite large both within and among sites, but the median value of R_{SBC} of 1.132 suggests that base cation dilution dominates ANC loss in these streams (value of 1.0 indicates that 100% of the ANC loss is attributable to SBC dilution; Figure 4.26). R_{SO4} variability was significantly less, with data from BLAC and UPTB falling very close to the median value of –0.013 (indicating a negative contribution to ΔANC); all except two points for NPLR were negative, again indicating consistent dilution of mine drainage SO_4^{2-} during episodes (Figure 4.27). R_{NO3} values were also much less variable, with data from UPTB showing the greatest variability among the sites (Figure 4.28); the median value of 0.061 suggests a relatively small (~6%) contribution to ΔANC. Finally, R_{OA} data was the least variable of all, showing a relatively consistent 8% contribution to ΔANC among the sites and sampled episodes (Figure 4.29).

Median values of the ion contribution ratios (R_{ion}) also provide evidence of the general causes of ANC depression at each stream site (Table 4.3). Data from BIGR and HRTB appear most consistent with an atmospheric acidification interpretation, since median values of R_{NO3} and R_{SO4} are positive for both streams; in addition, R_{OA} and R_{SBC} are both positive for both sites as well, suggesting positive contributions by flushing of natural organic acids and base cation dilution. At BIGR, the results suggest that 73% of the median ANC change is attributable to dilution of base cations, 10% attributable to flushing of sulfuric acid, 8% due to flushing of natural organic acids, and 6% due to flushing of nitric acid (ratios do not add up exactly to 100% since these are median—not mean—values). At HRTB, the percentage contributions are 40%, 39%, 7%, and 25%, respectively. Median results for BLAC suggest that dilution of base cations is the dominant mechanism of ANC depression at this site, as evidenced by the large positive value (1.37) of R_{SBC} and negative values for R_{NO3} (-0.28) and R_{SO4} (-0.14). Data from NPLR indicates that ANC depressions at this site are largely due to base cation dilution in excess of sulfuric acid dilution, with nitric and organic acid increases playing very small roles proportionally. Data for UPTB also suggests domination of base cation dilution in excess of nitric acid dilution, with a minor role for organic acid increases (Table 4.3).

The median ion contribution ratio data also reveal an important result when graphed vs. an "index" of mean spring baseflow ANC (ANC_{index}; Figure 4.30); the value of ANC_{index} for each site was taken as the mean baseflow value during the months of March through May of the three years. In general, the graphs indicate that R_{SBC} increases as ANC_{index} increases, while R_{SO4}, R_{NO3}, and R_{OA} all decrease as ANC_{index} increases, suggesting that SBC dilution generally becomes

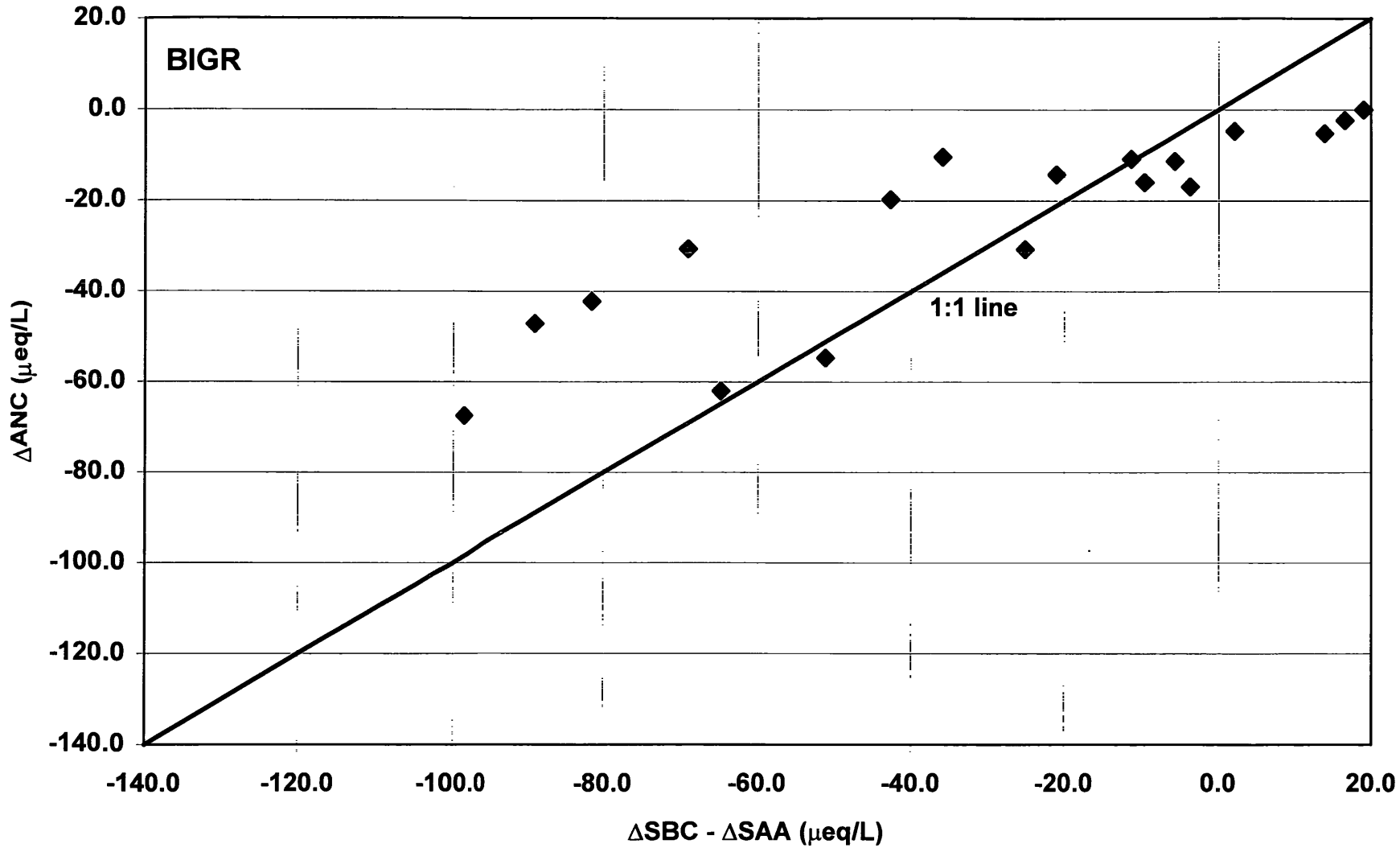

Figure 4.20. Relationship between ΔANC and ΔSBC – ΔSAA for all episodes sampled at the BIGR site.

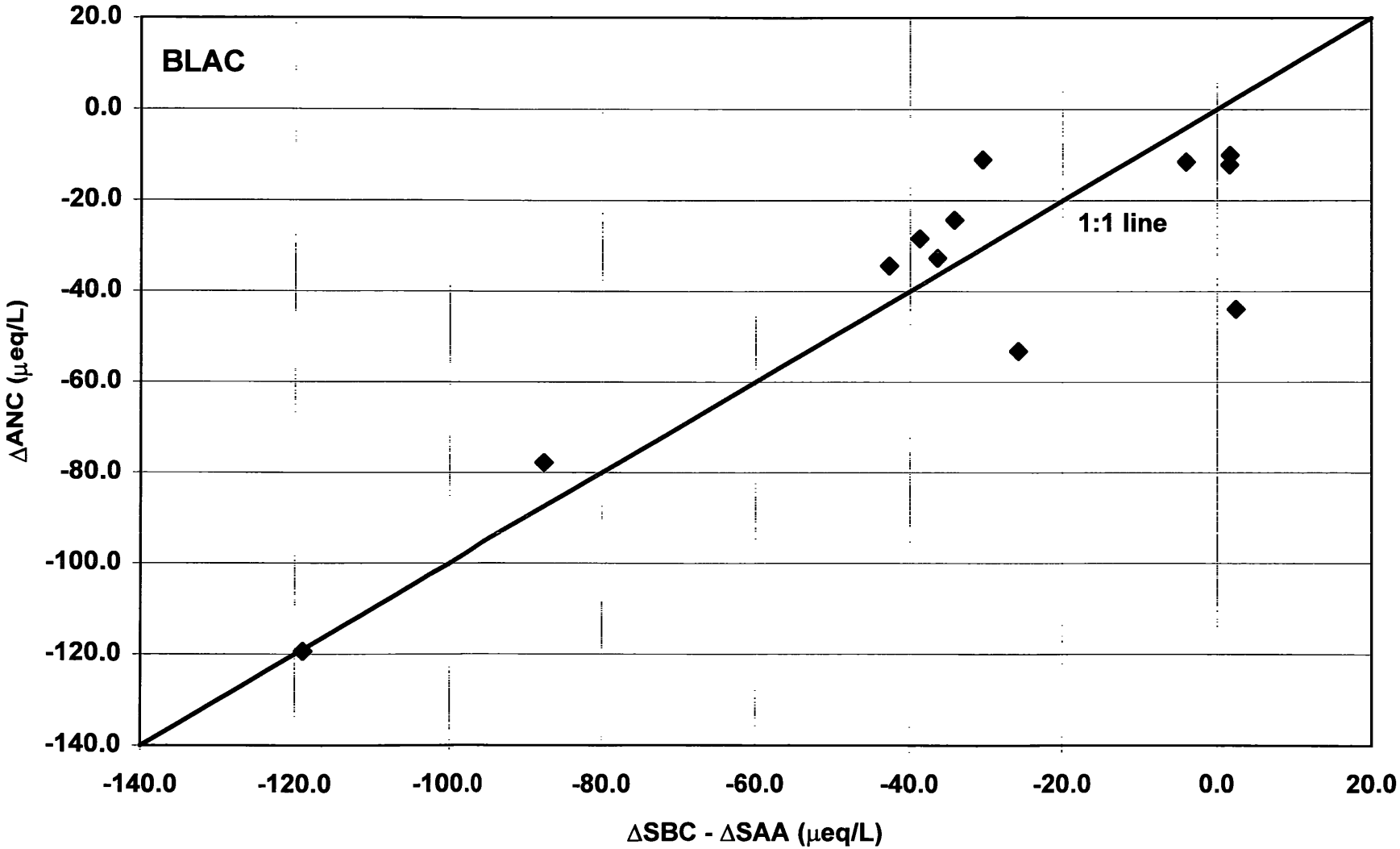

Figure 4.21. Relationship between ΔANC and ΔSBC – ΔSAA for all episodes sampled at the BLAC site.

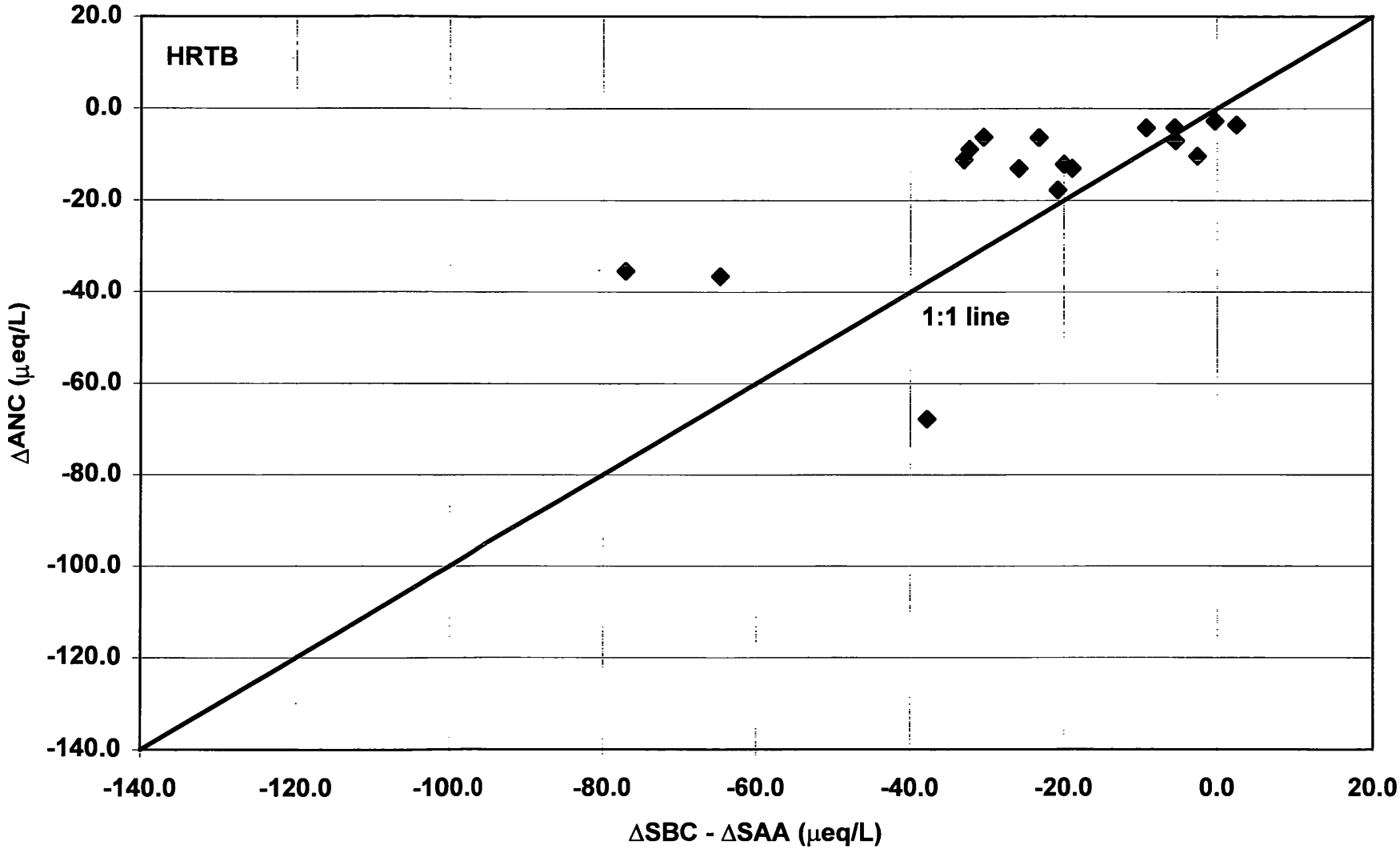

Figure 4.22. Relationship between ΔANC and ΔSBC – ΔSAA for all episodes sampled at the HRTB site.

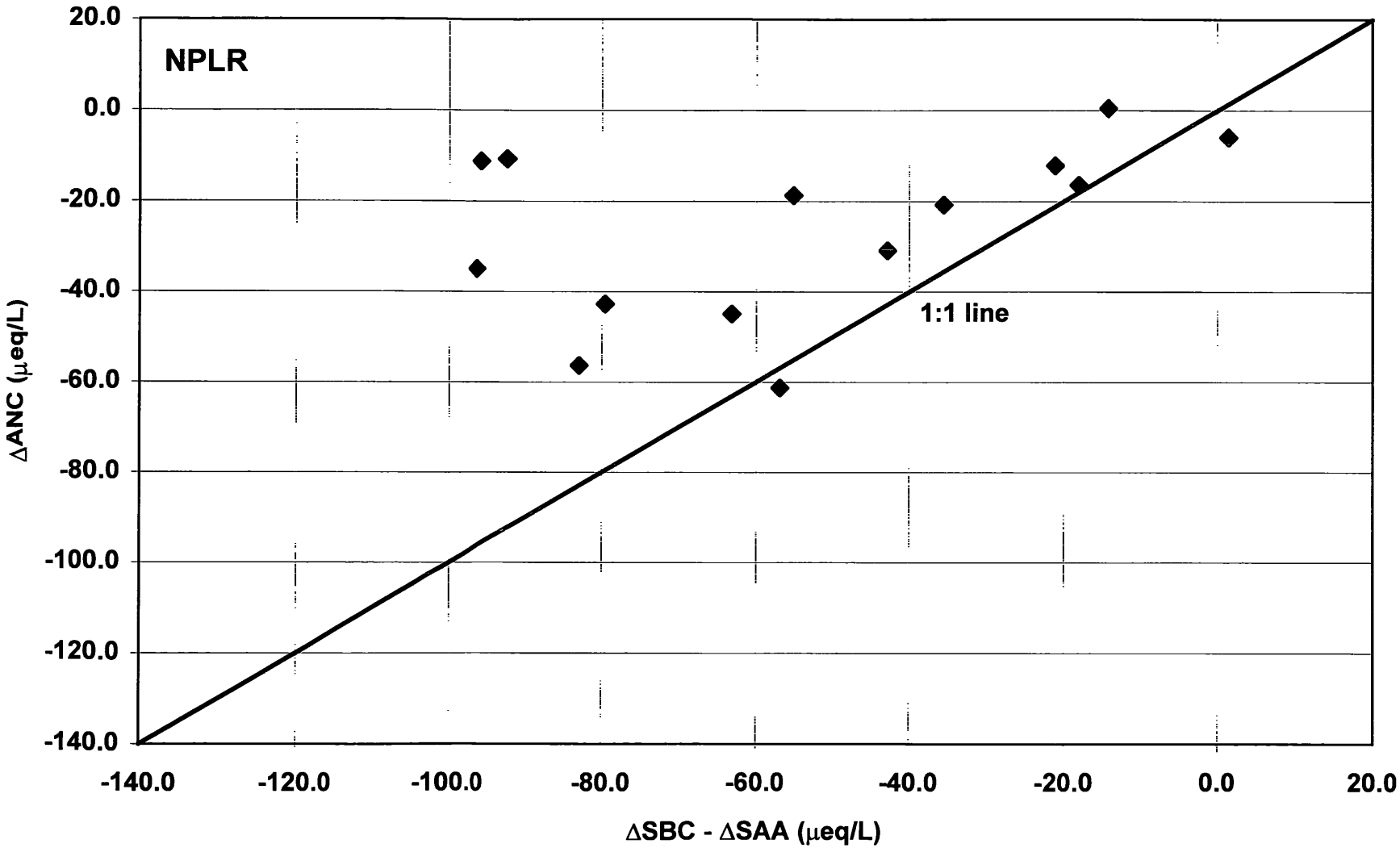

Figure 4.23. Relationship between ΔANC and ΔSBC – ΔSAA for all episodes sampled at the NPLR site.

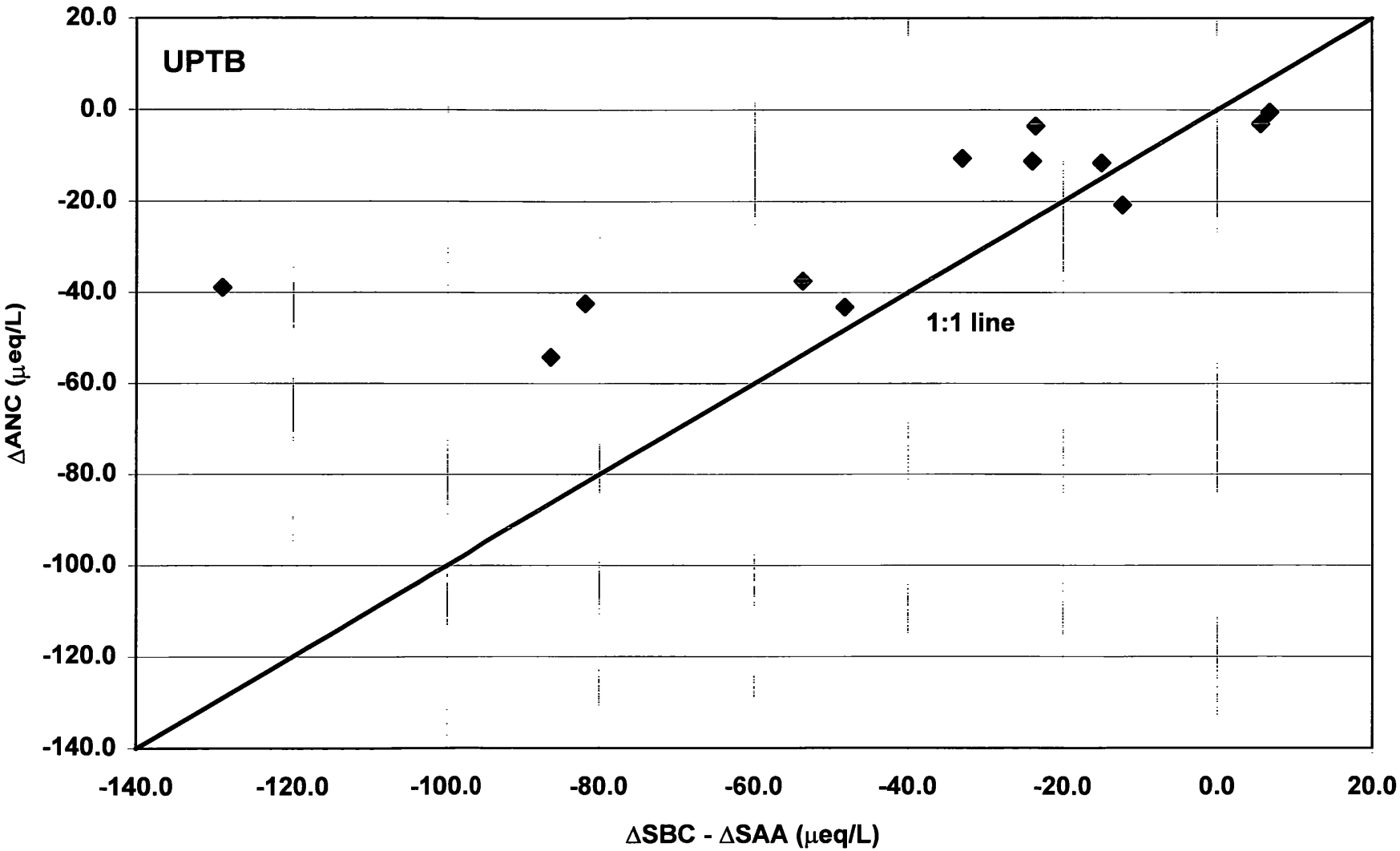

Figure 4.24 Relationship between ΔANC and ΔSBC – ΔSAA for all episodes sampled at the UPTB site.

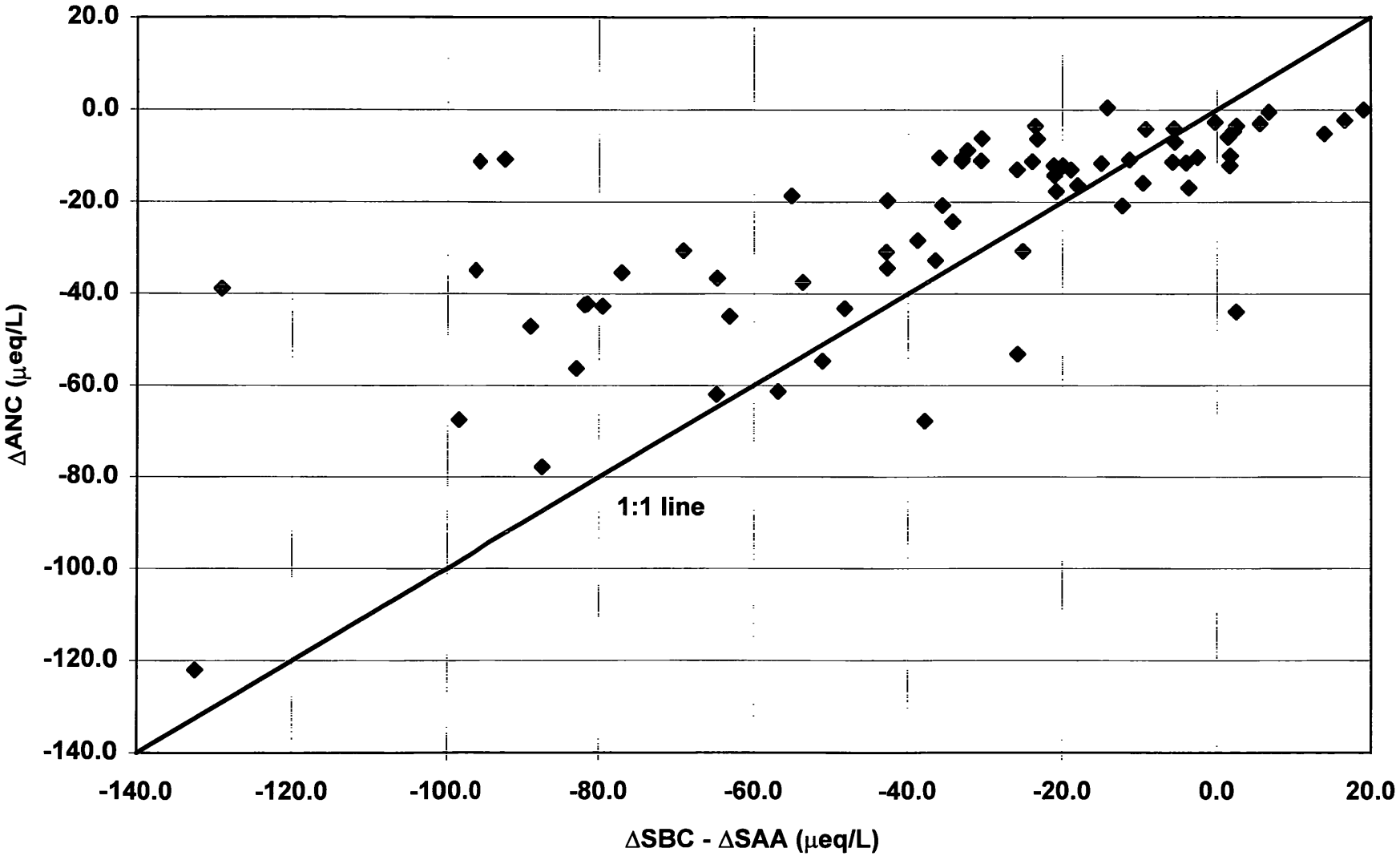

Figure 4.25 Relationship between ΔANC and ΔSBC – ΔSAA for all episodes sampled at all sites during the project (n = 75).

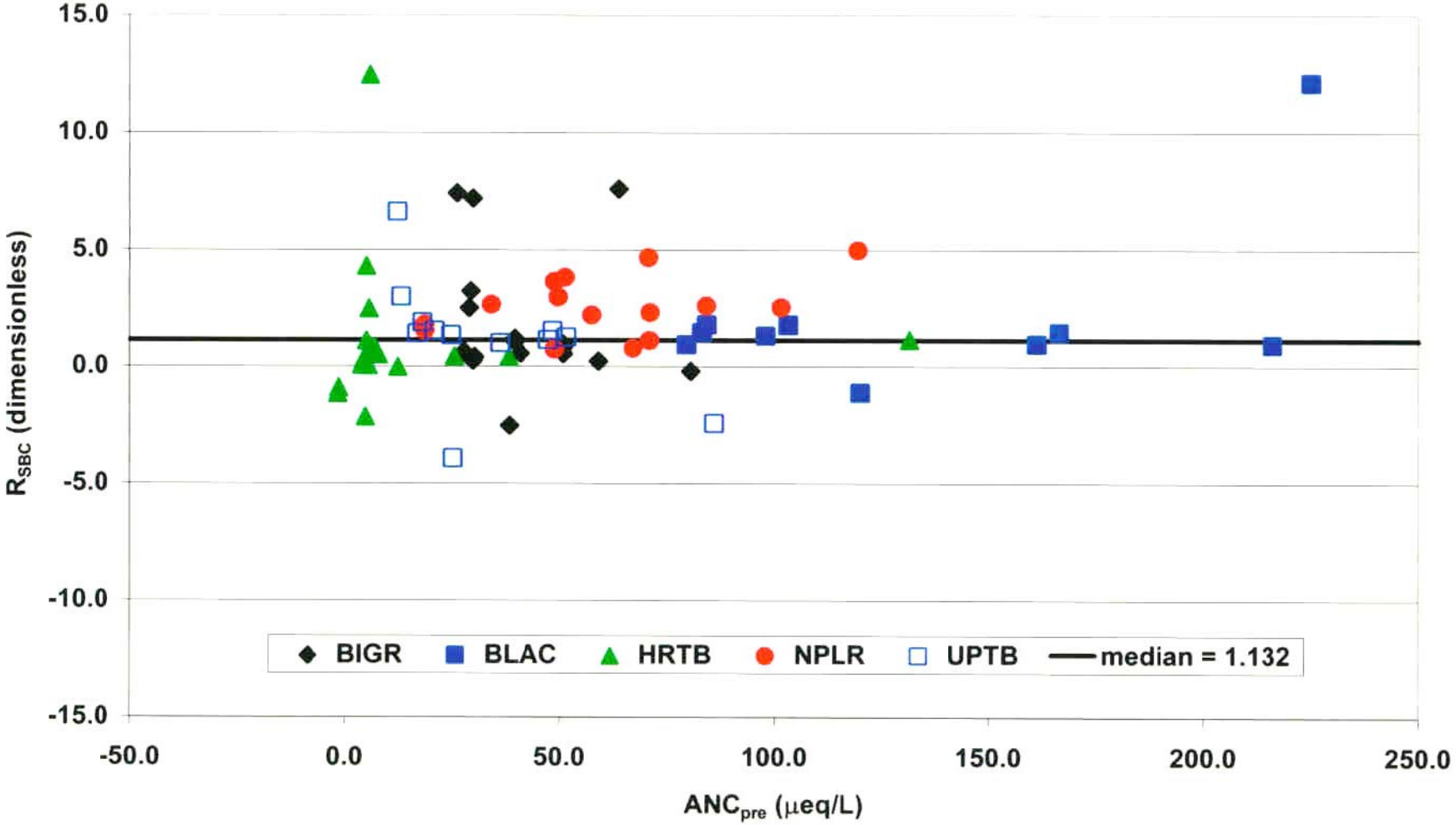

Figure 4.26. Graph of dimensionless ion contribution ratio for sum of base cations (R_{SBC}) for all episodes sampled at all sites during the project (median value of R_{SBC} also shown).

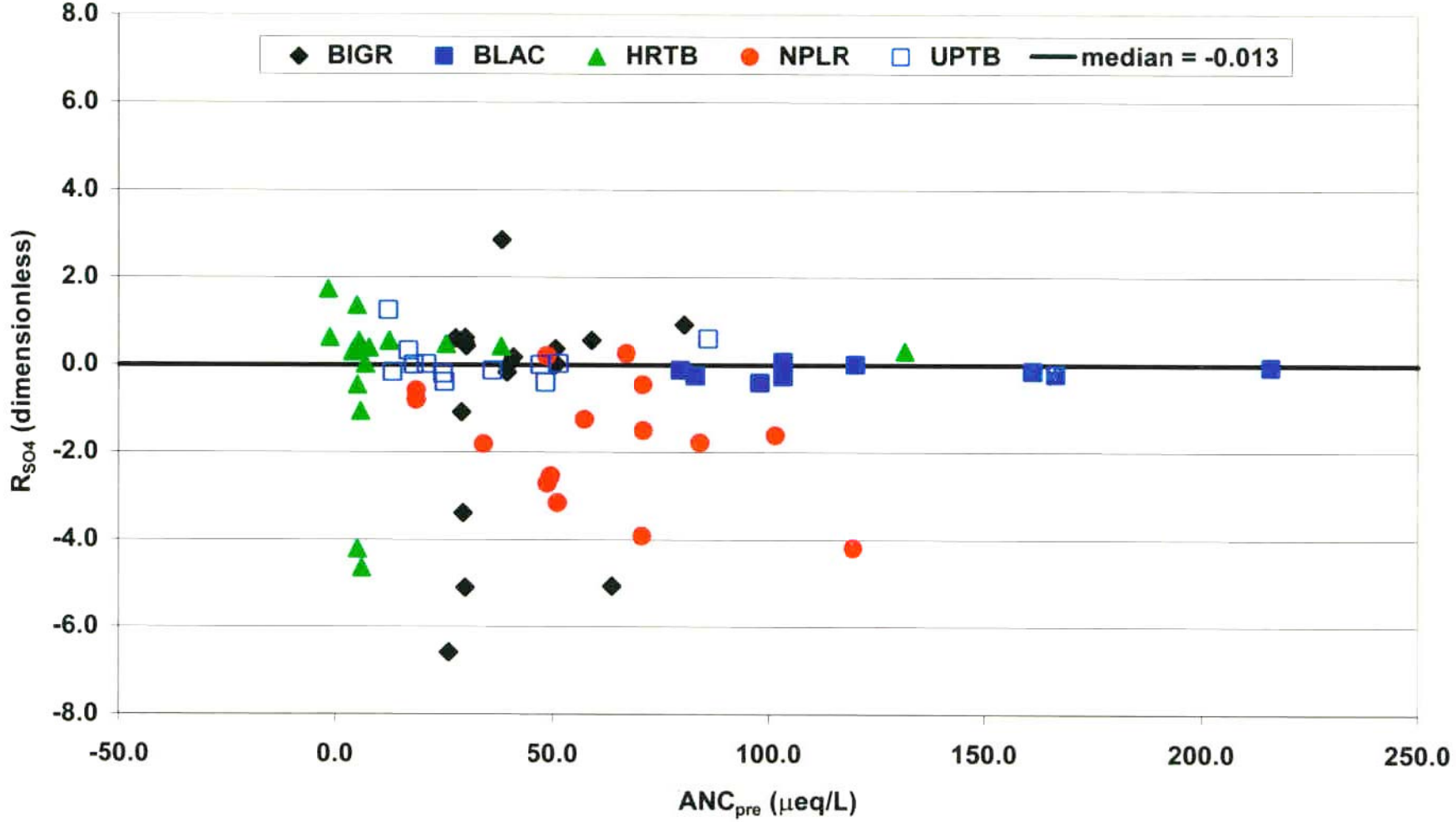

Figure 4.27. Graph of dimensionless ion contribution ratio for SO_4^{2-} (R_{SO4}) for all episodes sampled at all sites during the project (median value of R_{SO4} also shown).

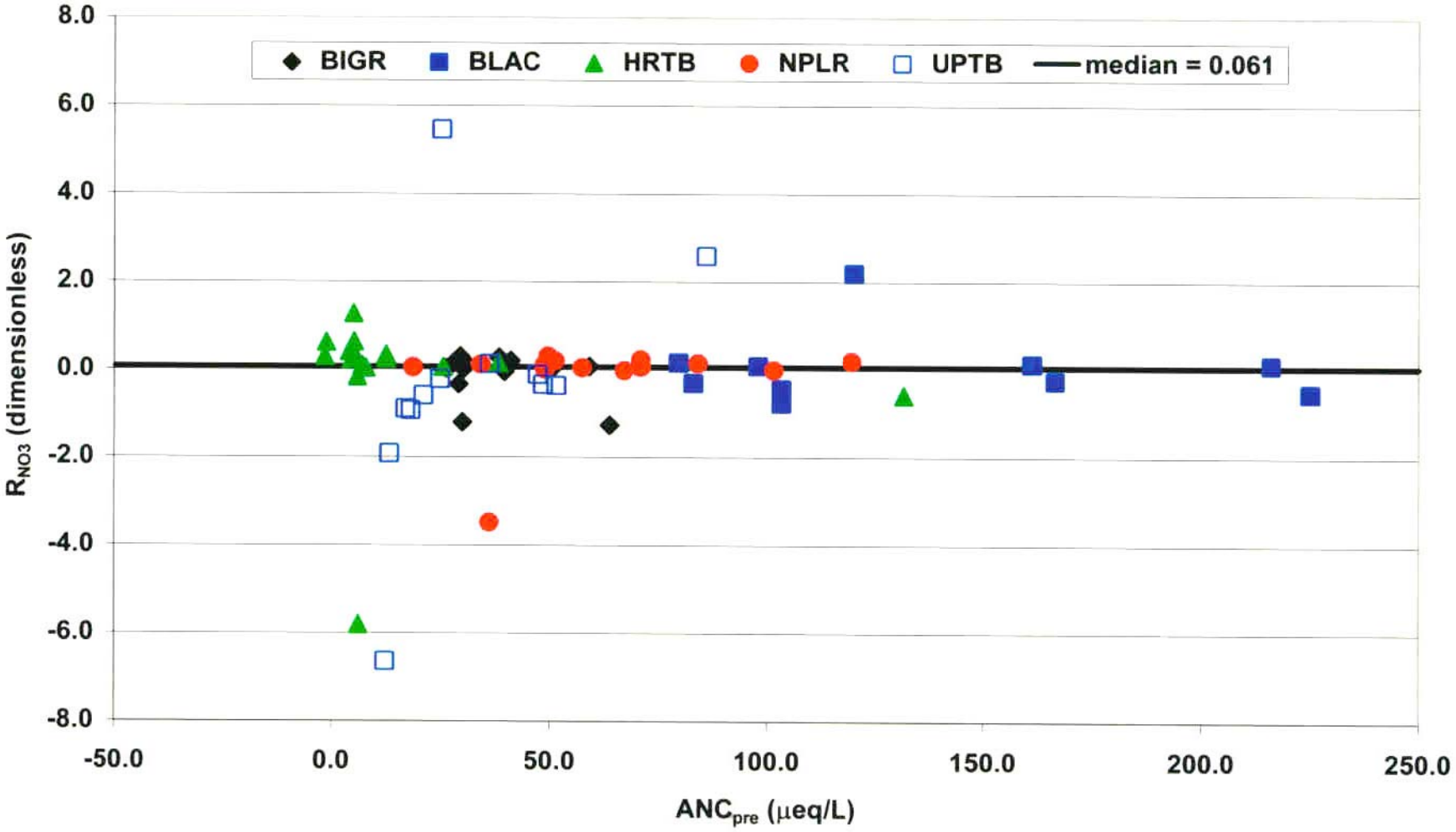

Figure 4.28. Graph of dimensionless ion contribution ratio for NO_3^- (R_{NO3}) for all episodes sampled at all sites during the project (median value of R_{NO3} also shown).

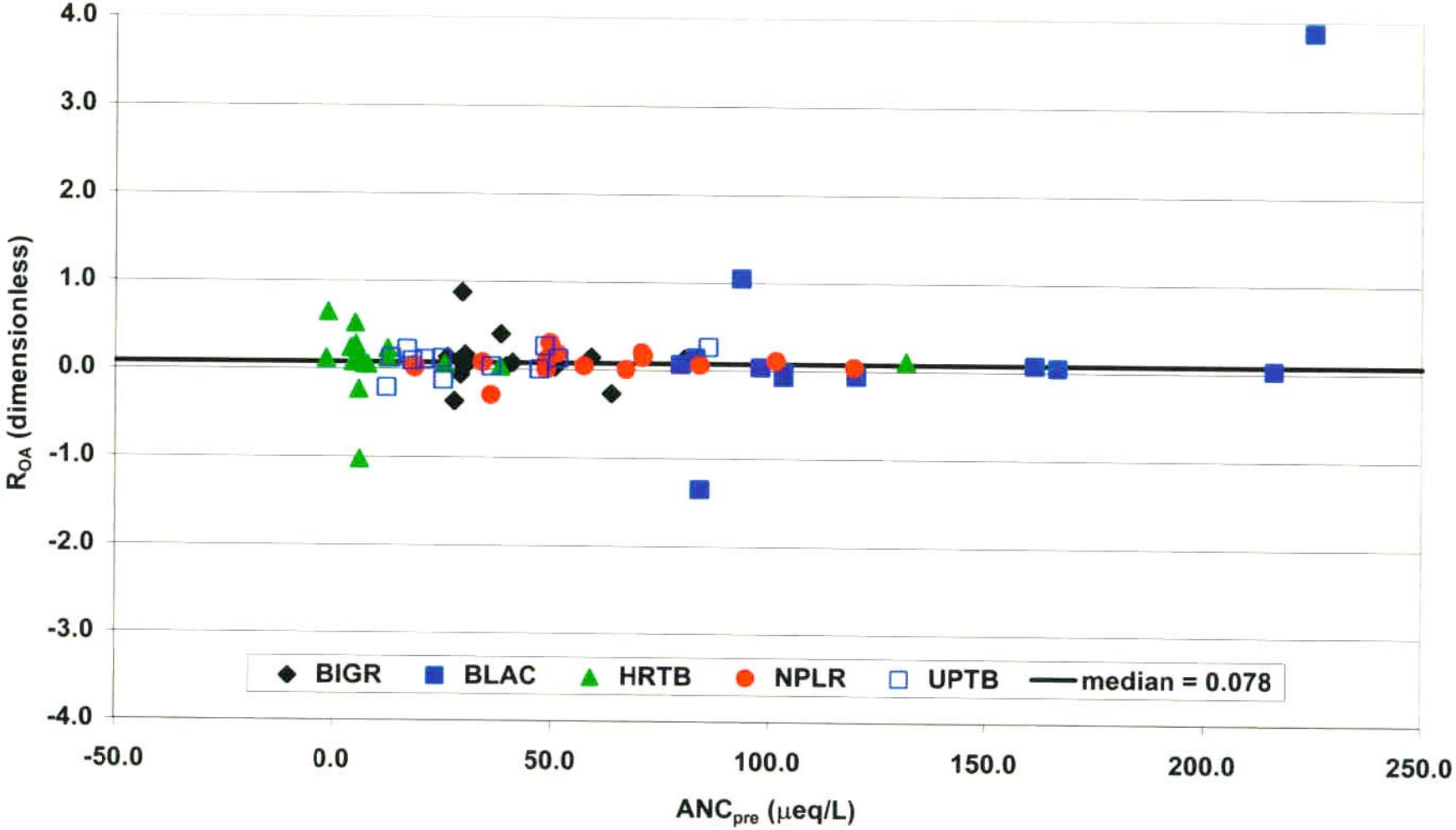

Figure 4.29. Graph of dimensionless ion contribution ratio for OA^- (R_{OA}) for all episodes sampled at all sites during the project (median value of R_{OA} also shown).

Table 4.3. Median values of ion changes (μeq/L) and ion contribution ratios (dimensionless) for episodes sampled at the five sites.

	ΔANC	ΔSBC	ΔNO_3^-	ΔSO_4^{2-}	ΔOA^-	R_{NO3}	R_{S04}	R_{OA}	R_{SBC}
BIGR	-16.4	-17.9	2.6	2.0	3.7	0.06	0.10	0.08	0.73
BLAC	-30.6	-51.3	4.8	-11.2	1.5	-0.28	-0.14	0.04	1.37
HRTB	-10.3	-1.2	4.9	11.8	2.7	0.25	0.39	0.11	0.40
NPLR	-19.7	-150.4	3.5	-87.5	4.8	0.06	-1.57	0.07	2.41
UPTB	-16.2	-67.3	-25.1	-0.3	4.4	-0.36	-0.01	0.12	1.35

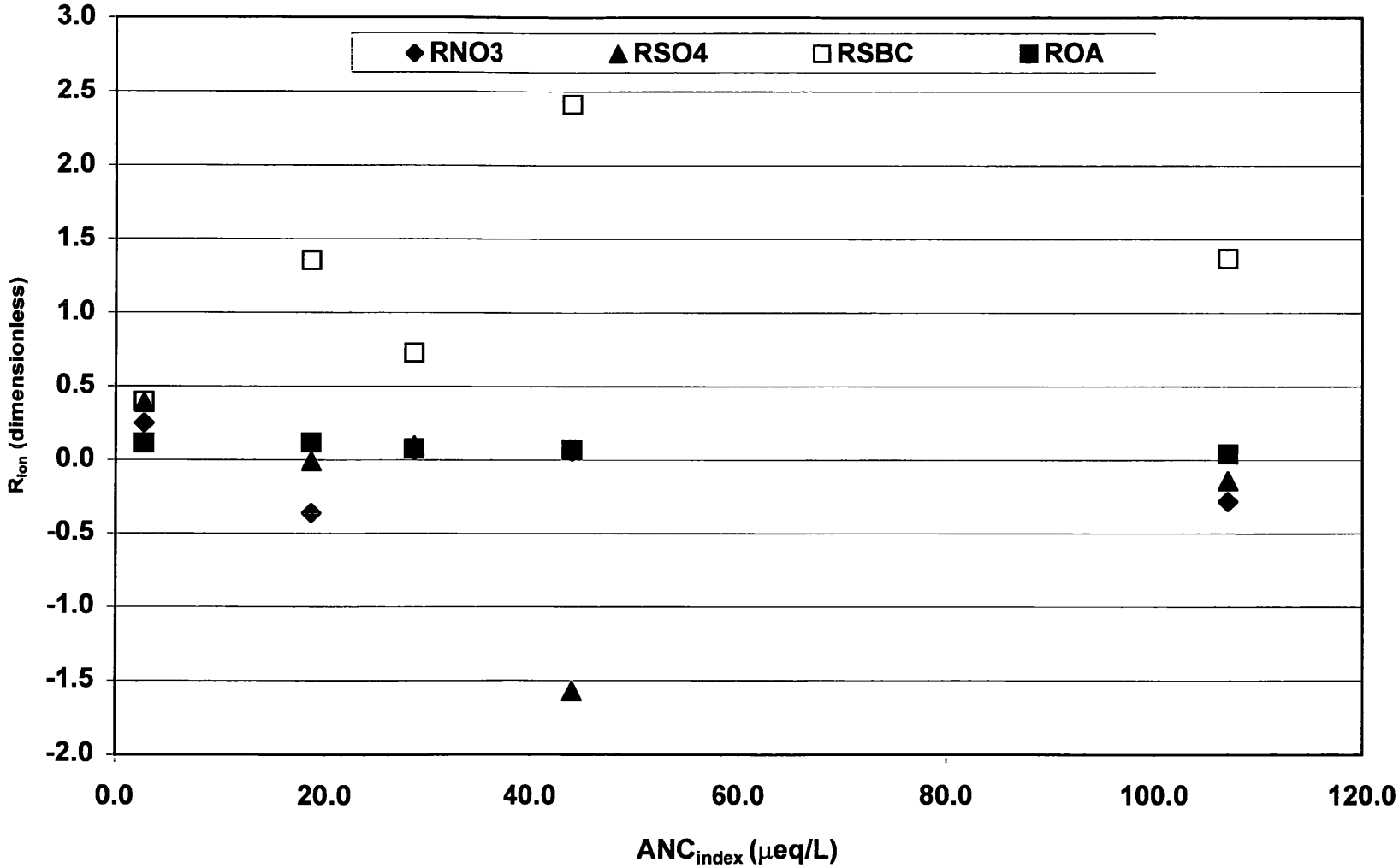

Figure 4.30. Graph of median ion contribution ratios (R_{SBC}, R_{SO4}, R_{NO3}, and R_{OA}) for all episodes sampled at each of the sites during the project vs. ANC_{index}.

relatively more important in higher ANC systems, while flushing of acids into streams becomes less important in higher ANC systems (all else being equal). This result is generally consistent with previous findings of Eshleman *et al.* (1995) for surface waters draining watersheds in the Adirondack and Catskill mountain regions of New York.

The absolute changes in ion concentrations also suggest mechanisms for ANC depression among the five streams. A graph of ΔSBC on $\Delta SO_4^{2-} + \Delta NO_3^- + \Delta OA^-$, partitioned into eight quadrants, can be used to ascribe these mechanisms (Figure 4.31). The fact that virtually all of the data points fall below the 1:1 line (in quadrants 2 through 5) indicates that episodic acidification is taking place during all of the sampled episodes and is largely controlled by the dynamics of base cations, SO_4^{2-}, NO_3^-, and OA^-. Episodes falling into quadrant 2 (dominated by many from BIGR and HRTB) indicate that both ΔSBC and ΔSAA are positive, but that $\Delta SAA > \Delta SBC$. Episodes falling into quadrants 3 and 4 (dominated by BIGR, BLAC, and HRTB) indicate that ΔSAA is positive and ΔSBC is negative (but ΔSBC is more negative resulting in ANC depression). Finally, episodes falling into quadrant 5 (dominated by NPLR, UPTB, and BLAC) are best characterized as "dilution episodes" in which ΔSAA and ΔSBC are both negative, but ΔSBC is more negative resulting in ANC depression.

Wigington *et al.* (1993) also found that episodic acidification of five acid-sensitive streams on the Northern Appalachian Plateau in Pennsylvania was dominated by base cation dilution (SBC) and H_2SO_4 (SO_4^{2-}) increases, while HNO_3 (NO_3^-) and strong organic acid (OA^-) increases were generally secondary or tertiary contributors to ANC depressions; Morgan *et al.* (1994) showed that episodic acidification on the Big Run watershed in western Maryland was dominated by ΔSBC and ΔSO_4^{2-}, with ΔNO_3^- and ΔOA^- playing much smaller roles. Data from Big Run also showed that ΔSBC contributed proportionally more to ΔANC than did ΔSO_4^{2-} in higher ANC systems (Morgan *et al.*, 1994), all else being equal.

The observed values of ΔANC and ANC_{min} are clearly controlled by the major ion changes that occur during hydrological mixing in streams and their watersheds, but our data suggest that these critical variables may also vary as a function of the particular hydrological event, antecedent chemical conditions, and local physiographic conditions (e.g., land use disturbances). Adding data from a previous study of episodic acidification at BIGR by Morgan *et al.* (1994) during the years 1990-92 to our results, it is evident that ANC_{min} measured during an event is well-predicted ($r^2 = 0.64$) by peak discharge at the nearby Savage River (near Barton) station; lower values of ANC_{min} occur during higher discharge conditions, all else being equal (Figure 4.32).

ANC_{min} and ΔANC are also shown to be well-predicted by ANC_{pre}, the antecedent or pre-event value of ANC in the stream (Figure 4.33). Using all 75 data points, simple linear regression models explain 77% and 43% of the total variation in these variables, respectively. This result more than any other provides support for a two-component mixing model approach to predicting changes in ANC in western Maryland streams in response to hydrological events. The data shown in Figure 4.33 also suggest that streams with pre-event ANC values greater than

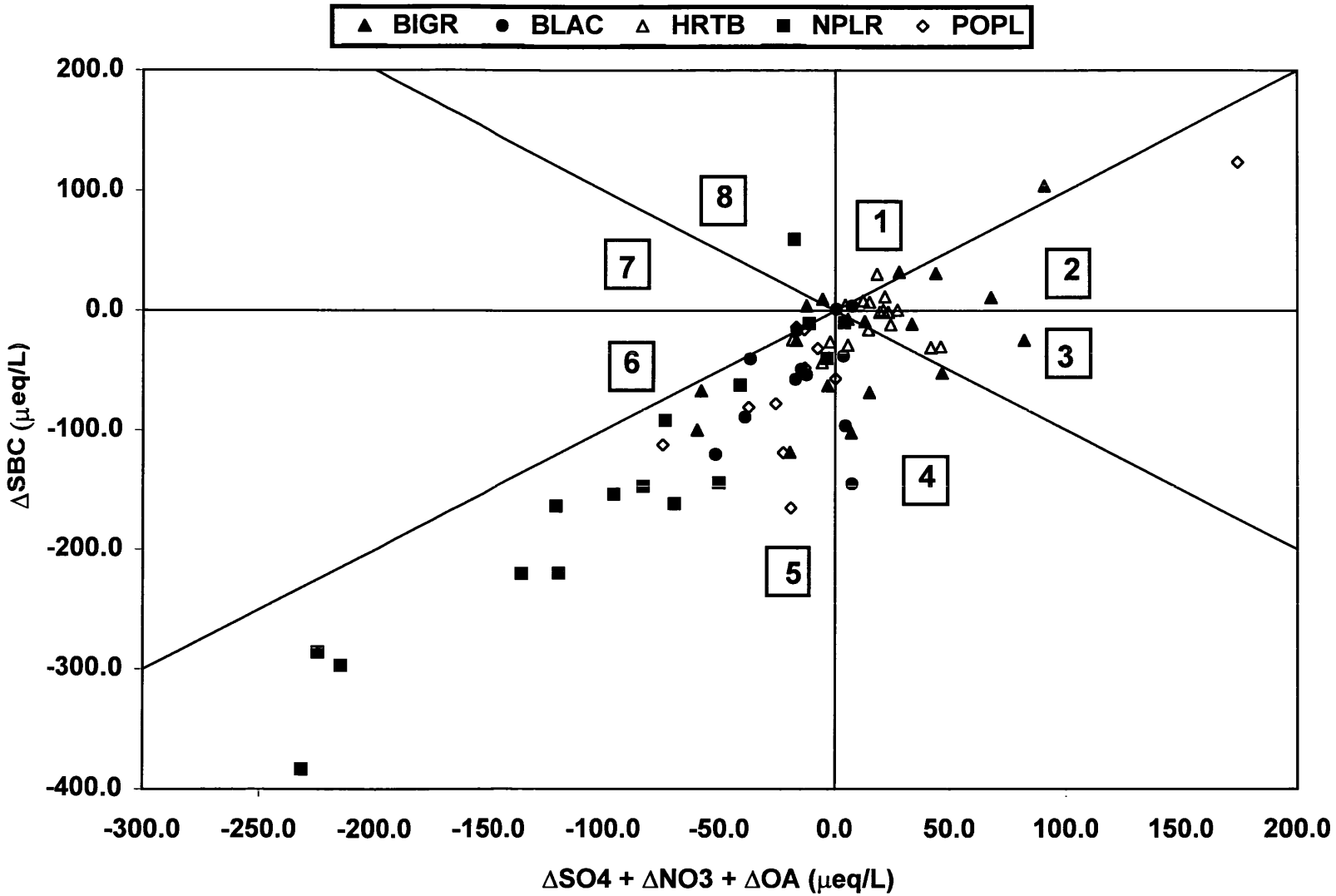

Figure 4.31. Graph of ΔSBC vs. $\Delta SO_4^{2-} + \Delta NO_3^- + \Delta OA^-$ for all episodes sampled during the project. See text for discussion of eight labeled quadrants.

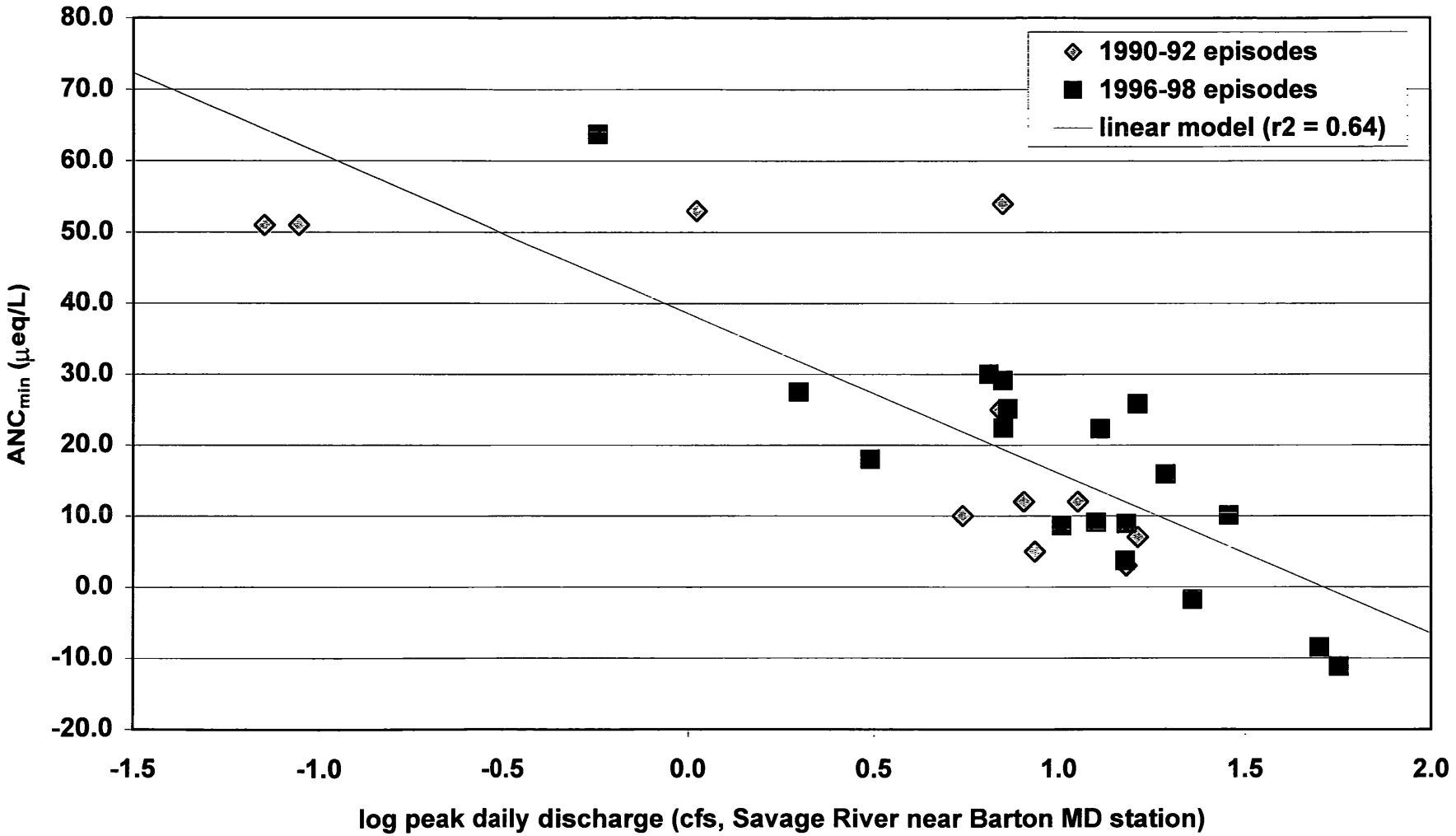

Figure 4.32. Relationship between ANC_{min} measured during episodes at BIGR vs. log peak daily discharge measured at the SAVR (Savage River near Barton) station. Data collected by Morgan *et al.* (1994) during 1990-92 also shown for comparison.

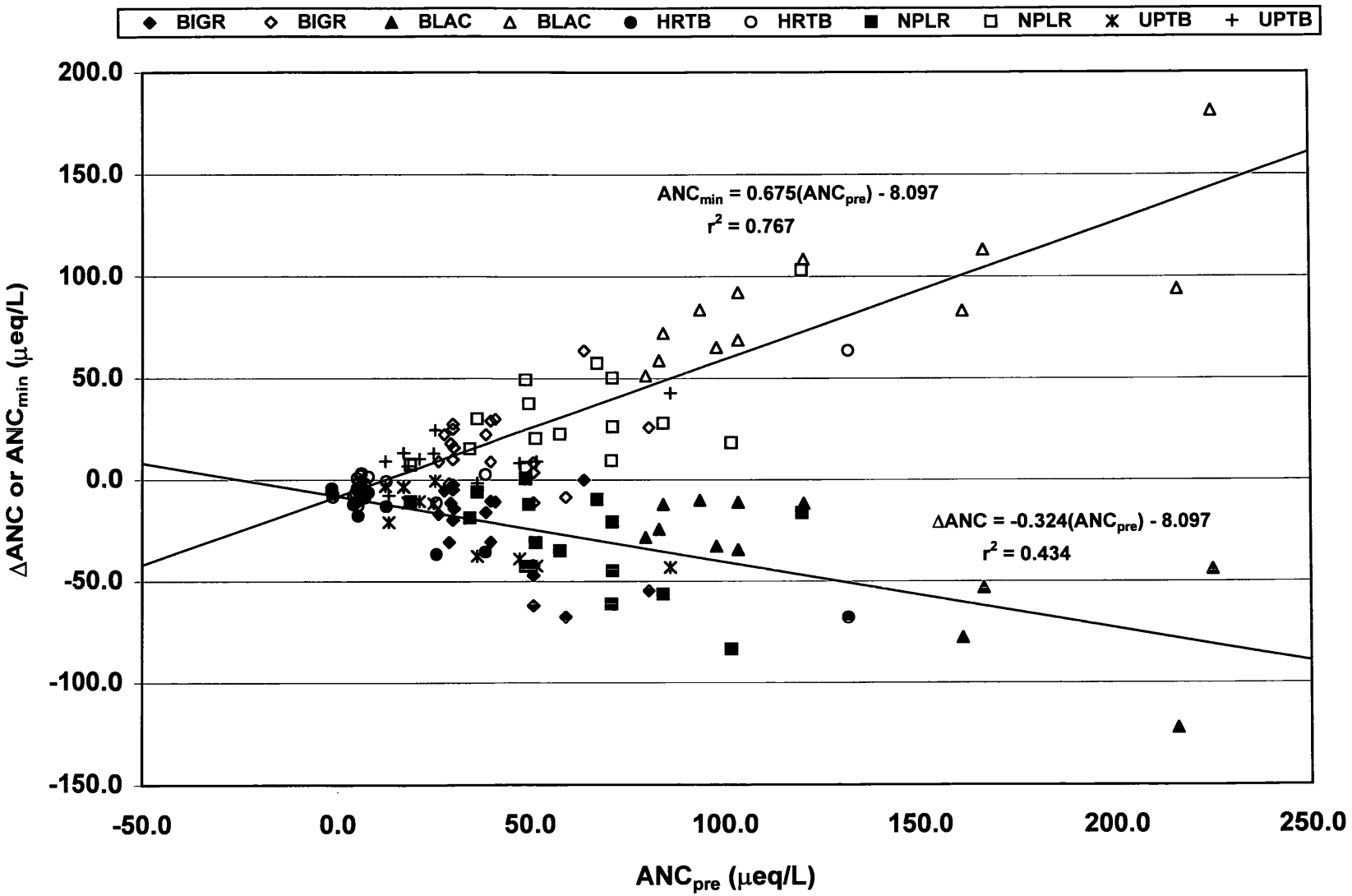

Figure 4.33. Relationships between ΔANC (solid symbols) and ANC_{min} (open symbols) vs. ANC_{pre} for all episodes sampled at all sites during the project. Linear regression models also shown.

about 75 μeq/L are unlikely to become episodically acidified (ANC < 0) during extreme events. It may in fact be possible to use 95% confidence limits on our regression model line to better identify the probability of a stream reaching negative ANC as a function of the antecedent condition. It is most interesting to compare the results shown in Figure 4.33 with similar results presented by Morgan *et al.* (1994) for streams in the Big Run watershed. Using data from six sites (total of 81 episodes), the linear regression models (ANC_{min} and ΔANC on ANC_{pre}) are virtually identical to the models found in this study. Finally, using only the five lowest values of ANC_{min} during the study and an "index" of mean value of spring baseflow ANC (ANC_{index}), we find a similar relationship; we also find a similar model for predicting ΔANC (computed as $\Delta ANC = ANC_{min} - ANC_{index}$; Figure 4.34).

D. Temporal Variations in Low-Level Dissolved Metals in Streamwater

In March 1997, we began collection of samples for analysis of the following low-level dissolved metals by ICP-AES: chromium, zinc, cadmium, beryllium, iron, cobalt, manganese, vanadium, and zinc. Low-level metals samples were also collected for one stormflow event (May 24-29, 1997) at four of the five sampling locations: BIGR, BLAC, HRTB, and NPLR. Event samples were filtered in the laboratory following the same protocols as for the other dissolved analytes. The most commonly detected low-level dissolved metals analyzed by AL were: zinc, iron, and manganese. Vanadium, cobalt, copper, chromium, cadmium, and beryllium were only detected in a few isolated samples. This might be more a result of limitations of the analytical equipment than an absence of these analytes in the samples. Therefore, relationships and trends could only be examined for zinc, iron, and manganese at the five sampling locations.

Baseflow samples were collected bi-weekly at all five sampling sites. BLAC exhibited the lowest average metal concentrations (Figure 4.35). The most commonly detected metals at the sites were: manganese, zinc, iron. Iron was the highest low-level metal at all sites except NPLR, which exhibited higher manganese concentrations. Of some concern are the concentrations of iron at HRTB for baseflow samples. Iron averaged about 600 μg/L for all baseflow samples but was measured to be as high as 4500 μg/L on one occasion. This is above the EcoTox threshold (ET) of 1000 ppb that has been established by USEPA. ET's have been defined as media-specific contaminant concentrations above which there is sufficient concern regarding adverse ecological effects to warrant further site investigation. The ET's are for screening purposes and can be used in baseline risk assessment. The ET's for surface water have been based on the Chronic Ambient Water Quality Criteria (CAWQC), developed by the USEPA Office of Water (USEPA, 1996). HRTB is the only site that had iron concentrations higher than the ET. The ET for manganese is 80 μg/L. This ET was exceeded at HRTB and at NPLR in baseflow grab samples.

We also collected extensive low-level metals data at HRTB and BLAC for three events, which also corresponded with the trace metal analyses that accompanied the expanded scope of work for the final year of the project. Additionally, samples were analyzed for low-level metals

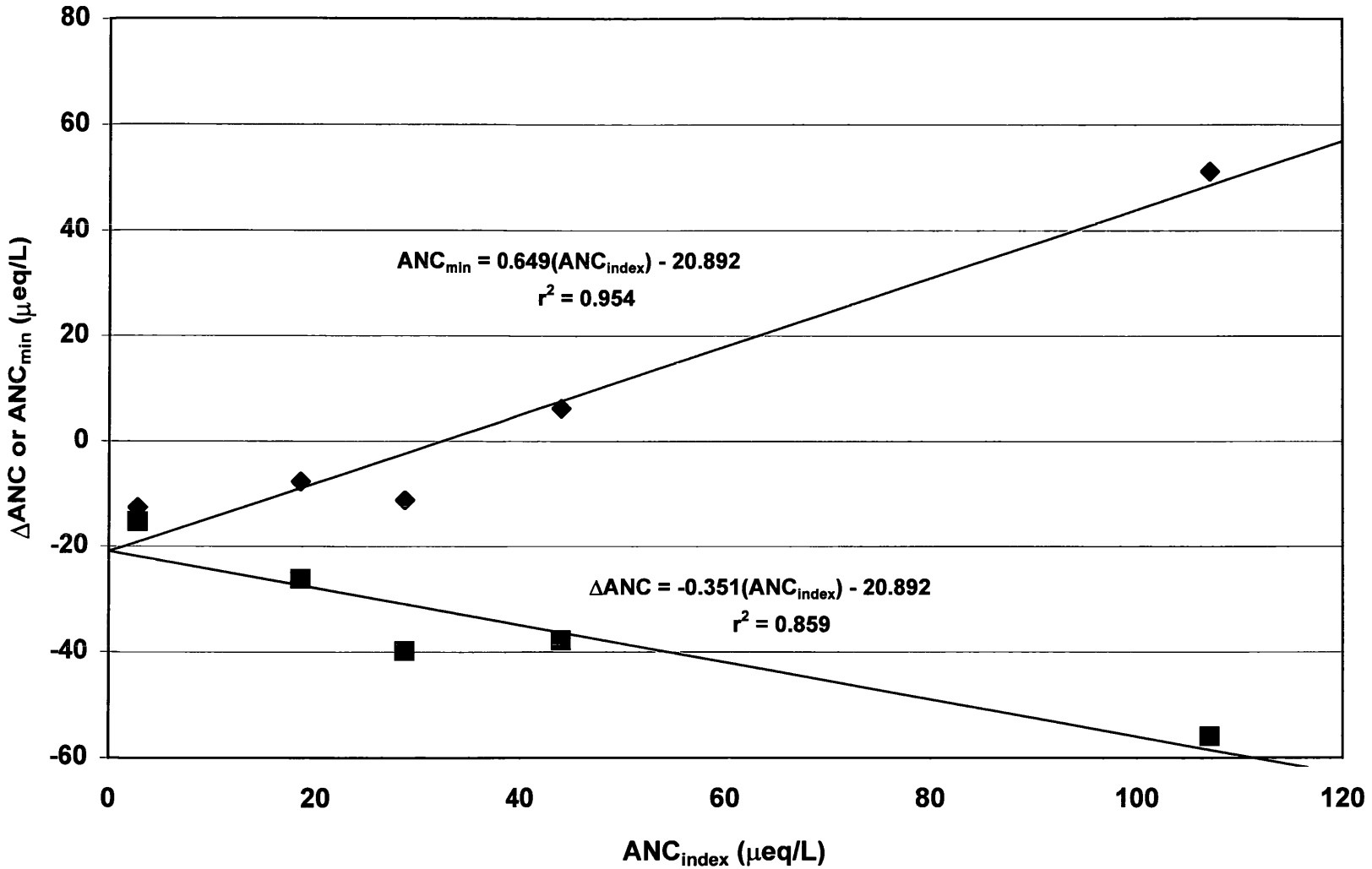

Figure 4.34. Relationships between ΔANC (solid squares) and ANC_{min} (solid diamonds) vs. ANC_{index} for the five study sites. Linear regression models also shown.

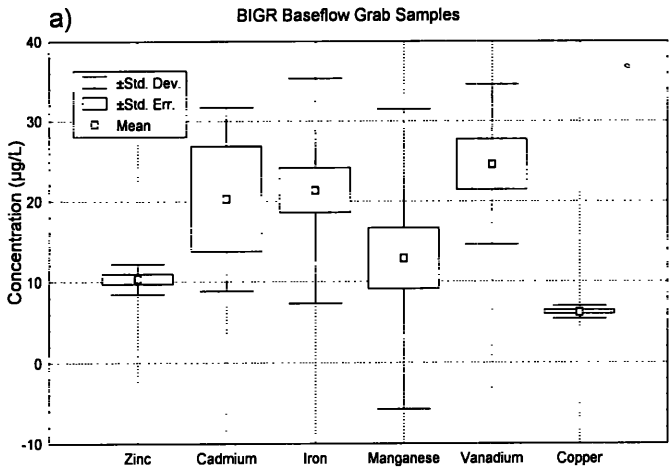

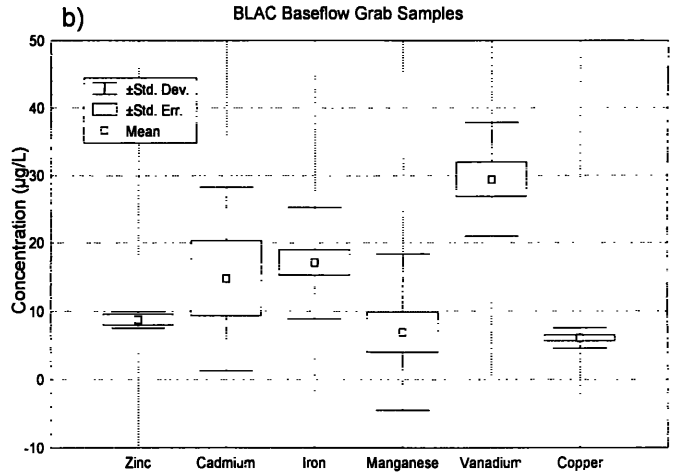

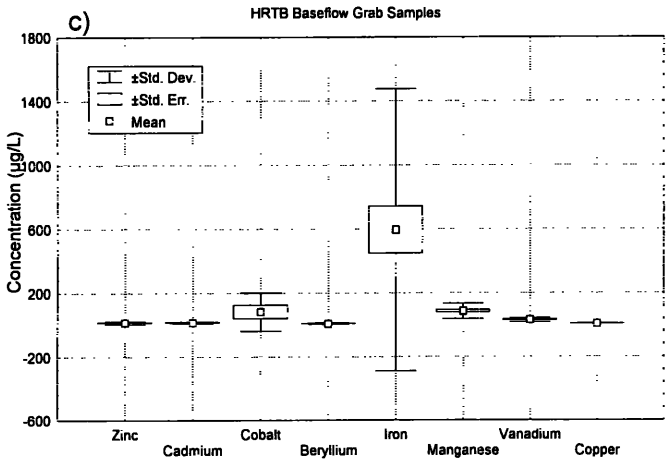

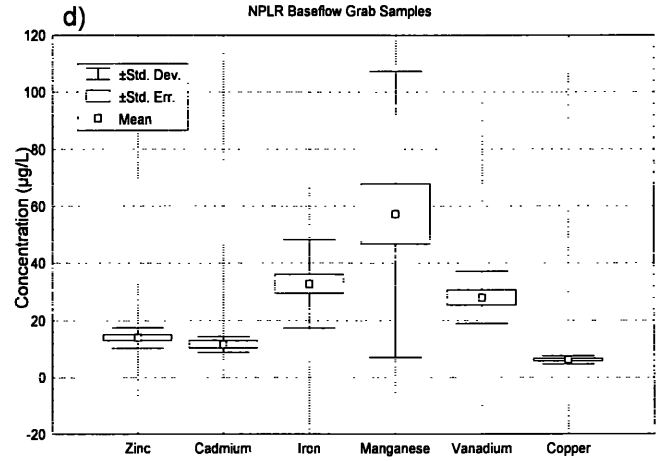

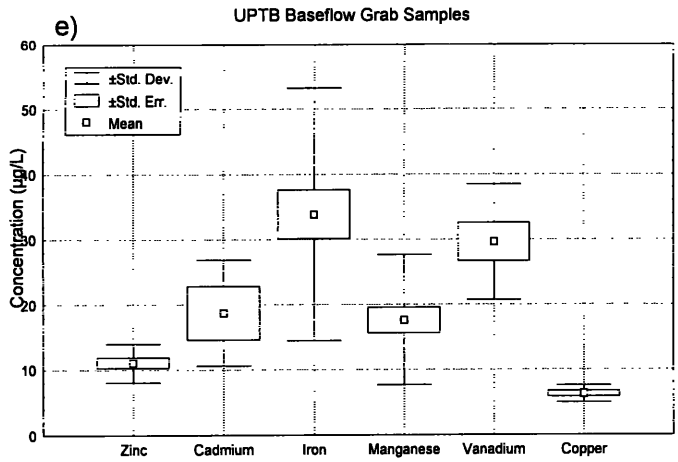

Figure 4.35. Mean low-level dissolved metal concentrations at a) BIGR, b) BLAC, c) HRTB, d) NPLR, and e) UPTB measured during the study.

at certain points on the storm hydrograph at all five sites for a number of events (Figures 4.36 – 4.40). Each intensively sampled event will be discussed individually.

The first event sampled for both low-level and trace metals was a rainfall event in late fall (November 6-10) of 1997. This event was of a moderate magnitude and was accompanied by minor changes in pH and ANC. ANC at HRTB dropped about 35 μeq/L and remained above zero (Figure 4.41), while ANC at BLAC dropped about 50 μeq/L but was well above 50 μeq/L for the duration of the event (Figure 4.42). Iron and manganese were detected at BLAC and HRTB before, during, and after the episode. Zinc was also detected at HRTB near the peak on the falling limb of the hydrograph. Rises in iron and manganese concentrations and the appearance of zinc at HRTB also correspond with marked decreases in ANC and pH. Concentrations for all metals at HRTB rose after increases in discharge and then remained above baseflow levels throughout the entire event. Manganese concentrations at HRTB both before, during, and after the event were above the ET of 80 μg/L, which is cause for concern.

The hydrograph at BLAC for this event exhibited two peaks in discharge. The peak in iron concentration occurred shortly after the first peak. The peak in manganese occurred near the second peak in discharge. At BLAC, both iron and manganese also remained above baseflow levels throughout the event, although they never approached the ET.

The first winter event (February 10-15, 1998) was a rain-on-snow event that was of a relatively short duration. This event was accompanied by only slight changes in pH and ANC (Figures 4.43, 4.44). ANC at HRTB never dropped below zero and ANC at BLAC only dropped about 10 μeq/L and remained well above 50 μeq/L. A larger quantity of metals was detected at both sites during this event then during the fall event. This would be expected if atmospheric pollutants were being deposited on and then accumulated in the snowpack. Zinc, iron, manganese, and copper were detected at HRTB during this event. Slight increases in manganese, iron, and zinc were observed shortly after the peak in the hydrograph. The copper results exhibited more noise and did not suggest a pattern related to flow or other variables. This might be due to measuring concentrations so close to the detection limit. It might also be important to point out that concentrations of manganese and iron at both sites were lower before, after, and during this February event than they were during November. At the conclusion of sampling for this event, all metals were either at or below the levels they were at the beginning of the event. Manganese, though, was again at concentrations higher than the ET. Concentrations were either near or above 100 μg/L during the entire event. Iron, manganese, and copper were detected at BLAC during the first February event, but no clear patterns in metal concentration could be detected from the results for BLAC.

The second winter event (February 16-21, 1998) was of a much greater magnitude than the first February event and was also a rain-on-snow event. ANC at HRTB dropped only about 10 μeq/L but fell below zero after the initial peak in flow and remained negative for the duration of the event (Figure 4.45). ANC at BLAC dropped about 35 μeq/L and fell below 50 μeq/L after peak discharge (Figure 4.46). Iron, manganese, zinc, and cadmium were detected at HRTB

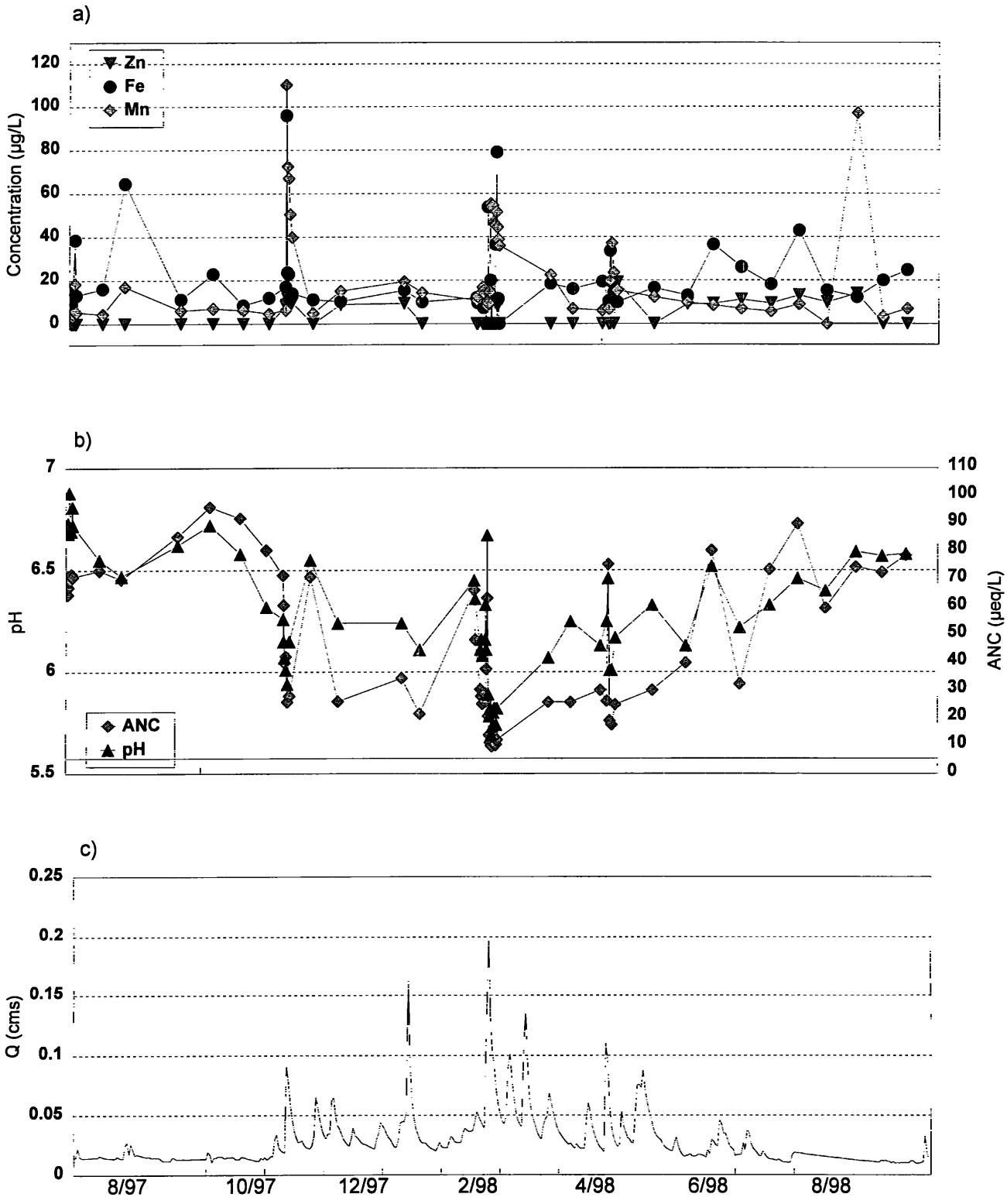

Figure 4.36. Temporal variations in a) Zn, Fe, and Mn, b) ANC and pH, and c) discharge at BIGR during the project.

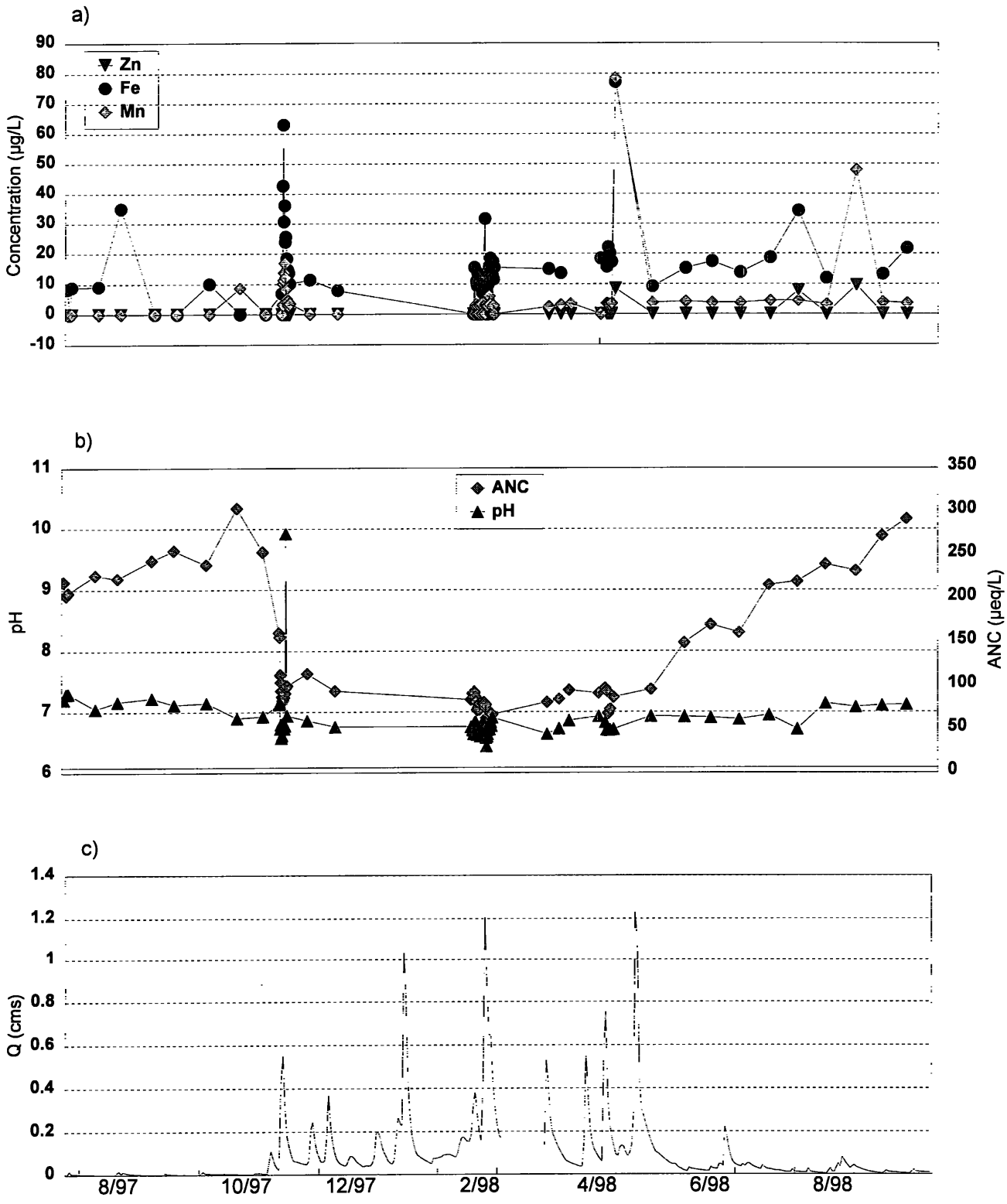

Figure 4.37. Temporal variations in a) Zn, Fe, and Mn, b) ANC and pH, and c) discharge at BLAC during the project.

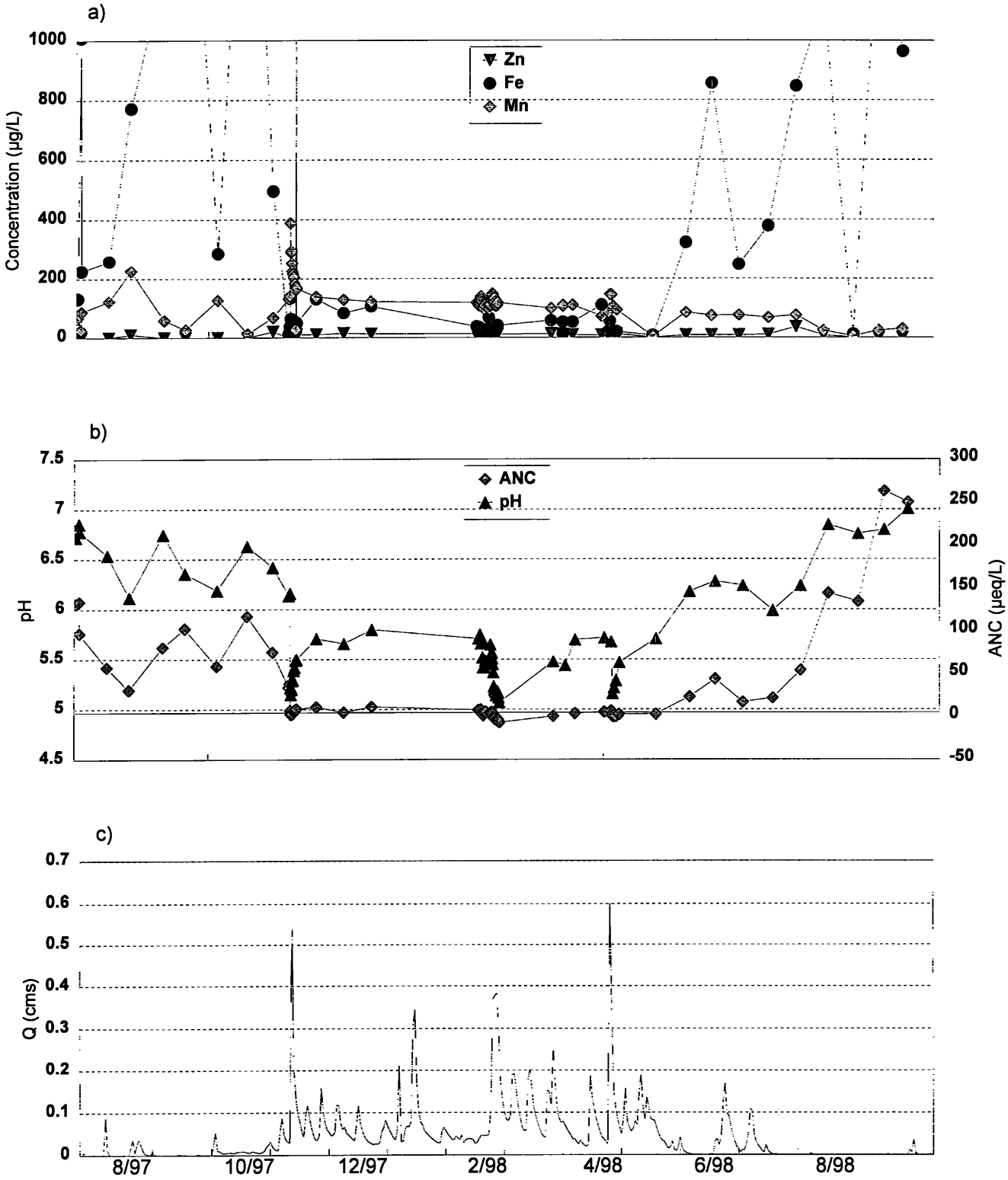

Figure 4.38. Temporal variations in a) Zn, Fe, and Mn, b) ANC and pH, and c) discharge at HRTB during the project.

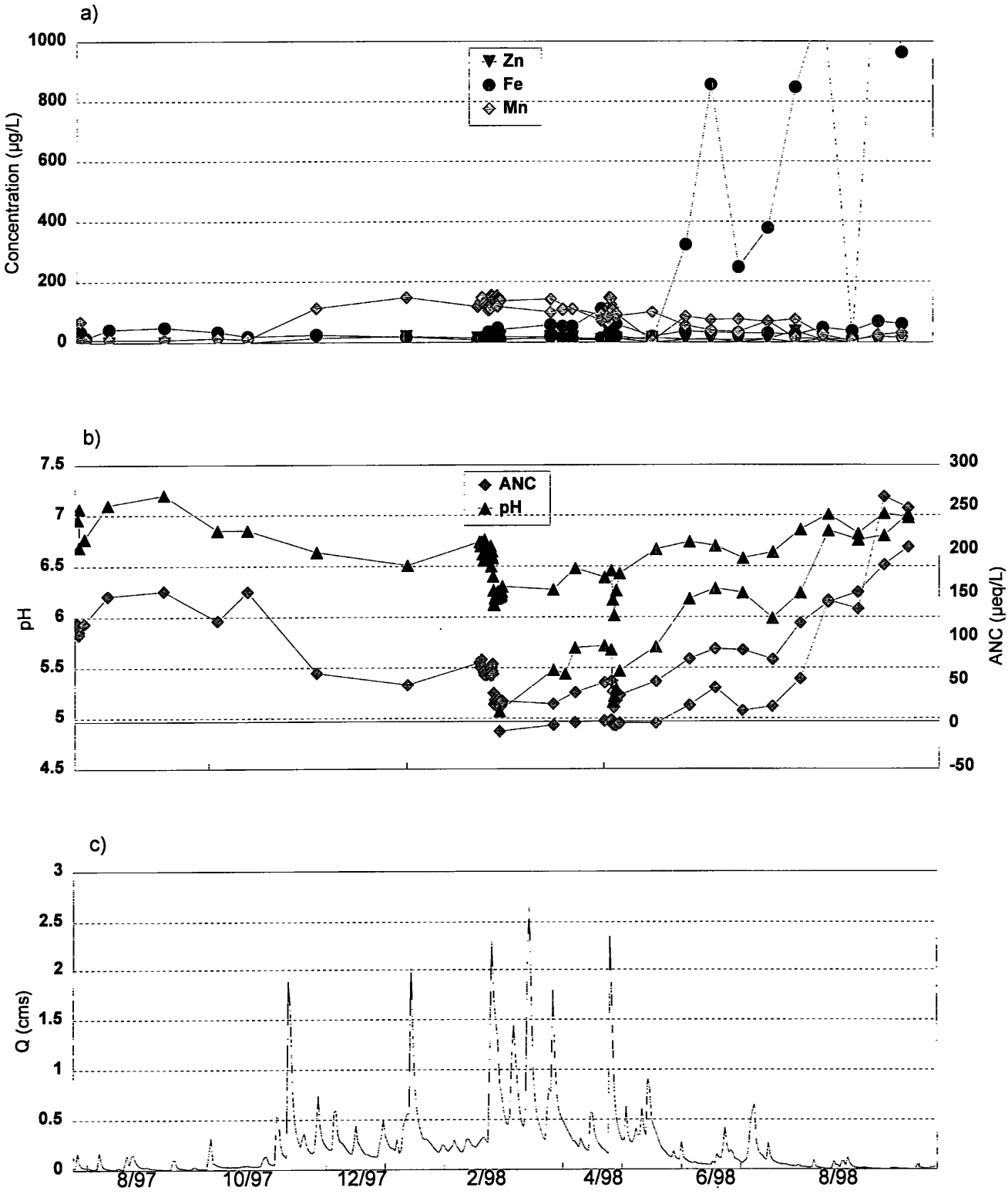

Figure 4.39. Temporal variations in a) Zn, Fe, and Mn, b) ANC and pH, and c) discharge at NPLR during the project.

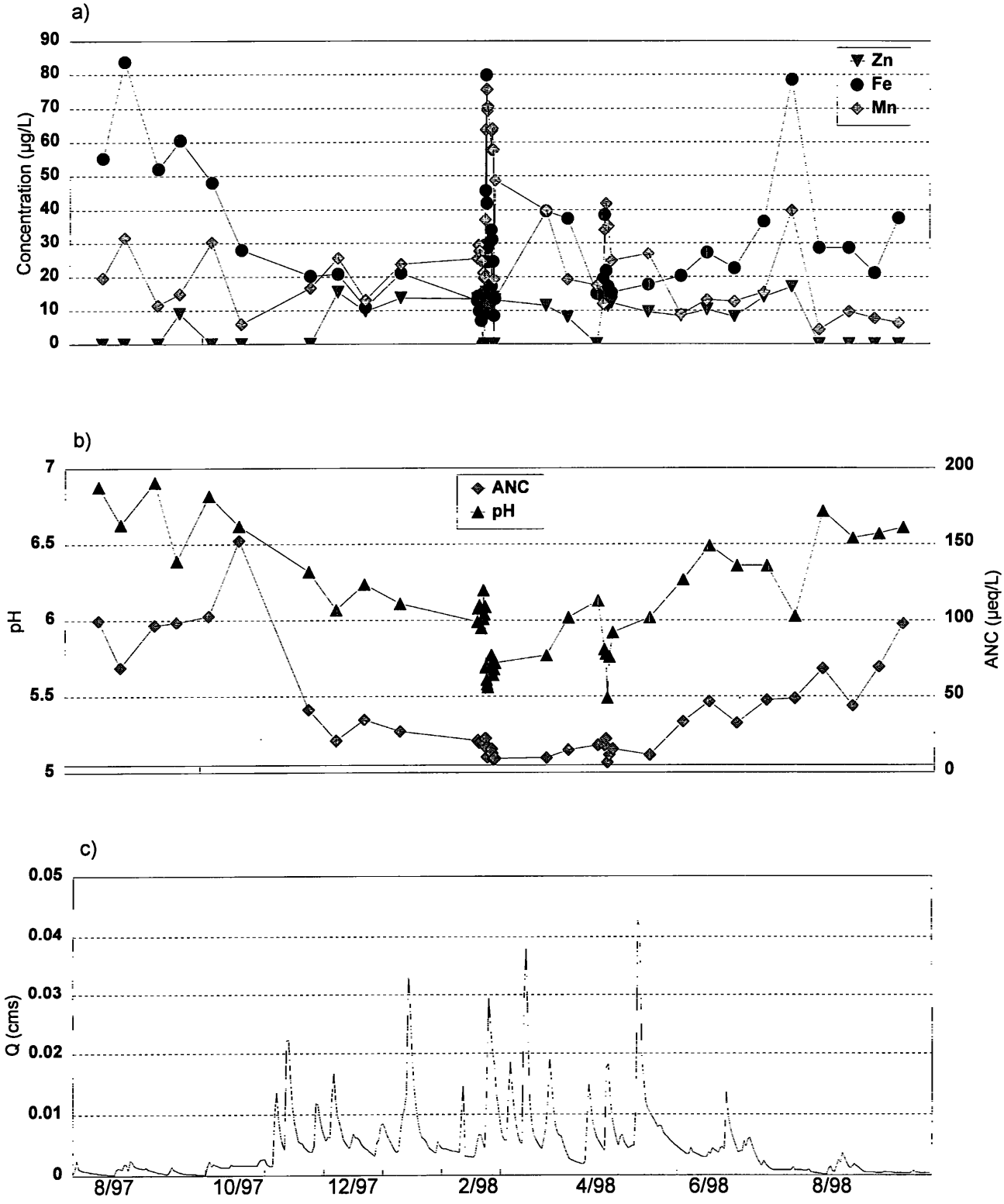

Figure 4.40. Temporal variations in a) Zn, Fe, and Mn, b) ANC and pH, and c) discharge at UPTB during the project.

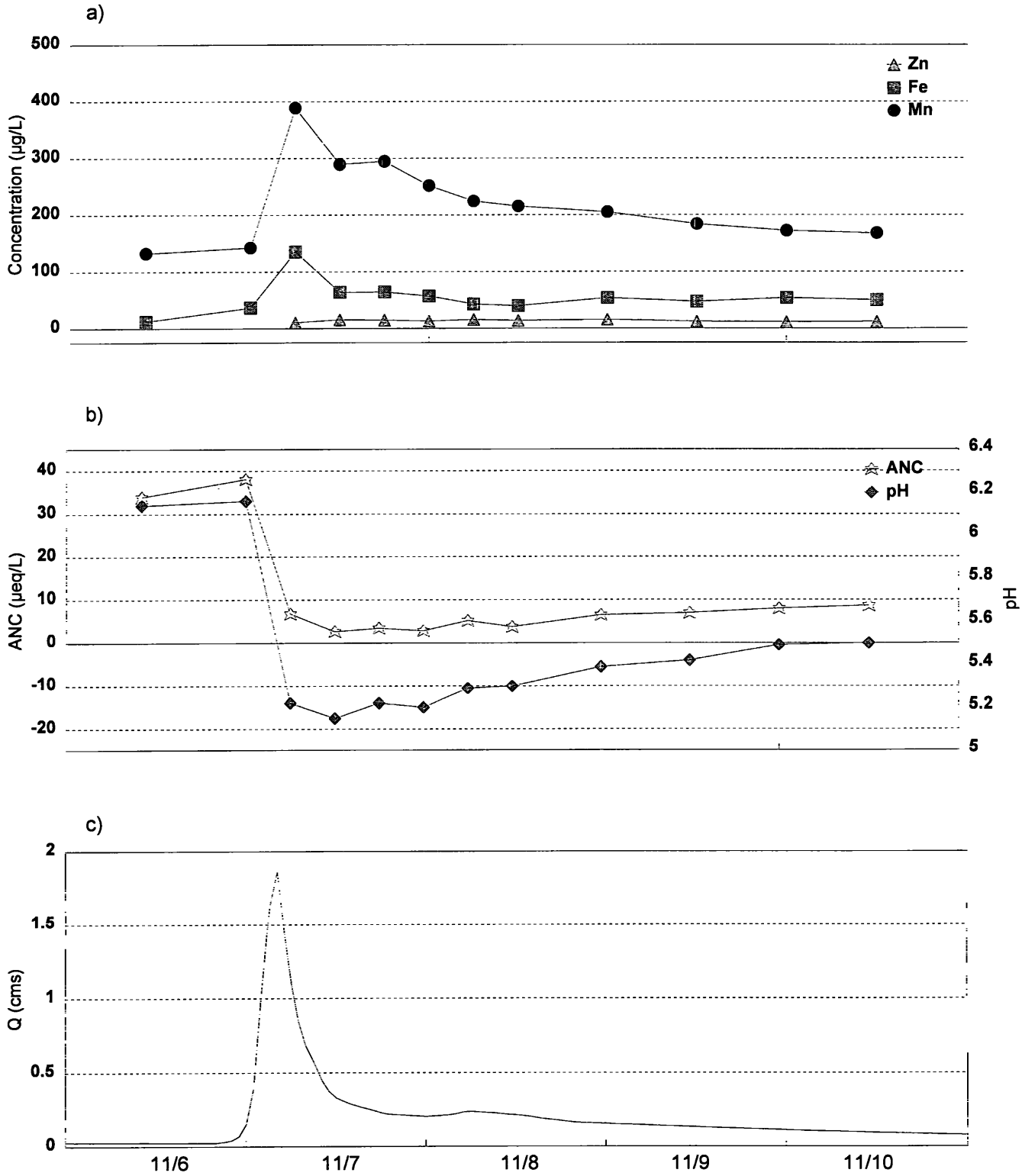

Figure 4.41. Temporal variation in a) dissolved low-level metals, b) ANC and pH, and c) discharge at HRTB during the period November 6-10, 1997.

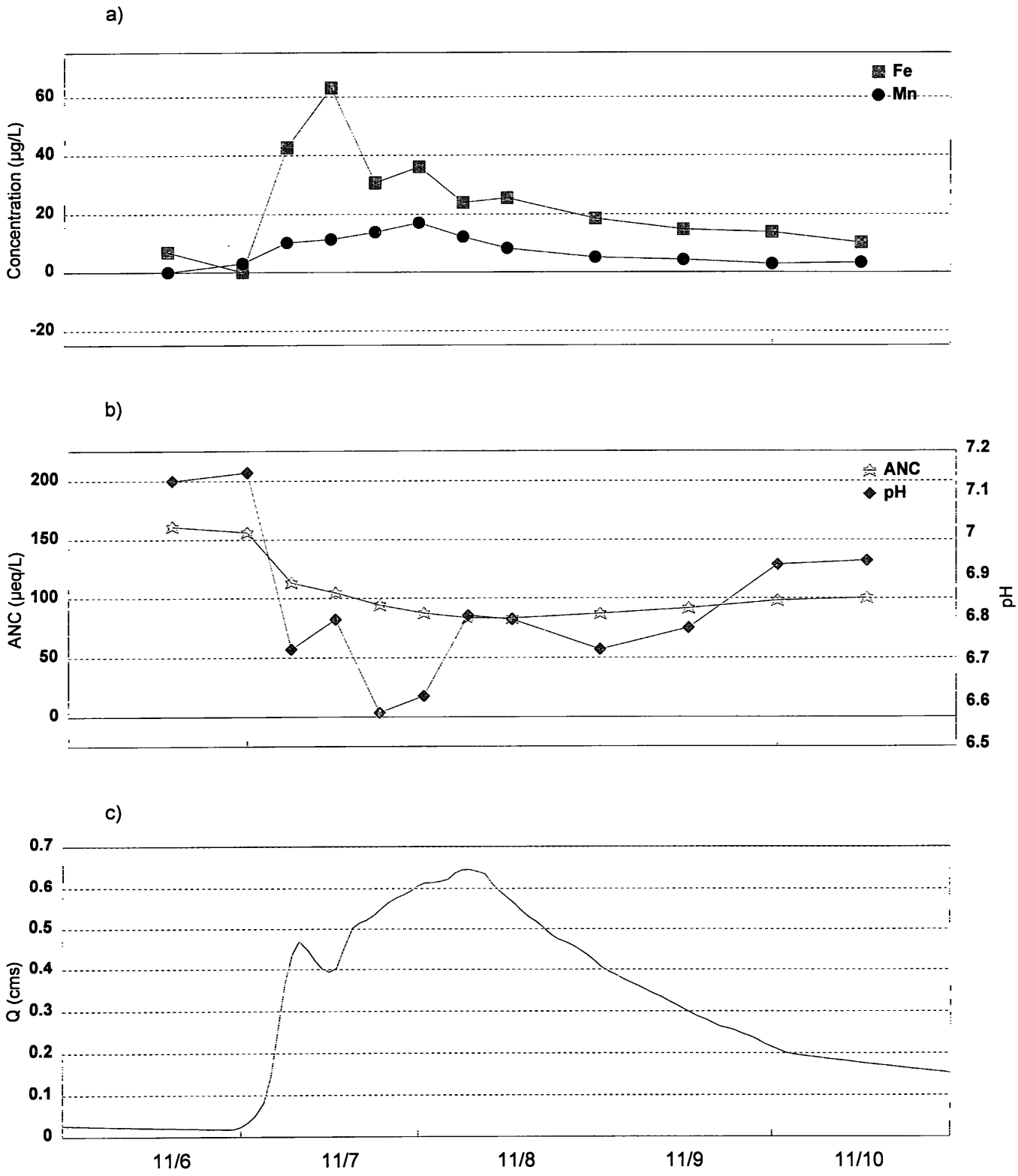

Figure 4.42. Temporal variations in a) dissolved low-level metals, b) ANC and pH, and c) discharge at BLAC during the period November 6-10, 1997.

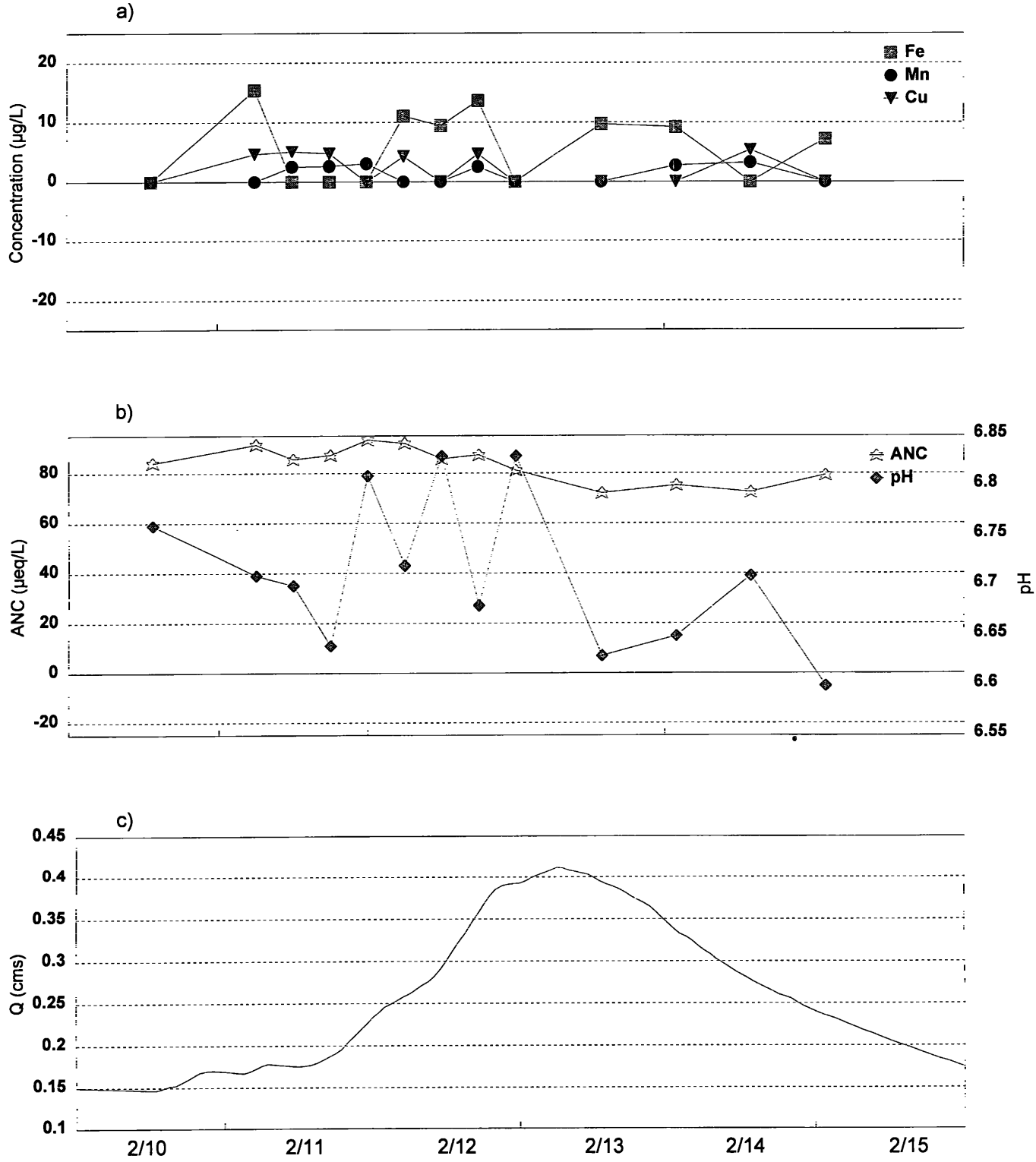

Figure 4.43. Temporal variations in a) dissolved low-level metals, b) ANC and pH, and c) discharge at BLAC during the period February 10-15, 1998.

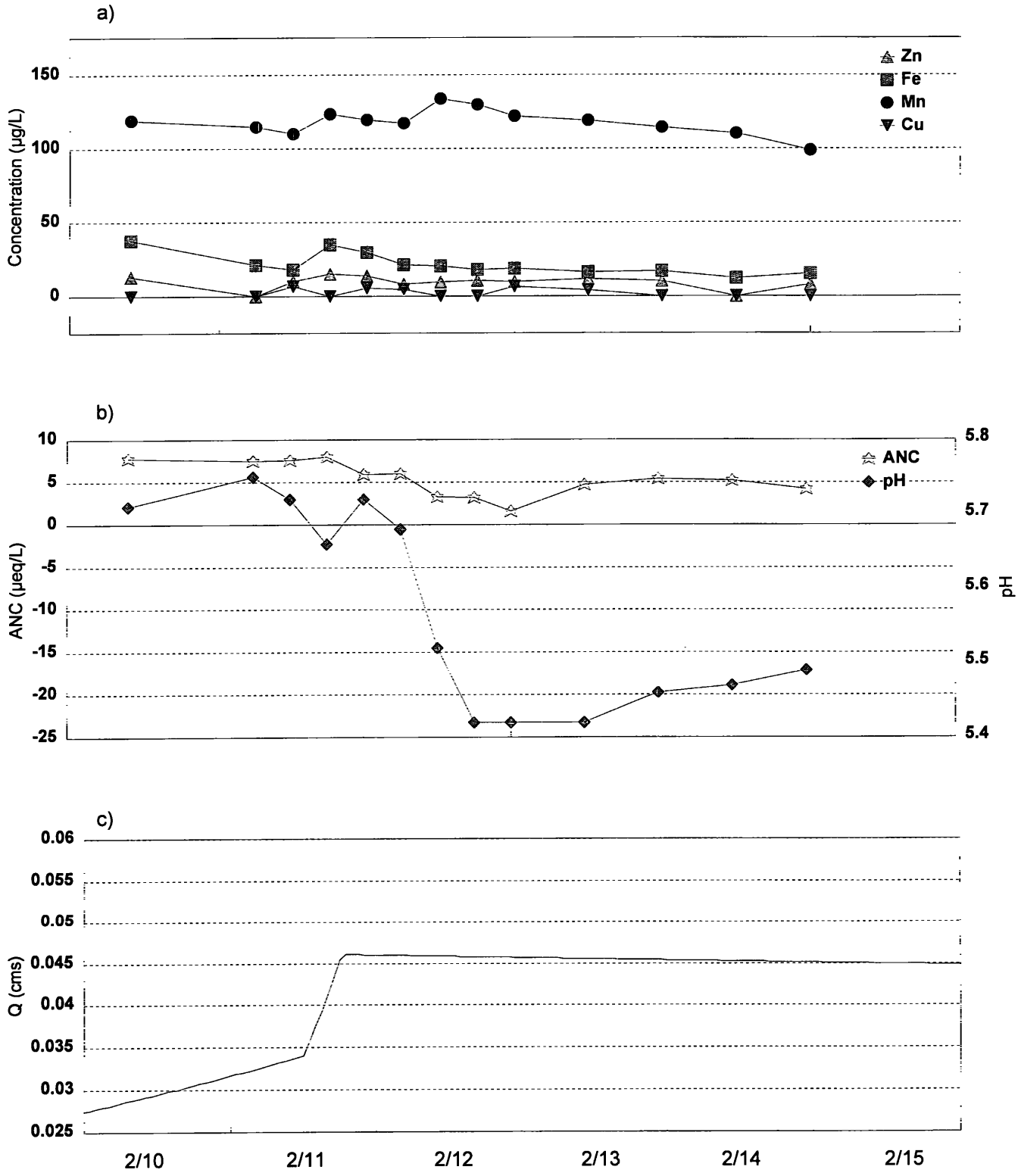

Figure 4.44. Temporal variations in a) dissolved low-level metals, b) ANC and pH, and c) discharge at HRTB during the period February 10-15, 1998.

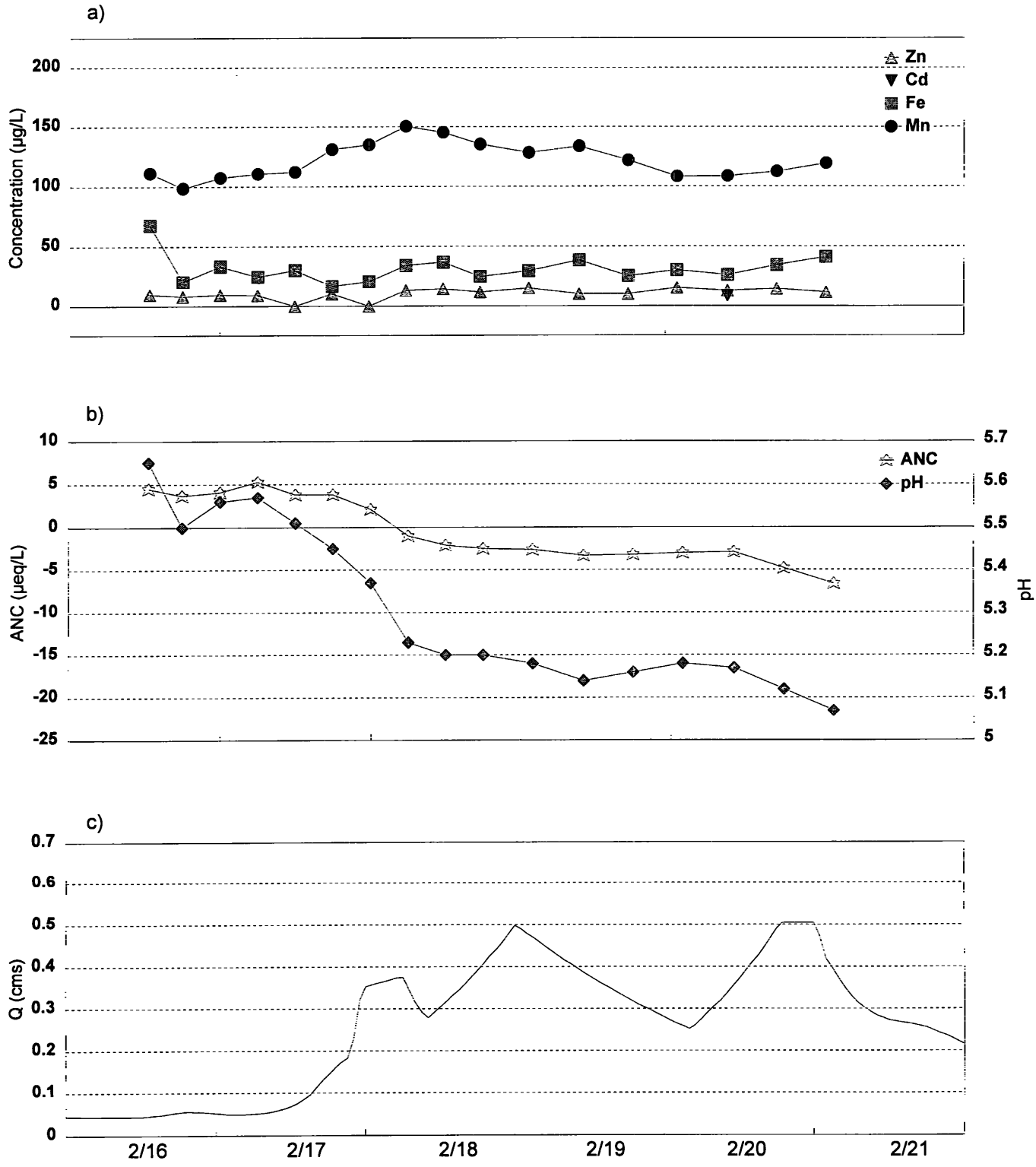

Figure 4.45. Temporal variations in a) dissolved low-level metals, b) ANC and pH, and c) discharge at HRTB during the period February 16-21, 1998.

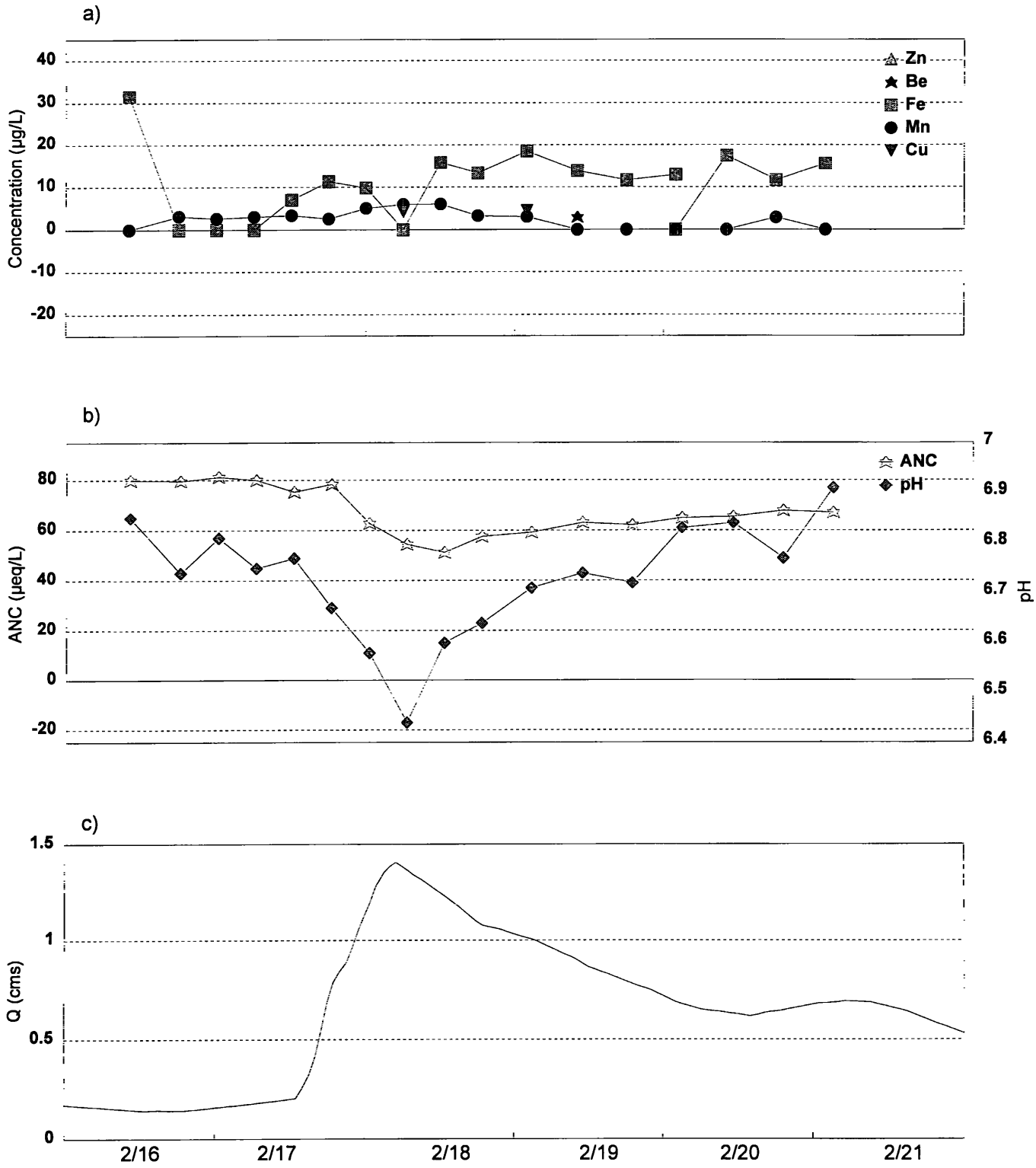

Figure 4.46. Temporal variations in a) dissolved low-level metals, b) ANC and pH, and c) discharge at BLAC during the period February 16-21, 1998.

during the second February event. Cadmium was only detected in one sample. Manganese, iron, and zinc concentrations were highest shortly after the initial peak in flow. This would be expected if significant amounts of atmospherically derived pollutants that had accumulated on the snowpack were released with the initial snowmelt. Concentrations were back down to about their initial concentration by the end of the event. Again, manganese concentrations were higher than the ET for the duration of the event.

Copper and beryllium were detected in only a few isolated samples during the second February event at BLAC (Figure 4.46), therefore patterns and trends could not be discerned. Manganese and iron were also detected at BLAC. Increases in manganese concentrations corresponded to the storm hydrograph. Iron concentrations were also highest just after the peak in discharge. All metal concentrations were back down to or lower than their initial concentration at the conclusion of the event.

Low-level metals analysis was also performed on samples collected from the other three project sites. For this February event at BIGR, ANC decreased by about 50 μeq/L to less than 10 μeq/L and the pH fell from 6.6 to about 5.8 after peak stream flow (Figure 4.47). The decreases in ANC and pH at BIGR for this event were accompanied by an increase in manganese and a decrease in iron concentrations. The increase in iron toward the end of the event could potentially be attributed to sample contamination, especially since copper and chromium were also detected in that single sample and this pattern was not observed for any of the other events. By the conclusion of sampling, manganese concentrations had not yet reached baseflow levels. Manganese concentrations remained below the 80 μg/L ET level.

UPTB exhibited similar responses in ANC and pH as BIGR (Figure 4.48). Zinc, iron, and manganese were detected at UPTB during the second February event. The drop in pH and ANC on the upper part of the falling limb of the storm hydrograph were accompanied by a drastic increase in manganese concentration and a slight increase in zinc concentration. Iron concentrations peaked at about 80 μg/L right at peak flow and then fell to about pre-event levels. None of the metals approached the ET's at UPTB for this event.

At NPLR, ANC decreased by about 50 μeq/L to less than 30 μeq/L during the second February event (Figure 4.49). Manganese, zinc and iron were detected throughout the event, while copper, cadmium and beryllium were detected in samples at sporadic points during the event. The drop in ANC and pH were accompanied by increases in manganese, zinc, and iron. Increases in zinc and iron were slight, while the increase in manganese was more marked. Manganese concentrations were higher than the ET of 80 μeq/L before, during, and after the event.

The spring event (April 18-23, 1998) was also sampled for low-level metals. At HRTB, ANC levels dropped below zero for most of the event (Figure 4.50) and were accompanied by a decrease in pH of about 0.5 units. Increases in iron and manganese were observed when pH and ANC dropped. Cadmium and copper were also detected in this sample. At the conclusion of the

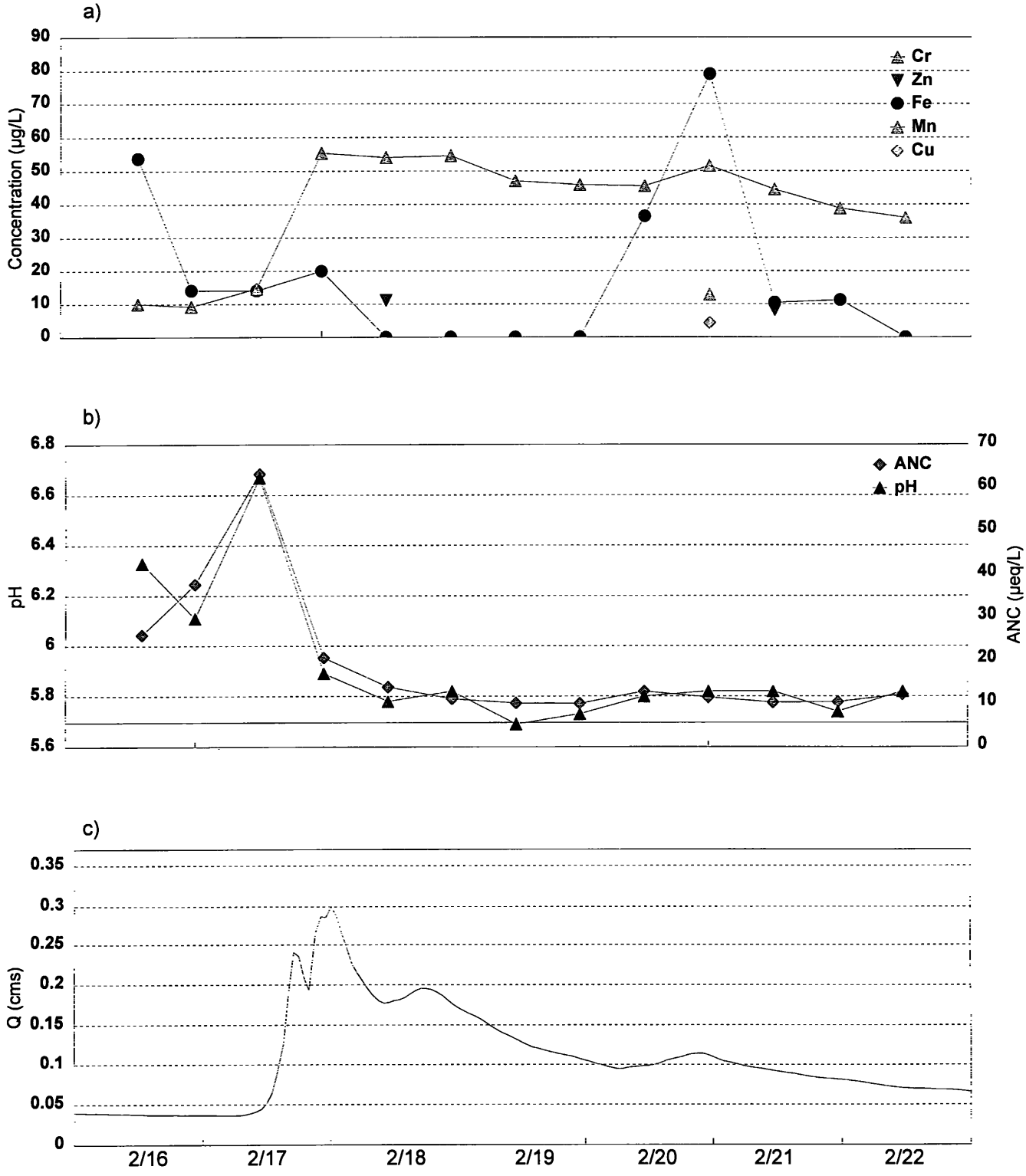

Figure 4.47. Temporal variations in a) dissolved low-level metals, b) ANC and pH, and c) discharge at BIGR during the period February 16-21, 1998.

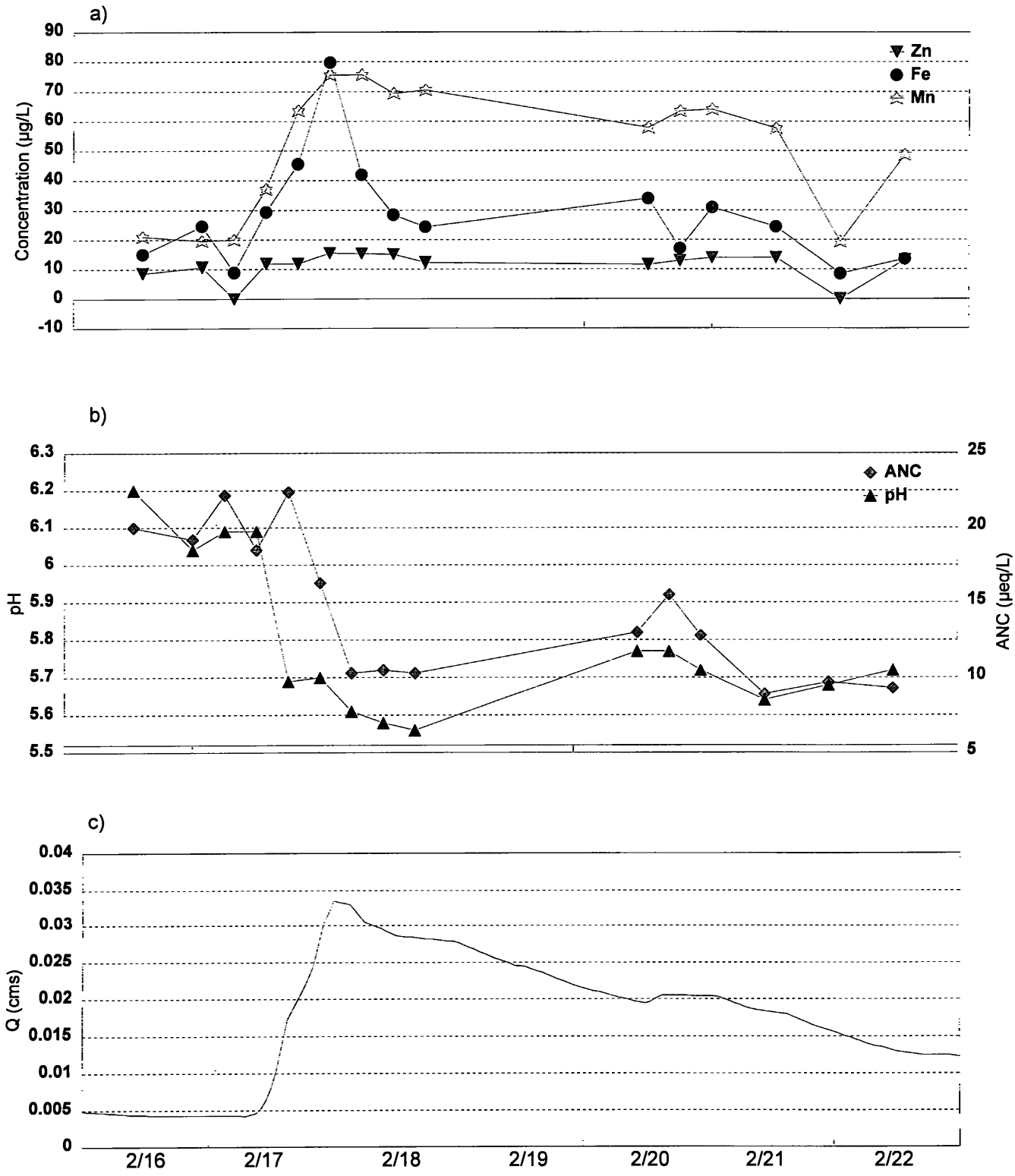

Figure 4.48. Temporal variations in a) dissolved low-level metals, b) ANC and pH, and c) discharge at UPTB during the period February 16-21, 1998.

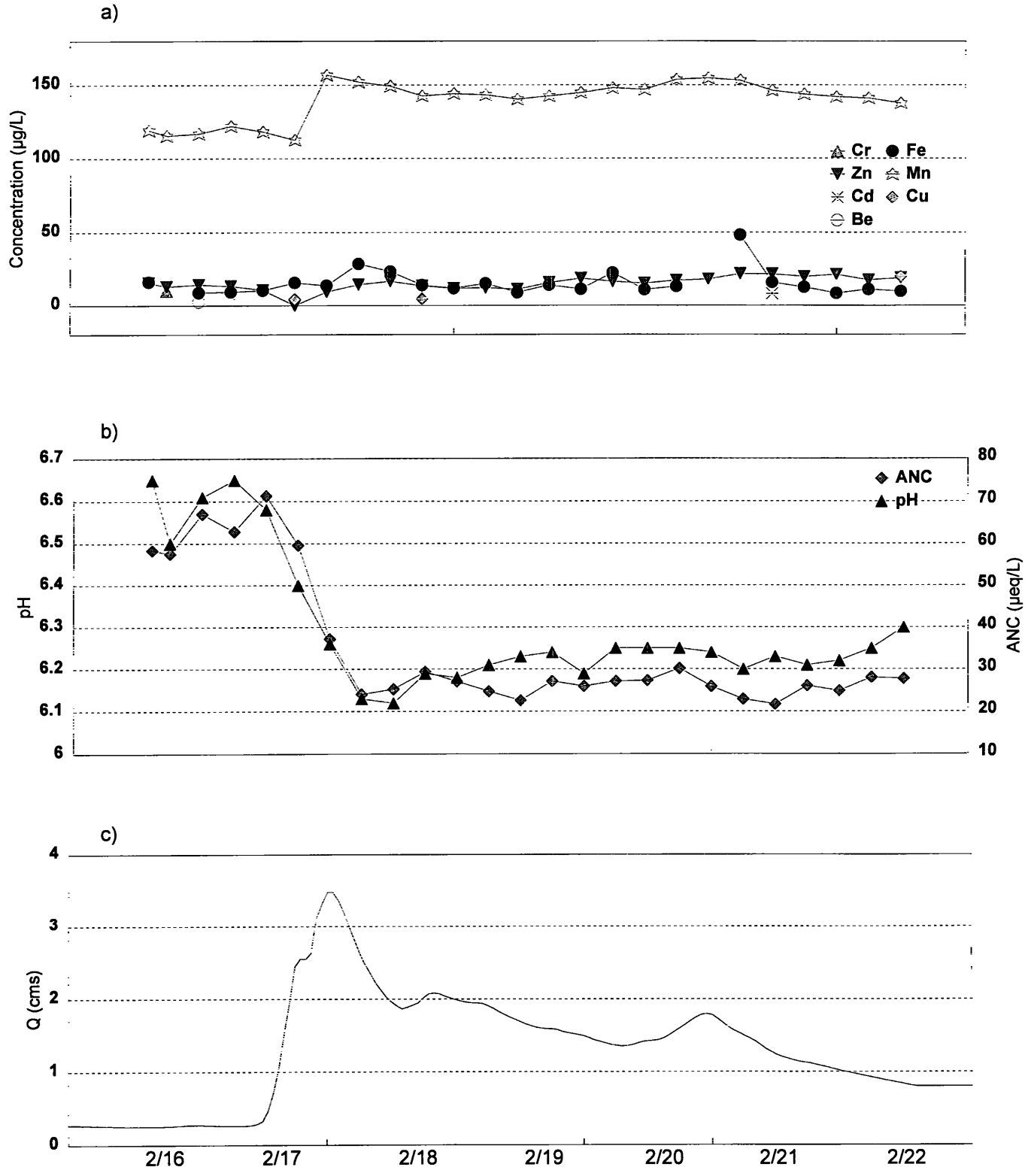

Figure 4.49. Temporal variations in a) dissolved low-level metals, b) ANC and pH, and c) discharge at NPLR during the period February 16-21, 1998.

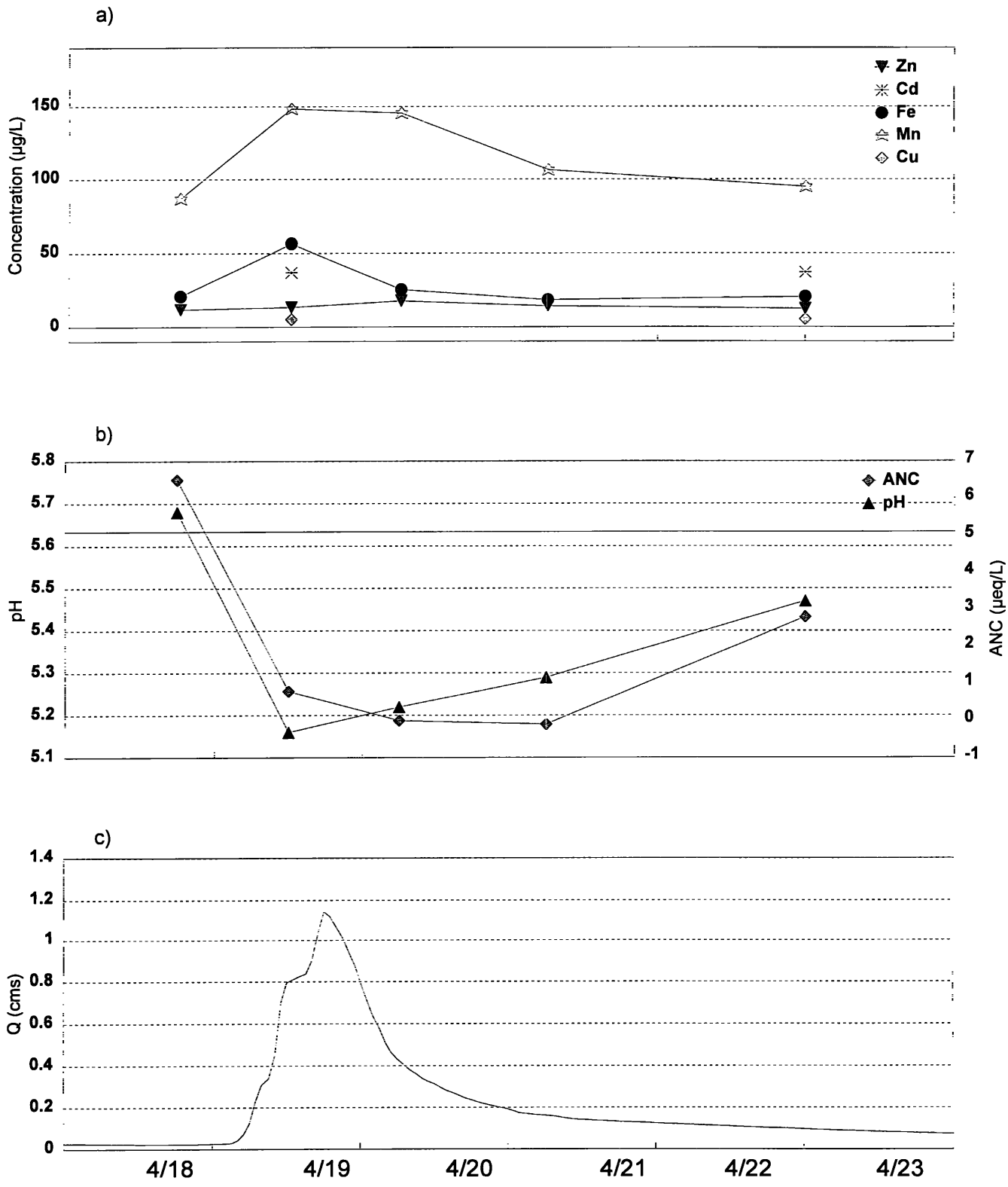

Figure 4.50. Temporal variations in a) dissolved low-level metals, b) ANC and pH, and c) discharge at HRTB during the period April 18-22, 1998.

event, iron and manganese were back down to pre-event levels, but manganese was above the ET of 80 μg/L for most of the episode.

At BLAC, ANC levels decreased by almost 30 μeq/L and pH fell to about 6.7 after peak discharge (Figure 4.51). Manganese, iron, copper, and cadmium were detected in samples during the event. There was not much temporal variation in concentrations of each metal. The sample analyzed at the conclusion of the event exhibited elevated metal concentrations. This was probably due to sample contamination, especially since this condition was never observed at BLAC during any of the other events.

The decreases in pH and ANC at BIGR for the April event were accompanied by an increase in manganese concentrations (Figure 4.52). Zinc was also detected in this sample. At peak flow, ANC and pH were higher than at baseflow. When pH and ANC increased, iron also increased. The iron concentration then decreased after peak flow. Copper was also detected at a few points during the event. Copper concentration increased with iron and then decreased to about its pre-event level.

Zinc, cadmium, copper, manganese, beryllium and iron were detected at UPTB during the April event (Figure 4.53). ANC levels dropped by about 15 μeq/L. The decreases in ANC and pH were accompanied by increases in the following metals: beryllium, copper, manganese, and zinc. Iron concentrations initially rose during the event but decreased with the drop in pH and ANC.

The April event at NPLR exhibited a change in ANC of about 20 μeq/L (Figure 4.54). Zinc, cadmium, iron, manganese and copper were detected at this site. Cadmium was detected in the first two samples and was not measure in any of the other samples. Manganese concentrations tracked the drop in ANC and pH and rose to above the ET of 80 μg/L. Iron initially increased and then decreased with the decrease in pH and continued to decrease for most of the event. Copper concentrations remained relatively stable in response to changes in flow and acid-base chemistry. A discernable pattern of response for zinc was also not observed.

We examined all data to determine if there were relationships among metal concentrations and pH, ANC, and stream discharge. Pearson correlation analysis was performed to determine if there were any linear relationships between the metals analyzed and the other water quality and quantity variables (Table 4.4). When all sites were grouped together, there was a significant relationship between manganese and flow (Figure 4.55a). There were significant positive linear relationships between discharge and manganese concentrations at BIGR, HRTB, NPLR, and UPTB (Figure 4.56). Manganese concentrations, though, at BLAC did not change in response to an increase in discharge. This relationship between manganese and discharge exhibited at all of the sites except BLAC might also be influenced by stream pH. BLAC had the highest pH levels and were fairly stable throughout most events (Figure 4.37), while the other sites underwent more dynamic pH changes during storm events. Therefore, the strong positive relationship between pH and manganese for all sites could be influencing this relationship.

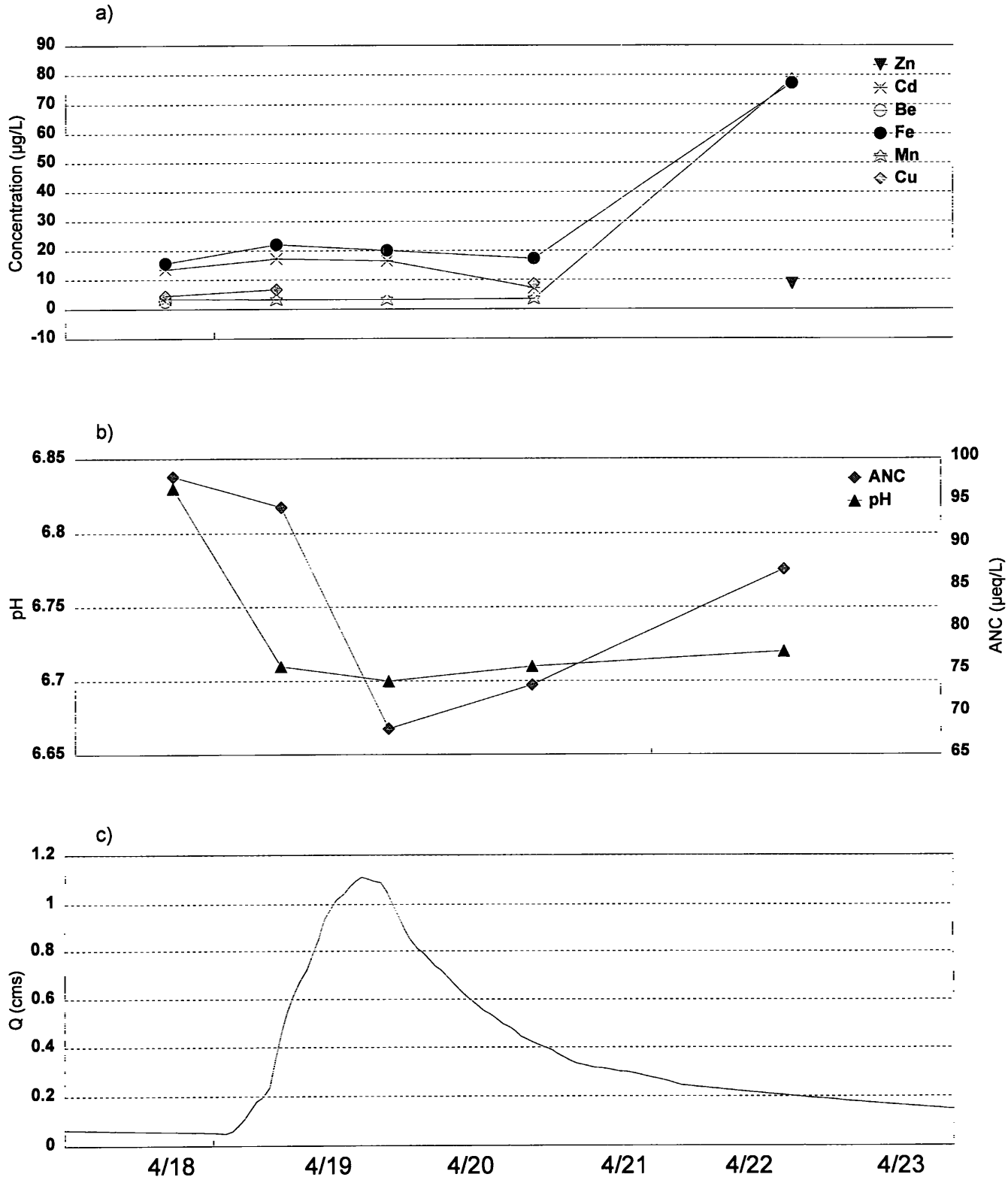

Figure 4.51. Temporal variations in a) dissolved low-level metals, b) ANC and pH, and c) discharge at BLAC during the period April 18-22, 1998.

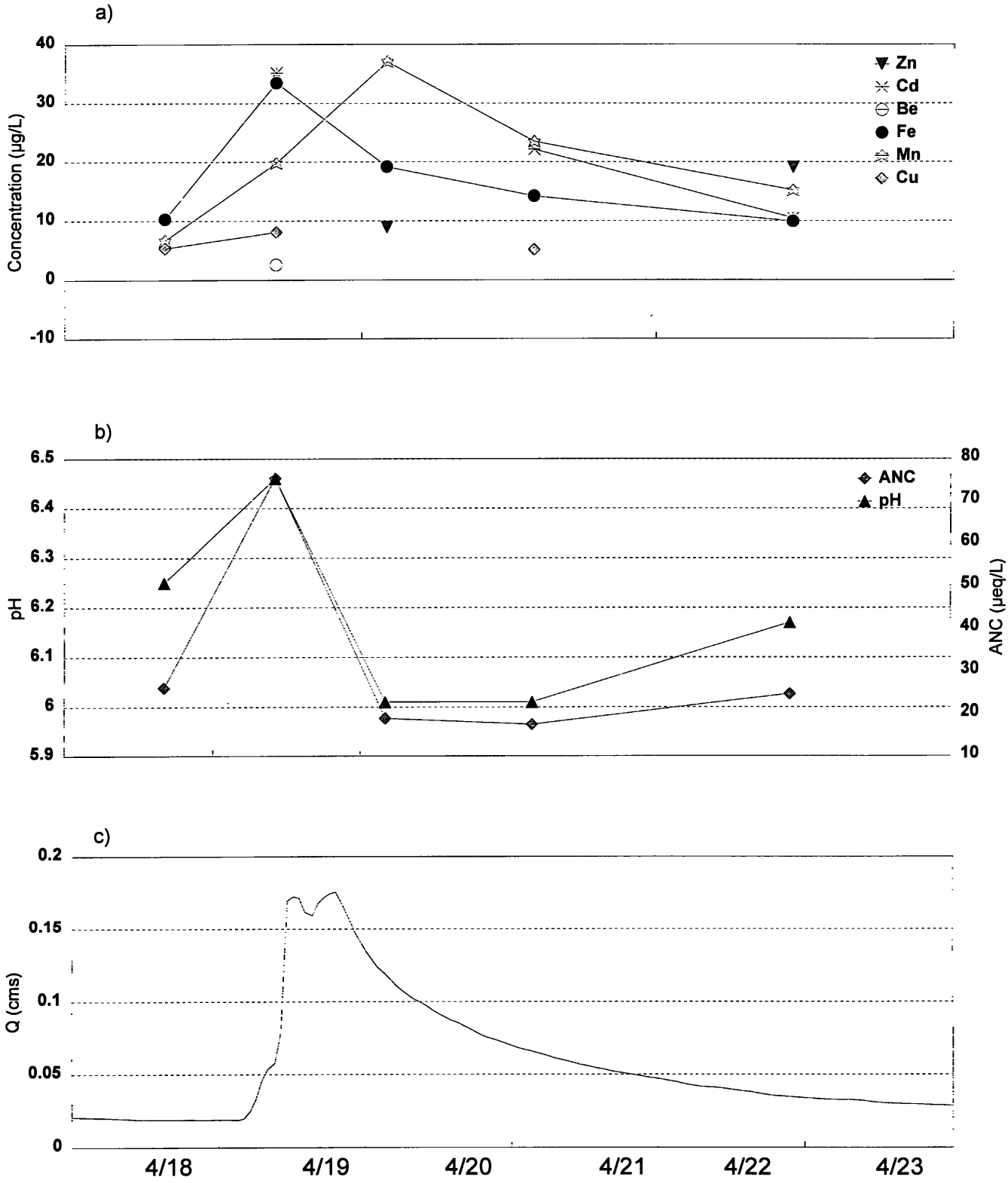

Figure 4.52. Temporal variations in a) dissolved low-level metals, b) ANC and pH, and c) discharge at BIGR during the period April 18-22, 1998.

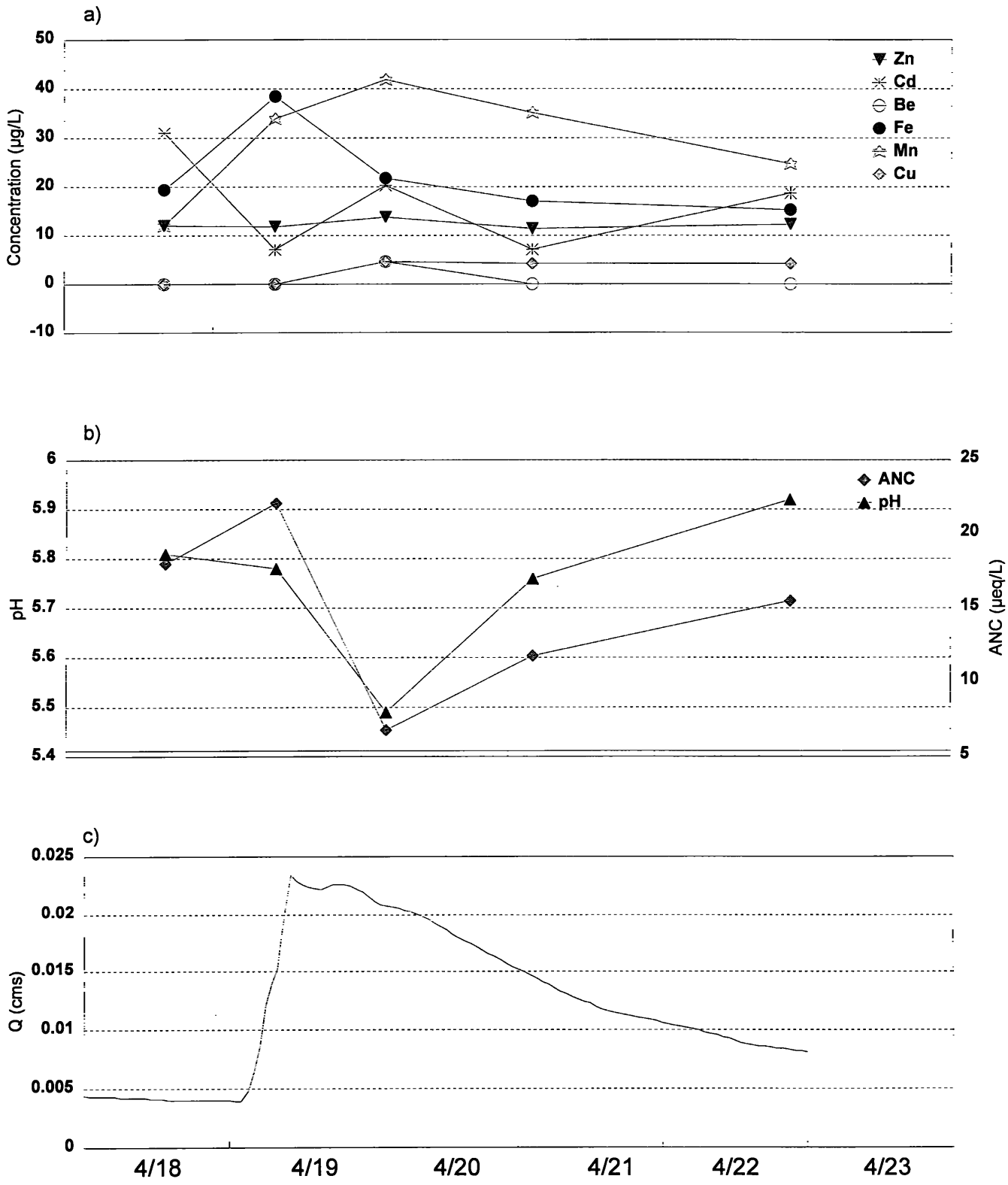

Figure 4.53. Temporal variations in a) dissolved low-level metals, b) ANC and pH, and c) discharge at UPTB during the period April 18-22, 1998.

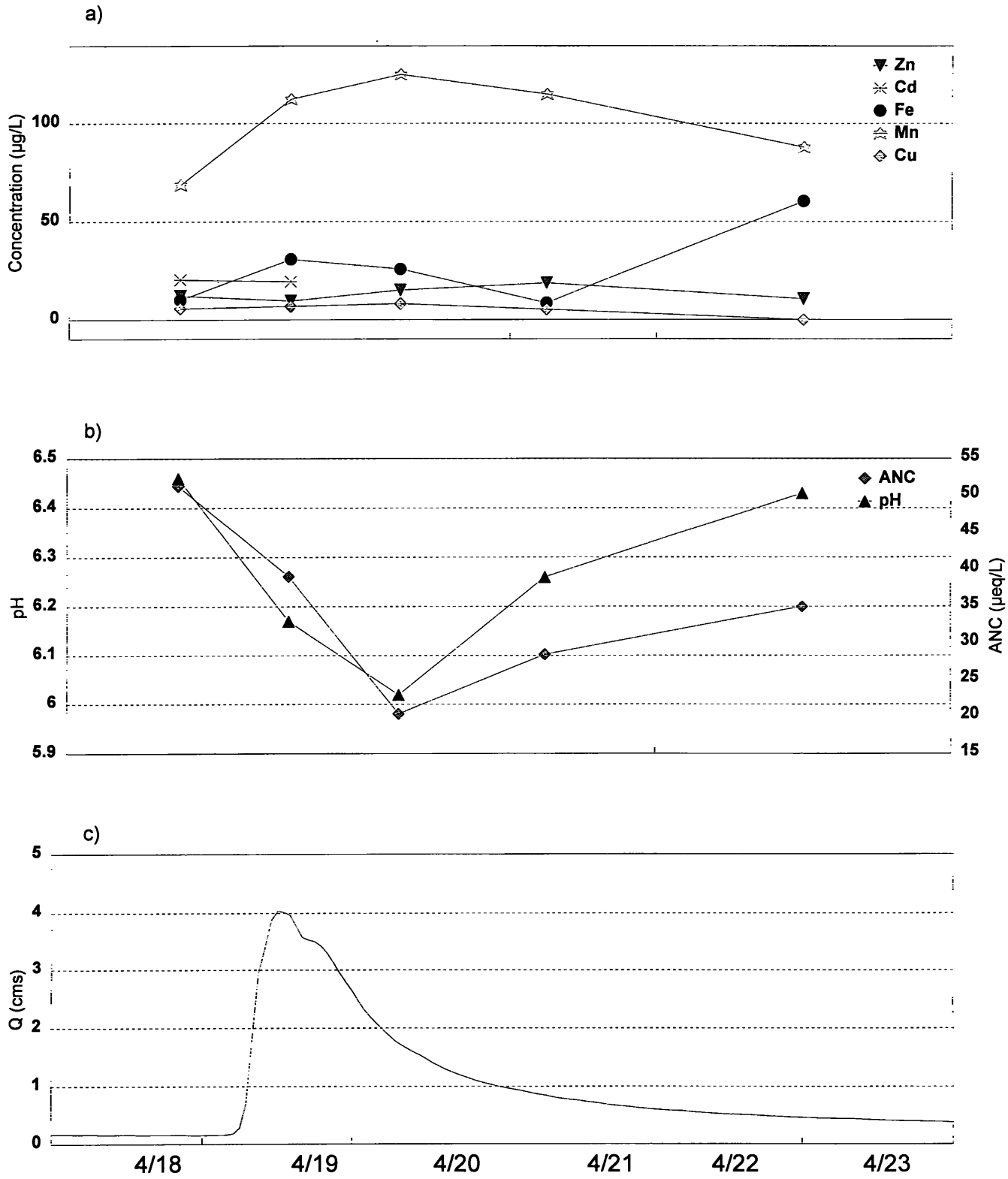

Figure 4.54. Temporal variations in a) dissolved low-level metals, b) ANC and pH, and c) discharge at NPLR during the period April 18-22, 1998.

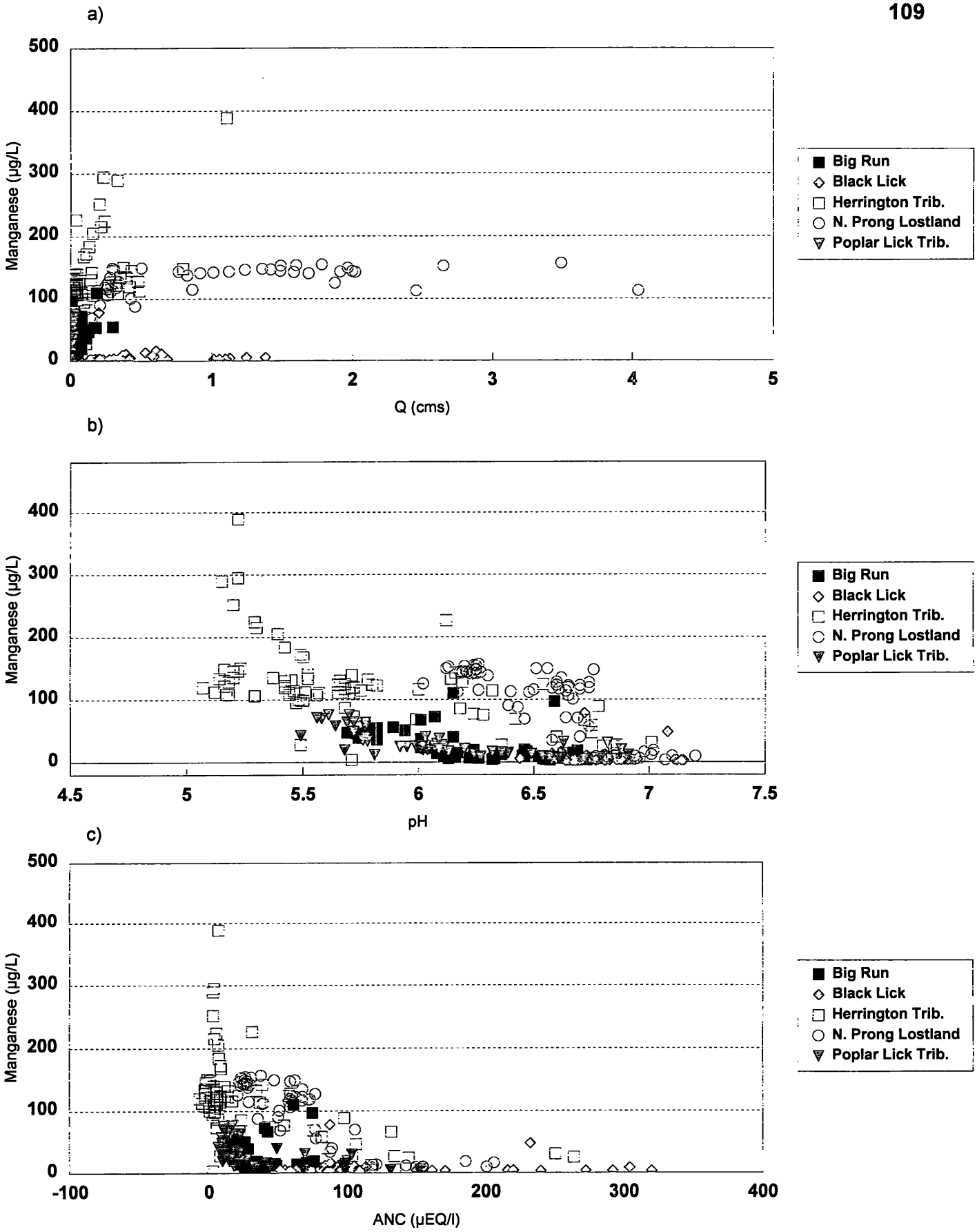

Figure 4.55. Relationship between measured dissolved manganese concentration and a) discharge, b) pH, and c) ANC at the five sites.

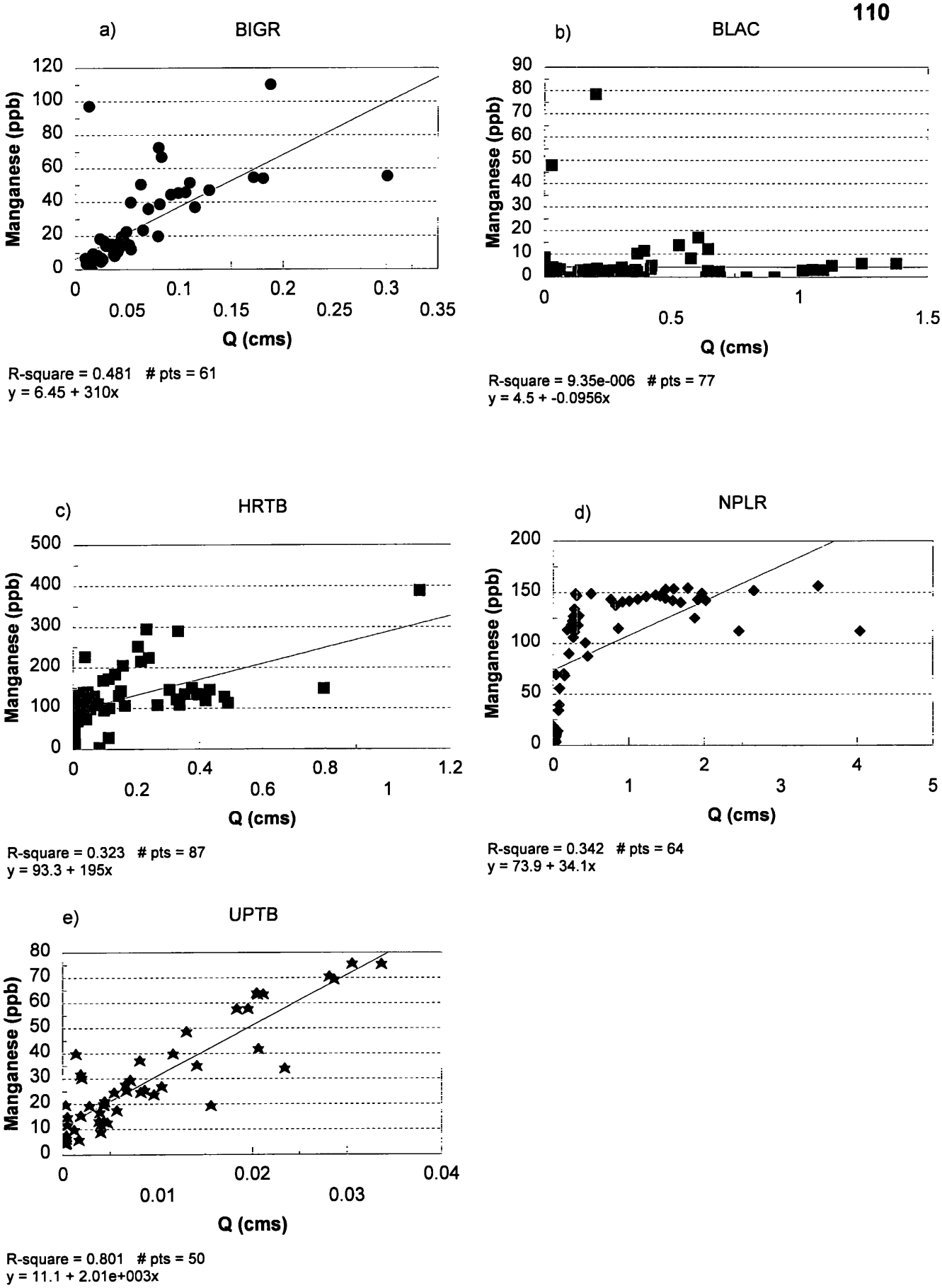

Figure 4.56. Relationship between manganese concentration and discharge at each sampling site.

Table 4.4. Correlation matrix for all low-level metals, discharge, ANC, and pH data. Marked correlations are significant at p <0.05.

Variable	Q	ANC	pH	Cr	Zn	Cd	Co	Be	Fe	Mn	V	Cu
Q	1.00											
ANC	-0.17*	1.00										
pH	-0.03	0.76*	1.00									
Cr	0.47	-0.36	-0.02	1.00								
Zn	0.16*	0.01	0.09	-------	1.00							
Cd	0.04	-0.02	-0.14	-------	-0.12	1.00						
Co	-0.52	0.51	0.67	-------	-0.68	-------	1.00					
Be	-0.28	0.11	0.00	-------	0.07	-0.20	-------	1.00				
Fe	-0.11	0.18*	0.09	-0.02	0.27*	-0.05	0.96*	0.74*	1.00			
Mn	0.35*	-0.48*	-0.56*	-0.12	0.18*	0.07	-0.71*	-0.07	-0.04	1.00		
V	0.15	-0.14	-0.15	-------	-0.21	0.18	-------	-0.87*	-0.15	0.28*	1.00	
Cu	0.05	0.06	0.07	-0.95	0.27	0.09	-------	0.30	-0.00	0.09	-0.23	1.00

The adsorption of manganese oxides are sensitive to pH. As pH increases, manganese is more highly adsorbed to soil particles (Drever, 1988). Therefore, we would expect the significant negative relationship between stream pH and manganese concentration (Table 4.4). We again observed significant relationships between manganese and pH for all of the sites except BLAC (Figure 4.57). Manganese concentrations were highest at HRTB, ranging from 400 ppb to below the detection limit. This stream typically exhibited the lowest pH values. Conversely, pH at BLAC rarely was lower than 6.5 and manganese concentration was usually at or below the detection limit. Therefore, manganese solubility at varying pH levels is more than likely influencing concentrations in the streams.

Similar results were also observed between ANC and manganese concentrations (Table 4.4). BLAC was the only site that did not exhibit a relationship between manganese and ANC (Figure 4.58). At HRTB and UPTB there also seems to be a threshold for manganese concentration in a specific range of ANC and pH (Figures 4.57, 4.58). At HRTB it appears that at about a pH of 5.3 and an ANC of close to zero, manganese concentrations markedly increase. The same pattern was also exhibited at UPTB at a pH of about 5.6 and an ANC of about 10-15 μeq/L. This threshold was not exhibited at NPLR or BIGR, but this might be because pH and ANC levels were never as low as they were at HRTB and UPTB. Therefore, during extreme episodic events accompanied by large decreases in pH and ANC, manganese concentrations are more likely to be of concern to aquatic biota than during events of lesser magnitude.

Zinc was another metal that was detected at the five sampling locations with regularity. Zinc concentrations at all five sites were related to pH, ANC, and discharge. There was a significant positive relationship between zinc concentration and discharge (Table 4.4). It was definitely not as strong as the relationships for manganese, though. The results were broken down by site (Figure 4.59). UPTB was the only site that had a significant positive relationship between discharge and zinc concentrations. This might be related to land use history, geology, or soil differences within the watershed.

When the results for iron are examined with all sites included together, correlation relationships between pH and discharge are not significant. There was a significant positive correlation between ANC and iron (Table 4.4). When the relationships were broken down by site, more subtle relationships were noticed. There were not significant relationships between iron concentrations and stream discharge at BLAC, NPLR, and UPTB. There were significant relationships, though, at HRTB and BIGR (Figure 4.60). Iron levels at HRTB tended to decrease with increased discharge, which was probably a dilution effect. At periods of extreme low flow, we saw extremely high concentrations of iron. This was probably a colloidal form of iron that is diluted by other sources of groundwater under different flow regimes. Iron at BIGR, though, tended to increase with increased discharge.

There were significant positive relationships between iron and pH at HRTB and NPLR (Figure 4.61). The relationship at HRTB supports the results we found for discharge and iron. ANC and pH at HRTB tended to increase dramatically during periods of low flow. Therefore, if

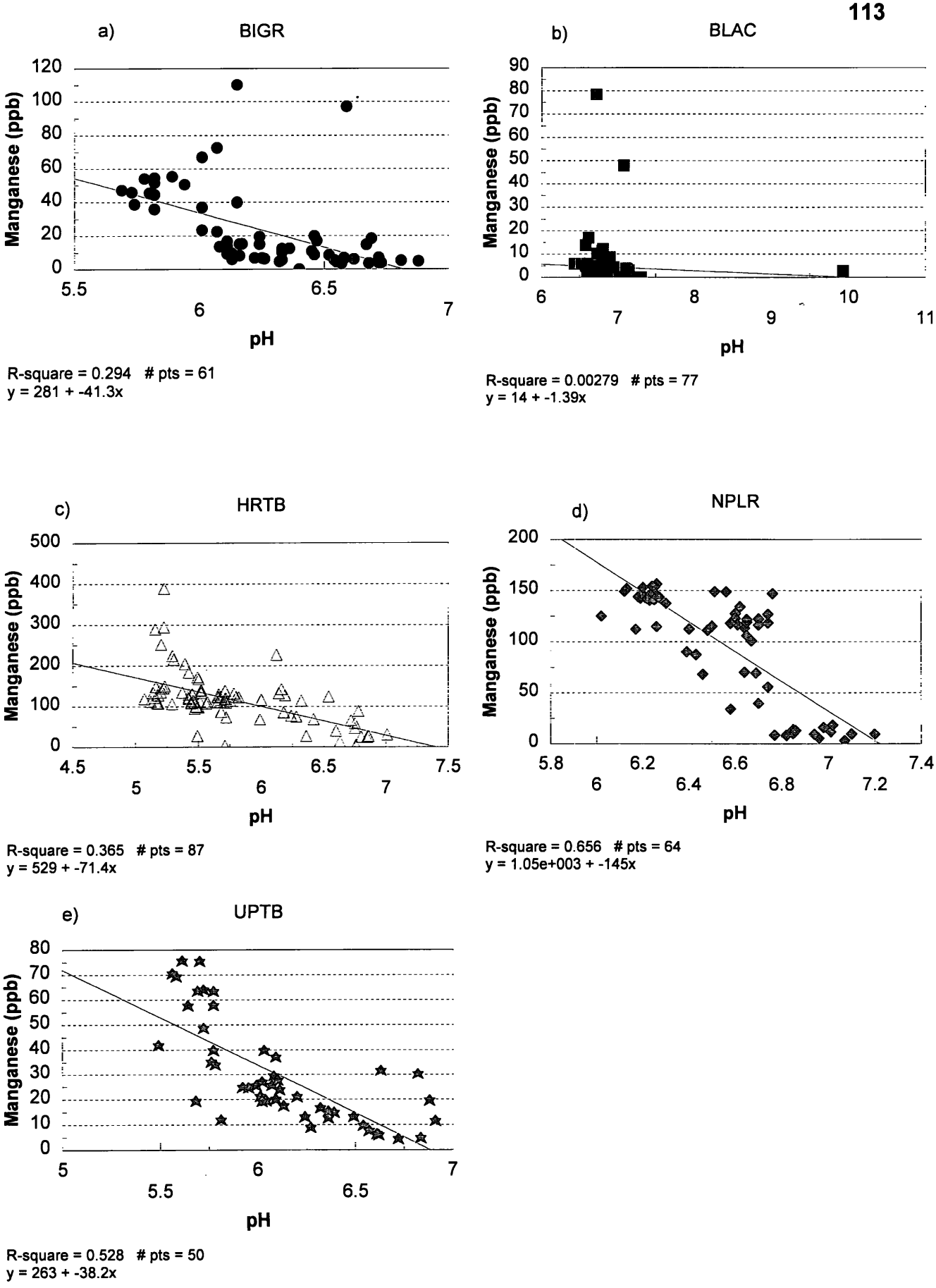

Figure 4.57. Relationship between manganese concentration and pH at each sampling site.

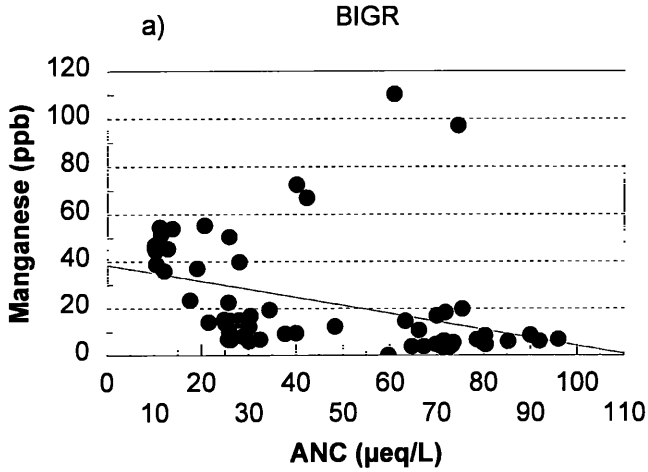

R-square = 0.145 # pts = 61
y = 38.5 + -0.342x

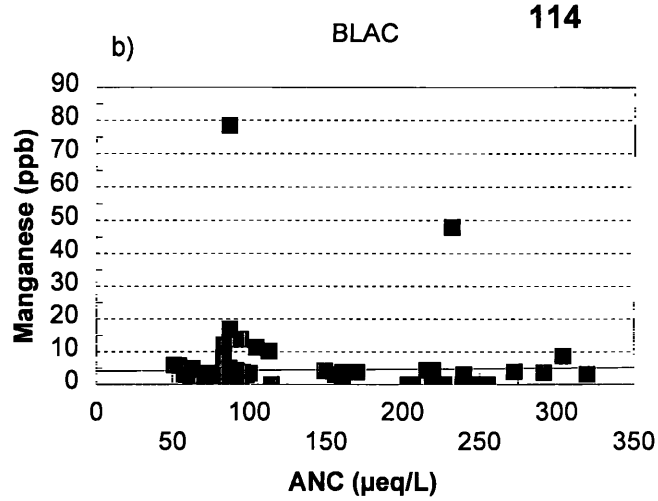

R-square = 0.00044 # pts = 77
y = 4.09 + 0.0031x

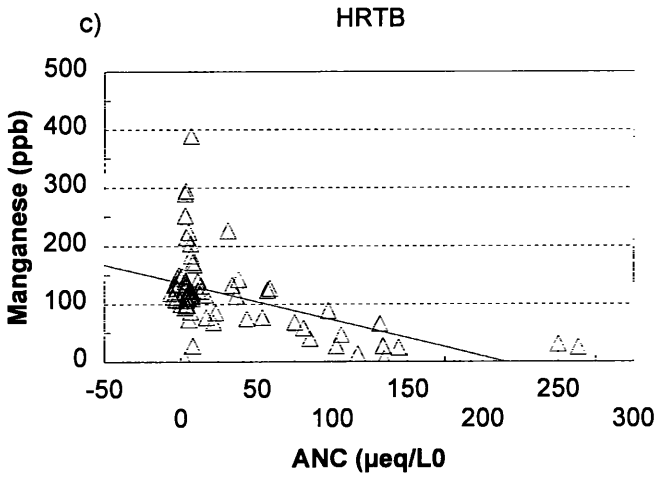

R-square = 0.275 # pts = 85
y = 136 + -0.632x

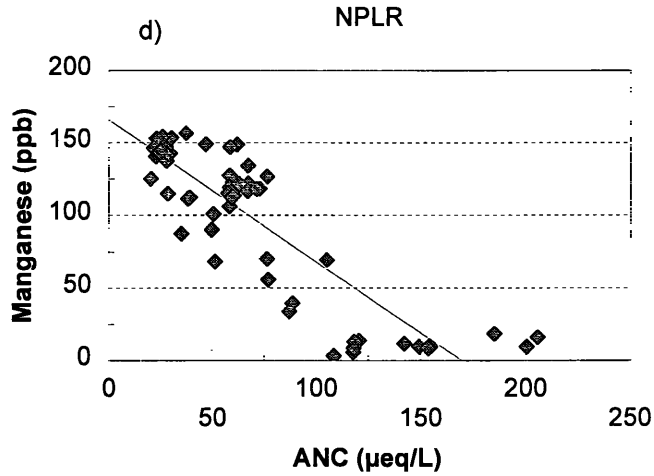

R-square = 0.779 # pts = 64
y = 166 + -0.978x

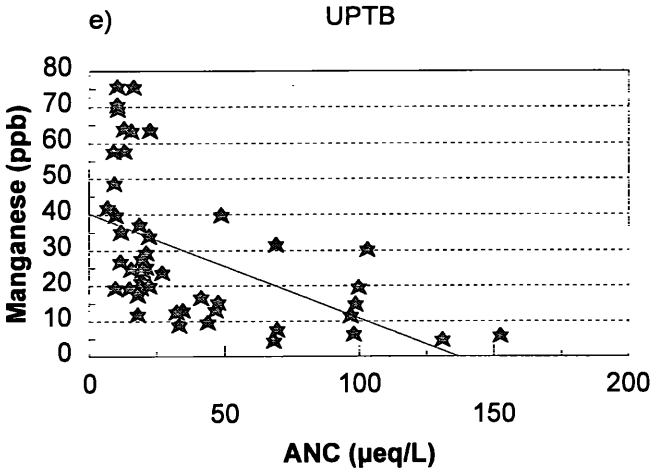

R-square = 0.257 # pts = 50
y = 40.3 + -0.295x

Figure 4.58. Relationship between manganese concentration and ANC at each sampling site.

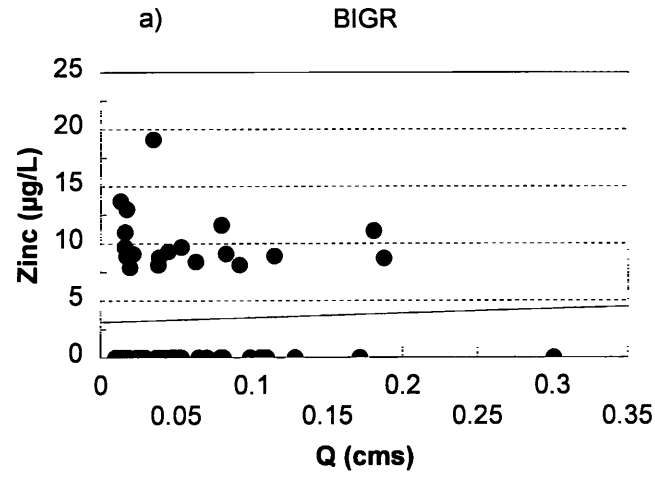

R-square = 0.00168 # pts = 61
y = 3.14 + 3.86x

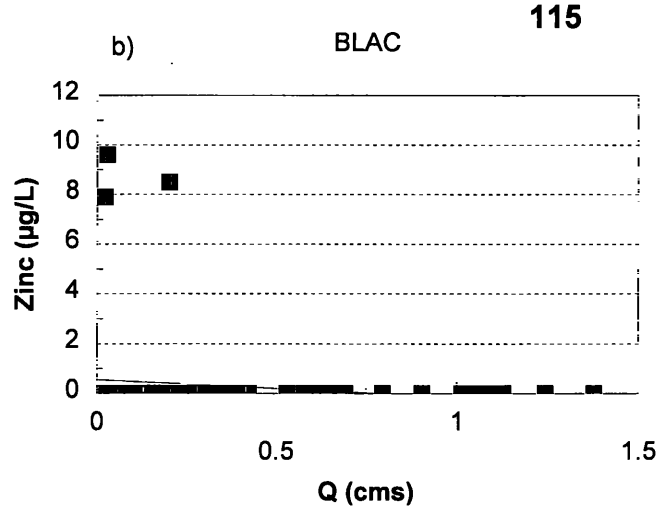

R-square = 0.0189 # pts = 77
y = 0.554 + -0.691x

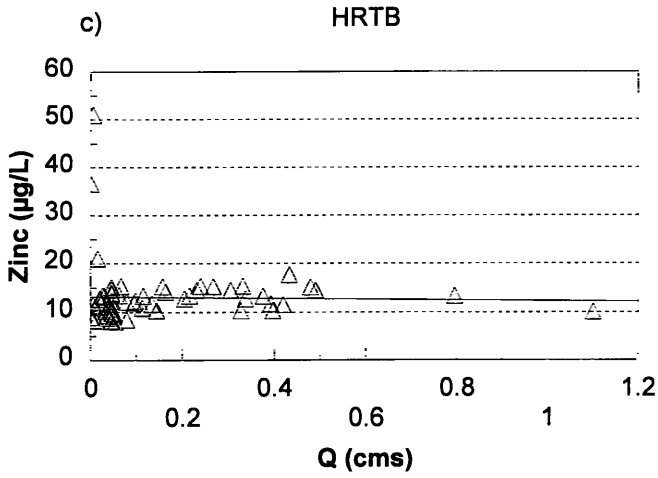

R-square = 0.000746 # pts = 66
y = 13.2 + -0.845x

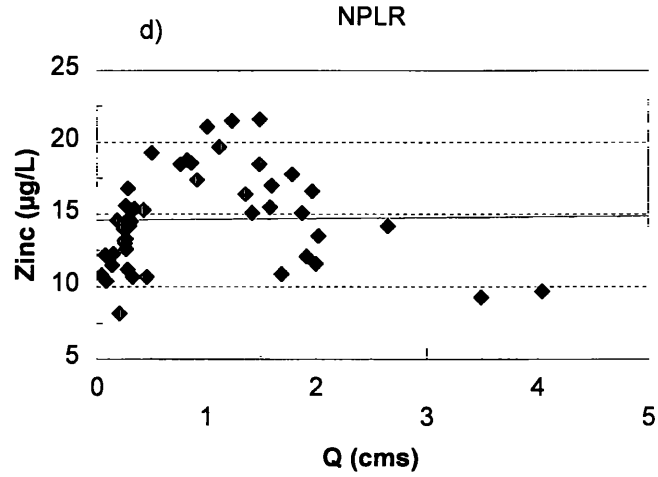

R-square = 0.000245 # pts = 48
y = 14.6 + 0.0569x

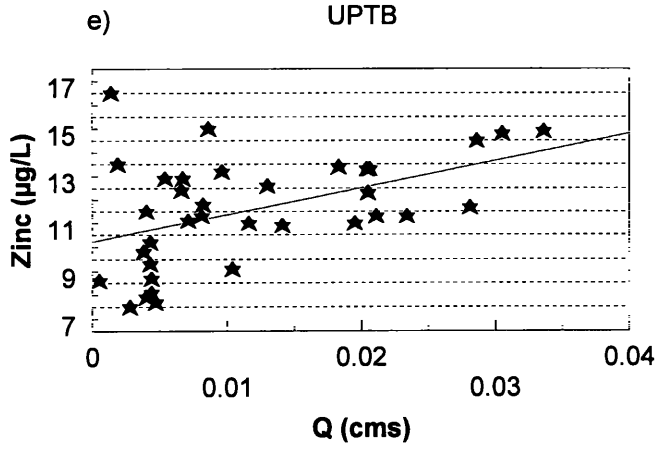

R-square = 0.216 # pts = 35
y = 10.7 + 114x

Figure 4.59. Relationship between zinc concentration and discharge at each sampling site.

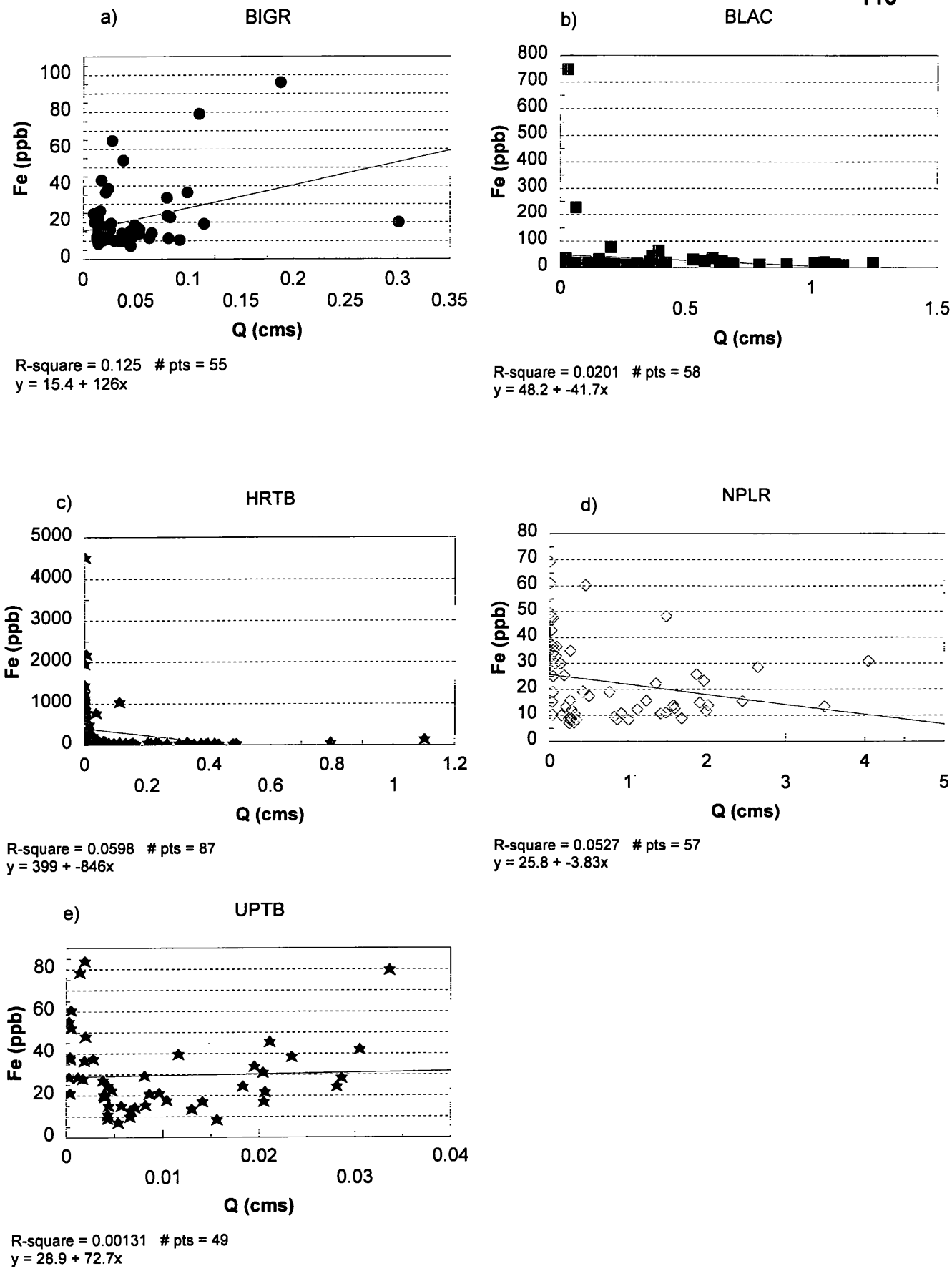

Figure 4.60. Relationship between iron concentration and discharge at each sampling site.

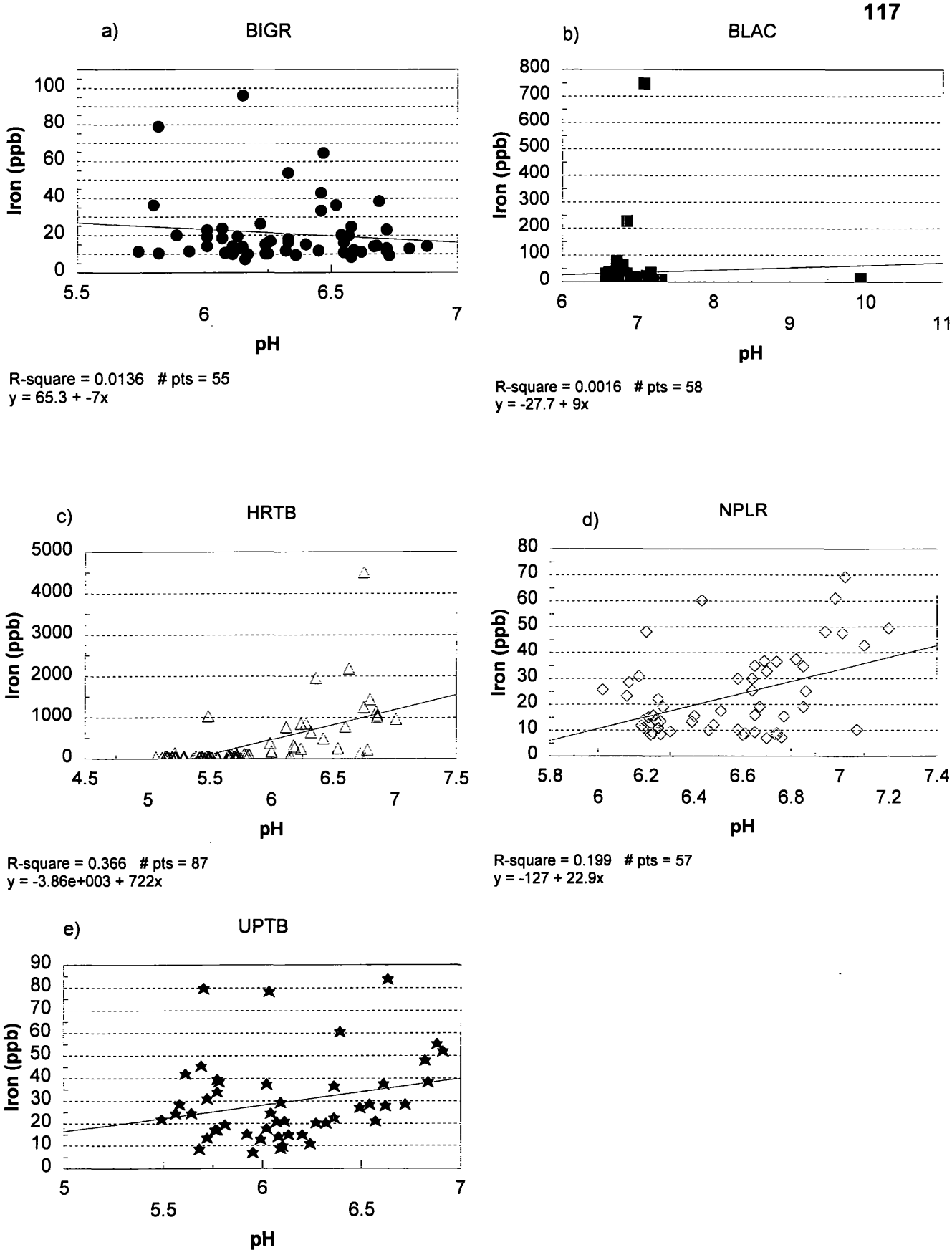

Figure 4.61. Relationship between iron concentration and pH at each sampling site.

we saw a relationship between iron and discharge, we would expect to see a relationship between ANC and pH and iron at HRTB. We would have expected to see positive relationships between iron and pH for the same sites where we saw a relationship for manganese and pH because iron adsorption is also affected by pH (Drever 1988). Differences in geology and soils in the watersheds of the different sampling sites might provide an explanation. HRTB and NPLR both exhibit evidence of prior coal mining activities within the watershed. Coal seam formations generally contain large amounts of iron.

Results from HRTB and NPLR indicated a corresponding relationship between ANC and iron concentration. Additionally, UPTB exhibited a significant positive linear relationship between iron and ANC (Figure 4.62).

E. Temporal Variations in Trace Metals in Streamwater

We also sampled four episodes to determine if trace metal release occurred as a function of pH-ANC or flow for two sampling sites–BLAC and HRTB. These four episodes were from: November 6-10, 1997; January 8-10, 1998; February 10-15, 1998, and February 17-21, 1998. Analytes determined for these episodes were total mercury, methyl mercury, cadmium, lead, arsenic, and selenium. Neither arsenic nor selenium was analytically speciated. Other parameters, such as pH, ANC and flow collected during the study, were used to determine patterns of trace metal activity during episodes.

Monthly baseflow measurements at BLAc and HRTB indicated that total mercury and particulate mercury dominated both systems (Figure 4.63), with total and particulate methyl mercury found at low levels (mean less than 0.1 ng/L). Mean total and particulate mercury concentrations were similar in both watersheds, with HRTB being slightly higher than BLAC for both mercury types.

In both BLAC and HRTB, particulate trace metals were below 0.1 μg/L for cadmium, lead, arsenic, and selenium (Figure 4.64). Total cadmium was low (less than 0.1 μg/L) for both watersheds, as was lead (less than 0.2 μg/L). Mean concentrations of total arsenic and selenium for both watersheds were above 0.3 μg/L. HRTB had a mean monthly arsenic concentration over 0.6 μg/L. These levels of selenium and arsenic indicate potential atmospheric input into the watersheds (assumed to be from wet or dry deposition).

During the first episode (November 6-10, 1997), total mercury levels paralleled initial flow increases at BLAC (Figure 4.65) but only up to near the hydrograph peak. However, total mercury tended to be elevated over baseline at peak flows. Total mercury levels rapidly diminished and were near baseline conditions by the end of the episode. Baseline total mercury was 0.15 ng/L and reached a high of 14.98 ng/L. Six observations during the episode showed total mercury levels over 6 ng/L at BLAC.

Of more biological concern is the presence of methylated mercury species since it is biologically available and generally leads to bioconcentration in organisms and biomagnification in food webs. During the first episode at BLAC, methyl mercury levels ranged from 0.01 to 0.19

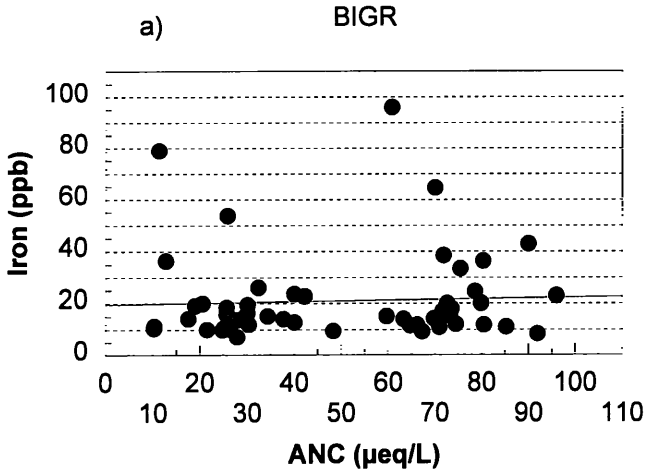

R-square = 0.00166 # pts = 55
y = 19.6 + 0.0276x

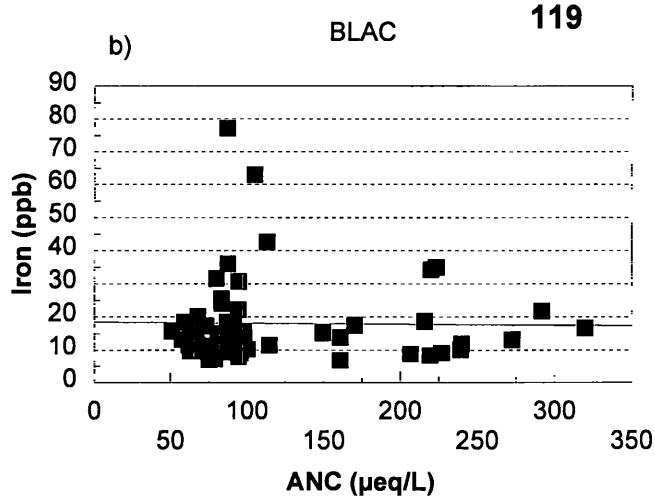

R-square = 0.000265 # pts = 56
y = 18.5 + -0.00309x

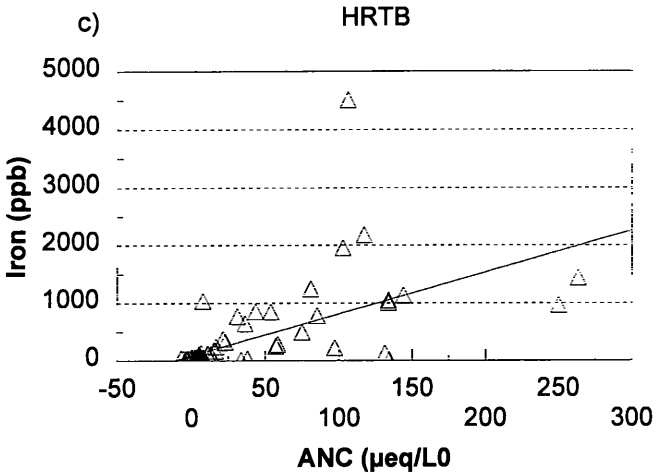

R-square = 0.357 # pts = 85
y = 87.3 + 7.24x

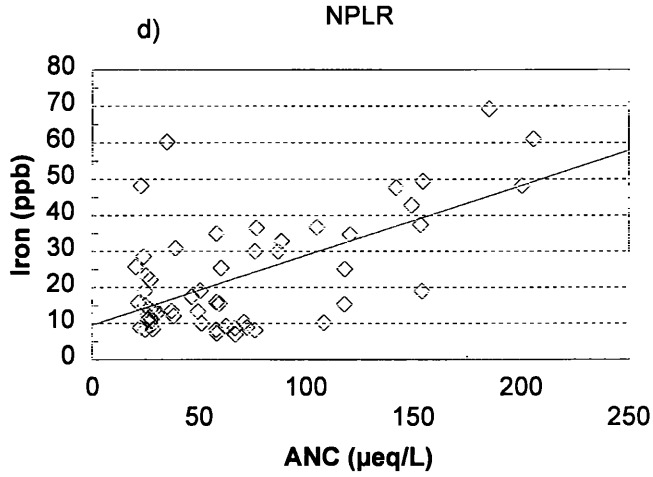

R-square = 0.38 # pts = 57
y = 9.6 + 0.193x

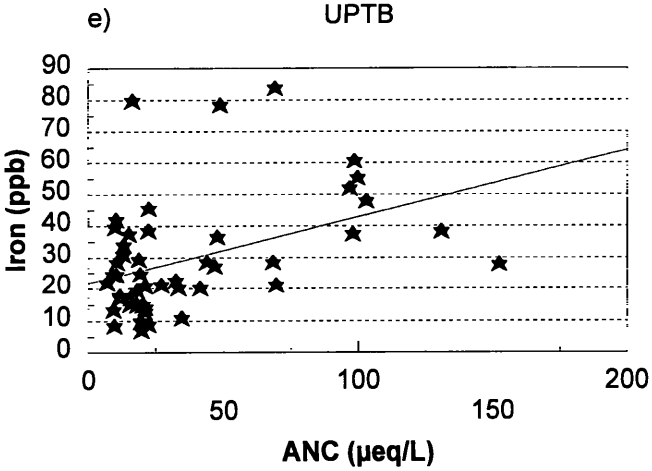

R-square = 0.166 # pts = 49
y = 21.7 + 0.212x

Figure 4.62. Relationship between iron concentration and ANC at each sampling site.

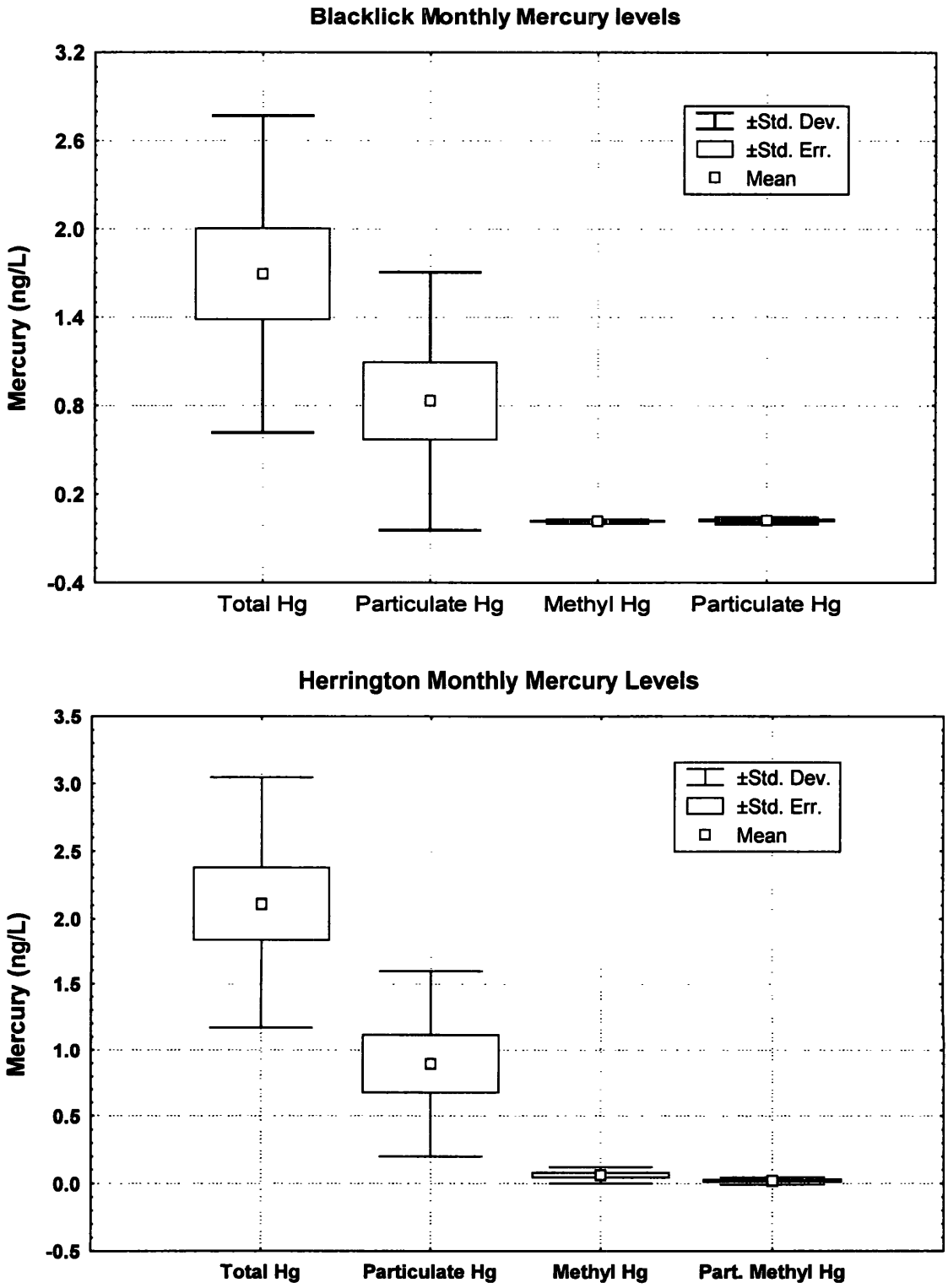

Figure 4.63. Monthly mercury levels for BLAC and HRTB, including total and particulate levels.

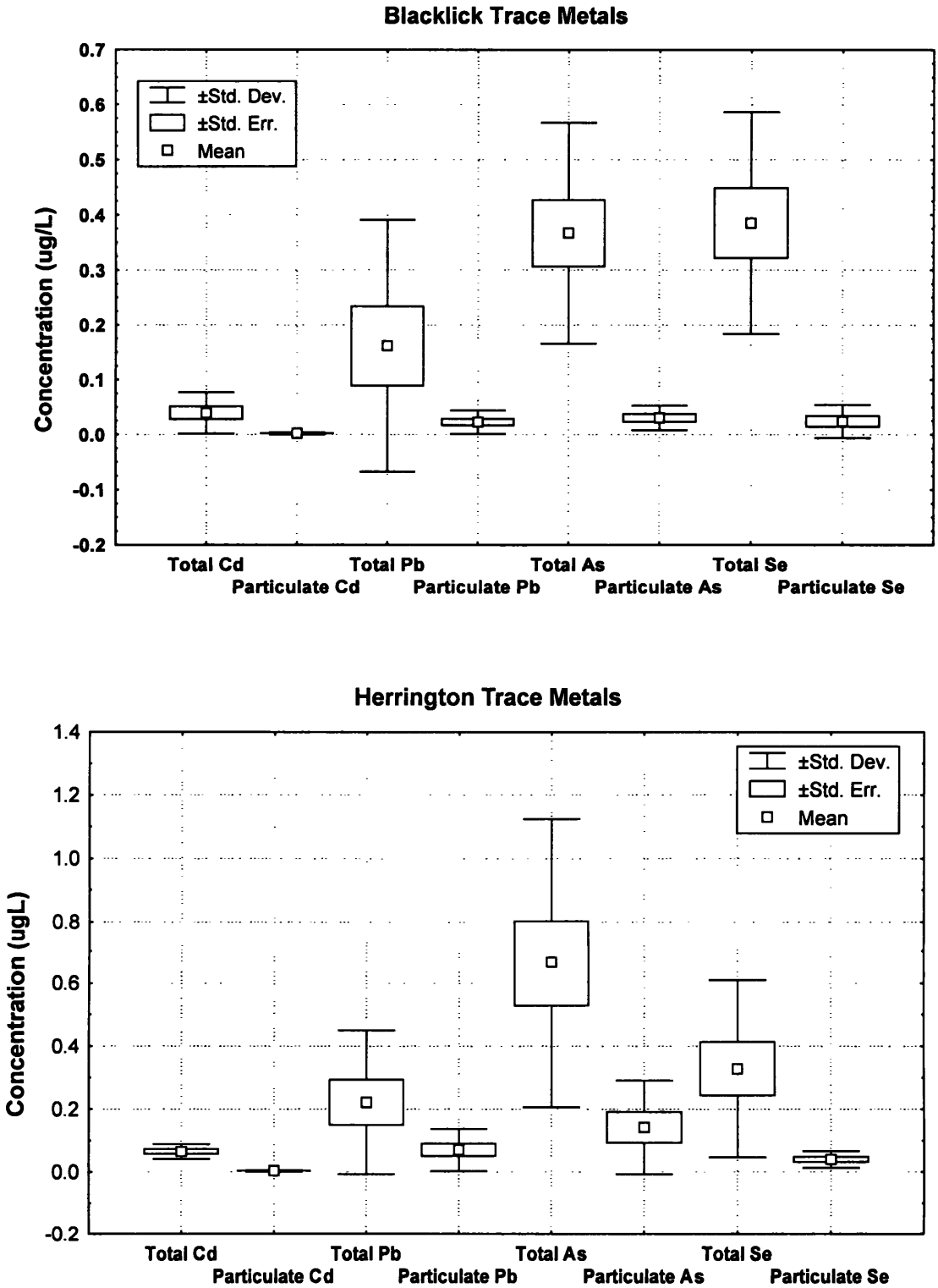

Figure 4.64. Monthly cadmium, lead, arsenic, and selenium levels for BLAC and HRTB, including total and particulate levels.

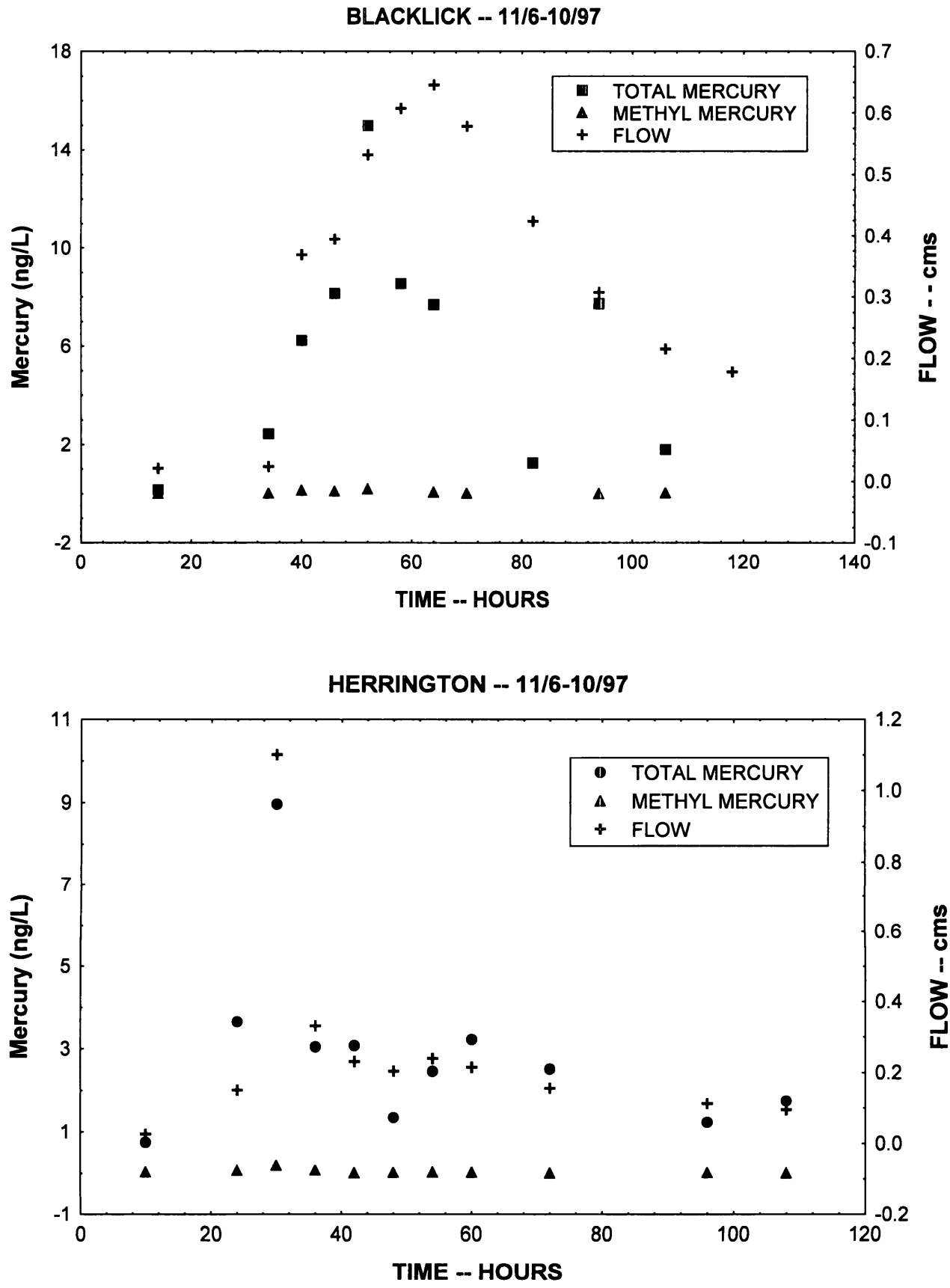

Figure 4.65. Total mercury and methyl mercury concentrations for the 11/6-10/97 episode at BLAC and HRTB.

ng/L—essentially staying constant over the entire episode (Figure 4.65), although there were increased methyl mercury levels at the hydrograph peak. This possibly indicates a deficit of methyl mercury in the BLAC watershed, a lack of biological activity to convert inorganic mercury to the methylated mercury species, low deposition rates for mercury, or some combination of the above factors.

The same episode at HRTB presented a slightly different pattern, although total mercury concentrations were slightly lower (maximum concentration of 15 ng/L at BLAC and 9 ng/L at HRTB). At HRTB, total mercury levels closely followed flow (Figure 4.65). Baseline total mercury was 0.75 ng/L and 1.7 ng/L at the end of measurement—total mercury did not fall to pre-episode levels. Methyl mercury levels essentially remained flat, with all measurements below 0.19 ng/L. Eight of the points were below 0.03 ng/L methyl mercury. Mercury levels at both BLAC and HRTB were below the USEPA EcoTox (ET) threshold (EPA, 1996) for inorganic mercury of 1.3 μg/L and 0.003 μg/L of methyl mercury.

For cadmium, lead, arsenic and selenium, there were interesting responses to flow at BLAC during the November episode (Figure 4.66). Cadmium and selenium showed little response to increasing flow (cadmium declined from the baseline over the episode and selenium concentrations remained below 0.29 μg/L). Arsenic concentrations increased with flow but arsenic levels never exceeded 2.0 μg/L. Lead increased initially but then dropped below pre-episodic levels. Both arsenic and lead levels at HRTB were elevated during the November episode, and generally followed flow (Figure 4.66) although lead levels quickly dropped after peak flow. Cadmium and selenium were essentially constant throughout the storm event, with both these elements found below 1.0 μg/L. Concentrations of these four trace elements were all very low at both BLAC and HRTB. These levels were below the ET for arsenic III of 190 μg/L and arsenic V of 8.1 μg/L, selenium of 5.0 μg/L, cadmium of 1.0 μg/L (hardness-dependent ambient water quality criterion, value listed based on 100 mg/L CaCO3), and lead of 2.5 μg/L (hardness-dependent ambient water quality criterion, value listed based on 100 mg/L CaCO3).

For the January episode (January 8-10, 1998), a similar pattern to the November episode in total mercury levels was seen at BLAC (Figure 4.67). Total mercury peaked at 41.4 ng/L just prior to peak flows, and then declined over the rest of the event. Again, methyl mercury remained low in proportion to total mercury. The highest methyl mercury level observed was 0.15 ng/L at the same time the highest total mercury was seen in the event. Lower levels of mercury were seen at HRTB in the January event than at BLAC (Figure 4.67), where total mercury concentrations did not exceed 13.2 ng/L. The flow-total mercury pattern was not as clear in the first event, with the peak total mercury concentration occurring long after the flow maximum. Methyl mercury again was low, with the maximum level observed of 0.18 ng/L.

At BLAC, arsenic levels closely parallel flow but it appears that a dilution effect is taking place since pre-event arsenic concentrations were running slightly over 3.0 μg/L (Figure 4.68), and then dropped below 1.0 μg/L at event's end. All trace element concentrations were below 3.5 μg/L. Lead showed a slight increase with flow but very quickly dropped to below pre-event

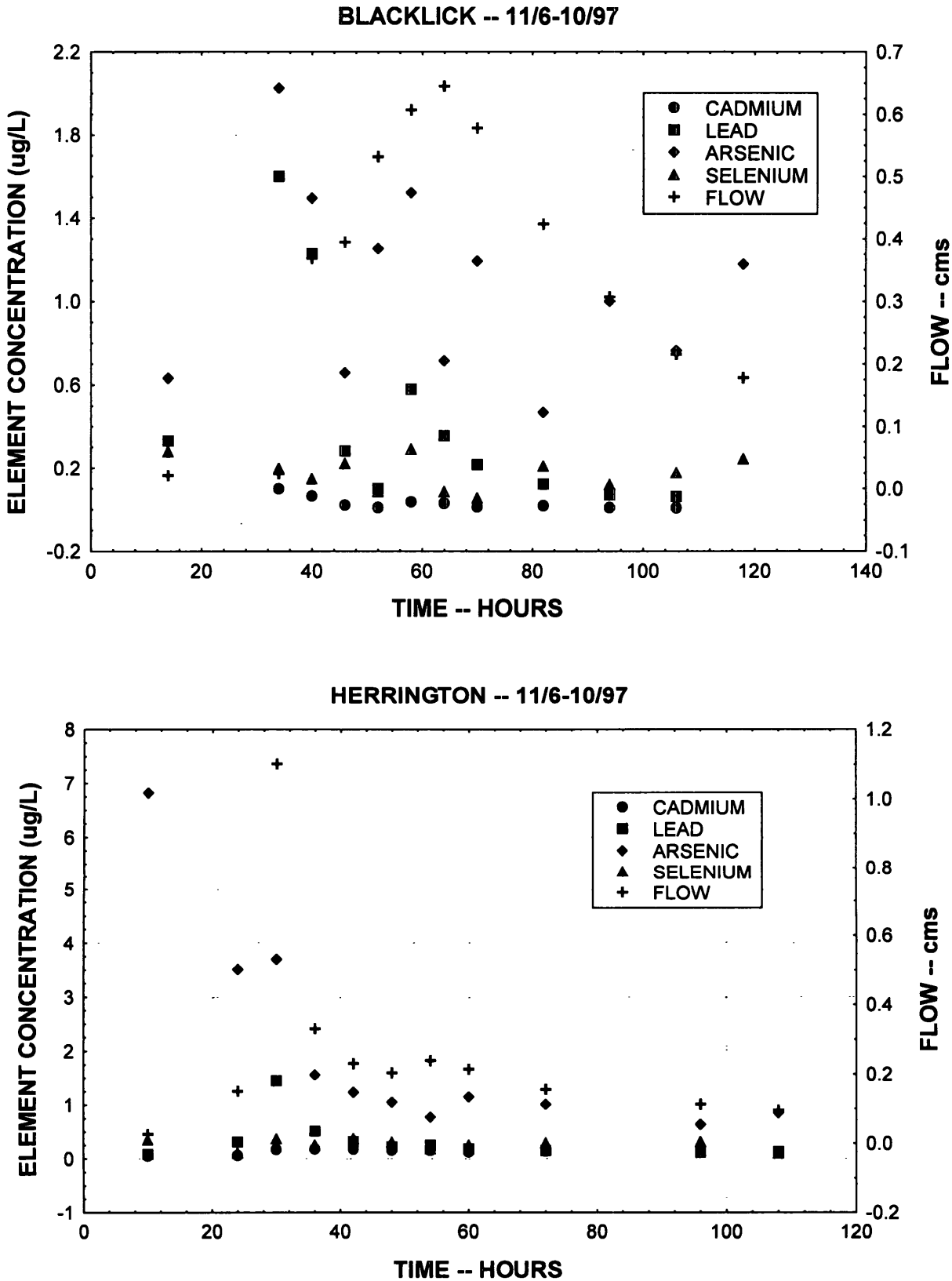

Figure 4.66. Cadmium, lead, arsenic and selenium concentrations for the 11/6-10/97 episode at BLAC and HRTB.

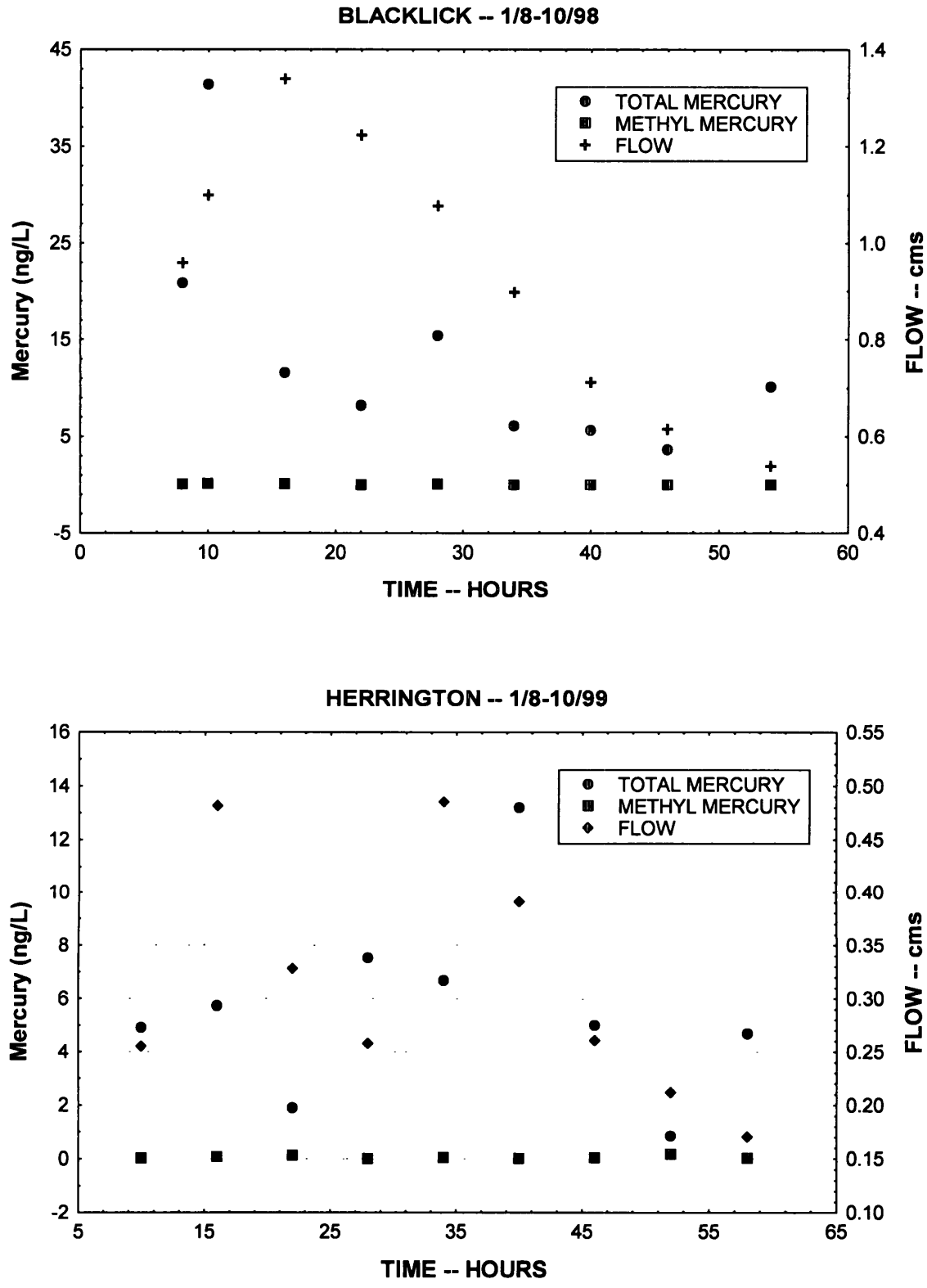

Figure 4.67. Total mercury and methyl mercury concentrations for the 1/8-10/98 episode at BLAC and HRTB.

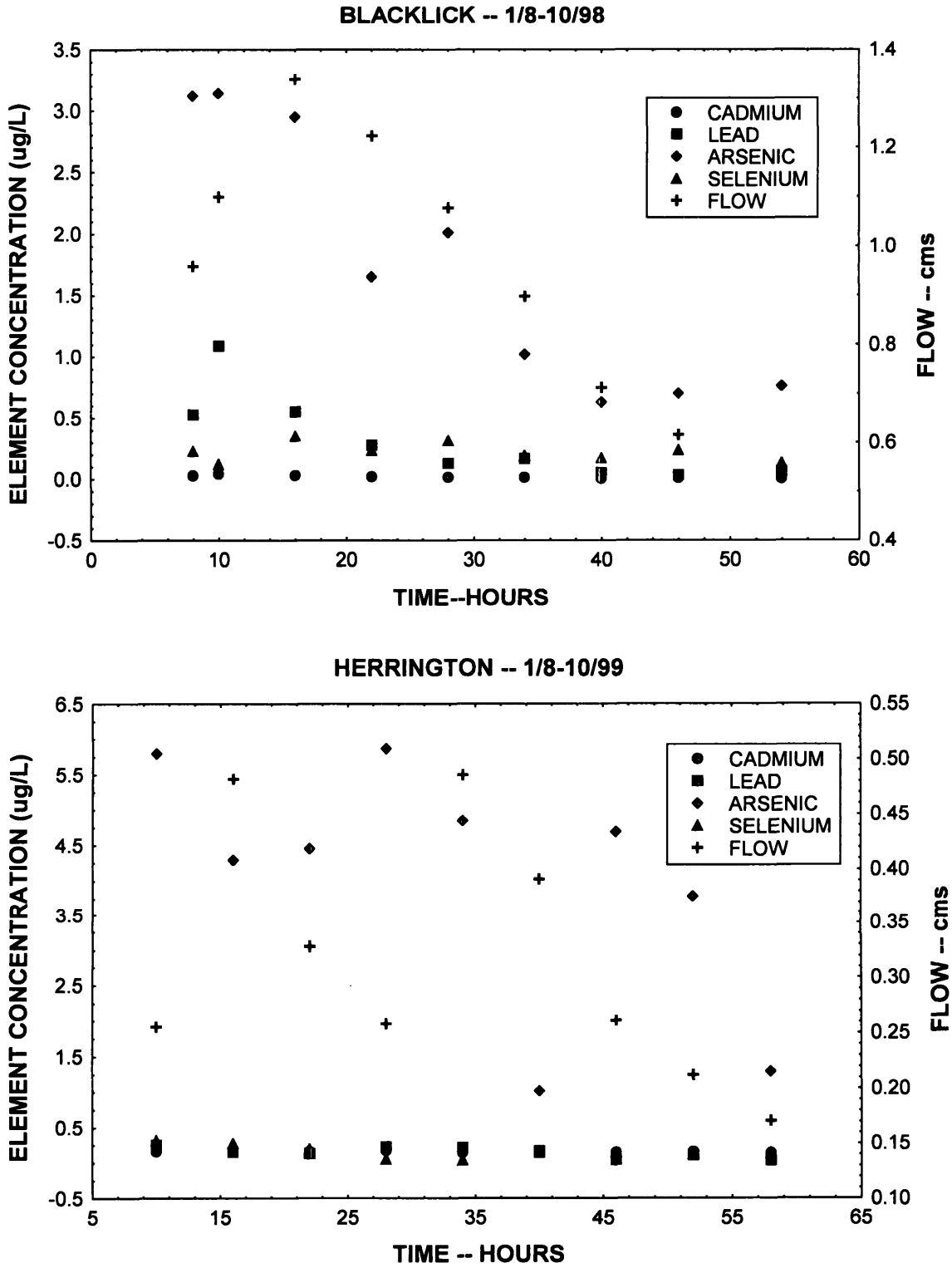

Figure 4.68. Cadmium, lead, arsenic and selenium concentrations for the 1/8-10/98 episode at BLAC and HRTB.

levels. Selenium and cadmium were low, and remained low during the event. At HRTB, arsenic again was high during the event but showed a very erratic pattern (Figure 4.68). All other trace metals did not vary with flow patterns—these metals were all below 0.5 μg/L.

The first winter episode in 1998 (February 10-15, 1998) again showed a dilution pattern for total mercury (Figure 4.69). The pre-event level for total mercury was 5.6 ng/L, and all other total mercury values were less than 3.5 ng/L. Again, methyl mercury was essentially flat over the entire event (Figure 4.69). At HRTB, all total mercury concentrations were below 3.1 ng/L, and methyl mercury was essentially level over the entire event (Figure 4.69).

For other trace metals at BLAC, levels were below 0.7 μg/L for this episode, and there was no apparent pattern in their response to flow (Figure 4.70). Arsenic showed a dilution effect, dropping from 3.8 μg/L to less than 0.50 μg/L over the course of the episode. At HRTB, arsenic was also elevated in the first phase of the event, and then dropped below 0.50 μg/L (Figure 4.70). All other trace metals at HRTB were below 0.50 μg/L.

The last episode sampled (February 17-21, 1998) for trace metals was the most interesting of the four, in spite of lacking some mercury data. For BLAC, there was an increase in total mercury (up to 10.4 ng/L) that almost exactly matched the hydrograph pattern (Figure 4.71), followed by a drop in total mercury as flows started to decrease. Again, methyl mercury remained relatively low over the event's duration. For HRTB, total mercury also increased to about 9.0 ng/L but then dropped as flows started to increase (Figure 4.71). Methyl mercury was level over the event.

Levels of trace elements were low (below 0.9 μg/L) at both BLAC and HRTB (Figure 4.72). However, trace metals at BLAC showed patterns of metal concentration associated with flow, and this was the only episode where these patterns were distinct. Although concentrations are low, lead, arsenic and selenium tracked flow. Cadmium did not vary greatly with flow at BLAC. The HRTB pattern for trace metals was not as distinct as that of BLAC, but lead, arsenic and selenium levels did mimic the hydrograph. Again, cadmium did not vary over the event.

We also examined all episodic data to determine if there were relationships among pH, ANC and flow that would be influencing the release of trace metals in either watershed. First, we wanted to see if ANC or pH influenced the metal release (since ANC and pH are closely correlated, pH was employed in the analysis). For BLAC and HRTB, there did not appear to be any distinct pattern with pH and mercury release (Figure 4.73), as one would see with aluminum-pH interactions. Methyl mercury was very low in both systems and did not show any response to pH. However, observation of any pH-total mercury response is restricted since the pH range was from 5.0 to 7.2, and lower pH systems may show an increased mercury release. For the other trace metals (cadmium, lead, arsenic, and selenium), again there also did not appear to be any patterns associated with pH and trace metal levels during episodes (Figure 4.73). For all four episodes, arsenic was the only trace metal that was elevated over 2 μg/L during any episode. Selenium, lead and arsenic just did not respond to pH.

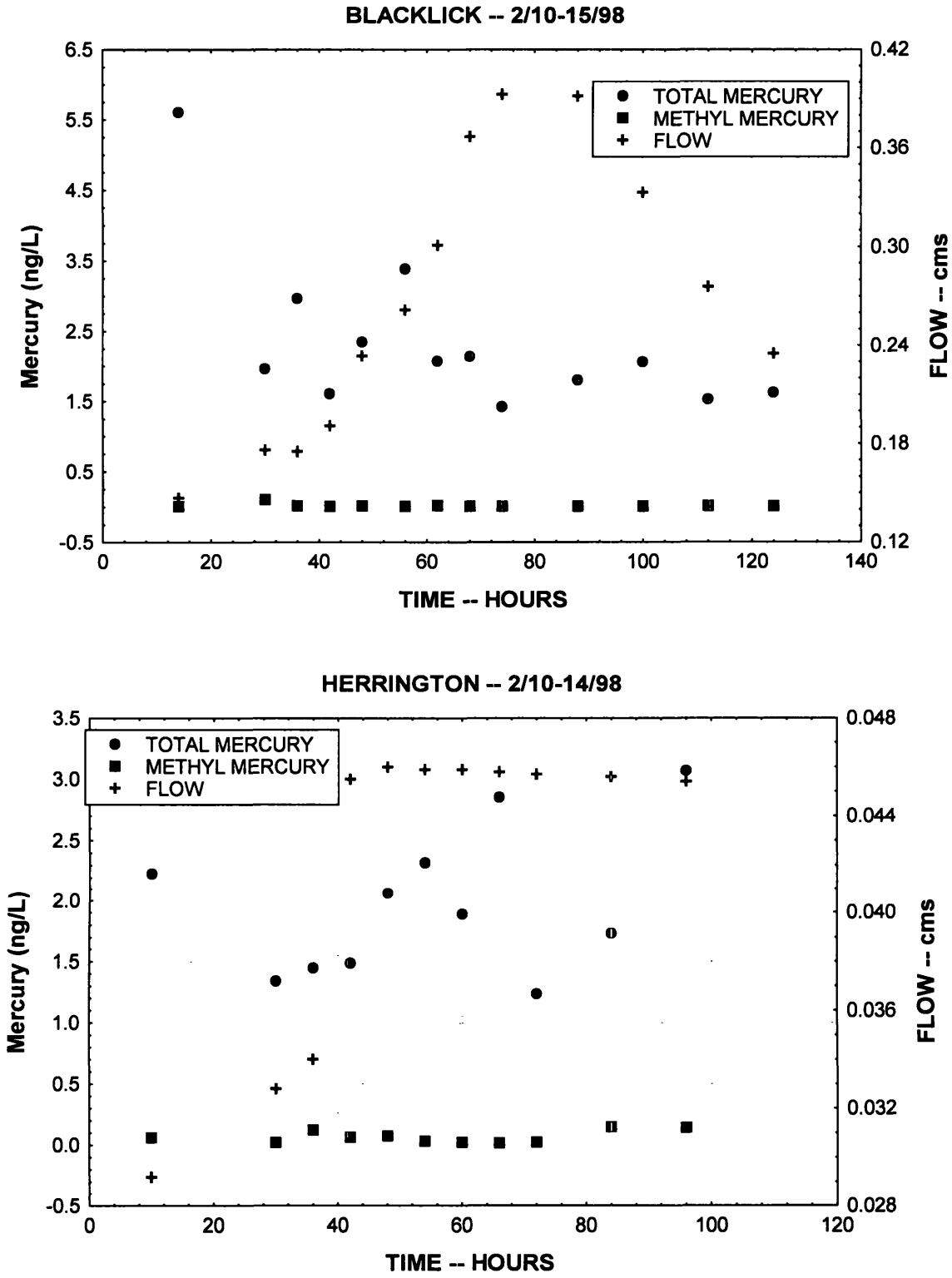

Figure 4.69. Total mercury and methyl mercury concentrations for the 2/10-15/98 episode at BLAC and HRTB.

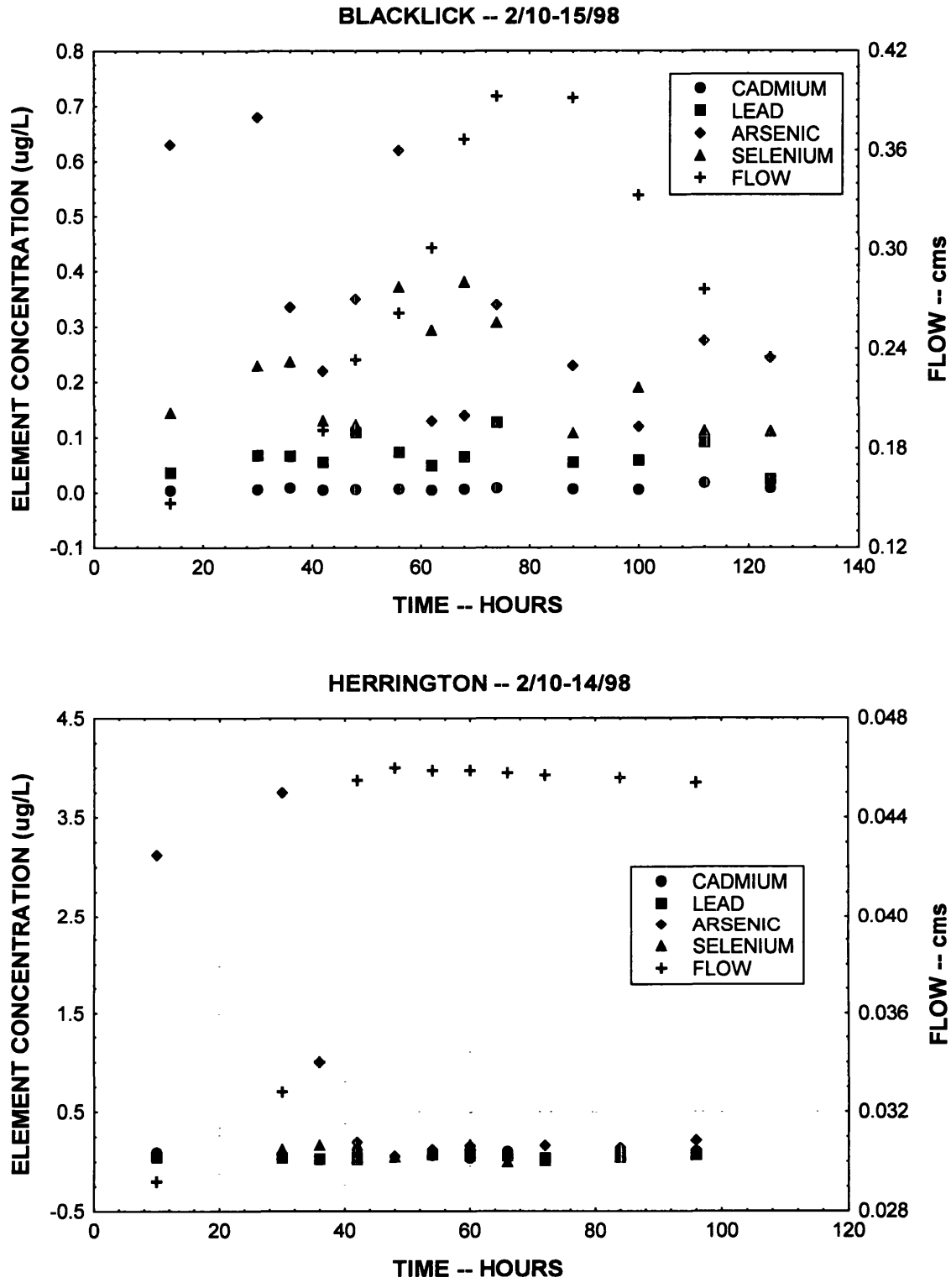

Figure 4.70. Cadmium, lead, arsenic and selenium concentrations for the 2/10-15/98 episode at BLAC and HRTB.

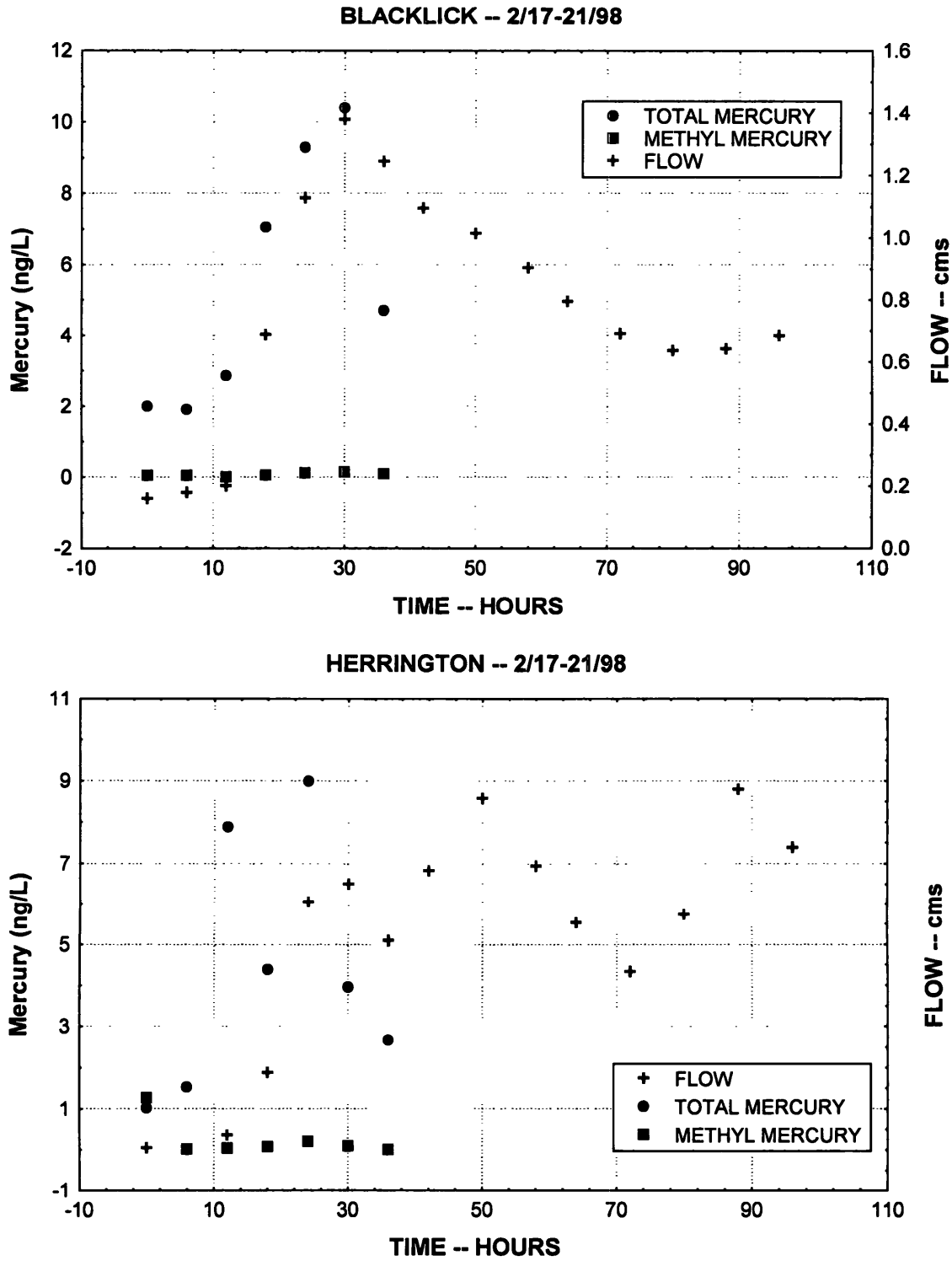

Figure 4.71. Total mercury and methyl mercury concentrations for the 2/17-21/98 episode at BLAC and HRTB.

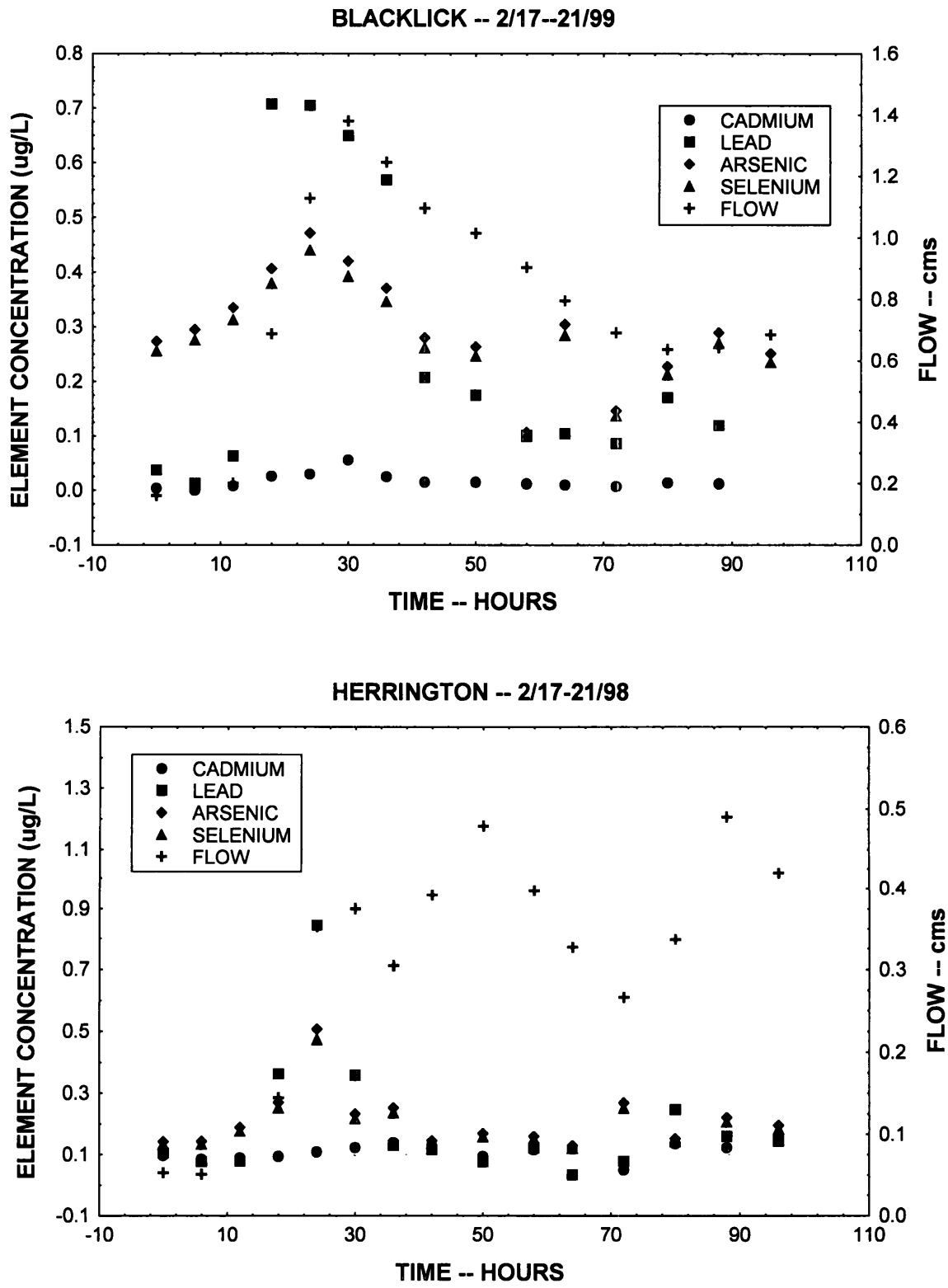

Figure 4.72. Cadmium, lead, arsenic and selenium concentrations for the 2/17-21/98 episode at BLAC and HRTB.

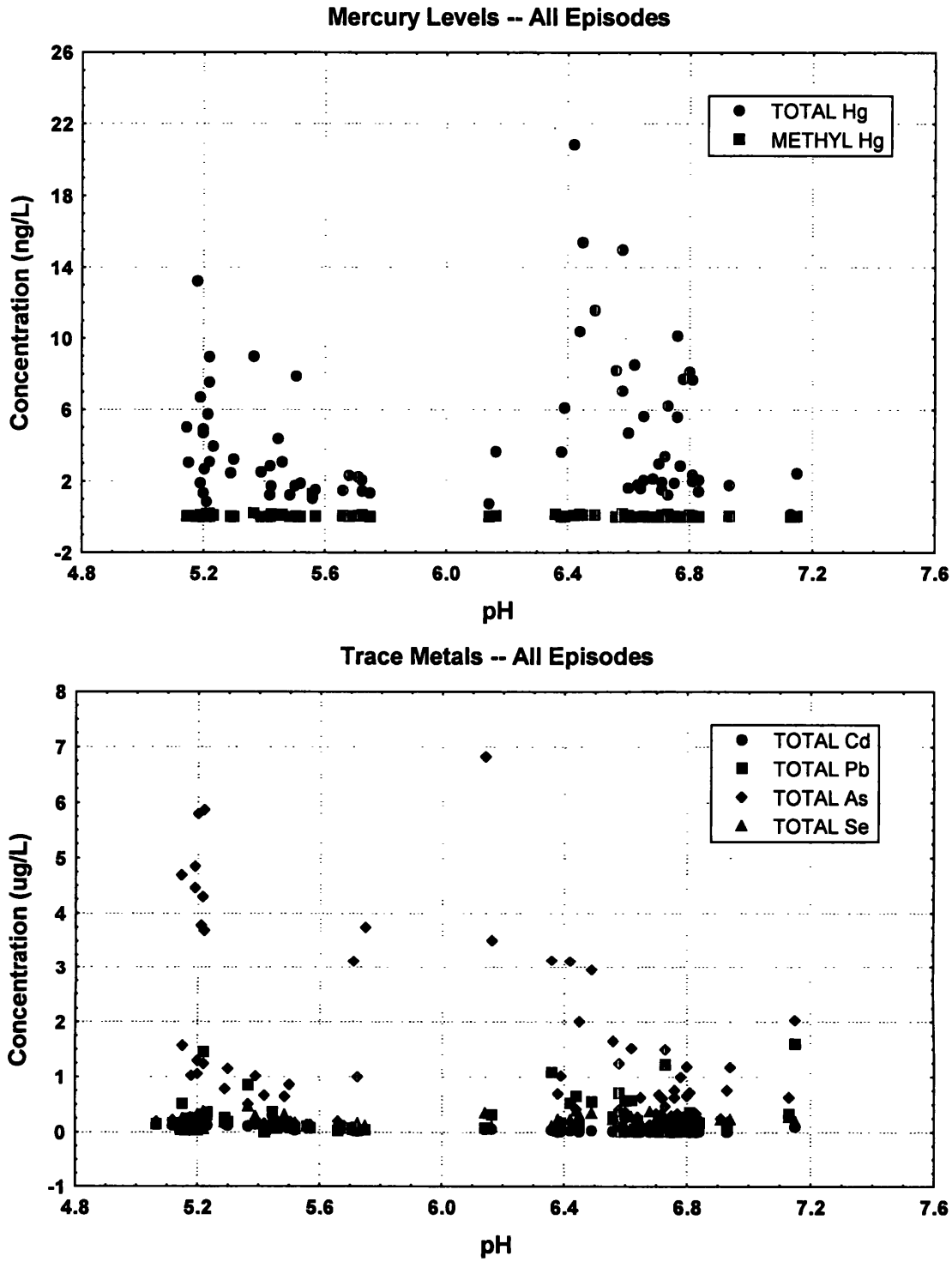

Figure 4.73. Mercury and trace metal levels for all episodes as a function of pH.

We then examined mercury release as a function of flow for all episodes (Figure 4.74). Methyl mercury was essentially level and did not show any flow response. However, there was a relationship between total mercury and flow (expressed as Y = 1.789 + 7.743X) present for all episodes. We need to point out that this pattern is just for these two watersheds, and within the flow regime of 0.0 to 1.4 cms. Total mercury observed during the episodes was approximately 21 ng/L.

We also observed one other interesting pattern during the episode analysis. Total cadmium-flow patterns were quite distinct for BLAC and HRTB (Figure 4.75). BLAC cadmium levels were generally lower than HRTB, and show a linear increase with flow. HRTB displays more of a threshold effect where cadmium levels are variable at low flows, and then increase with flows over 0.1 cms. No other trace metal showed this pattern. Differential sensitivity to acidification my be responsible for this cadmium pattern since HRTB is frequently acidic (ANC < 0 μeq/L) during storm events, whereas BLAC never experienced an ANC less than 50 μeq/L during the study.

During the acme of acid rain research, a major focus centered on how changes in ANC, pH, and solutes drove episodic acidification effects during storm events (Wigington *et al.*, 1996a; b). Concurrent with episodic ANC changes, there was also interest in how aluminum, and other metals, increases toxicity to fishes. Aluminum is mobilized at low pH from soils, and converted to a free ionic species (inorganic monomeric aluminum) that contributes to fish mortality (Baker *et al.*, 1996). The proximal cause of fish mortality due to low pHs results from effects on gill ionic regulation (Rosseland *et al.*, 1990). The primary effect leads to a loss of body salts, with a secondary effect on internal water balance in internal tissues and structures. Typically, fish response to low pH is driven by the number and density of gill chloride cells and variations in the tight junctions between cells (McDonald *et al.*, 1991), with mortality caused by a failure of ionic regulatory mechanisms (Rosseland *et al.*, 1990). Aluminum is also implicated, at low pHs, because of its effects on gill physiology. Epidermal gas transfer is essentially blocked if either aluminum or aluminum bound to mucus precipitates on gill surfaces, blocking gas diffusion processes across gill lamellae (Ultsch and Gros, 1979). Consequently, fish exposed to acidic stresses are subject to both an osmoregulatory stress and a respiratory stress, resulting in acute and chronic effects.

Little attention was paid to the link between other trace metals and episodes during the acidification years. However, Driscoll *et al.* (1980) not only examined aluminum but also looked at other metals such as zinc and manganese associated with acid deposition. Most metal work focused on lakes where metal concentrations (Al, Zn, and Hg) increased to levels having biological consequences (Dickson, 1975; Hutchinson and Sprague, 1986). Mercury in lakes is of concern because of sediment processes that convert inorganic mercury to methylated mercury, with concomitant bioaccumulation (Hakanson, 1980; Sloan and Schofield, 1983; Suns *et al.*, 1987; Almer *et al.*, 1978; Fagerstrom and Jarnelov, 1972). There are correlations among lead,

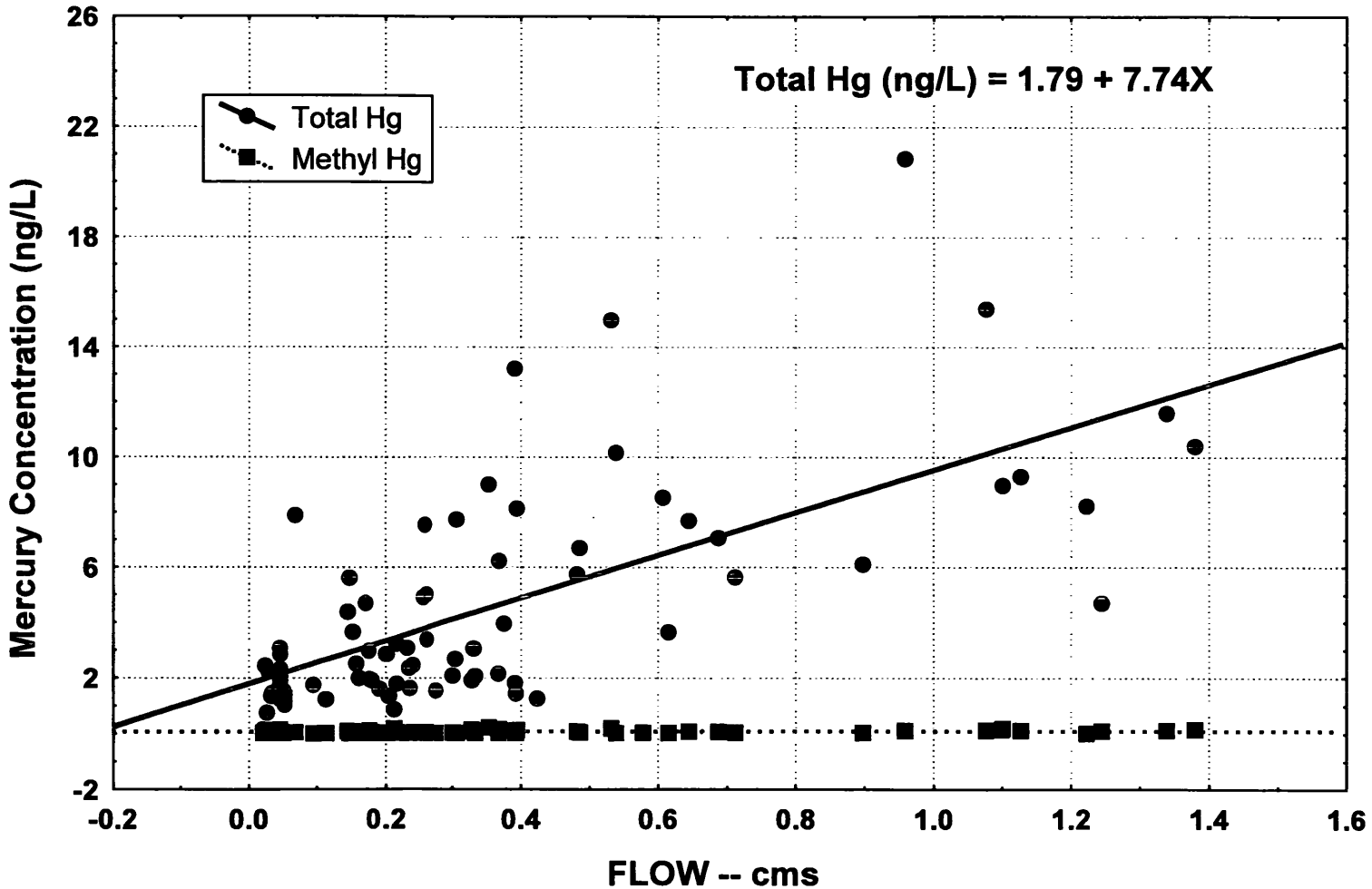

Figure 4.74. Total mercury and methyl mercury as a function of flow for all episodes.

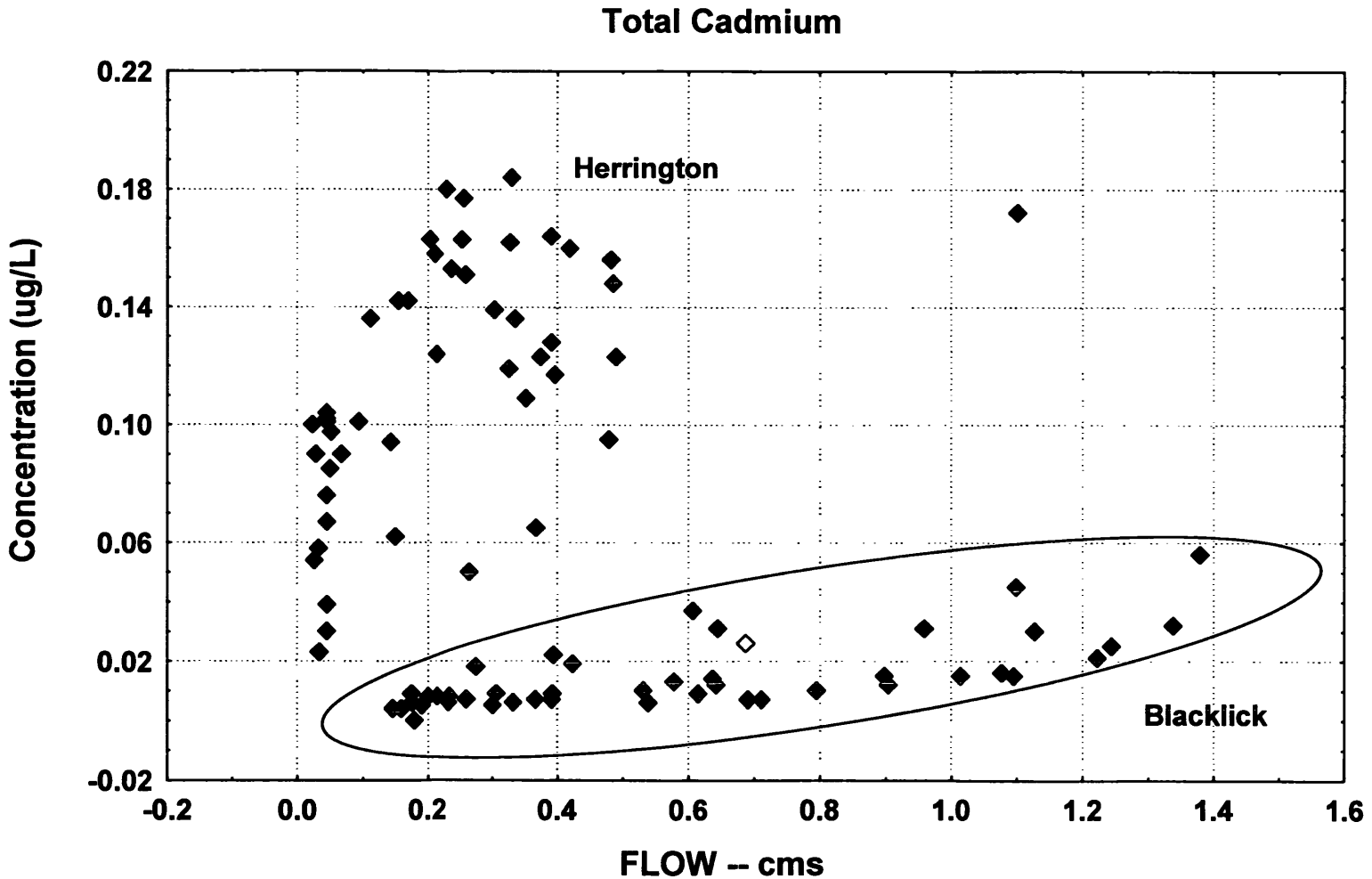

Figure 4.75. Total cadmium concentration as a function of flow for both sites for all episodes.

copper and cadmium levels in fishes with pH (Suns *et al.*, 1987; Anderson and Borg, 1988; Hutchinson and Sprague, 1986).

Borg (1986) found metal concentrations of 1.1-10 μg/L Zn, 0.06-0.52 μg/L Cu, 0.13-0.57 μg/L Pb, and 0.004- 0.066 μg/L Cd during spring snowmelts in four mountain streams near Lofsdalen, Sweden. Lead levels generally agree with results obtained for both HRTB and BLAC. Cadmium levels at BLAC were similar to the Swedish streams but much higher at HRTB (about 0.18 μg/L). Concentration of these four trace elements was very low at BLAC and HRTB. These levels were below the EPA EcoTox threshold (USEPA, 1996) for cadmium of 1.0 μg/L (hardness-dependent ambient water quality criterion, value listed based on 100 mg/L $CaCO_3$), and lead of 2.5 μg/L (hardness-dependent ambient water quality criterion, value listed based on 100 mg/L $CaCO_3$).

Borg (1986) also noted that trace metal concentrations did not fluctuate as greatly as Al, Fe or Mn (highly correlated to pH), although metal maximums correlated to high discharge periods. During the study, Borg (1986) also observed temporal variations in Al (upper levels of 300-420 μg/L), Fe (7,000 μg/L), and Mn (300-420 μg/L)—closely correlated to pH variation during snowmelt.

Of interest is the recent paper by Tarvainen *et al.* (1997) where several metals (Mn, Zn, Cu, Ni, Cr, Pb, As, and Cd) were studied in Finnish surface waters subjected to trace metal deposition. They note that discrete patterns of atmospheric metal distribution are found in headwater lakes. However, land-use, overburden metal concentration, and the presence of humic substances influence the trace metal distribution in both lakes and streams. In a similar, but earlier study, Iivonen *et al.* (1992) found that bioaccumulation of several trace metals increased with increasing acidity and decreasing ANC. Consequently, there is an important link between trace metals and acidification processes.

However, the most relevant work to this study is that done by Church *et al.* (1998) on Bear Branch – a small tributary to Hunting Creek in the Catoctin Mountains of central Maryland. During 1994, they sampled two intensive events in May and August (one event in July was unsuitable for analysis), sampling for trace element loadings and major dissolved ion concentrations. Interestingly, Church *et al.* (1998) determined that relative particulate loadings were not important as a transport mechanism for most trace elements during storm events.

During the first event in July 1994 (3.7 cm rainfall), dissolved metal loadings for the crustal elements Al, Fe, and Mn followed discharge and suspended sediments, indicating that they may have been mobilized by acidity. This pattern was also observed for dissolved Zn, Ni, and Cu. Church *et al.* (1998) hypothesized that this pattern reflected stabilization by strong organic ligands. Cd, Cr, and Pb first increased and then decreased, with Cd decreasing rapidly. During the event, As increased rapidly but Se displayed a pattern more similar to that observed for Cd, Cr, and Pb. Overall, the particulate trace element loading was of minor significance, in comparison to the dissolved elements, for Al, Fe, Cr, As, and Se (for Mn, Cd, Cu, Ni, and Zn the entire fraction was in the dissolved phase).

The August 1994 event (9.1 cm rainfall) produced two peaks in discharge (Church *et al.*, 1998). The second peak, following about 12 hours after the event's start, corresponded to the peak dissolved loading for of crustal elements Al, Fe, Mn along with Zn and Se. All other elements displayed less dramatic loadings, with Ni, Cd, and Se peaking almost as much in the event's beginning as later. Cu, Pb, and Cr did not display much loading during the event.

Elements sampled commonly among Bear Branch, HRTB, and BLAC were compared to the observed maximum loadings during events (Table 4.5). Cd is higher at Bear Branch than at HRTB or BLAC. However, both HRTB and BLAC have substantially higher peak event levels of Pb, As, and Se, especially As. Cd throughfall deposition is roughly similar for both Bear Branch and HRTB, with lead slightly higher for Bear Branch than HRTB (Castro *et al.*, 1999). However, both As and Se deposition are substantially higher at HRTB than at Bear Branch. Church *et al.* (1998) noted that Al, Zn, Ni, Mn, and Cd are transmitted through the Bear Branch watershed; Cu, Cr, Se, As, Fe, and Pb are largely retained in the Bear Branch watershed, presumably as organically-bound phases. Presumably As, and Se, may be stored in soil organic fractions, released and transported out during storm events. Analysis of input-output budgets indicated that 50-90% of the input of Pb, As, and Se was retained in the HRTB watershed, 25% of Fe, Cu, and Cr retained, and that the watershed was a net source of Zn, Ni, and Cd (Castro *et al.*, 1999).

Of course, mercury is the key element of interest in acidic deposition work since it is toxic, wide-spread, and bioaccumulated (Monson and Brezonik, 1999). Mercury levels at both BLAC and HRTB were below the EPA EcoTox threshold (EPA 1996) for inorganic mercury of 1.3 μg/L and 0.003 μg/L of methyl mercury. Methyl mercury, during episodes, ranged from 0.01-0.19 ng/L at both BLAC and HRTB. However, mercury bioaccumulation and biomagnification of even ultra-trace levels (subnanogram/L) in aquatic food chains may present problems to higher consumers (fish to humans). The key concern is methyl mercury since this is the major bioaccumulative species of mercury.

The increasing regional significance of methyl mercury may be found in the recent paper by Yeardley *et al.* (1998). As part of the EPA Environmental Monitoring and Assessment Program (EMAP), fish tissue samples from 167 lakes in the northeastern United States were analyzed for Al, As, Cd, Cr, Cu, Fe, Hg, Ni, Pb, Se, and Zn. Using EPA hazard assessment models, only methyl mercury was determined to be an element of regional concern to fish consumers, with 26% of the lakes exceeding the human critical value of 0.2 μg/g.

Monson and Brezonik (1999) point out that there are several questions relating to methyl mercury bioavailability, including the availability and form of methyl mercury for uptake. Generally, it is agreed that bioavailable mercury is a function of methyl mercury concentration (Wiener *et al.*, 1990), but many factors may modulate uptake kinetics (Monson and Brezonik, 1999). Of concern also is the potential role of methyl mercury as an endocrine disrupting chemical at ultralow levels (Colburn *et al.*, 1993).

Monthly total and particulate levels of Hg, Cd, Pb, As and Se were low, as were the levels of total and particulate CH_3Hg. Monthly mean baseflow levels for total Hg were 1.7 ng/L at BLAC and 2.1 ng/L at HRTB. Cd, Pb, As, and Se all had mean monthly averages below 0.7 μg/L at both sites. For Hg, particulate Hg was a significant component of total Hg. However, it is apparent

that western Maryland streams have higher trace metal concentrations than central and eastern Maryland during episodes, in part reflecting higher deposition rates in the area. However, not all metals sampled at the other sites were sampled in western Maryland so that complete comparisons (spatially and temporally) are difficult to make. Elevated levels of As, Pb and Se may be of concern during storm events.

F. Extensive Stream Sampling

Following identification of significant relationships between important chemical variables identified as part of our intensive study of five western Maryland streams (e.g., linear relationship between ANC_{min} and ANC_{index}, etc.), we undertook a synoptic sampling of 33 stream sites in the Savage River watershed to attempt to verify these relationships. Interestingly, results from the surveys indicate that there was no statistically significant difference between the spring stormflow ANC and spring baseflow ANC at the 33 sites (Figure 4.76); the mean (paired) difference between these samples was only 0.7 μeq/L (std. dev. = 31.6 μeq/L). Spring stormflow ANC was significantly different from fall baseflow ANC, however (mean difference = -14.3 μeq/L; std. dev. = 32.1 μeq/L; $\alpha = 0.05$; Figure 4.76). Despite these results, graphs of spring episode ANC on (a) spring baseflow ANC (Figure 4.77) and (b) fall baseflow ANC (Figure 4.78) indicate the same type of linear relationship noted for the intensive sites (Figures 4.33, 4.34), although the slopes of the regression equations were very close to unity. Several different explanations for these results are plausible: (1) episodic acidification is not regionally important in western Maryland streams, despite the fact that it is clearly observed in our intensive studies;

Table 4.5. Comparison of Cd, Pb, As, and Se among Bear Branch, Herrington Creek tributary (HRTB), and Black Lick Run (BLAC) for maximum levels (μg/L) observed during events. Elemental levels at HRTB and BLAC were corrected for the particulate fraction using base flow data for total and particulate elemental fractions.

Element	Bear Branch[1]	HRTB[2]	BLAC[2]
Cd	1.01	0.17	0.095
Pb	0.22	0.98	1.37
As	0.59	4.64	2.88
Se	0.14	0.41	0.41

[1]Total dissolved element
[2]Total corrected dissolved element

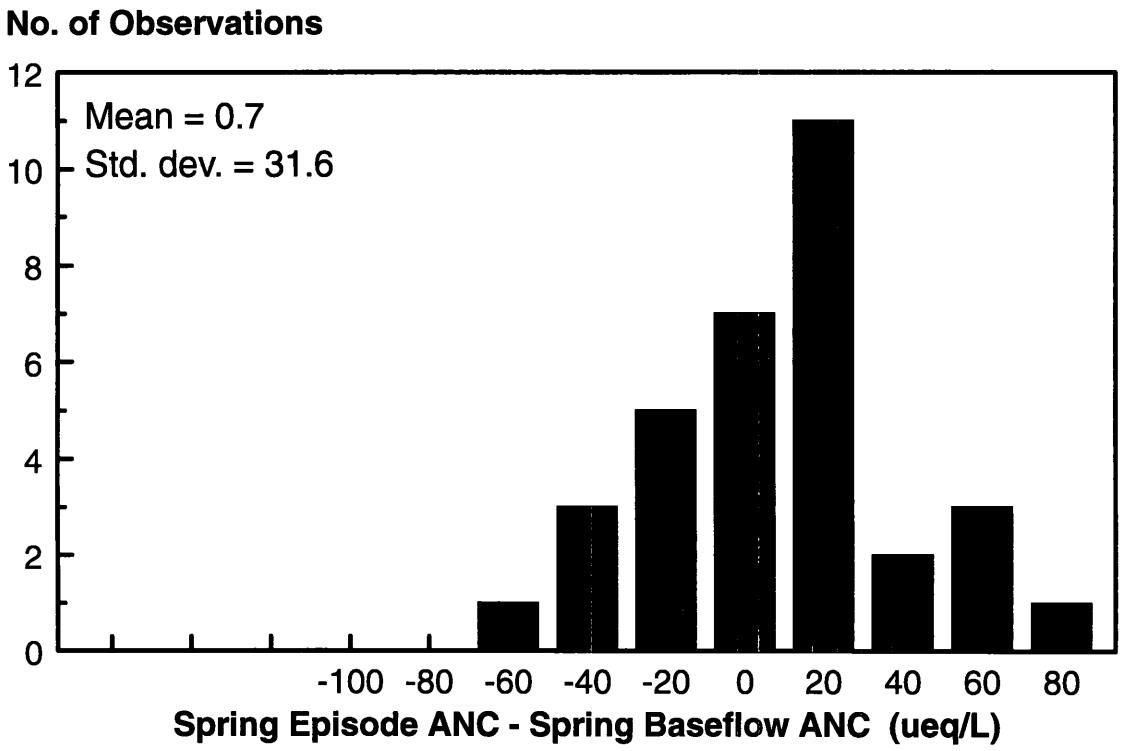

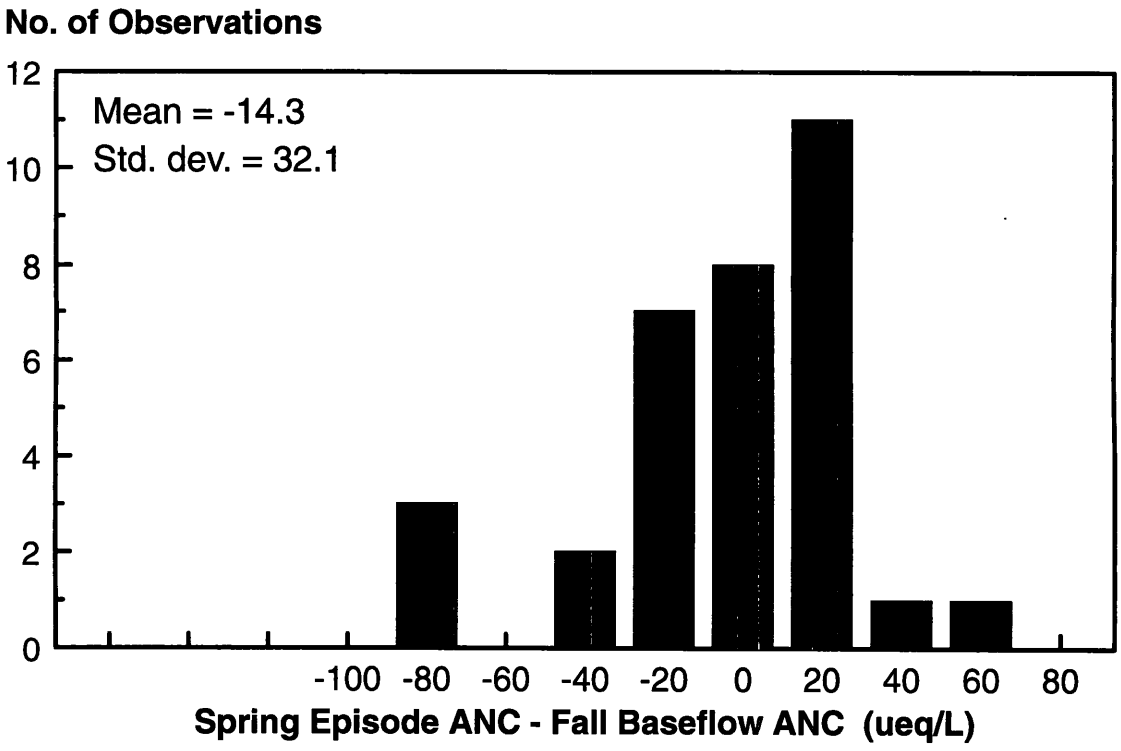

Figure 4.76. Frequency distribution of the difference between a) spring episode ANC and spring baseflow ANC and b) spring episode ANC and fall baseflow ANC for the 33 synoptic Savage River sampling sites.

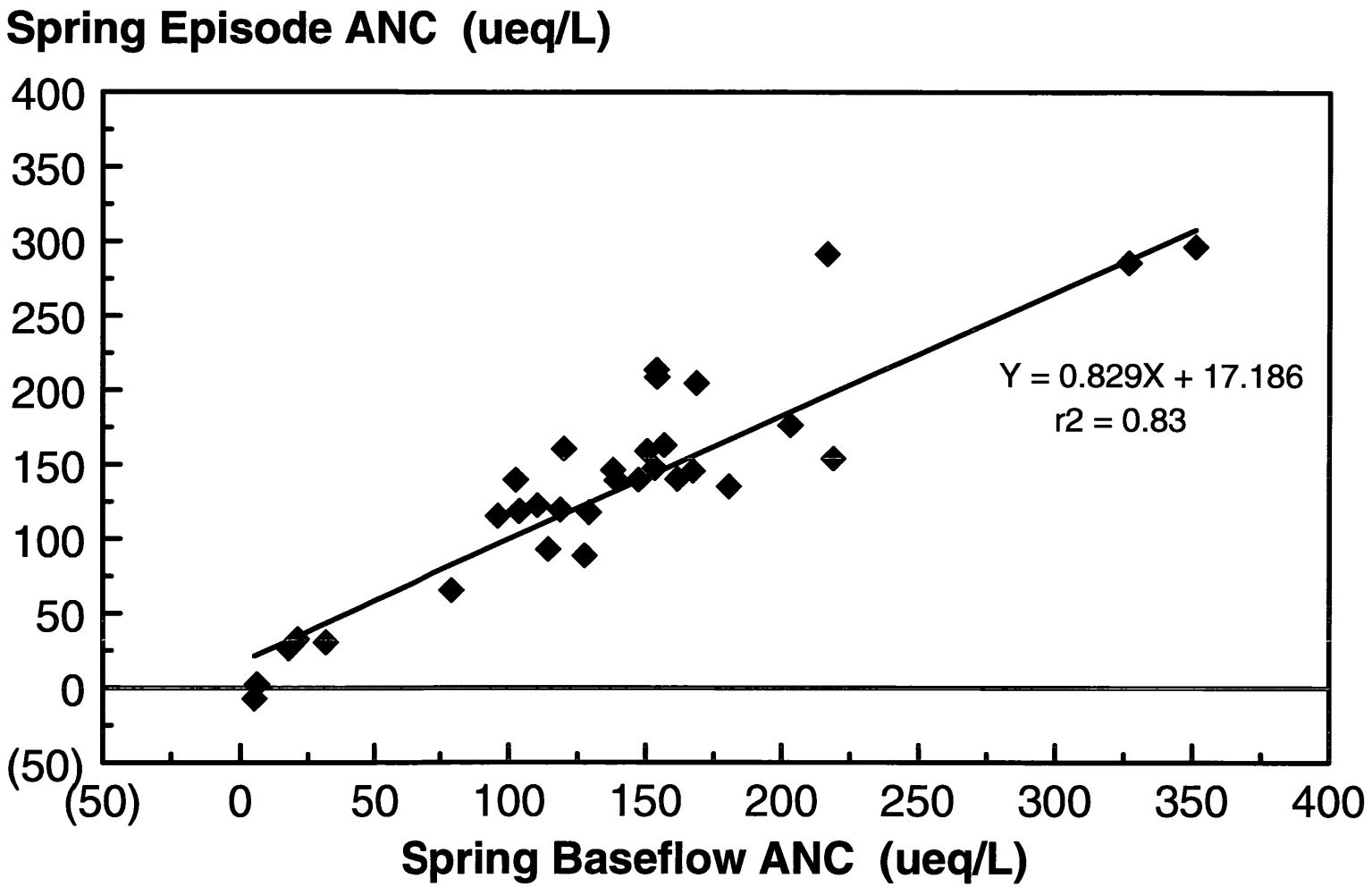

Figure 4.77. Observed statistical relationship between spring episode ANC and spring baseflow ANC for the 33 synoptic Savage River sampling sites.

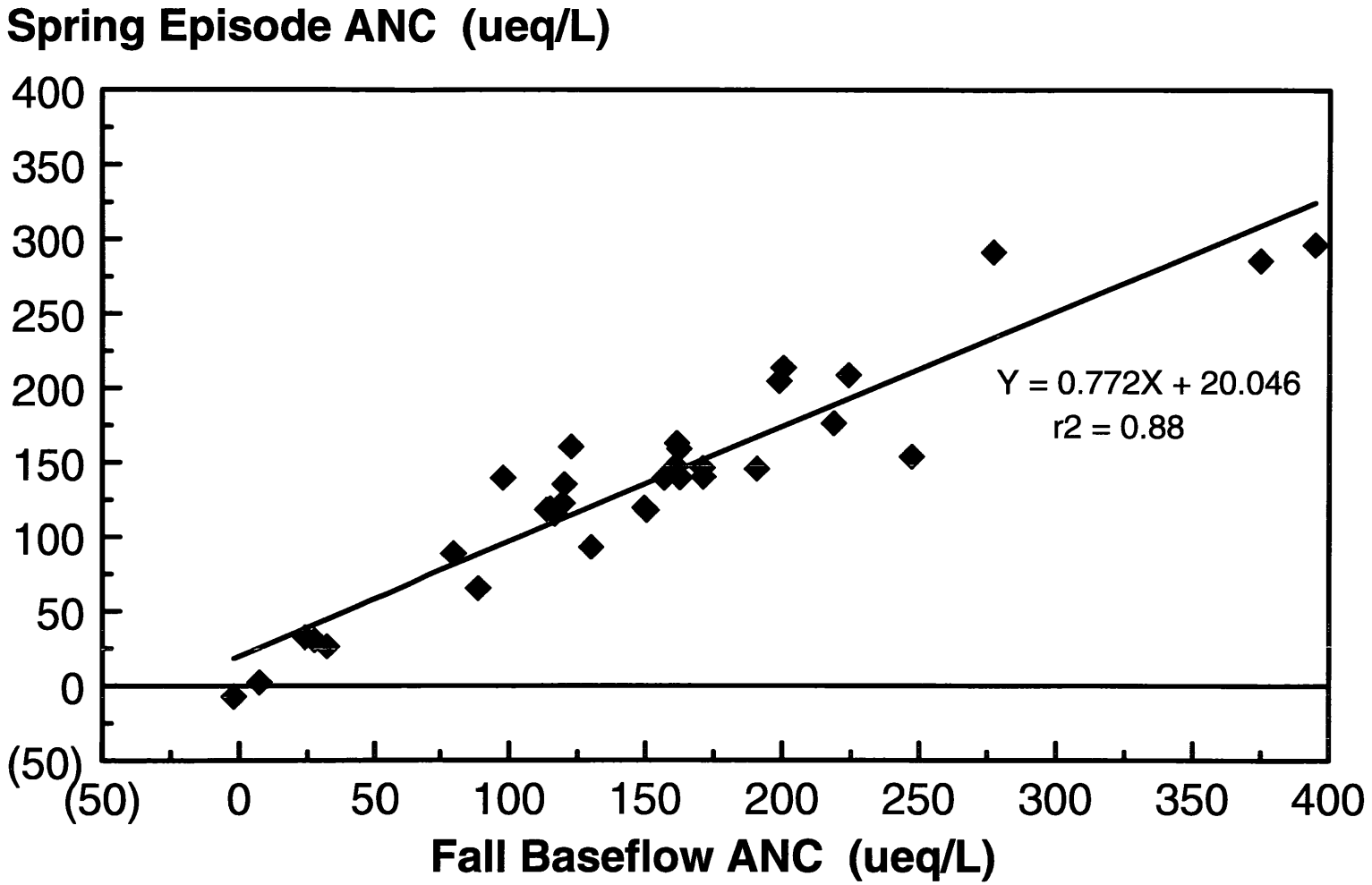

Figure 4.78. Observed statistical relationship between spring episode ANC and fall baseflow ANC for the 33 synoptic Savage River sampling sites.

(2) the particular spring episode sampled was not of sufficient magnitude to elicit a strong acidification response in the regional stream network; or (3) our synoptic sampling design simply was unable to capture the period of ANC_{min} that we were targeting. We favor either of the latter two explanations: first of all, the annual hydrographs for the five sites clearly portray the June 1997 stormflow event as quite modest—particularly when compared with the 1996 flood events which elicited dramatic ANC excursions (Figure 4.2). Second, since results from our intensive studies clearly illustrate that maximum ANC depression often occurs one or more days following the discharge peak, it is quite possible that our sampling design actually ended up sampling the streams too early. Unfortunately, budgetary constraints and uncooperative weather conditions in the third year of the project precluded additional synoptic sampling of another major episode as a way of testing the episodic model.

G. Hydrochemical Modeling of Episodic Acidification

Based on the results of the analysis of the chemical characteristics of episodic acidification in the five western Maryland streams, we attempted to apply a two-component mixing model (2CMM) as a means of providing improved estimates of regional episodic acidification of the entire population of streams in the region. The first step in this modeling effort was to estimate the proportion of streams that are currently experiencing episodic acidification by applying the model to the regional description of stream population based on the 1987 Maryland Synoptic Stream Chemistry Survey (MSSCS). Using Figure 4.34 derived from data from our five intensive sites, streams with ANC_{index} values less than about 32 μeq/L would be expected to become acidic (ANC < 0) during extreme hydrological events; streams with ANC_{index} values above this value would experience dramatic ANC decreases, but to ANC_{min} levels above zero.

Based on the results from the 1987 MSSCS described by Knapp *et al.* (1988) which excludes streams affected by acid mine drainage (AMD), 10.7% of stream kilometers on Maryland's Appalachian Plateau (AP) have a spring baseflow ANC < 0 μeq/L, 12.2% of streams have ANC < 25 μeq/L, and 15.7% have ANC < 50 μeq/L (Figure 4.79). Interpolating between the 25 and 50 μeq/L levels, we find that approximately 13.2% of the cumulative AP stream length in Maryland is predicted to have an ANC < 0 during extreme episodic conditions—a value that is not much higher than the 10.7% of streams that are chronically acidic during the spring period. The estimated proportion of episodically acidified streams increases, however, if we use an ANC sensitivity criterion of 25 μeq/L—noting that this ANC level corresponds roughly to a pH of 5.5, considered nearing the sensitivity threshold for brook trout of the median pH of 5.0-5.2 (Baker *et al.*, 1996) where trout abundance is reduced, and where significant chronic/acute effects may occur (Morgan, 1995). Using this sensitivity level (corresponding to an ANC_{index} value of about 71 μeq/L) and again interpolating, we predict that 19.7% of the cumulative Maryland AP stream length experiences deleterious acid episodes during extreme stormflow events—an estimate that nearly doubles the percentage based on the spring baseflow survey.

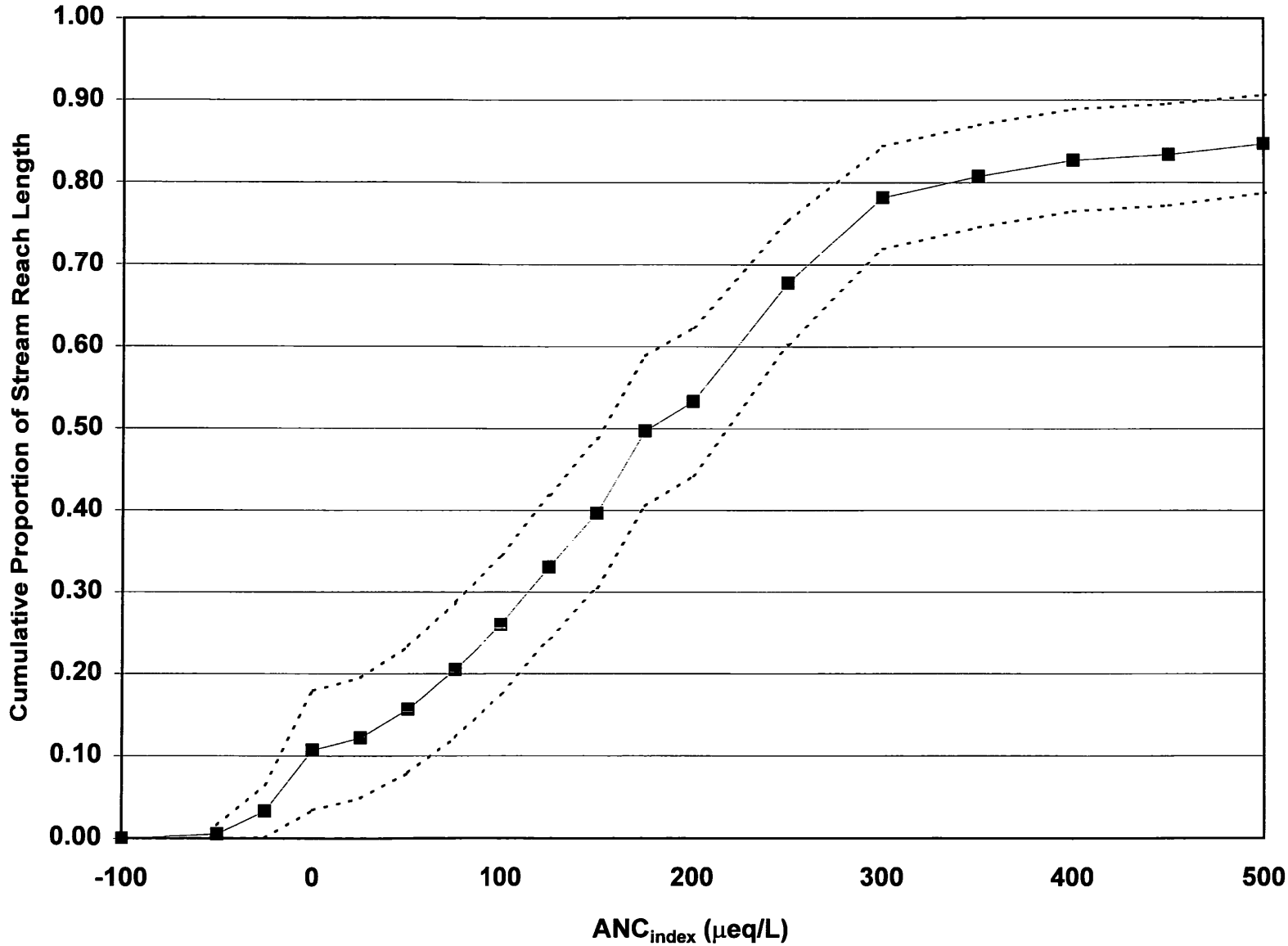

Figure 4.79. Cumulative proportion of stream reach length as a function of measured baseflow ANC (ANC_{index}) measured in Appalachian Plateau (AP) streams in western Maryland during the 1987 Maryland Synoptic Stream Chemistry Survey (MSSCS; from Knapp *et al.*, 1988); 95% confidence bounds also shown. Distribution truncated above ANC > 500 μeq/L.

The analysis can also be performed by considering uncertainties associated with both the regression model (i.e., using the lower 95% confidence limit for *prediction*; Figure 4.80) and the regional population estimates (Figure 4.79). Again, assuming streams with episodic ANC_{min} values < 25 μeq/L would experience deleterious effects on brook trout populations, we find that the relevant 95% upper and lower confidence bounds correspond to ANC_{index} values of 96 and 47 μeq/L, respectively. Combining with the confidence bounds shown in Figure 4.79 for regional estimation, we estimate with 95% confidence that the percentage of cumulative stream reach on the Maryland AP that experiences deleterious acid episodes is between 8.0% and 34.5%. It is interesting to note that the regional estimates made in this report are very similar to estimates provided by Eshleman (1995) using a previously published regression model based on data collected throughout the AP region (streams in Maryland and Pennsylvania; Figure 4.81). Comparing the models shown in Figure 4.80 and Figure 4.81, it is apparent that both the slopes and y-intercepts of the models are nearly identical, yielding similar estimates of regional acidification of western Maryland streams.

While our field/modeling study suggests that a relatively large proportion of the cumulative stream length on the AP in western Maryland currently experiences deleterious acid episodes, one of our research objectives was to predict the proportion that might experience such episodes in the future, given reductions in acid deposition loading to the region. The modeling approach of Eshleman *et al.* (1995)—known as REALSM (Regional Episodic Acidification of Lakes and Streams Model)–can be used to address this question, if a robust model calibration can be obtained using the field data. We tested the model using data from two episodes (9/5/96 and 2/18/98) that had been sampled for the three field sites (BIGR, BLAC, and HRTB) that are not believed to be influenced by land use disturbances or acid mine drainage. Model calibrations for these two episodes are presented in Figure 4.82 and Figure 4.83, respectively. The models only roughly reproduce the patterns of the data, namely the variation of R_{ion} with ANC_{pre}, but this may be mostly related to the fact that we have only three data points with which to calibrate the model; given the site-to-site variations in the characteristics of episodic acidification discussed previously, it seems reasonable to go ahead and apply the model to the regional population described by Knapp *et al.* (1988). A major limitation in testing the model calibration is the unavailability of SO_4^{2-}, NO_3^-, OA^- and SBC data for the regional stream population. In their 1987 survey, Knapp *et al.* (1988) did not measure major ion concentrations, so we are forced to assume regional mean concentrations, which cannot be verified using a regional data set. As described by Eshleman *et al.* (1995), our approach to prediction will thus be to use regional mean values of SO_4^{2-} (165.4 μeq/L), NO_3^- (19.9 μeq/L), and OA^- (9.7 μeq/L) during "index" conditions (based on the 9/5/96 episode) and compute SBC by difference (SBC = SAA + ANC). Similarly, we will use mean ion changes reported for the 9/5/96 episode (ΔSO_4^{2-} = 26.5 μeq/L; ΔNO_3^- = 7.9 μeq/L; ΔOA^- = 9.2 μeq/L), again computing ΔSBC by difference. REALSM (coded in a MS-Excel spreadsheet) is then run using a regional "F-factor"(or range of F-factor values) for different values of $\%\Delta SO_4^{2-}$ (%ΔS) and $\%\Delta NO_3^-$ (%ΔN) that represent target values for acid

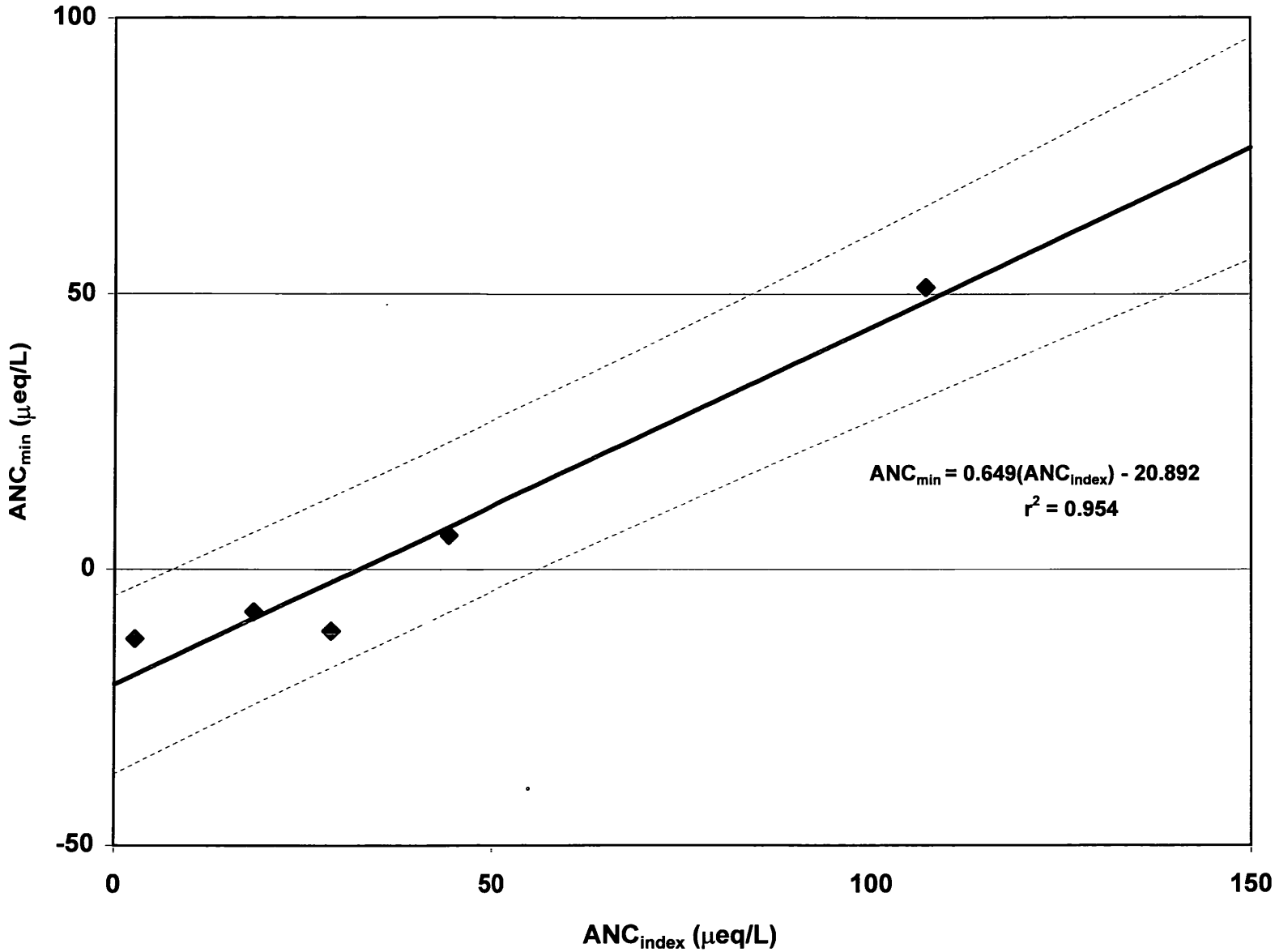

Figure 4.80. Relationship between ANC_{min} and ANC_{index} for the five study streams. Linear regression model and 95% confidence bounds for prediction also shown.

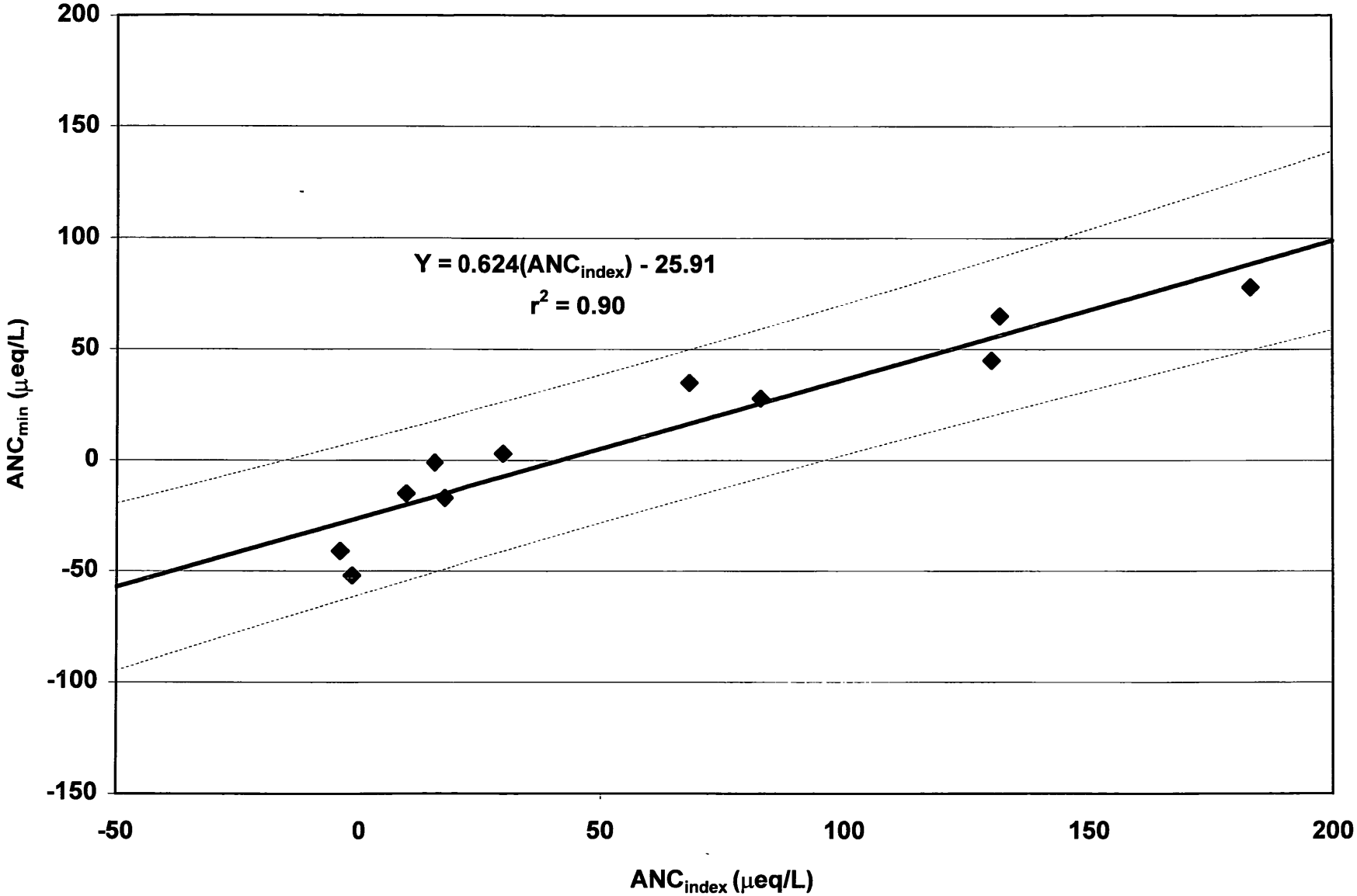

Figure 4.81. Relationship between ANC_{min} and ANC_{index} for 11 streams on the Appalachian Plateau (AP) in Pennsylvania and Maryland (published by Eshleman, 1995). Linear regression model and 95% confidence bounds for prediction also shown.

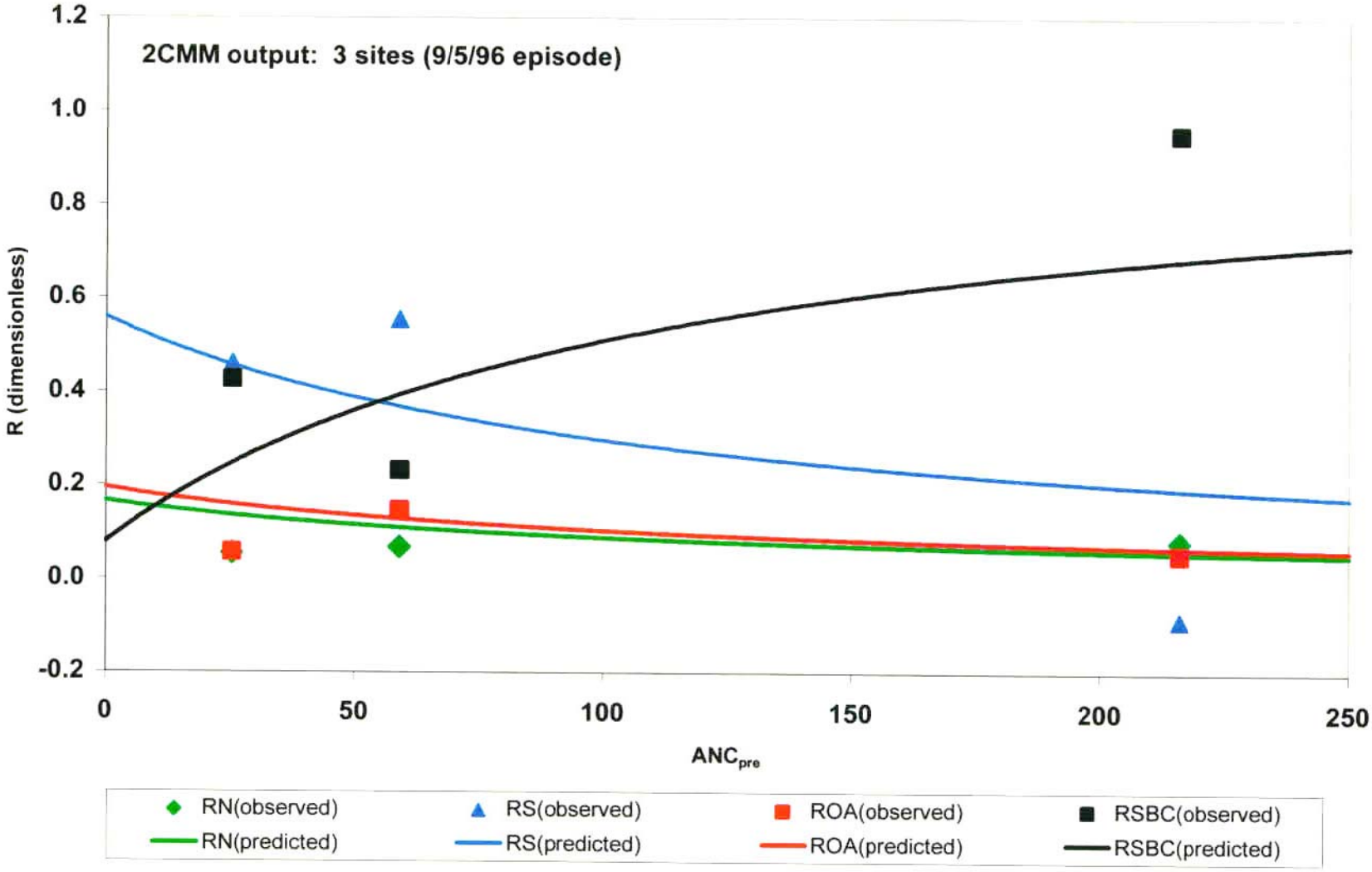

Figure 4.82. Ion contribution ratios (R_{ion}) for BIGR, BLAC, and HRTB for the 9/5/96 episode. Calibration results for 2CMM also shown for comparison.

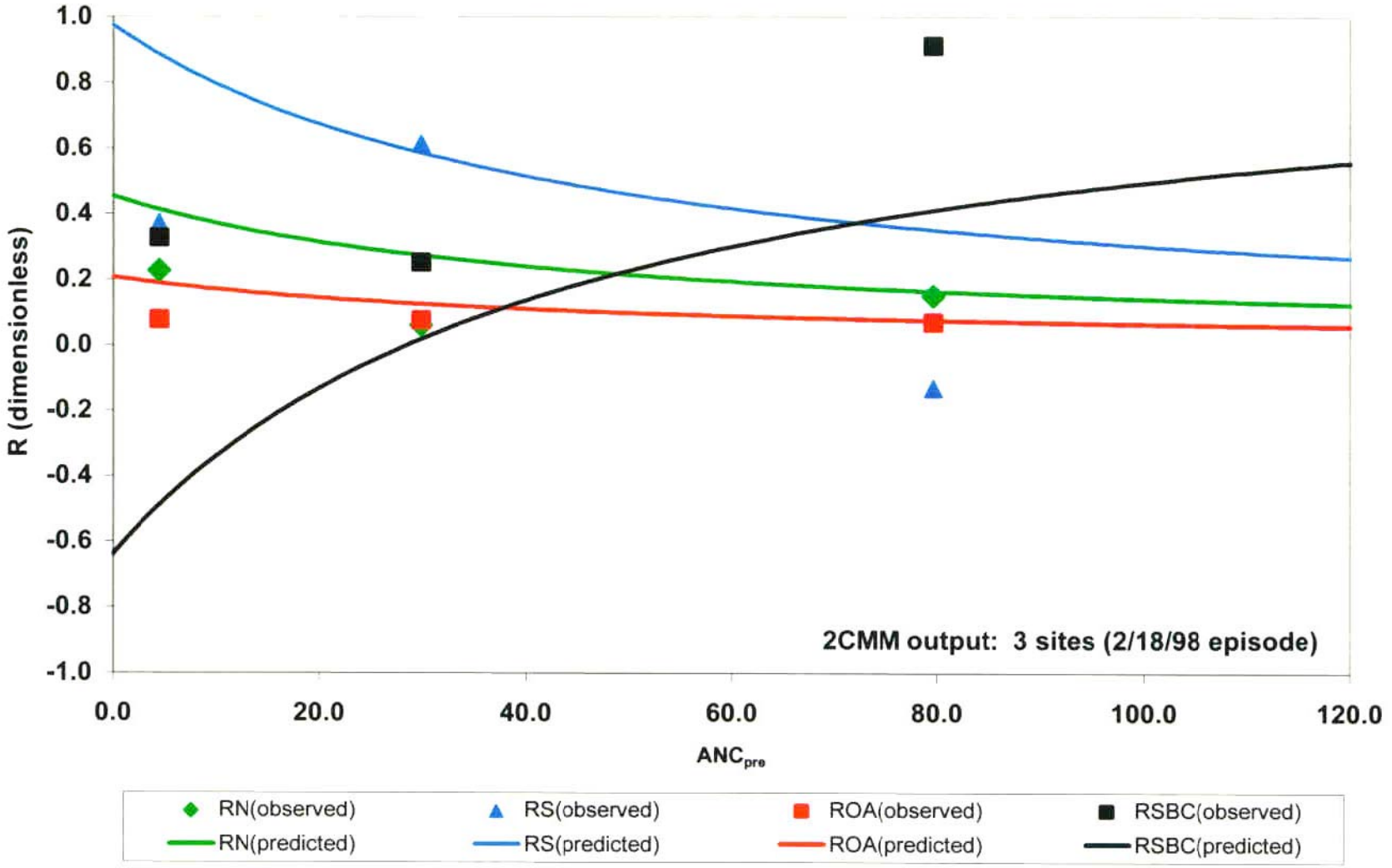

Figure 4.83. Ion contribution ratios (R_{ion}) for BIGR, BLAC, and HRTB for the 2/18/98 episode. Calibration results for 2CMM also shown for comparison.

abatement. It should be noted that the behavior of REALSM is consistent with previous analyses by Morgan *et al.* (1994) that suggested that forested watersheds in western Maryland are approximately at "steady state" with respect to atmospheric sulfur deposition. These results (and the REALSM predictions) suggest that reductions in sulfur deposition will cause proportional declines in stream SO_4^{2-} concentrations—both under baseflow and episodic conditions

Using the ANC < 25 μeq/L criterion, results of the model runs (presented in Table 4.6) suggest that western Maryland streams will respond to decreases in sulfate deposition of the magnitude of 40% (corresponding to values of %ΔS of –40%), given F-factor values in the range 0.5-0.6 and no change in nitrate concentrations. During index conditions, the percentage of affected streams declines from a current estimate of 12.2% to a predicted value of 3.3%, while under extreme episodic conditions, the percentage of affected streams declines only marginally (from 15.7% to 10.7%). Using an F-factor value of 0.7, the declines under index and episodic conditions are even smaller (12.2% to 10.7% and 15.7% to 12.2%, respectively). The model predicts, however, that fewer stream systems would be episodically-affected if %ΔS is increased to –60%. As expected, the model shows that including a significant decrease in nitric acid concentrations (%ΔN = -50%) has almost no effect on the percentages of affected systems, since HNO_3 is a relatively minor contributor to episodes in these streams in western Maryland.

H. Analysis of Long-Term Changes in Streamwater

Long-term monitoring (1990 to present) of streamwater chemical composition (both bi-weekly and episodic sampling) and discharge at the Upper Big Run (BIGR) site support the conclusion that little improvement in water quality has been brought about by the 1990 Clean Air Act Amendments which mandated 40% cutbacks in sulfur emissions nationally. We graphed the occurrences of (minimum) episodic ANC conditions measured during a previous study with those observed during the present study and found little in the way of a temporal pattern suggesting improvement (Figure 4.84). The range in the observations has changed little from 1990 to present, with a suggestion that—if anything—minimum ANC conditions may have actually moved somewhat lower; we believe, however, that this suggestion is a sampling artifact that is explained by the fact that the 1996 water year contained several extreme hydrological events with rather long (~ 50-100 year) recurrence intervals. Given the inverse dependence of ANC_{min} on discharge (Figure 4.32), we believe this is a reasonable interpretation of this interesting data set.

We also used the method described by Eshleman *et al.* (1998) to examine long-term changes in SO_4^{2-} and NO_3^- fluxes (and discharge-weighted mean concentrations) at BIGR during the period 1990-present; since a continuously-recording stream gage was only put into operation in late 1995, we needed to use auxiliary flow data from the Savage River at Barton site as a means of estimating daily discharge values for BIGR for the 1990-94 period; fortunately, a linear regression model is able to explain a very high percentage of the total variation in discharge at BIGR (see Eshleman *et al.*, 1998). Graphs of the raw SO_4^{2-} and NO_3^- concentration data and

Table 4.6. Predicted percentages of affected Appalachian Plateau cumulative stream length in western Maryland under current and future conditions (see text for description of scenarios).

Current Conditions (ANC < 25 μeq/L)		Scenarios			Future Conditions (ANC < 25 μeq/L)	
Index	Episodic	F	%ΔS	%ΔN	Index	Episodic
12.2	15.7	0.5	-40	0	3.3	10.7
12.2	15.7	0.6	-40	0	3.3	10.7
12.2	15.7	0.7	-40	0	10.7	12.2
12.2	15.7	0.5	-60	0	3.3	3.3
12.2	15.7	0.6	-60	0	3.3	3.3
12.2	15.7	0.7	-60	0	3.3	10.7
12.2	15.7	0.5	-40	-50	3.3	10.7

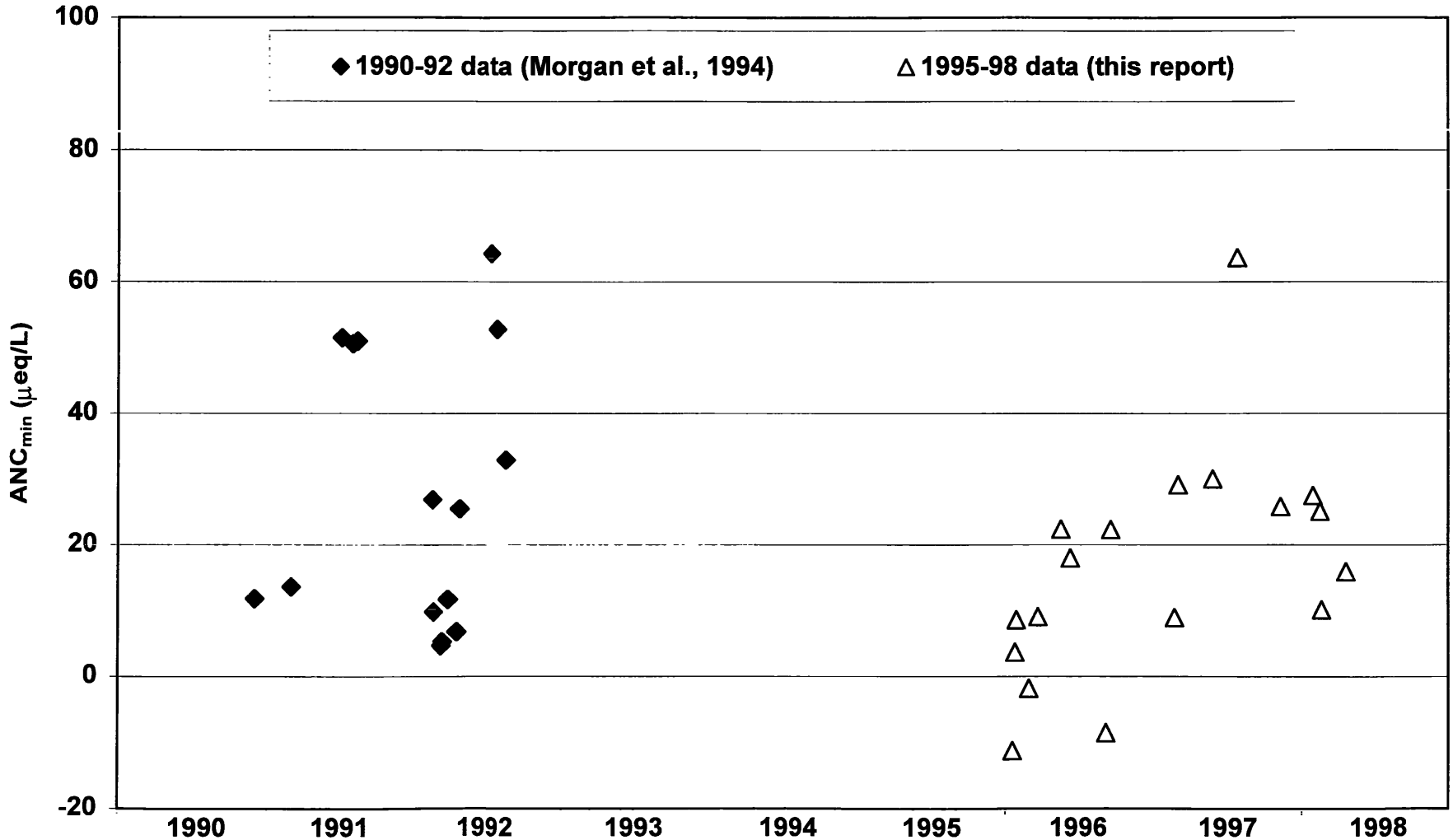

Figure 4.84. Temporal sequence of observed values of ANC_{min} measured at BIGR during episodes as part of this study and as part of a previous study reported by Morgan *et al.* (1994).

computed long-term monthly fluxes for BIGR are shown in Figures 4.85 – 4.88, respectively. While suggesting a clear seasonal pattern of higher fluxes during the dormant season in response to higher discharge, the SO_4^{2-} data suggest no clear trends over the nine-year period (Figures 4.85, 4.87); the NO_3^- data, while also indicating a clear seasonal pattern, also suggest a long-term decline in monthly flux during the period, however (Figures 4.86, 4.88).

The long-term trend in NO_3^- flux and concentration is even more obvious when the data are aggregated to annual water year periods (Figures 4.89, 4.90, respectively). Nitrate flux and annual discharge-weighted concentrations clearly peaked in 1991 and have been mostly declining ever since; several deviations from the long-term decline appear attributable to annual variations in runoff (Figure 4.91). The mean annual NO_3^- flux during the three water years of the present study (about 120 eq/ha-yr) is only about 50% as large as the annual flux in water year 1991, indicating a dramatic decline. While some researchers have proposed long-term nitrogen saturation of watersheds in western Maryland, Eshleman *et al.* (1998) has proposed forest disturbances such as gyspy moth defoliation as a cause of this long-term pattern in nitrate-N flux, showing that the summers of 1990 and 1991 were the last periods of significant gypsy moth defoliation in this watershed. An on-going USEPA-sponsored research project is currently exploring various approaches to modeling the effects of forest disturbances on nitrate-N export and the data presented here will eventually be used in calibration of a watershed model of this process (Eshleman *et al.*, 2000).

In contrast to the NO_3^- flux and concentration trends, comparable data for SO_4^{2-} suggest a far less dramatic decline (Figures 4.92, 4.93, respectively). Annual SO_4^{2-} fluxes appear to be driven mostly by the flux of water from the watershed, noting the similarity between Figure 4.92 and Figure 4.91. While it does appear that annual discharge-weighted SO_4^{2-} concentrations have declined during the nine-year period (Figure 4.93), the best explanation for this behavior may be due to an increase in precipitation and runoff, rather than any change in atmospheric deposition of sulfur to the watershed.

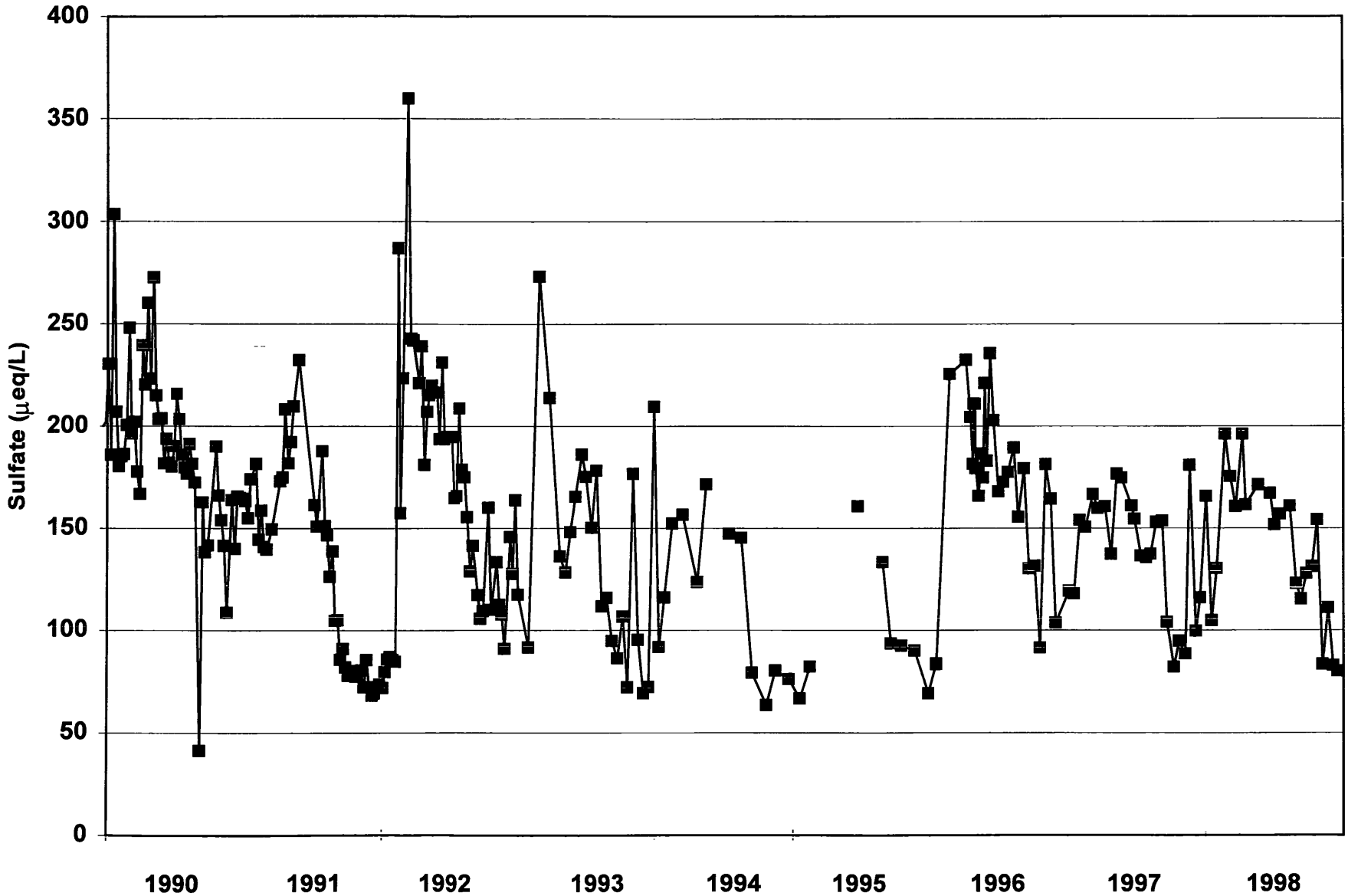

Figure 4.85. Graph of (approximately) bi-weekly measurements SO_4^{2-} concentration in streamwater measured at BIGR as part of this study and as part of a previous study reported by Morgan *et al.* (1994).

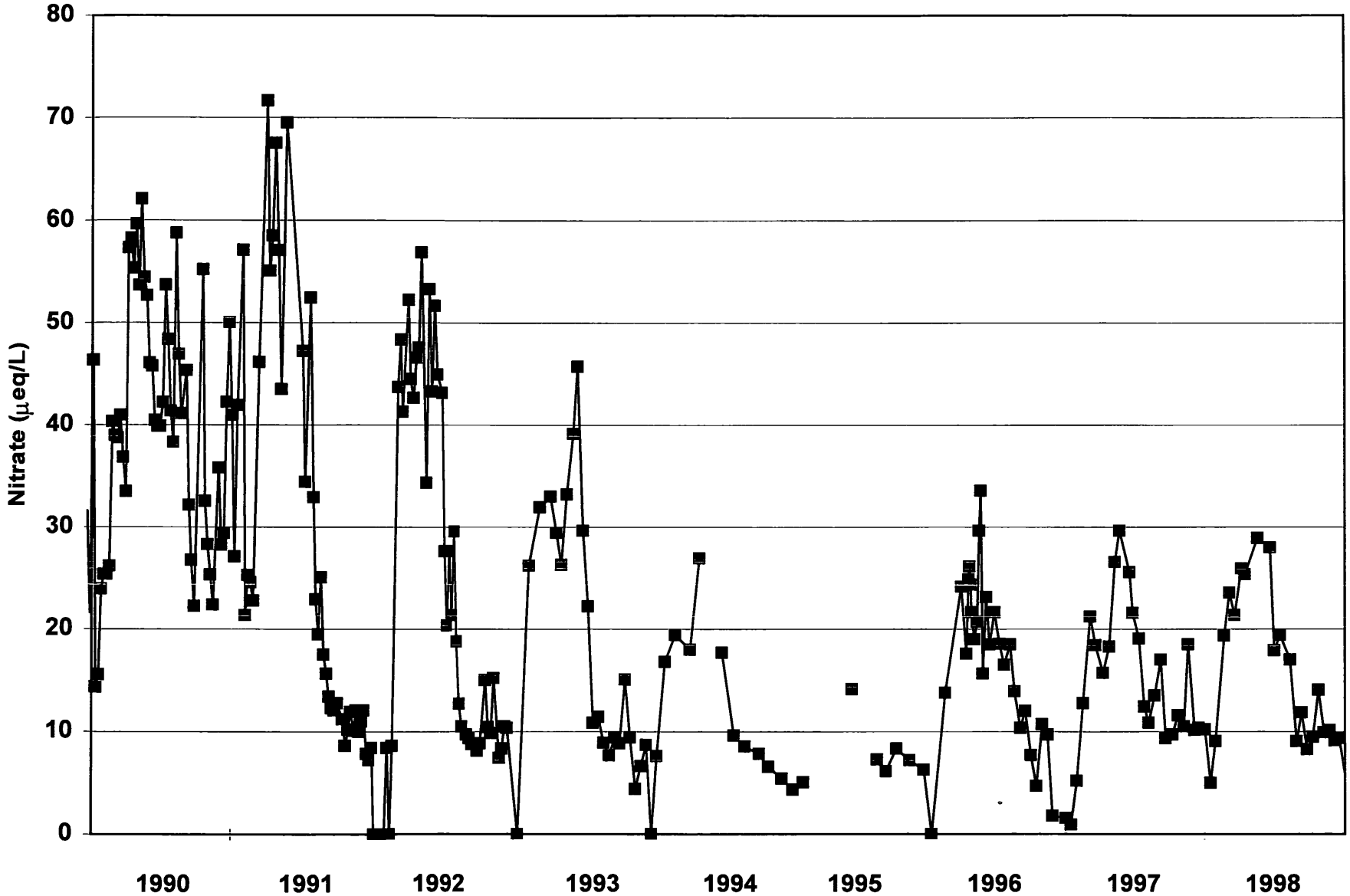

Figure 4.86. Graph of (approximately) bi-weekly measurements NO_3^- concentration in streamwater measured at BIGR as part of this study and as part of a previous study reported by Morgan *et al.* (1994).

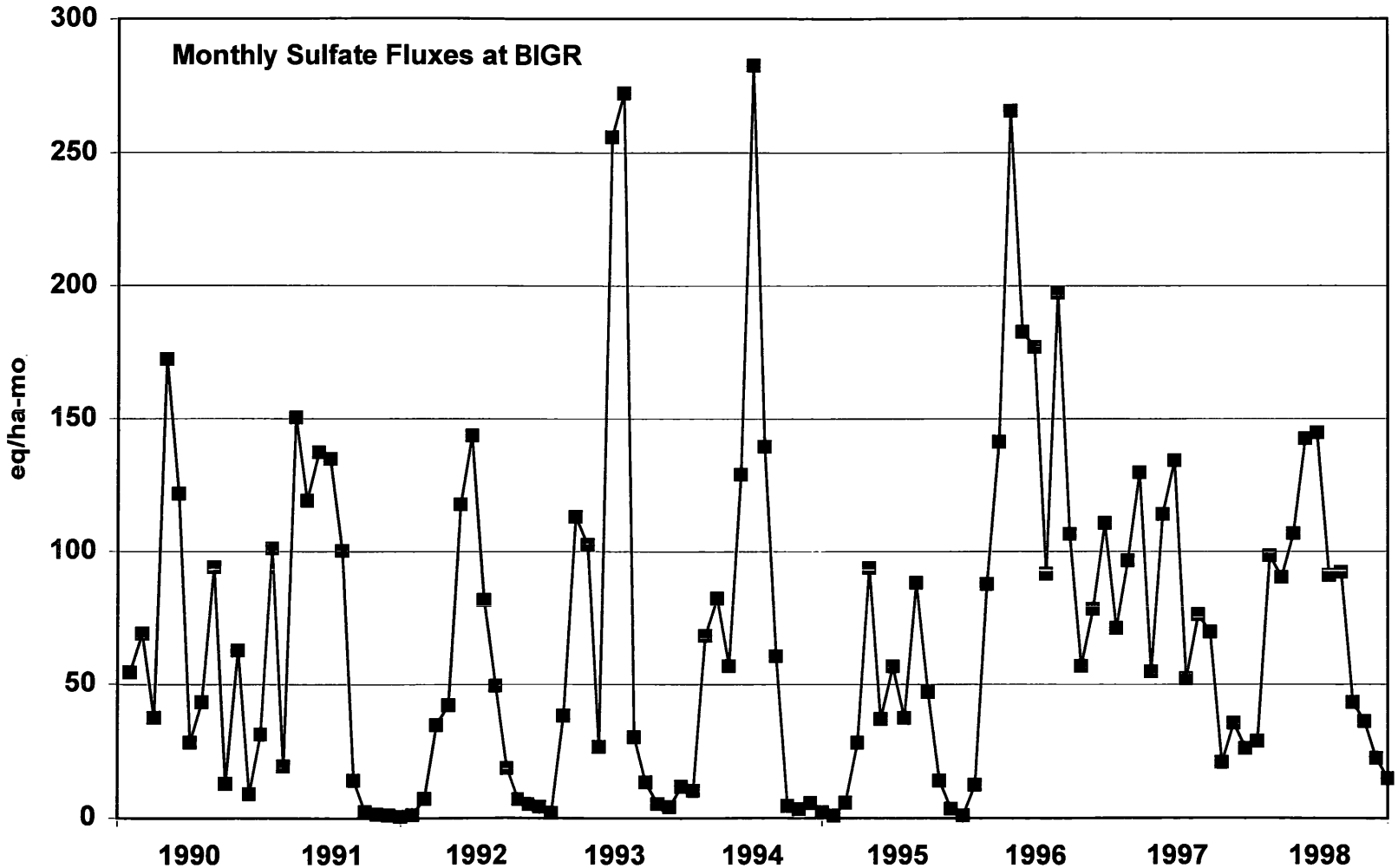

Figure 4.87. Computed monthly streamwater fluxes of SO_4^{2-} at BIGR based on discharge and concentration data collected during this study and as part of a previous study reported by Morgan *et al.* (1994).

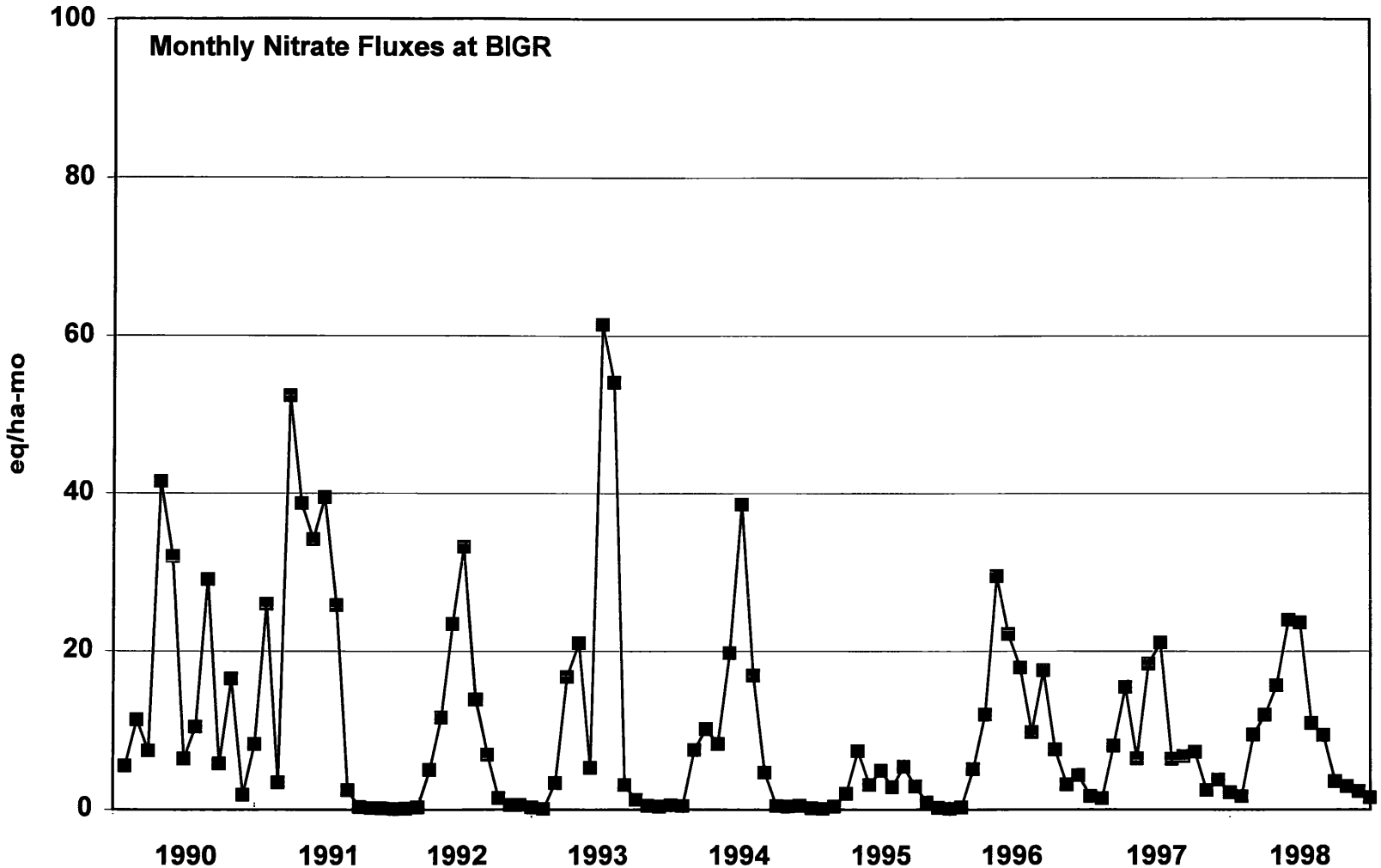

Figure 4.88. Computed monthly streamwater fluxes of NO_3^- at BIGR based on discharge and concentration data collected during this study and as part of a previous study reported by Morgan *et al.* (1994).

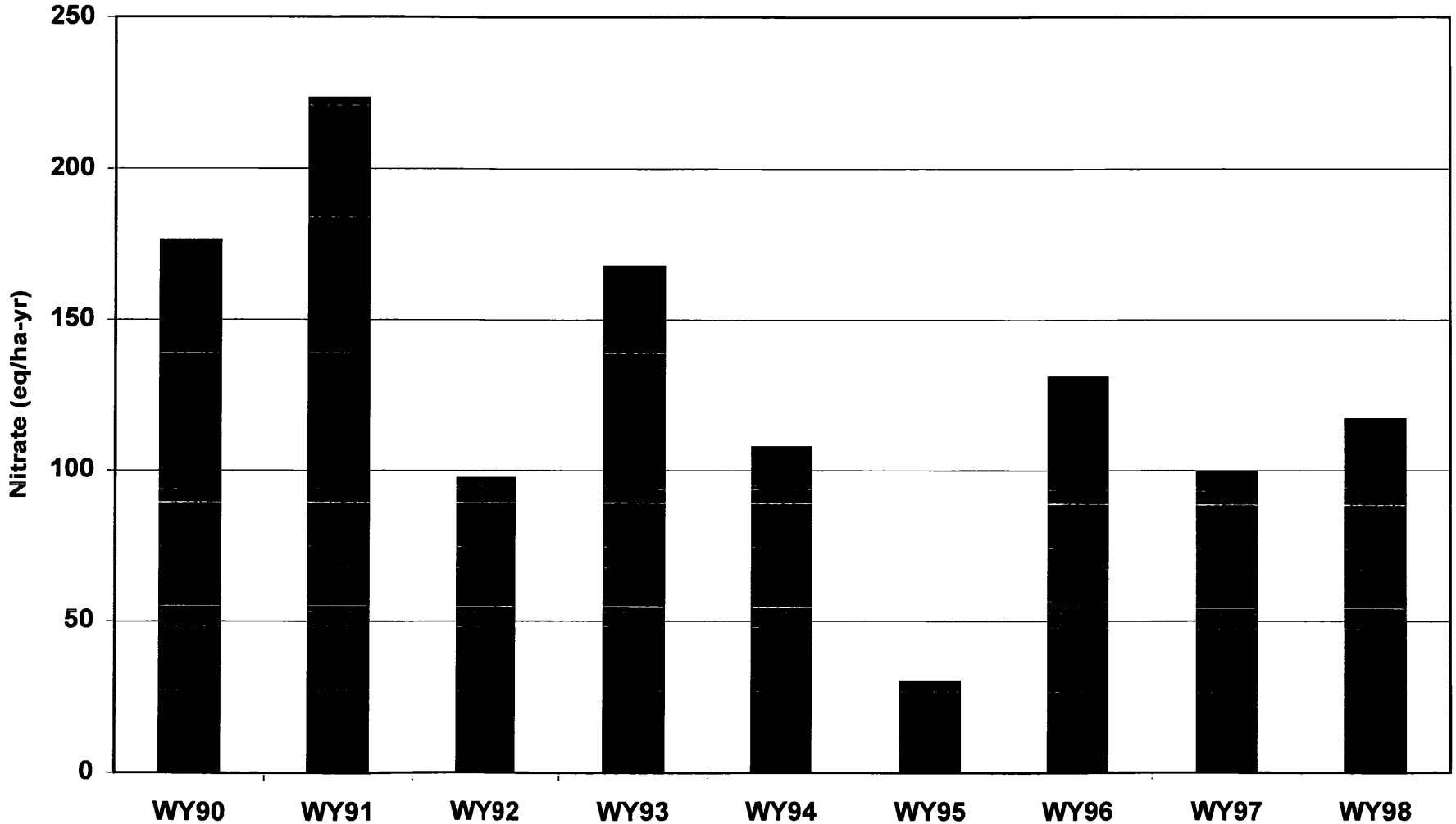

Figure 4.89. Computed annual fluxes of NO_3^- at BIGR (water years 1990-98) based on discharge and concentration data collected during this study and as part of a previous study reported by Morgan *et al.* (1994).

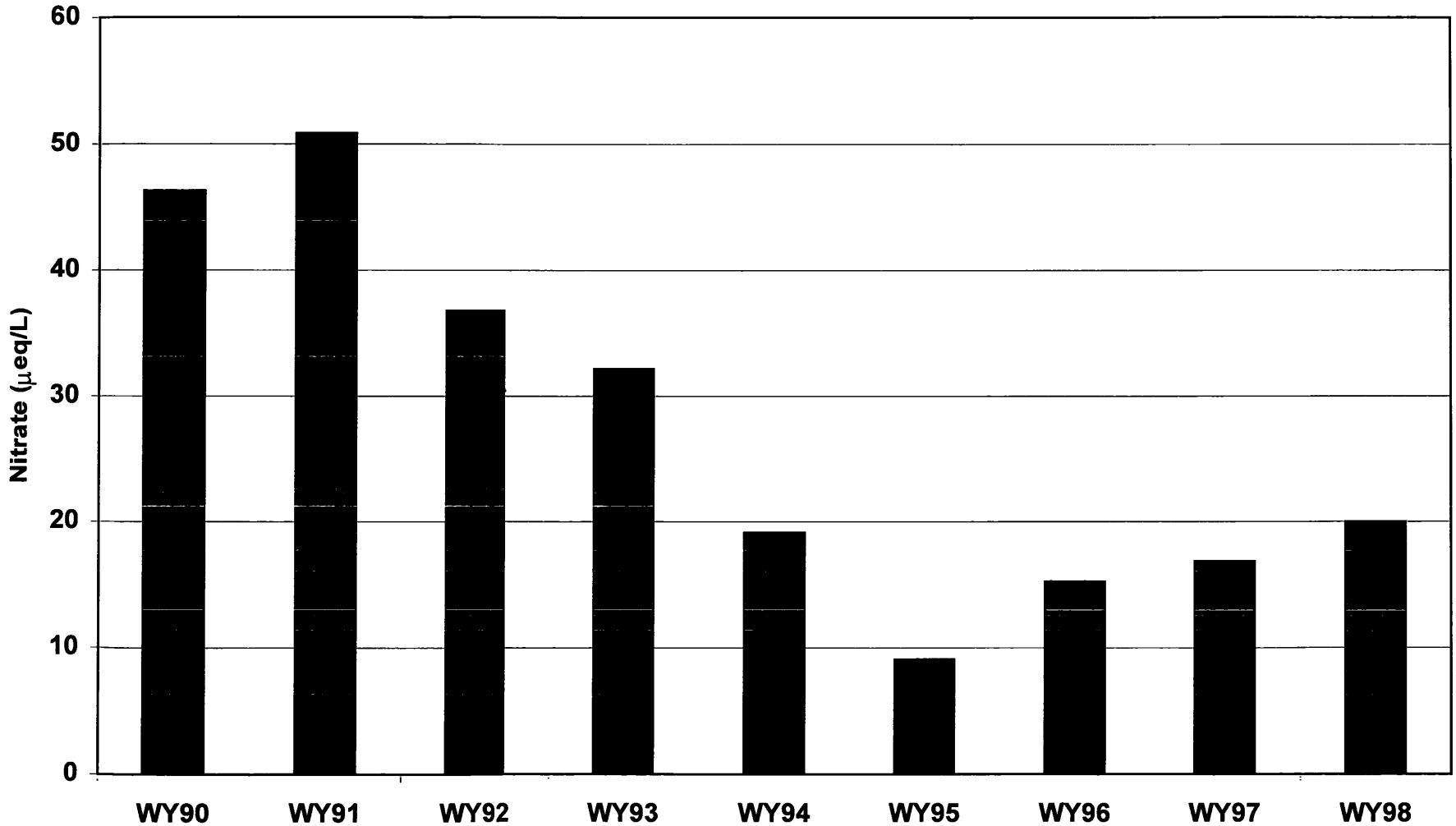

Figure 4.90. Computed annual discharge-weighted streamwater concentrations of NO_3^- at BIGR (water years 1990-98) based on discharge and concentration data collected during this study and as part of a previous study reported by Morgan *et al.* (1994).

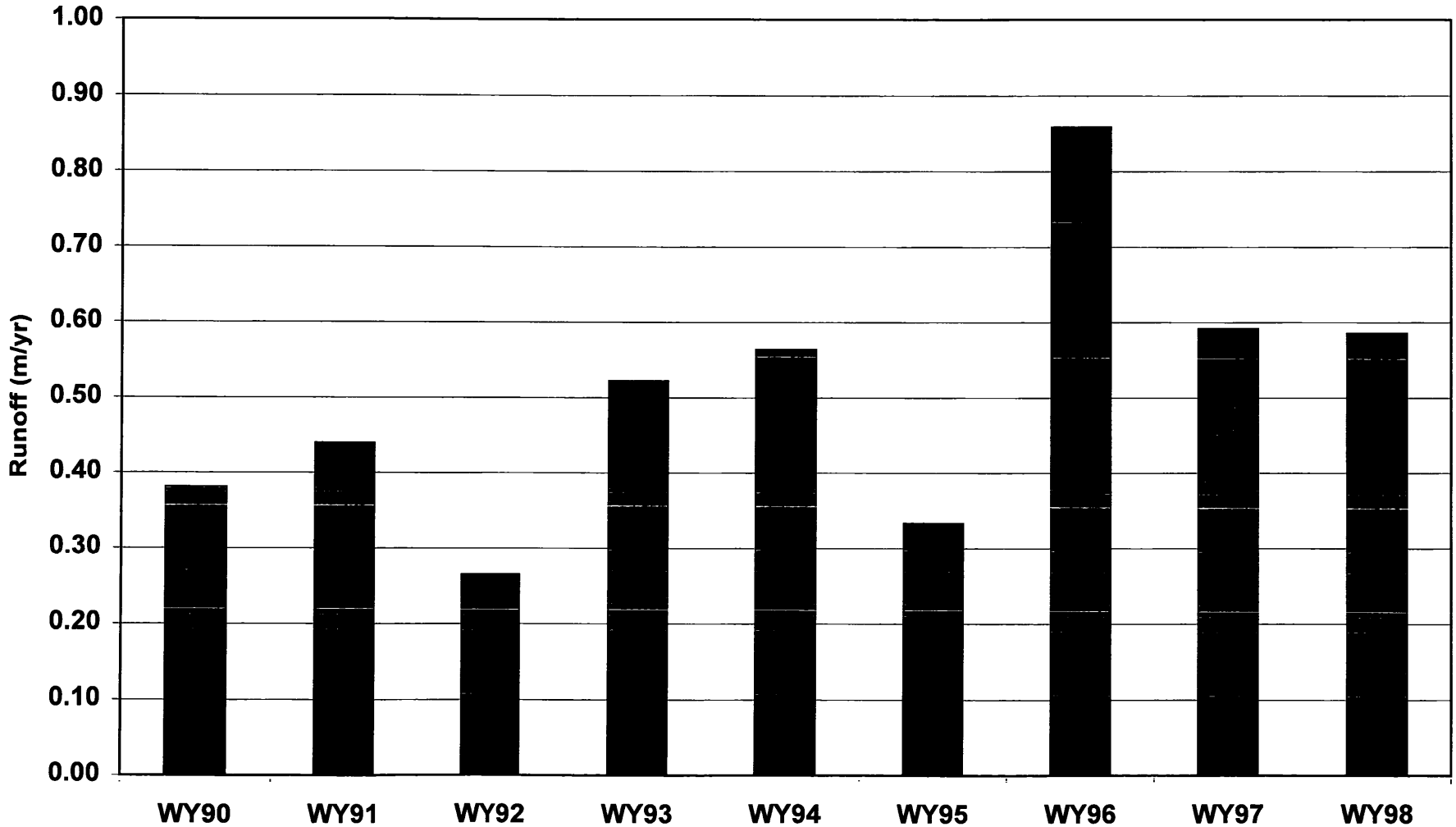

Figure 4.91. Computed annual runoff of water at BIGR (water years 1990-98) based on discharge data collected during this study (and using long-term discharge records from the SAVR site).

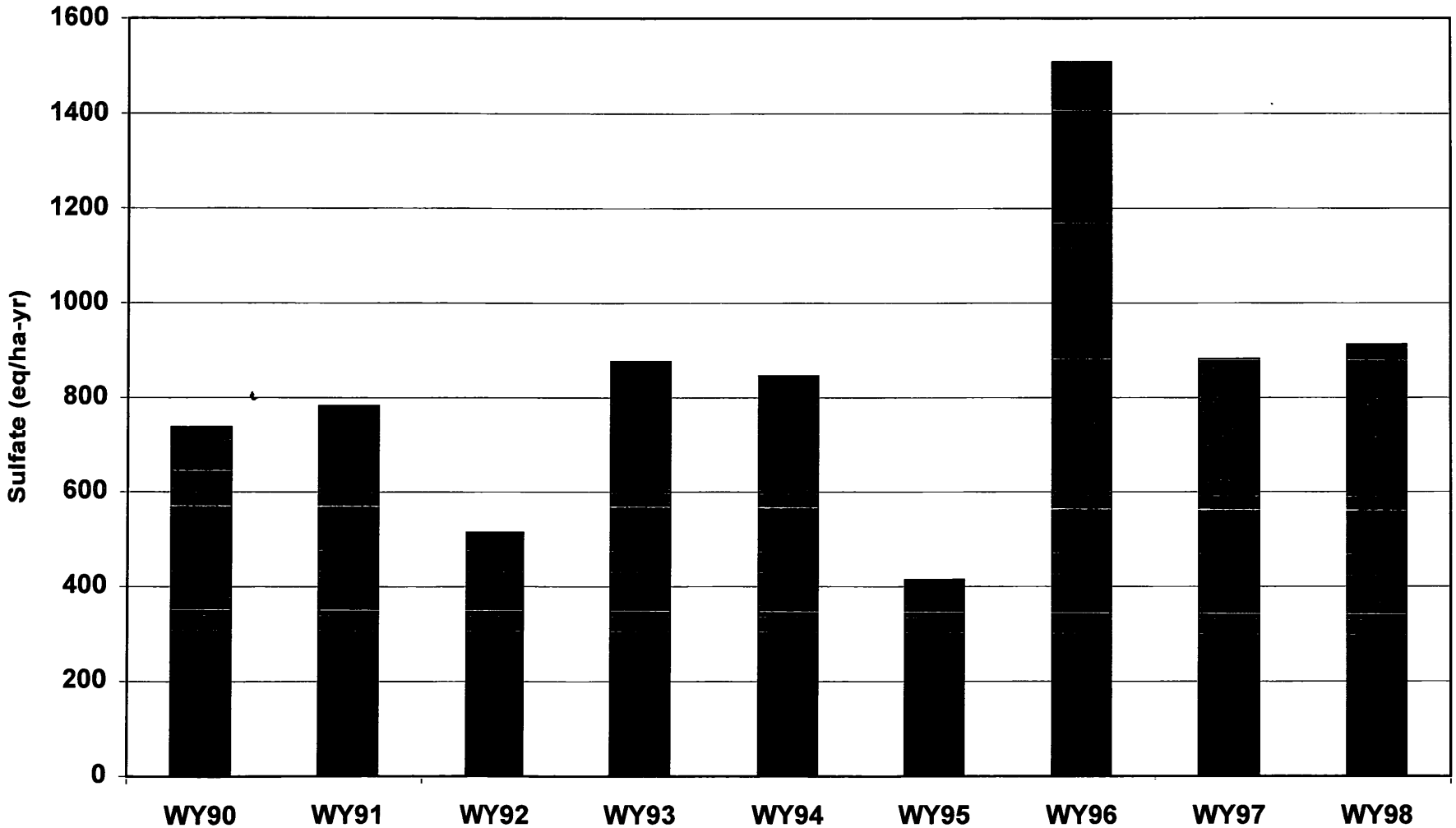

Figure 4.92. Computed annual streamwater fluxes of SO_4^{2-} at BIGR (water years 1990-98) based on discharge and concentration data collected during this study and as part of a previous study reported by Morgan *et al.* (1994).

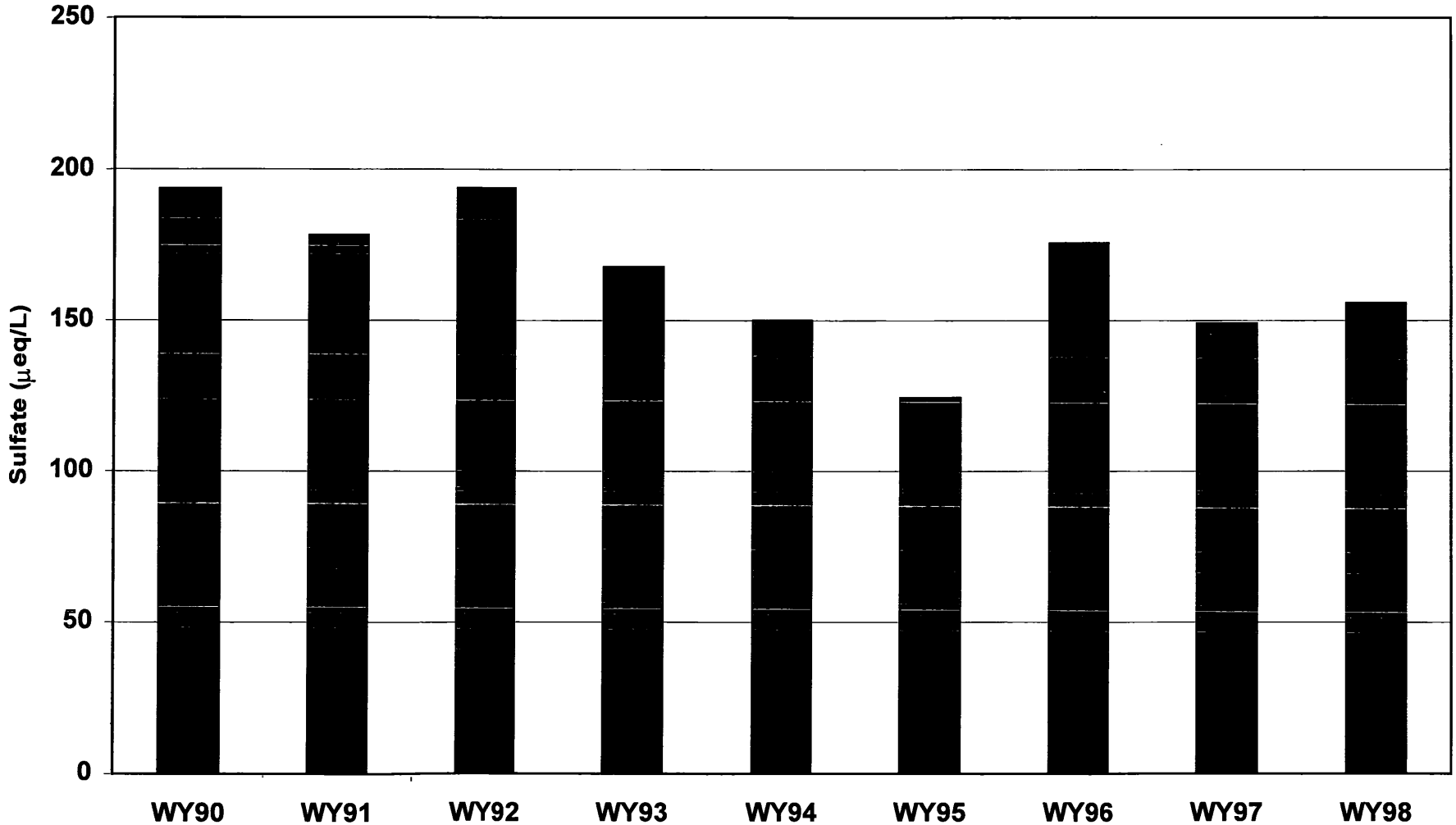

Figure 4.93. Computed annual discharge-weighted streamwater concentrations of SO_4^{2-} at BIGR (water years 1990-98) based on discharge and concentration data collected during this study and as part of a previous study reported by Morgan *et al.* (1994).

5. Conclusions

The results of this field study of episodic acidification clearly demonstrate that episodic acidification of surface waters—the transient loss of ANC that accompanies rainfall and snowmelt events—is ubiquitous in western Maryland watersheds. All five study streams experienced dramatic depressions in ANC, especially during or immediately following high stream discharge conditions caused by intense rainfall, rapidly melting snow, or a combination of rain-on-snow. In particular, data associated with two major floods in 1996—one in mid-January due to rain-on-snow and and a second in September due to the remnants of Hurricane Fran—illustrate the magnitude of ANC decline. During one of more of these two episodes, ANC in three of the five streams was "over-titrated" to negative values, also causing major depressions in pH (to values less than 5.0) and increases in exchangeable reactive Al concentrations (to levels exceeding 50 μg/L). These levels are clearly within the range of conditions that should be considered deleterious to populations of fish and other aquatic biota.

While the conditions measured during the two "Floods of 1996" are illustrative of the most extreme hydrological and hydrochemical conditions observed during the study, data from these and many other episodes conform to a predictable pattern that provides evidence for the underlying causes of episodic acidification in western Maryland streams, as well as in streamwaters in general. Minimum values of ANC (ANC_{min}) and changes in ANC (ΔANC) based on 75 discrete episode-stream observations were found to be predictable, varying linearly with the antecedent (i.e., pre-event) value of ANC (ANC_{pre}); ANC_{min} at our long-term monitoring site (Upper Big Run) was also found to vary as a linear function of the log of peak daily discharge. All of these results strongly support the previous conclusion based on data from a variety of watersheds in the eastern U.S. that episodic acidification is inherently a hydrological mixing process that can usually be described by a simple two-component mixing model (Eshleman, 1988; Eshleman *et al.*, 1995).

Using this rather robust modeling approach, the episodic response of an entire population of streams within a region can be estimated using calibration data from a small number of streams such as was obtained in the current study. For streams draining the Appalachian Plateau in western Maryland, the combined field/modeling study suggested that about 20% (95% confidence limits = 8%, 35%) of the cumulative length of streams in the region is either *episodically* or *chronically* acidified, based on an ANC_{min} criterion of 25 μeq/L. Compared to an estimate (based on the 1997 MSSCS reported by Knapp *et al.*, 1988) that 12% of the combined stream length is *chronically* acidified to this extremely low ANC level, episodic acidification may currently be causing deleterious impacts on fish populations in approximately the same number and length of streams in the region as is chronic acidification.

While the estimates of current regional acidification are based on a robust model that is also verifiable using data obtained from other watersheds draining the Appalachian Plateau (both in Maryland and Pennsylvania), determining the specific role of atmospheric deposition of sulfuric and nitric acids (as well as the role of natural strong organic acids) in the episodic acidification process is far more difficult. In general, our data support the conclusion that hydrological

dilution of base cations during stormflow events was the primary cause of ANC depression in the five study streams; this interpretation is further supported by the fact that dilution of base cations is more important in the higher ANC streams, a result that is also consistent with the conceptual acidification model employed. In the average episode observed, base cation dilution was just about equal (on an equivalent basis) to the depression in ANC, with nitric acid and organic acid concentrations increasing very slightly; the median change in sulfuric acid concentration was actually found to be negligible—a quite interesting result not necessarily inconsistent with an "acid rain" interpretation.

In fact, a conceptual model known as REALSM could be calibrated using data from two episodes that were particularly well-characterized. Results from application of the calibrated model to the regional stream population suggest that abatement of episodic acidification should occur in western Maryland once sulfuric acid concentrations are reduced by 40% from current levels (consistent with the 1990 Federal Clean Air Act Amendments [CAAA] and subsequent atmospheric emission controls), although there is substantial uncertainty associated with these predictions. In particular, the current model is quite sensitive to the value of the regional "F-factor", which is very difficult to estimate. One interesting result of the modeling study is that reductions in nitric acid concentrations—even by dramatic percentages—do not cause a significant abatement of episodic acidification at the regional scale, despite the fact that nitric acid is a more consistent contributor to episodic acidification than is sulfuric acid. This result is consistent with a previous finding of Eshleman *et al.* (1995) for episodic acidification of Adirondack lakes associated with spring snowmelt. An important limitation of the conceptual model is an inability to explicitly consider the timeframes associated with the abatement of acidification due to biogeochemical "lags" in the watershed system that are not incorporated into the model.

Finally, data collected as part of this project and a previous field study at the Upper Big Run site provide little evidence of any long-term decline in sulfate concentrations in streamwater during the period 1990-98, while the data clearly demonstrate an exponential decline in nitrate concentrations during the same period. Additional research is needed to explain why sulfate concentrations are not declining in this system, despite the known reduction in acid deposition of sulfur brought about by the CAAA. Analyses by Morgan *et al.* (1994) suggested that streams in western Maryland are approximately at "steady state" with respect to atmospheric sulfur deposition, so we expected that reductions in sulfur deposition would cause proportional declines in stream sulfate concentrations which have apparently not taken place. One possible explanation for this unexpected behavior is that watershed sources of sulfate in this region may be more significant than previously thought. In contrast, we propose that the decline in rather high nitrate concentrations in this system can be explained by recovery of the forest from disturbances during the late 1980's and early 1990's that was caused by gypsy moth defoliation, rather than by a watershed response to deposition of atmospheric nitrogen. On-going analyses of these data—as well as data collected in other forested watersheds in the mid-Atlantic region—should provide a particularly significant test of the competing "nitrogen saturation" and "forest

disturbance" hypotheses (Eshleman *et al.*, 2000). We thus conclude that both the inputs of nitric and sulfuric acid from the atmosphere—as well as the production of both of these mineral acids on the watershed by natural or anthropogenically-influenced processes—have the capability of contributing to episodic acidification of streams in the western Maryland region. The model predicts that abatement of atmospheric deposition will gradually reduce the intensity of episodic acidification, but the time lags associated with this reversal are currently unknown.

6. Acknowledgements

The research described in this report was conducted by the Appalachian Laboratory of the University of Maryland Center for Environmental Science under contract no. CB95-009-002 with the State of Maryland, Department of Natural Resources (DNR), Monitoring and Non-tidal Assessment Division. We gratefully acknowledge financial support provided by DNR, as well as permission granted to establish field sites and conduct the field study in the Savage and Potomac-Garrett State Forests. We sincerely thank Dr. Paul Miller for his personal contribution to this "long-term" environmental research project. We thank Mr. J.R. Holtsmaster and Mr. Matt Kline for help during installation of field equipment, and Dr. Rob Mason at the Chesapeake Biological Laboratory for performing trace metal analyses on a rather large number of streamwater samples. We acknowledge Dr. M. Robbins Church (U.S. Environmental Protection Agency), Mr. Frank Deviney (University of Virginia), and an anonymous reviewer for their constructive comments on an earlier draft of the report. This report is technical report TS-239-00 from the University of Maryland Center for Environmental Science.

7. References Cited

Almer, B., W.T. Dickson, C. Ekstrom, and E. Hornstrom. 1978. Sulphur pollution and the aquatic ecosystem. Pp. 272- 311. In: J.O. Nriagu (ed.), *Sulphur in the Environment*, John Wiley and Sons, New York, NY.

Anderson, P. and H. Borg. 1988. Effects of liming on the distribution of cadmium in water, sediment, and organisms in a Swedish lake. *Canadian Journal of Fisheries and Aquatic Sciences* 45:1154-1162.

Baker, J.P., D.P. Bernard, S.W. Christensen, and M.J. Sale. 1990. Biological Effects of Changes in Surface Water Acid-Base Chemistry, *State of Science and Technology Report 13*, National Acid Precipitation Assessment Program, Washington, DC.

Baker, J.P., J. Van Sickle, C.J. Gagen, D.R. DeWalle, W.E. Sharpe, R.F. Carline, B.P. Baldigo, P.S. Murdoch, D.W. Bath, W.A. Kretser, H.A. Simonin, and P.J. Wigington, Jr. 1996. Episodic acidification of small streams in the northeastern United States: effects on fish populations. *Ecological Applications* 6:422-437.

Borg, H. 1986. Metal speciation in acidified mountain streams in central Sweden. *Water, Air and Soil Pollution* 30:1007-1014.

Bricker, O.P. and K.C. Rice. 1989. Acidic deposition to streams. *Environmental Science and Technology* 23:379-385.

Carline, R.F., D.R. DeWalle, W.E. Sharpe, B.A. Dempsey, C.J. Gagen, and B. Swistock. 1992. Water chemistry and fish community responses to episodic stream acidification in Pennsylvania, USA. *Environmental Pollution* 78:45-48.

Castro, M.S., R.P. Mason, J.R. Scudlark, and T.M. Church. 1999. Input-output budgets of major ions, trace elements and mercury for a forested watershed in western Maryland. Draft Report: Maryland Department of Natural Resources, Power Plant Research Program, Annapolis, MD.

Chen, C.W., S.A. Gherini, N.E. Peters, P.S. Murdoch, R.M. Newton, and R.A. Goldstein. 1984. Hydrologic analyses of acidic and alkaline lakes. *Water Resources Research* 20:1875-1882.

Christopherson, N. and R.F. Wright. 1981. Sulfate budget and a model for sulfate concentrations in stream water at Birkenes, a small forested catchment in southernmost Norway. *Water Resources Research* 17:377-389.

Church, T.M., J.R. Scudlark, K.M. Conko, O.P. Bricker, and K.C. Rice. 1998. Transmission of atmospherically deposited trace elements through an undeveloped, forested Maryland watershed. Final Report (CBWP-MANTA-AD-98-2): Maryland Department of Natural Resources, Chesapeake Bay and Watershed Programs, Monitoring and Non-Tidal Assessment, Annapolis, MD.

Colburn, T., F.S. van Saal, and A.M. Soto. 1993. Developmental effects of endocrine-disrupting chemicals in wildlife and humans. *Environmental Health Perspectives* 101:378-384.

Cosby, B.J., G.M. Hornberger, J.N. Galloway, and R.F. Wright. 1985. Modeling the effects of acid deposition: assessment of a lumped parameter model of soil water and streamwater chemistry. *Water Resources Research* 21:1591-1601.

Davies, T.D., M. Tranter, P.J. Wigington, Jr., and K.N. Eshleman. 1992. Acidic episodes in surface waters in Europe. *Journal of Hydrology* 132:25-69.

Dickson, W. 1975. The acidification of Swedish lakes. *Report–Institute of Freshwater Research Drottningholm* 54:8-20.

Drever, J.I. 1988. *The Geochemistry of Natural Waters*. Prentice-Hall, Inc., Englewood Cliffs, NJ, 388 pp.

Driscoll, C.T., J.P. Baker, J.J. Bisogni, and C.L. Schofield. 1980. Effect of aluminum speciation on fish in dilute acidified waters. *Nature* 284:161-164.

Eshleman, K.N. 1988. Predicting regional episodic acidification of surface waters using empirical models. *Water Resources Research* 24:1118-1126.

Eshleman, K.N., P.J. Wigington, Jr., T.D. Davies, and M. Tranter. 1992. Modelling episodic acidification of surface waters: the state of science. *Environmental Pollution* 77:287-295.

Eshleman, K.N. 1995. Predicting regional episodic acidification of streams in western Maryland. CBRM-AD-95-7, Final report for State of Maryland, Department of Natural Resources, Annapolis, MD.

Eshleman, K.N., P.J. Wigington, Jr., T.D. Davies, and M. Tranter. 1995. A two-component mixing model for predicting regional episodic acidification of surface waters during spring snowmelt. *Water Resources Research* 31:1011-1021.

Eshleman, K.N., R.P. Morgan II, J.R. Webb, F.A. Deviney, and J.N. Galloway. 1998. Temporal patterns of nitrogen leakage from mid-Appalachian forested watersheds: Role of insect defoliation. *Water Resources Research* 34:2017-2030.

Eshleman, K.N., R.H. Gardner, S.W. Seagle, N.M. Castro, D.A. Fiscus, J.R. Webb, J.N. Galloway, F.A. Deviney, and A.T. Herlihy. 2000. Effects of disturbance on nitrogen export from forested lands of the Chesapeake Bay watershed. *Environ. Monitor. Assess.* 63:187-197.

Fagerstrom, T. and A. Jarnelov. 1972. Some aspects of the quantitative ecology of mercury. *Water Research* 6:1193-1202.

Haines, T.A. 1981. Acidic precipitation and its consequences for aquatic ecosystems: a review. *Transactions of the American Fisheries Society* 110:669-707.

Hakanson, L. 1980. The quantitative impact of pH, bioproduction and Hg-contamination on the Hg-content of fish (pike). *Environmental Pollution* (B) 1:285-290.

Hendershot, W.H., S. Savoie, and F. Courchesne. 1992. Simulation of stream-water chemistry with soil solution and groundwater flow contributions. *Journal of Hydrology* 136:237-252.

Hutchinson, N.J. and J.B. Sprague. 1986. Toxicity of trace metal mixtures to American flagfish (Jordanella floridae) in soft, acidic water and implications for cultural acidification. *Canadian Journal of Fisheries and Aquatic Sciences* 43:647-55.

Iivonen, P., S. Piepponen, and M. Verta. 1992. Factors affecting trace-metal bioaccumulation in Finnish headwater lakes. *Environmental Pollution* 78:87-95.

Kaufmann, P.R. *et al.* 1988. Chemical characteristics of streams in the mid-Atlantic and southeastern United States, population descriptions and physico-chemical relationships,

EPA/600/3-88/021a, U.S. Environmental Protection Agency, Office of Research and Development, Washington, DC.

Kaufmann, P.R., A.T. Herlihy, M.E. Mitch, J.J. Messer, and W.S. Overton. 1991. Stream chemistry in the eastern United States, 1. Synoptic survey design, acid-base status, and regional patterns. *Water Resources Research* 27:611-627.

Knapp, C.M., W.P. Saunders, Jr., D.G. Heimbuch, H.S. Greening, and G.J. Filbin. 1988. Maryland synoptic stream chemistry survey: estimating the number and distribution of streams affected by or at risk from acidification, *Report AD-88-2*, Maryland Department of Natural Resources, Annapolis, MD.

Landers, D.H., W.S. Overton, R.A. Linthurst, and D.F. Brakke. 1988. Eastern lake survey: regional estimates of lake chemistry. *Environmental Science and Technology* 22:128-135.

Linthurst, R.A., D.H. Landers, J.M. Eilers, D.F. Brakke, W.S. Overton, E.P. Meier, and R.E. Crowe. 1986. Characteristics of lakes in the eastern United States, population descriptions and physico-chemical relationships, *EPA/600/4-86/007a*, U.S. Environmental Protection Agency, Washington, DC.

McDonald, D.G., J. Freda, V. Cavdek, R. Gonzalez, and S. Zia. 1991. Interspecific variations in gill morphology of freshwater fish in relation to tolerance of low-pH environments. *Physiological Zoology* 64:124-144.

Molot, L.A., P.J. Dillon, and B.D. LaZerte. 1989. Factors affecting alkalinity concentrations of streamwater during snowmelt in central Ontario. *Canadian Journal of Fisheries and Aquatic Science* 46:1658-1666.

Monson, B.A. and P.L. Brezonik. 1999. Influence of food, aquatic humus, and alkalinity on methylmercury uptake by *Daphnia magna*. *Environmental Toxicology and Chemistry* 18:560-566.

Morgan II, R.P. 1995. Assessment of critical pH for brook trout, smallmouth bass, blueback herring, and white sucker in Maryland. Maryland Critical Loads Study, Input Data, Volume 3. Maryland Department of Natural Resources, Annapolis, MD.

Morgan, II, R.P., C.K. Murray, and K.N. Eshleman. 1994. Episodic water chemistry changes in a western Maryland watershed. *Report CBRM-AD-94-8*, Maryland Department of Natural Resources, Annapolis, MD.

Neal, C., C.J. Smith, J. Walls, P. Billingham, S. Hill, and M. Neal. 1990. Hydrochemical variations in Hafren Forest stream waters, Mid-Wales. *Journal of Hydrology* 116:185-200.

Oliver, B.G., E.M. Thurman, and R.L. Malcolm. 1983. The contribution of humic substances to the acidity of colored natural waters. *Geochimica Cosmochimica Acta* 47:2031-2035.

Potter, F.I., J.A. Lynch, and E.S. Corbett. 1988. Source areas contributing to the episodic acidification of a forested headwater stream. *Journal of Contaminant Hydrogeology* 3:293-305.

Rantz, S.E., *et al.* 1982a. Measurement and computation of streamflow: Volume 1. Measurement of stage and discharge. *U.S. Geological Survey Water-Supply Paper 2175.*

Rantz, S.E., *et al.* 1982b. Measurement and computation of streamflow: Volume 2.

Computation of discharge. *U.S. Geological Survey Water-Supply Paper 2175.*

Reuss, J.O., B.J. Cosby, and R.F. Wright. 1987. Chemical processes governing soil and water acidification. *Nature* 329: 27-31.

Robson, A. and C. Neal. 1990. Hydrograph separation using chemical techniques: an application to catchments in mid-Wales. *Journal of Hydrology* 116:345-363.

Rosseland, B.O., and O.K. Skogheim. 1984. A comparative study on salmonid fish species in acid aluminum-rich water. II. Physiological stress and mortality of one- and two-year-old fish. Institute of Freshwater Research, National Swedish Board of Fisheries Report 106:186-194.

Schaefer, D.A., C.T. Driscoll, R. van Dreason, and C.P. Yatsko. 1990. The episodic acidification of Adirondack lakes during snowmelt. *Water Resources Research* 26:1639-1647.

Schindler, D.W. 1988. Effects of acid rain on freshwater ecosystems. *Science* 239:149-157.

Sloan, R. and C.L. Schofield. 1983. Mercury levels in brook trout (*Salvelinus fontinalis*) from selected acid and limed Adirondack lakes. *Northeast Environmental Science* 2:165-170.

Suns, K., G. Hitchin, B. Loescher, E. Pastorek, and R. Pearce. 1987. Metal accumulations in fishes from Muskoka-Hariburton lakes in Ontario (1978-1984). Ontario Ministry of the Environment Report, Water Resources Branch, Rexdale, Ontario.

Tarvainen, T., P. Lahermo, and J. Mannio. 1997. Sources of trace metals in streams and headwater lakes in Finland. *Water, Air and Soil Pollution* 94:1-32.

Tranter, M., T.D. Davies, P.J. Wigington, Jr., and K.N. Eshleman. 1994. Episodic acidification of freshwater systems in Canada—physical and geochemical processes. *Water, Air and Soil Pollution* 72:19-39.

Ultsch, G.R., and G. Gros. 1979. Mucus as a diffusion barrier to oxygen: Possible role in O_2 uptake at low pH in carp (*Cyprinus carpio*) gills. *Comparative Biochemistry and Physiology* 62A: 685-689.

USEPA. 1987. Handbook of Methods for Acid Deposition Studies, Laboratory Analysis of for Surface Water Chemistry, *EPA 600/4-87/026*, U.S. Environmental Protection Agency, Office of Research and Development, Washington, D.C.

USEPA. 1989. Handbook of Methods for Acid Deposition Studies, Field Operations for Surface Water Chemistry, *EPA/600/4-89/020*, U.S. Environmental Protection Agency, Office of Research and Development, Washington, D.C.

USEPA. 1991. Part 1: Quality Assurance Plan for the Long-Term Monitoring Project. In: Data User's Guide to the U.S. EPA Long-Term Monitoring Project: Quality Assurance Plan and Data Dictionary, *EPA/600/3-91-072*, U.S. Environmental Protection Agency, Environmental Research Laboratory, Corvallis, Oregon.

USEPA. 1996. ECO Update, *EPA 540/F-95/038*, United States U.S. Environmental Protection Agency, Office of Solid Waste and Emergency Response, Washington, DC.

Webb, J.R., B.J. Cosby, J.N. Galloway, and G.M. Hornberger. 1989. Acidification of native brook trout streams in Virginia. *Water Resources Research* 25:1367-1377.

Wiener, J.G., W.F. Fitzgerald, C.J. Watras, and and R.G. Rada. 1990. Partitioning and bioavailability of mercury in an experimentally acidified Wisconsin lake. *Environmental Toxicology and Chemistry* 9:909-918.

Wigington, P.J., Jr., T.D. Davies, M. Tranter, and K.N. Eshleman. 1990. Episodic Acidification of Surface Waters Due to Acidic Deposition, *State of Science and Technology Report 12*, National Acid Precipitation Assessment Program, Washington, DC.

Wigington, P.J., T.D. Davies, M. Tranter, and K.N. Eshleman. 1992. Comparison of episodic acidification in Canada, Europe and the United States. *Environmental. Pollution* 78:29-35.

Wigington, P.J., Jr., J.P. Baker, D.R. DeWalle, W.A. Kretser, P.S. Murdoch, H.A. Simonin, J. Van Sickle, M.K. McDowell, D.V. Peck, and W.R. Barchet. 1993. Episodic acidification of streams in the northeastern United States: chemical and biological results of the Episodic Response Project, *EPA/600/R-93/190*, U.S. Environmental Protection Agency, Washington, DC.

Wigington, P.J., J.P. Baker, D.R. DeWalle, W.A. Kretser, P.S. Murdoch, H.A. Simonin, J. Van Sickle, M.K. McDowell, D.V. Peck, and W.R. Barchet. 1996a. Episodic acidification of small streams in the northeastern United States: episodic response project. *Ecological Applications* 6:374-388.

Wigington, P.J., D.R. DeWalle, P.S. Murdoch, W.A. Kretser, H.A. Simonin, J. Van Sickle, and J.P. Baker. 1996b. Episodic acidification of small streams in the northeastern United States: ionic controls of episodes. *Ecological Applications* 6:389-407.

Yeardley, R.B., J.M. Lazorchak, and S.G. Paulsen. 1998. Elemental fish tissue contamination in northeastern U. S. lakes: Evaluation of an approach to regional assessment. *Environmental Toxicology and Chemistry* 17:1875-1884.

Appendix A. Absolute ion changes and ion contribution ratios

The tables in Appendix A display the absolute ion changes and ion contribution ratios that were computed from data collected during episodes sampled at the five stations during the period January 1996 through April 1998 (Tables A.1-A.5).

Appendix A (Table A1). Absolute ion changes (μeq/L) and ion contribution ratios (dimensionless) for episodes sampled at BIGR.

SAMPLE	STRCODE	DATE	ΔANC	ΔSBC	ΔNO_3^-	ΔSO_4^{2-}	ΔOA^-	R_{NO3}	R_{S04}	R_{OA}	R_{SBC}
pre-event	BIGRA02	01/15/96									
episode	BIGRA14	01/19/96									
delta			-62.0	-68.3	5.8	1.9	7.3	0.069	0.023	0.088	0.820
pre-event	BIGRA02	01/15/96									
episode	BIGRB13	01/25/96									
delta			-47.1	-102.2	4.6	-0.9	3.4	0.042	-0.009	0.032	0.935
pre-event	BIGRA02	01/15/96									
episode	BIGRA05	01/28/96									
delta			-42.2	-52.2	7.3	35.1	4.1	0.074	0.356	0.042	0.529
pre-event	BIGRA07	02/21/96									
episode	BIGRB23	02/28/96									
delta			-30.7	-99.9	-13.7	-43.7	-2.3	-0.341	-1.086	-0.058	2.485
pre-event	BIGR001	03/07/96									
episode	BIGRD17	03/21/96									
delta			-16.9	-67.0	0.1	-59.3	1.2	0.016	-6.582	0.136	7.430
pre-event	BIGR001	05/09/96									
episode	BIGRF08	05/17/96									
delta			-5.2	9.7	-2.0	-9.2	5.6	0.131	0.599	-0.365	0.635
pre-event	BIGR001	06/05/96									
episode	BIGRG09	06/09/96									
delta			-11.3	-24.7	2.3	-26.0	6.7	0.299	-3.395	0.875	3.222
pre-event	BIGR001	08/28/96									
episode	BIGRI07	09/07/96									
delta			-67.5	-24.6	7.2	59.0	15.5	0.068	0.555	0.146	0.232
pre-event	BIGRK00	09/16/96									
episode	BIGRK10	09/18/96									
delta			-15.9	31.3	3.3	35.5	5.0	0.264	2.851	0.401	-2.516
pre-event	BIGR001	02/06/97									
episode	BIGRM12	02/22/97									
delta			-30.6	-118.3	-5.4	-18.1	3.8	-0.055	-0.184	0.039	1.200
pre-event	BIGR001	02/06/97									
episode	BIGRN19	03/03/97									
delta			-10.4	-62.7	-2.9	-2.1	1.8	-0.048	-0.036	0.029	1.055
pre-event	BIGR001	05/22/97									
episode	BIGRP15	05/27/97									
delta			-10.8	-6.9	2.4	2.1	1.0	0.195	0.173	0.078	0.554
pre-event	BIGR001	07/22/97									
episode	BIGRR21	07/25/97									
delta			0.0	104.1	17.3	69.4	3.7	-1.261	-5.059	-0.273	7.592
pre-event	BIGR001	10/29/97									
episode	BIGRT09	11/09/97									
delta			-54.7	11.0	8.6	51.3	7.6	0.153	0.908	0.134	-0.194
pre-event	BIGRV01	01/22/98									
episode	BIGRV24	01/28/98									
delta			-2.3	4.2	-3.6	-8.4	-0.5	0.219	0.502	0.028	0.251
pre-event	BIGRV01	01/22/98									
episode	BIGRX11	02/15/98									
delta			-4.7	32.4	5.4	23.0	-0.5	-1.205	-5.095	0.107	7.193
pre-event	BIGRV01	01/22/98									
episode	BIGRY12	02/19/98									
delta			-19.7	-11.2	2.7	27.5	3.3	0.061	0.614	0.074	0.251
pre-event	BIGR001	04/15/98									
episode	BIGRZ09	04/20/98									
			-14.2	-8.9	0.1	9.2	3.6	0.007	0.420	0.166	0.408

Appendix A (Table A2). Absolute ion changes (μeq/L) and ion contribution ratios (dimensionless) for episodes sampled at BLAC.

SAMPLE	STRCODE	DATE	ΔANC	ΔSBC	ΔNO_3^-	ΔSO_4^{2-}	ΔOA^-	R_{NO3}	R_{SO4}	R_{OA}	R_{SBC}
pre-event	BLACI01	09/05/96									
episode	BLACI09	09/07/96									
delta			-119.4	-126.4	15.1	-9.0	4.4	0.110	-0.066	0.032	0.924
pre-event	BLACK00	09/16/96									
episode	BLACK06	09/17/96									
delta			-53.2	-48.9	-8.6	-7.7	1.5	-0.253	-0.225	0.045	1.434
pre-event	BLACM01	02/19/97									
episode	BLACM12	02/22/97									
delta			-34.4	-120.3	-31.0	-19.2	-1.6	-0.452	-0.280	-0.023	1.755
pre-event	BLACM01	02/19/97									
episode	BLACN08	02/28/97									
delta			-11.1	-89.1	-38.7	3.0	-3.5	-0.776	0.060	-0.070	1.786
pre-event	BLACP03	05/24/97									
episode	BLACP15	05/27/97									
delta			-11.5	3.9	7.6	0.0	-0.2	2.193	-0.006	-0.058	-1.129
pre-event	BLAC001	07/22/97									
episode	BLACR17	07/24/97									
delta			-43.9	-40.2	-1.8	-47.9	12.8	-0.539	-14.460	3.875	12.123
pre-event	BLACT00	11/06/97									
episode	BLACT07	11/08/97									
delta			-77.8	-96.4	12.9	-15.5	7.2	0.127	-0.153	0.071	0.955
pre-event	BLAC001	01/05/98									
episode	BLACU03	01/08/98									
delta			-24.3	-57.4	-12.5	-10.5	5.7	-0.312	-0.263	0.143	1.432
pre-event	BLACV01	01/22/98									
episode	BLACV24	01/28/98									
delta			-10.0	-16.3	16.5	-32.8	-0.5	-32.869	65.270	1.051	-32.452
pre-event	BLACX00	02/10/98									
episode	BLACX09	02/13/98									
delta			-12.1	1.2	11.6	-12.0	0.9	-16.870	17.461	-1.357	1.765
pre-event	BLACY01	02/16/98									
episode	BLACY08	02/18/98									
delta			-28.4	-37.9	6.2	-5.4	2.8	0.150	-0.130	0.068	0.912
pre-event	BLACZ01	04/18/98									
episode	BLACZ08	04/20/98									
delta			-32.7	-53.6	3.3	-17.2	1.4	0.080	-0.419	0.034	1.305

Appendix A (Table A3). Absolute ion changes (μeq/L) and ion contribution ratios (dimensionless) for episodes sampled at HRTB.

SAMPLE	STRCODE	DATE	ΔANC	ΔSBC	ΔNO_3^-	ΔSO_4^{2-}	ΔOA^-	R_{NO3}	R_{SO4}	R_{OA}	R_{SBC}
pre-event	HRTB001	01/17/96									
episode	HRTBB01	01/22/96									
delta			-10.3	-24.4	3.6	-23.9	1.6	0.631	-4.215	0.280	4.304
pre-event	HRTB001	01/17/96									
episode	HRTBB14	01/26/96									
delta			-17.7	-26.0	6.4	-11.1	2.3	0.271	-0.467	0.098	1.097
pre-event	HRTB001	02/06/96									
episode	HRTBB21	02/27/96									
delta			-12.1	-1.2	8.3	6.2	5.0	0.401	0.300	0.240	0.059
pre-event	HRTBD10	03/19/96									
episode	HRTBD13	03/20/96									
delta			-7.0	7.1	4.9	5.0	5.1	0.620	0.623	0.646	-0.888
pre-event	HRTBF01	05/15/96									
episode	HRTBF05	05/16/96									
delta			-4.2	11.6	3.0	17.5	1.2	0.297	1.729	0.122	-1.148
pre-event	HRTBG05	06/08/96									
episode	HRTBG07	06/09/96									
delta			-4.1	8.3	4.9	5.3	2.0	1.264	1.352	0.523	-2.139
pre-event	HRTBI01	09/05/96									
episode	HRTBI06	09/07/96									
delta			-36.6	-31.0	4.0	33.6	4.1	0.055	0.462	0.057	0.426
pre-event	HRTB001	02/18/97									
episode	HRTBM06	02/20/97									
delta			-13.0	0.4	6.9	11.5	2.6	0.335	0.555	0.127	-0.017
pre-event	HRTB001	02/18/97									
episode	HRTBN15	03/02/97									
delta			-13.0	0.6	6.6	14.3	6.2	0.250	0.540	0.233	-0.022
pre-event	HRTB001	05/22/97									
episode	HRTBP11	05/26/97									
delta			-3.5	30.6	2.2	13.1	2.9	-0.179	-1.062	-0.233	2.474
pre-event	HRTB001	07/22/97									
episode	HRTBR15	07/24/97									
delta			-67.8	-43.4	-21.9	11.9	4.2	-0.581	0.317	0.112	1.152
pre-event	HRTBT01	11/07/97									
episode	HRTBT03	11/07/97									
delta			-35.4	-30.3	11.0	32.1	2.8	0.144	0.421	0.037	0.397
pre-event	HRTB001	01/05/98									
episode	HRTBU06	01/09/98									
delta			-8.8	-28.8	3.3	0.3	2.0	0.096	0.008	0.058	0.839
pre-event	HRTBV01	01/22/98									
episode	HRTBV13	01/25/98									
delta			-2.7	4.8	2.2	1.8	0.4	-5.806	-4.642	-1.026	12.474
pre-event	HRTBX00	02/10/98									
episode	HRTBX08	02/13/98									
delta			-6.2	-15.9	1.0	11.8	1.7	0.033	0.389	0.055	0.522
pre-event	HRTB001	02/16/98									
episode	HRTBY16	02/21/98									
delta			-11.1	-11.7	8.1	13.4	2.7	0.227	0.372	0.076	0.325
pre-event	HRTB001	04/15/98									
episode	HRTBZ08	04/20/98									
			-6.3	-1.1	6.8	13.1	3.3	0.279	0.539	0.136	0.046

Appendix A (Table A4). Absolute ion changes (μeq/L) and ion contribution ratios (dimensionless) for episodes sampled at NPLR.

SAMPLE	STRCODE	DATE	ΔANC	ΔSBC	ΔNO_3^-	ΔSO_4^{2-}	ΔOA^-	R_{NO3}	R_{S04}	R_{OA}	R_{SBC}
pre-event	NPLR001	01/16/96									
episode	NPLRB10	01/24/96									
delta			-61.3	-286.0	3.9	-240.6	12.0	0.063	-3.924	0.196	4.665
pre-event	NPLR001	02/13/96									
episode	NPLRB09	02/24/96									
delta			-11.2	-144.2	4.3	-55.9	1.2	0.046	-0.596	0.013	1.537
pre-event	NPLR001	02/13/96									
episode	NPLRB24	02/28/96									
delta			-10.7	-161.8	2.2	-75.6	3.9	0.024	-0.819	0.043	1.753
pre-event	NPLRD10	03/19/96									
episode	NPLRD14	03/20/96									
delta			-18.7	-153.8	5.9	-106.2	4.7	0.102	-1.823	0.080	2.641
pre-event	NPLRF01	05/15/96									
episode	NPLRF09	05/17/96									
delta			-5.9	-10.8	1.9	-13.5	0.2	-3.485	24.312	-0.292	-19.535
pre-event	NPLRG05	06/08/96									
episode	NPLRG07	06/09/96									
delta			-42.7	-297.0	-0.2	-223.9	9.2	-0.003	-2.723	0.112	3.614
pre-event	NPLR001	08/28/96									
episode	NPLRI09	09/07/96									
delta			-83.4	-383.4	-2.7	-246.4	17.4	-0.018	-1.624	0.114	2.528
pre-event	NPLRM01	02/19/97									
episode	NPLRM04	02/20/97									
delta			-56.3	-220.4	11.2	-151.7	5.0	0.132	-1.786	0.059	2.595
pre-event	NPLRN08	02/28/97									
episode	NPLRN17	03/02/97									
delta			-12.1	-62.4	6.1	-53.9	6.5	0.291	-2.556	0.308	2.957
pre-event	NPLRP02	05/25/97									
episode	NPLRP08	05/26/97									
delta			-20.8	-39.9	8.2	-17.0	5.2	0.226	-0.467	0.143	1.098
pre-event	NPLRR01	07/22/97									
episode	NPLRR17	07/24/97									
delta			-16.4	-92.0	3.4	-77.7	0.8	0.185	-4.196	0.043	4.968
pre-event	NPLRT00	11/06/97									
episode	NPLRT08	11/08/97									
delta			-44.9	-147.1	3.5	-97.3	10.9	0.055	-1.517	0.170	2.292
pre-event	NPLRV01	01/22/98									
episode	NPLRV09	01/24/98									
delta			0.5	-10.0	1.3	2.8	0.0	0.092	0.196	0.000	0.712
pre-event	NPLRX03	02/11/98									
episode	NPLRY01	02/16/98									
delta			-9.6	59.5	2.4	-19.8	-0.5	-0.031	0.255	0.007	0.769
pre-event	NPLRY01	02/16/98									
episode	NPLRY12	02/19/98									
delta			-34.9	-220.2	2.5	-126.2	4.1	0.025	-1.254	0.041	2.188
pre-event	NPLRZ01	04/18/98									
episode	NPLRZ07	04/20/98									
delta			-30.9	-163.7	7.8	-136.5	8.1	0.181	-3.172	0.187	3.803

Appendix A (Table A5). Absolute ion changes (μeq/L) and ion contribution ratios (dimensionless) for episodes sampled at UPTB.

SAMPLE	STRCODE	DATE	ΔANC	ΔSBC	ΔNO_3^-	ΔSO_4^{2-}	ΔOA^-	R_{NO3}	R_{SO4}	R_{OA}	R_{SBC}
pre-event	POPL001	01/17/96									
episode	POPL001	01/22/96									
delta			-37.5	-56.9	6.4	-8.0	1.7	0.113	-0.141	0.030	0.998
pre-event	POPL001	02/22/96									
episode	POPL001	02/28/96									
delta			-20.8	-112.4	-72.6	-6.7	4.9	-1.919	-0.178	0.129	2.969
pre-event	POPLF01	05/15/96									
episode	POPLF12	05/18/96									
delta			-3.0	-15.8	-15.9	3.0	-0.5	-6.644	1.239	-0.213	6.618
pre-event	POPLG04	06/08/96									
episode	POPLG21	06/12/96									
delta			-11.6	-31.5	-5.5	-5.1	2.9	-0.231	-0.215	0.122	1.324
pre-event	POPLI01	09/05/96									
episode	POPLI05	09/06/96									
delta			-54.2	-200.1	-46.9	-55.6	35.5	-0.352	-0.418	0.266	1.503
pre-event	POPLM01	02/19/97									
episode	POPLM12	02/22/97									
delta			-38.9	-165.0	-18.7	-0.9	0.4	-0.128	-0.006	0.003	1.132
pre-event	POPLM22	02/26/97									
episode	POPLN16	03/02/97									
delta			-3.5	-47.7	-31.4	10.6	7.6	-0.911	0.308	0.219	1.383
pre-event	POPLR03	07/22/97									
episode	POPLR19	07/24/97									
delta			-43.2	123.7	131.5	29.6	13.4	2.588	0.583	0.263	-2.434
pre-event	POPLT00	11/06/97									
episode	POPLT06	11/08/97									
delta			-42.4	-118.8	-35.9	1.2	12.1	-0.373	0.012	0.126	1.235
pre-event	POPLV01	01/22/98									
episode	POPLV05	01/23/98									
delta			-0.5	-13.6	-18.9	1.4	0.4	5.453	-0.404	-0.124	-3.925
pre-event	POPLX01	02/13/98									
episode	POPLY09	02/18/98									
delta			-10.6	-77.7	-31.6	0.0	5.7	-0.610	-0.001	0.110	1.501
pre-event	POPLZ01	04/18/98									
episode	POPLZ07	04/20/98									
delta			-11.2	-80.9	-40.9	-0.6	3.9	-0.942	-0.013	0.090	1.865

Appendix B. Laboratory Analysis: Quality Assurance/Quality Control (QA/QC)

Introduction

The primary objective of a good laboratory quality assurance plan is to ensure the quality of the data that is generated by the laboratory. Each method of analysis must then employ specific quality control steps to ensure data quality. To ensure attainment of the quality assurance objectives, standard operating procedures have been implemented that detail the requirements for the correct performance of analytical, or laboratory, procedures. The quality of all data generated and processed during the Episodic Acidification Project has been monitored for both precision and accuracy. The internal quality assurance/quality control protocols for chemical analysis followed guidelines from the "Handbook of Methods for Acid Deposition Studies: Laboratory Analyses for Surface Water Chemistry" (USEPA, 1987).

Precision was determined by measuring the agreement among individual measurements of the same property, under similar conditions. Precision can be assess through the analysis of laboratory duplicates, or splits, and field duplicates. The degree of agreement between replicates can be expresses as the percent relative standard deviation (RSD):

$$Percent\ RSD = \frac{SD}{X} X\ 100$$

Because analysis of laboratory duplicates indicates precision associated with laboratory procedures only, not total precision, field duplicate samples collected bi-weekly from one of the five sampling sites were used to assess precision associated with sample collection, preservation, and storage procedures.

Accuracy can be defined as a measure of the closeness of an individual measurement to the true or expected value. Analyzing a reference material, or quality control check solution (QCCS), of known concentration is a method of determining accuracy. QCCS were independently made and analyzed after calibration, at specified intervals during sample analysis, and at the conclusion of sample analysis to ensure accurate measurement throughout the analysis run.

Deionized water blanks serve as a check of laboratory- or field-induced contamination. Field blanks were collected approximately monthly to assess field and laboratory contamination. Laboratory blanks were analyzed at predetermined intervals as outlined in the standard operating procedures for each analyte.

Additional methods employed by the laboratory to demonstrate quality of the chemical data include routine analysis of a field natural audit sample, calculation of anion/cation balances, and performance of conductivity checks. The laboratory also participates annually in an interlaboratory audit program.

The quality assurance plan in the analytical laboratory has yielded excellent results. A detailed description of the calibration and a summary of the quality control procedures and

results for each analysis performed by the analytical laboratory at the University of Maryland Center for Environmental Science Appalachian Laboratory (AL).

Specific Analyses

Closed pH

The pH meter was calibrated using a set of two buffers, that bracketed the pH of the samples. In 1996, a quality control check solution (QCCS) with a theoretical pH value of 4.00 was used to verify calibration. In 1997, the pH QCCS was changed to 5.00 because it was closer to the expected median of samples analyzed by the laboratory. The measured value of the QCCS is required to be with 0.05 pH units. The QCCS was analyzed using the same procedures as for routine samples. If the QCCS was not within the acceptable range, then the solution was remade and analyzed again. If it failed to pass the second time, the meter was re-calibrated, and all samples that were measured since the last acceptable QCCS were re-analyzed. The average pH of all pH 5.00 QCCS analyzed for the duration of the project was 5.00 (Table B.1).

A laboratory blank was analyzed with each batch of samples. The average pH value for the lab blank was 5.63. The pH of laboratory blanks can be variable due to the nature of the matrix but it should typically be between 5.40 and 6.20.

Laboratory duplicates for closed pH were analyzed every ten samples. Acceptable precision criteria for pH require that duplicates be within 0.10 pH units of the routine sample analysis. Analysts achieve an average difference of 0.03 pH units (Table B.2), which is within the acceptable precision limits for laboratory duplicate analysis for pH.

Acid Neutralizing Capacity (ANC)

Acid neutralizing capacity (ANC) was measured using the acidimetric Gran titration technique with electrometric pH detection. The pH meter used for the titration was calibrated using a set of two pH buffers that bracketed sample pH. A QCCS with a theoretical value of 5.00 was used to verify calibration. Any time that the QCCS was outside of the acceptable limits, the meter was re-calibrated and the QCCS was subsequently re-analyzed. The normality of the acid titrant was also cross-checked on a routine basis to verify method accuracy.

Prior to sample analysis a deionized water lab blank and sodium carbonate standard with a calculated ANC of 50 μeq/L were analyzed to verify method and analyst accuracy. A standard with an ANC of 50 μeq/L was chosen because it most closely reflected the median ANC value of the samples. The average ANC of the QCCS measured for the episodic acidification project was 49.2 μeq/L (Table B.1). The accuracy goal for analysis of the QCCS for ANC is $\pm$ 5%. Therefore, the acceptable range for the QCCS if 47.5 and 52.5. Most QCCS values were well within the accepted limits (Figure B.1). Whenever the QCCS was outside of the acceptable range, samples were re-analyzed. When values were outside of the accepted limits, it usually indicated that the acid titrant was due to be re-standardized. The mean ANC for all blanks analyzed was 0.5 μeq/L, which is well below the acceptable limit of 10 μeq/L, and indicates an

overall lack of contamination (Table B.3). Laboratory duplicate analysis also yielded excellent precision results for ANC (Table B.2).

Specific Conductance

Specific conductance was measured using a conductivity cell and meter with temperature compensation to 25°C. Before sample analysis, the conductivity meter was subjected to an electronics check over the range of 1.0 µS/cm to 1000 µS/cm. This was used to verify that the meter was operating correctly. A series of calibration check solutions that bracketed the expected conductance values were then made and measured to check the calibration of the conductivity cell. A laboratory blank was also analyzed prior to sample analysis. If the initial conductance values of all of the calibration check solutions and the blank were within acceptable limits, sample analysis could proceed. The 74 µS/cm check solution was also measured every ten samples and all calibration check solutions were re-analyzed at the conclusion of sample analysis (Table B.1). An average laboratory blank was well below the acceptance criteria of 1 µS/cm. Laboratory duplicates were measured every ten samples and were required to be within one percent RSD. The average duplicate precision for specific conductance was 0.71 % RSD (Table B.2).

Major Anions

Anions were measured using ion chromatography. Calibration for chloride, nitrate-nitrogen, and sulfate were conducted over at least a four point range, bracketing the expected concentrations of the ions of interest. Sample concentration was computed using peak area. The linear range of the calibration curve had to greater than 99.5% before analysis of samples could be performed. Calibration plots of each analysis batch are archived at AL.

Lab duplicate analysis was conducted approximately every ten samples. A laboratory blank was analyzed at the beginning of analysis (Table B.3). A QCCS was measured at the beginning and the end of sample analysis. The QCCS had a theoretical value of 1.0 mg/L for chloride, 0.5 mg/L for nitrate-nitrogen, and 5.0 mg/L for sulfate. The mean values for the anion QCC were all within the recommended EPA quality assurance criteria for these analytes (Table B.1). All blanks analyzed were below the detection limit for all three analytes (Table B.3). Duplicate laboratory analysis yielded an average percent RSD of 0.5 for chloride, 0.5 for nitrate-nitrogen, and 0.6 for sulfate (Table B.2). These values verify that precision for the method was within acceptable limits.

Major Cations

Base cations were also measured using ion chromatography. Calibration for cations (sodium, ammonium, potassium, magnesium, and calcium) was also conducted over a four to six point range, bracketing the expected concentrations of the ions of interest. Sample concentration was computed by peak area using a calibration curve. The linear range of the calibration curve

had to be greater than 99.5 percent before analysis of samples could be performed. Calibration plots of each analysis batch are archived at AL.

Lab duplicate analysis was conducted approximately every ten samples. Duplicate precision was high for cation analysis (Table B.3). A QCCS was measured at the beginning and the end of sample analysis. A laboratory blank was analyzed at the beginning of sample analysis. Theoretical values for the cation check solutions are summarized in Table B.1. Analysis of laboratory blanks (Table B.3) demonstrated an overall lack of contamination for cation analysis.

Dissolved Organic Carbon (DOC)

DOC was measured using the UV-persulfate oxidation methods. Calibration was conducted over a five point range, bracketing the expected DOC concentrations. Sample concentration was computed from instrument response using a calibration curve. The linear range of the calibration curve had to be greater than 99.5 percent before sample analysis could commence.

Check solutions were measured at the beginning of sample analysis and once every 20 samples. The solutions had theoretical values of 2 and 10 mg/L DOC. The average values for all check solutions analyzed were 2.1 mg/L for the 2 QCCS and 9.9 for the 10 QCCS (Table B.1). Laboratory duplicates were analyzed once per sample batch and yielded a precision value of 3.03 percent RSD (Table B.2). The acceptable limit of precision for DOC analysis is ten percent RSD. Laboratory blanks were also well within acceptable limits for DOC (Table B.3).

Dissolved Silica

Dissolved silica concentration was measured by inductively-coupled plasma atomic emission spectroscopy (ICP-AES). Calibration was conducted over a four point range and sample concentration was computed from instrument response using a calibration curve. A 1.5 mg/L QCCS was measured at the beginning of sample analysis and once approximately every 20 samples. The average QCCS value for silica analysis was 1.479 mg/L (Table B.1), which reflects a high degree of method accuracy. Average laboratory blank analysis was 0.009 mg/L (Table B.3), indicating extremely low laboratory contamination. Duplicate precision was calculated to be 2.34 percent RSD for silica analysis (Table B.3). This is well within recommended EPA guidelines for laboratory duplicate analysis of silica.

Aluminum

Total, exchangeable, and non-exchangeable reactive aluminum concentrations were measured using flow injection analysis. Calibration was conducted over a five point range, bracketing the expected aluminum concentrations. The linear range of the calibration curve had to be greater than 99.5 before sample analysis could begin. Data quality for total aluminum was also very good. A 0.075 mg/L QCCS was measured prior to sample analysis and once approximately every twenty samples. Analysts achieved a mean QCCS value of 0.073 mg/L (Table B.1). Therefore, method accuracy was well within the recommended USEPA guidelines. Blank analysis resulted in a mean of 0.005 mg/L (Table B.3) for aluminum, which indicates very

little or no sample contamination. Duplicate precision was also excellent for aluminum analysis. Average percent RSD for aluminum duplicates was 0.47 (Table B.2).

Low-level Metals

In May of 1997, prior to sample collection, a series of blanks were collected at each sampling location to assess sources of potential sample contamination during event sampling. First, a deionized water blank was drawn directly from the system into a clean ISCO sample bottle. This sample was then poured off into a triple-rinsed bottle typically used for metals analysis and preserved appropriately. None of the metals were detected in this first blank, helping to demonstrate that the source of deionized water and the sample bottles were free from contamination at our detection limits. Next, deionized water blanks were poured off into clean ISCO sample bottles and placed in the sampler for the typical duration of an event to determine if samples became contaminated from sitting in the sampler for a week (called a cube blank). Half of this sample was then poured off and preserved, while the other half was filtered in the laboratory to identify potential contamination from the filtering protocol. The last blank that was collected was a tubing blank. Deionized water was drawn through the ISCO sample collection tubing, or pump tubing, to determine if the tubing was a source of sample contamination. Therefore, three blanks were collected at each of the five streams.

Results from the blank analysis are summarized in Table B.4. None of the cube blanks had detectable levels of metals. The only blanks that exhibited any contamination were the tubing blanks at two of the streams. There was slight cobalt and manganese contamination of the Herrington Tributary tubing blank and slight iron contamination of the Poplar Lick Tributary tubing blank. Since all of these concentrations are fairly close to the instrument detection limit, contamination of cobalt and manganese should be considered to be extremely minimal. There was substantial iron contamination, though, in the Herrington Tributary tubing blank. Because the other tubing blanks were "clean", we hypothesize that the source of these metals in the tubing blanks was not the pump tubing but was perhaps some sort of particulate matter that did not get flushed properly from the tubing before sample collection. This was taken into consideration for future event sampling for metals.

Additional quality control procedures for low-level metals analyses included the analysis of laboratory blanks, calibration checks, laboratory duplicates, and sample spikes. None of the analytes were at detectable levels in the laboratory blanks, therefore contamination was not detected in the analytical method. Accuracy was excellent for the metals analysis. Results for the 30 μg/L calibration check solution are summarized in Table B.5. Precision for laboratory analyses were also very good, with average relative standard deviations (% RSD) for duplicate analysis within the recommended 10 percent of the mean (Table B.6). Sample spikes were analyzed to determine any sources of interference. A known amount of analytes are added to a volume of sample in order to measure percent recovery of the analytes when the sample is analyzed. Table B.7 summarizes the results for matrix spike analysis and all were within 15 percent of the recommended recovery range.

QA/QC Checks

Anion/Cation Balances

A method of evaluating overall internal quality control is the calculation of ion ratios and balances. Results depicted in Figure B.1 demonstrate that almost all of the analyzed samples (excluding field blanks) passed the ion ratio check. Therefore, almost all of the calculated ion ratios were between 85 and 115 percent. The target for the ion ratio check is 1.0 and the median value was slightly greater than 1.0. Ion differences were also calculated for all analyzed samples, with the exception of field blanks. Figure B.2 demonstrates that all but a extremely small portion of the samples analyzed passed the ion difference check (-10% < % ion difference > 10%).

Conductivity Checks

The specific conductance of a sample can be estimated by summing the equivalent conductances for each measured ion. Calculated conductance can then be compared to measured conductance as an additional quality control check. Figure B.3 illustrates the strong positive relationship (r^2= 0.876) between the measured and calculated conductances for all analyzed samples. When conductivity differences were calculated (Figure 4), most samples were within the recommended limits (0 $\pm$ 20%).

Collection and Analysis of Natural Audit Sample

Natural audit samples are another useful part of a comprehensive Quality Assurance Plan. Because they are collected from streams, they are more representative of the actual sample matrix than a manufactured calibration check solution. In January of 1997, a field natural audit sample was collected from Upper Big Run in order to establish an internal audit sample (FNBR001). Approximately 50 liters of sample were filtered using a 0.45 μm filter capsule and a Masterflex pump. The sample was returned to AL, where it was refrigerated for approximately 20 days and periodically check for stability by analyzing sample ANC. Once the sample was stable, it was poured off into 500 mL aliquots. The audit samples are stored in the dark at 4°C and are analyzed periodically for all analytes except closed pH and aluminum. Although there are no actual right or wrong results for any of the analytes, like when a known QCCS is measured, variations in analyte concentration can help determine or diagnose any sources of analytical error. They are especially useful as a diagnostic tool when any changes in the operating conditions of an instrument (i.e., column or electrode replacement). Results from analysis of the audit sample verify the stability of the analytical results (Table B.8).

Analysis of Field Duplicates

Field duplicates were collected bi-weekly from one of the five routine sampling sites to provide a means of assessing precision associated with sample collection, preservation, and storage procedures, as well as with analytical procedures. Overall, the results from the field

duplicate analysis were excellent (Table B.9) and indicate consistent sample collection, storage, and analytical procedures.

Analysis of Field Blanks

Field blanks were collected approximately monthly to assess field contamination. Analysis of these blanks indicated that contamination during sample collection and processing was negligible (Table B.10).

Interlaboratory Audit

The laboratory also participates in the National Water Research Institute (NWRI) Ecosystem Interlaboratory Quality Assurance Program annually as an additional quality assurance measure. Twelve natural water samples were analyzed for the following analytes: open pH, specific conductance, DOC, ANC, nitrate-nitrogen, ammonia, sodium, magnesium, silica, sulfate, chloride, potassium, and calcium. Results from the October 1996 study were good with the laboratory receiving ideal ratings for six of the analytes (Table B.11). A slight bias was indicated for magnesium and calcium.

Results from the 1998 inter-comparison study were similar to the results from 1996. Bias was indicated for magnesium and calcium again. Additionally, conductance results were suggested to be slightly biased. Bias was not detected for any of the other analytes (Table B.12).

LITERATURE CITED

USEPA. 1987. Handbook of methods for acid deposition studies: Laboratory analysis for surface water chemistry. United States Environmental Protection Agency, Acid Deposition and Atmospheric Research Division, Office of Acid Deposition, Environmental Monitoring and Quality Assurance, Office of Research and Development, Washington, D.D. EPA-600/4-87/026.

Table B.1. Summary of QCCS analysis.

Analyte	Theoretical Value	Mean	N	Std. Dev.	Minimum	Maximum
Closed pH	5.00	5.00	80	0.02	4.95	5.03
	4.00	4.02	44	0.02	3.96	4.06
ANC	50.0	49.2	197	2.99	40.7	56.5
Conductance	14.7	14.9	97	0.42	14.1	16
	74.0	72.9	97	1.67	70.2	77.7
	147.0	144.5	96	3.05	138.8	152.6
Chloride	1.000	1.068	110	0.03	1.017	1.180
Nitrate-N	0.500	0.486	110	0.03	0.404	0.625
Sulfate	5.000	4.865	110	0.17	4.294	5.577
Sodium	0.300	0.285	53	0.15	0.147	0.644
Ammonium	0.300	0.270	52	0.08	0.092	0.496
Potassium	0.500	0.459	53	0.10	0.203	0.556
Magnesium	2.000	1.858	53	0.29	1.085	2.038
Calcium	4.000	3.725	53	0.57	2.029	4.102
DOC	10.0	9.9	212	0.21	9.3	10.5
	2.0	2.1	222	0.11	1.7	2.5
Silica	1.500	1.479	53	0.10	1.319	1.747
Aluminum	0.075	0.073	179	0.05	0.060	0.084

Table B.2. Summary of precision analysis for the project. Values are in percent relative standard deviation (% RSD) unless otherwise noted.

Analyte	Precision	N	Std. Dev.	Minimum	Maximum	Std. Error
Closed pH	0.03 units	109	0.03	0.00	0.17	0.896
ANC	0.93	244	10.87	-76.0	67.7	11.64
Conductance	0.71	151	1.09	0	11.11	1.54
Chloride	0.51	70	0.70	0	3.99	1.38
Nitrate-N	0.45	70	0.57	0	2.39	1.26
Sulfate	0.61	70	0.99	0	6.22	1.63
Sodium	1.99	173	2.11	0	11.60	1.35
Ammonium	3.35	54	8.79	0	50	2.63
Potassium	0.80	176	0.80	0.006	5.79	1.00
Magnesium	1.37	174	1.32	0	8.77	0.97
Calcium	3.78	173	4.63	0	51.54	1.22
DOC	3.03	190	3.38	0	19.03	1.12
Silica	2.34	87	1.83	0.00	4.78	0.78
Aluminum	0.47	77	1.79	0.000	3.49	3.81

Table B.3. Summary of laboratory blank analyses.

Analyte	Mean	N	Std. Dev.	Minimum	Maximum	Std. Error
Closed pH	5.63	104	0.18	5.27	6.18	0.03
ANC	0.45	245	2.32	-7.10	17.8	5.16
Conductance	0.69	90	0.19	0.38	1.69	0.28
Chloride	0.006	111	0.04	0	0.22	6.67
Nitrate-N	0.001	120	0.01	0	0.06	10.00
Sulfate	0.002	120	0.02	0	0.27	10.00
Sodium	0.104	90	0.92	0	8.69	10.00
Ammonium	0.001	89	0.01	0	0.11	12.00
Potassium	0.002	89	0.01	0	0.10	5.00
Magnesium	0.001	89	0.004	0	0.03	4.00
Calcium	0.015	89	0.04	0	0.21	2.67
DOC	-0.07	91	0.12	-0.43	0.75	1.71
Silica	0.009	33	0.05	0	0.09	5.56
Aluminum	0.005	57	0.01	0	0.01	2.00

Table B.4. Summary of field blank analysis for low-level metals. Concentrations are in µg/L.

Blank Type	Cr	Zn	Cd	Be	Fe	Co	Mn	V	Cu
BIGR Filtered Cube Blank	<4.2	<7.9	<6.7	<2.6	<6.9	<8.2	<2.4	<15	<4.2
BLAC Filtered Cube Blank	<4.2	<7.9	<6.7	<2.6	<6.9	<8.2	<2.4	<15	<4.2
HRTB Filtered Cube Blank	<4.2	<7.9	<6.7	<2.6	<6.9	<8.2	<2.4	<15	<4.2
NPLR Filtered Cube Blank	<4.2	<7.9	<6.7	<2.6	<6.9	<8.2	<2.4	<15	<4.2
POPL Filtered Cube Blank	4.4	<7.9	<6.7	<2.6	<6.9	<8.2	<2.4	<15	<4.2
BIGR Unfiltered Cube Blank	<4.2	<7.9	<6.7	<2.6	<6.9	<8.2	<2.4	<15	<4.2
BLAC Unfiltered Cube Blank	<4.2	<7.9	<6.7	<2.6	<6.9	<8.2	<2.4	<15	<4.2
HRTB Unfiltered Cube Blank	<4.2	<7.9	<6.7	<2.6	<6.9	<8.2	<2.4	<15	<4.2
NPLR Unfiltered Cube Blank	<4.2	<7.9	<6.7	<2.6	<6.9	<8.2	<2.4	<15	<4.2
POPL Unfiltered Cube Blank	<4.2	<7.9	<6.7	<2.6	<6.9	<8.2	<2.4	<15	<4.2
BIGR Tubing Blank	<4.2	<7.9	<6.7	<2.6	<6.9	<8.2	<2.4	<15	<4.2
BLAC Tubing Blank	<4.2	<7.9	<6.7	<2.6	<6.9	<8.2	<2.4	<15	<4.2
HRTB Tubing Blank	<4.2	<7.9	<6.7	<2.6	48.8	10.7	3.5	<15	<4.2
NPLR Tubing Blank	<4.2	<7.9	<6.7	<2.6	<6.9	<8.2	<2.4	<15	<4.2
POPL Tubing Blank	<4.2	<7.9	<6.7	<2.6	8.3	<8.2	<2.4	<15	<4.2

Table B.5. Average values for the 30 µg/L calibration check solution for low-level metals analysis.

Analyte	Mean QCCS	Standard Deviation
Chromium	27.7	2.45
Zinc	31.1	2.78
Cadmium	29.8	2.07
Beryllium	30.3	1.11
Iron	31.1	2.01
Cobalt	28.2	4.22
Manganese	30.4	0.45
Vanadium	27.2	5.87
Copper	29.4	1.77

Table B.6. Summary of precision for laboratory duplicates for low-level metals analysis.

Analyte	Mean % RSD	Standard Deviation
Chromium	0	0
Zinc	1.27	2.45
Cadmium	0	0
Beryllium	0	0
Iron	4.81	7.22
Cobalt	8.09	12.87
Manganese	1.18	3.22
Copper	0	0
Vanadium	0	0

Table B.7. Average percent recovery values for low-level metals sample spikes.

Analyte	Average % Recovery	Standard Deviation
Chromium	101.7	3.64
Zinc	108.1	1.05
Cadmium	101.1	3.22
Beryllium	108.2	0.98
Iron	99.5	10.05
Cobalt	110.4	8.78
Manganese	109.7	3.41
Copper	103.2	4.62
Vanadium	99.2	11.76

Table B.8. Natural audit sample analytical results.

Analyte	Mean	N	Std. Dev.	Std. Error	Minimum	Maximum
Open pH	6.47	130	1.29	0.20	6.19	6.71
ANC	34.3	130	2.75	0.08	32.7	39.2
Conductance	29.0	123	0.95	0.03	27.8	30.5
Chloride	0.857	117	0.09	0.11	0.784	1.085
Nitrate-N	0.220	117	0.06	0.27	0.194	0.280
Sulfate	7.391	117	0.17	0.02	7.165	7.629
Sodium	0.435	109	0.11	0.25	0.378	0.511
Ammonium	0	109	0	0	0	0
Potassium	0.672	109	0.17	0.25	0.589	0.753
Magnesium	1.049	109	1.15	1.10	0.973	1.072
Calcium	2.599	109	1.23	0.47	2.473	2.899
DOC	0.8	94	0.17	0.21	0.7	1.3
Silica	1.878	45	0.15	0.08	1.813	2.087

Table B.9. Summary of results from precision analysis of field duplicate samples. Units are in percent RSD unless otherwise specified.

Analyte	Mean	Std. Dev.	Minimum	Maximum	Std. Error
Closed pH	0.1 units	0.06	0	0.3	0.97
ANC	2.4 μeq/L	3.57	0	24.3	1.50
Conductance	1.0	1.31	0	6.0	1.34
Chloride	1.1	1.86	0	9.4	1.69
Nitrate-N	1.1	1.53	0	6.2	1.43
Sulfate	0.8	1.44	0	6.5	1.70
Sodium	2.3	3.65	0	18.9	1.61
Ammonium	61.9	47.6	5.3	100	0.77
Potassium	1.3	2.02	0	10.9	1.54
Magnesium	0.6	1.05	0	6.0	1.78
Calcium	0.8	0.92	0	4.5	1.19
DOC	0.01 mg/L	0.63	-0.62	1.22	
Silica	2.79	3.72	0.02	11.73	1.33
Total Aluminum	0.001 mg/L	0.007	0	0	7.39
Organic Aluminum	0.001 mg/L	0.003	0.02	0.01	3.66

Table B.10. Summary of analyses of field blank samples.

Analyte	Mean	Std. Dev.	Minimum	Maximum	Std. Error
Closed pH	5.91	0.20	5.48	6.21	0.03
ANC	-0.2	1.21	-2.0	2.9	7.17
Conductance	1.01	0.21	0.69	1.5	0.21
Chloride	0.007	0.03	00	0.138	4.36
Nitrate-N	0	0	0	0	0
Sulfate	0	0	0	0	0
Sodium	0.006	0.011	0	0.033	1.78
Ammonium	0.001	0.003	0	0.009	2.39
Potassium	0.001	0.006	0	0.024	4.36
Magnesium	0	0	0	0	0
Calcium	0.026	0.050	0	0.159	1.87
DOC	0.137	0.17	-0.17	0.42	1.24
Silica	0.34	0.57	0	0.94	1.68
Total Aluminum	0.004	0.006	0	0.019	1.43
Organic Aluminum	0.003	0.006	0	0.017	2.15

Table B.11. Summary of results from 1996 NWRI interlaboratory audit.

Analyte	Rating
Conductance	Flagged low on 3 samples
Open pH	Flagged low on 3 samples
DOC	Ideal
ANC	Ideal
Nitrate-N	Ideal
Ammonium	No bias
Sodium	Ideal
Magnesium	Flagged high on 4 samples – slightly biased
Silica	No bias
Sulfate	No bias
Chloride	Ideal
Potassium	Ideal
Calcium	Flagged high on 7 samples – biased

Table B.12. Summary of results from 1998 NWRI interlaboratory audit.

Analyte	Rating
Conductance	Flagged high on 3 samples – slightly biased
Open pH	Flagged low on 2 samples
DOC	Ideal
ANC	Ideal
Nitrate-N	Flagged high on 6 samples
Ammonium	Flagged high on 2 samples
Sodium	Flagged high on 2 samples
Magnesium	Flagged high on 7 samples – biased
Silica	No bias
Sulfate	Flagged high on 4 samples
Chloride	No bias
Potassium	Flagged high on 9 samples
Calcium	Flagged high on 9 samples – biased

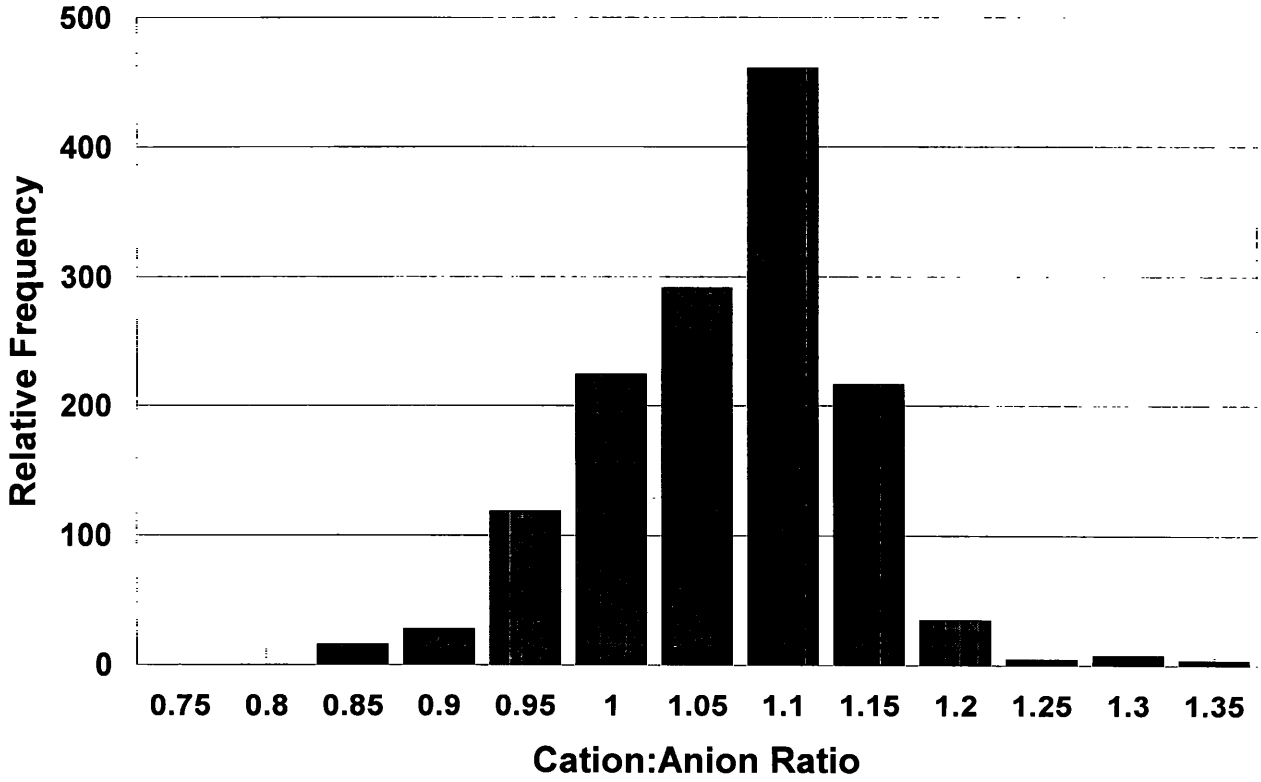

Figure B.1. Relative frequency distribution of the computed cation-anion ratios for all streamwater samples.

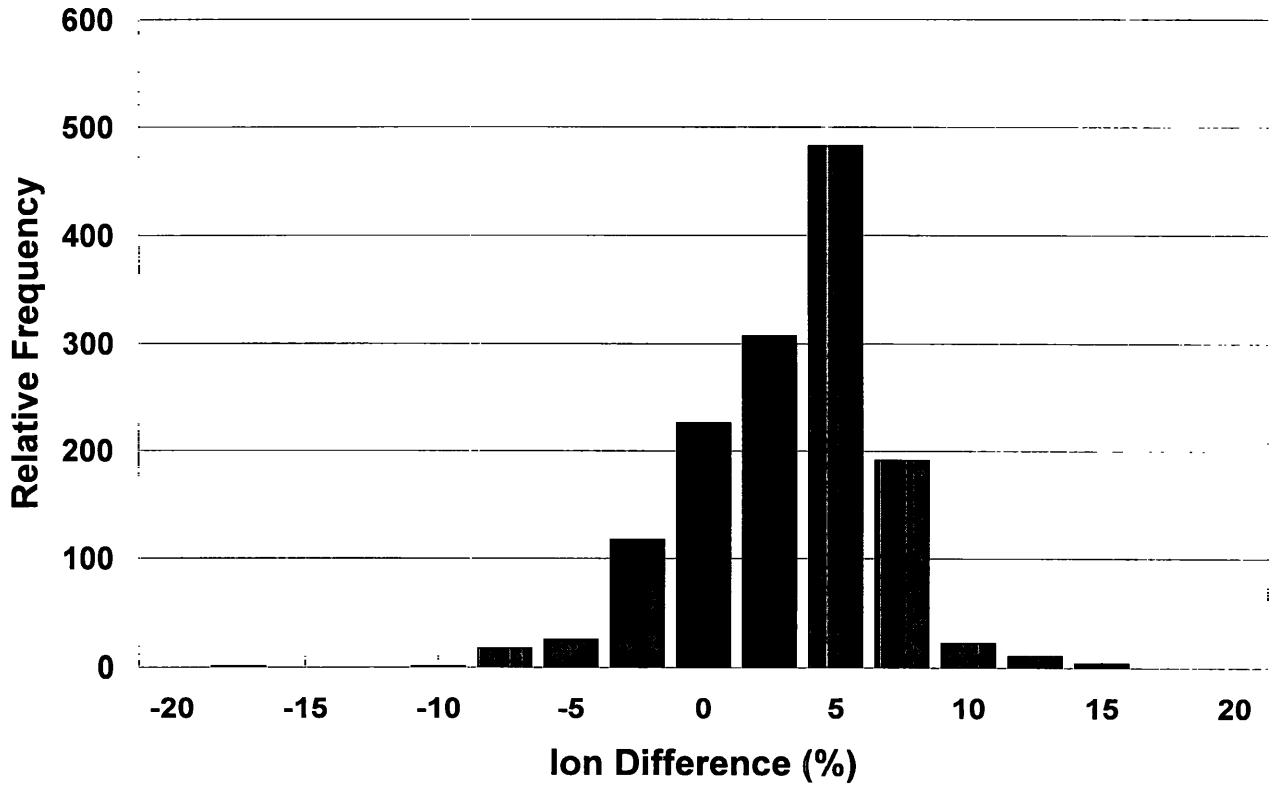

Figure B.2. Relative frequency distribution of the computed ion differences for all streamwater samples.

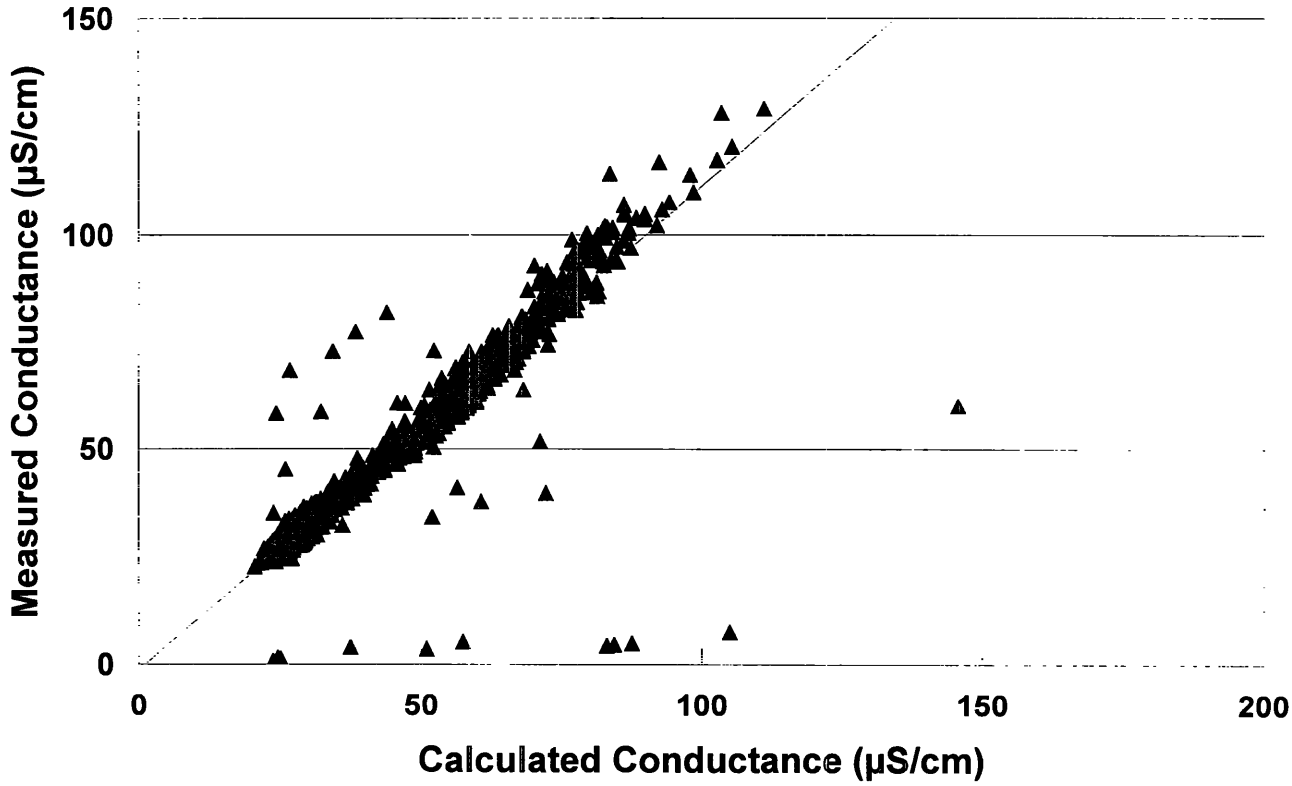

Figure B.3. Relationship between calculated and measured conductance for all streamwater samples (Y = -1.25 + 1.12X; r2 = 0.876; n = 1416).

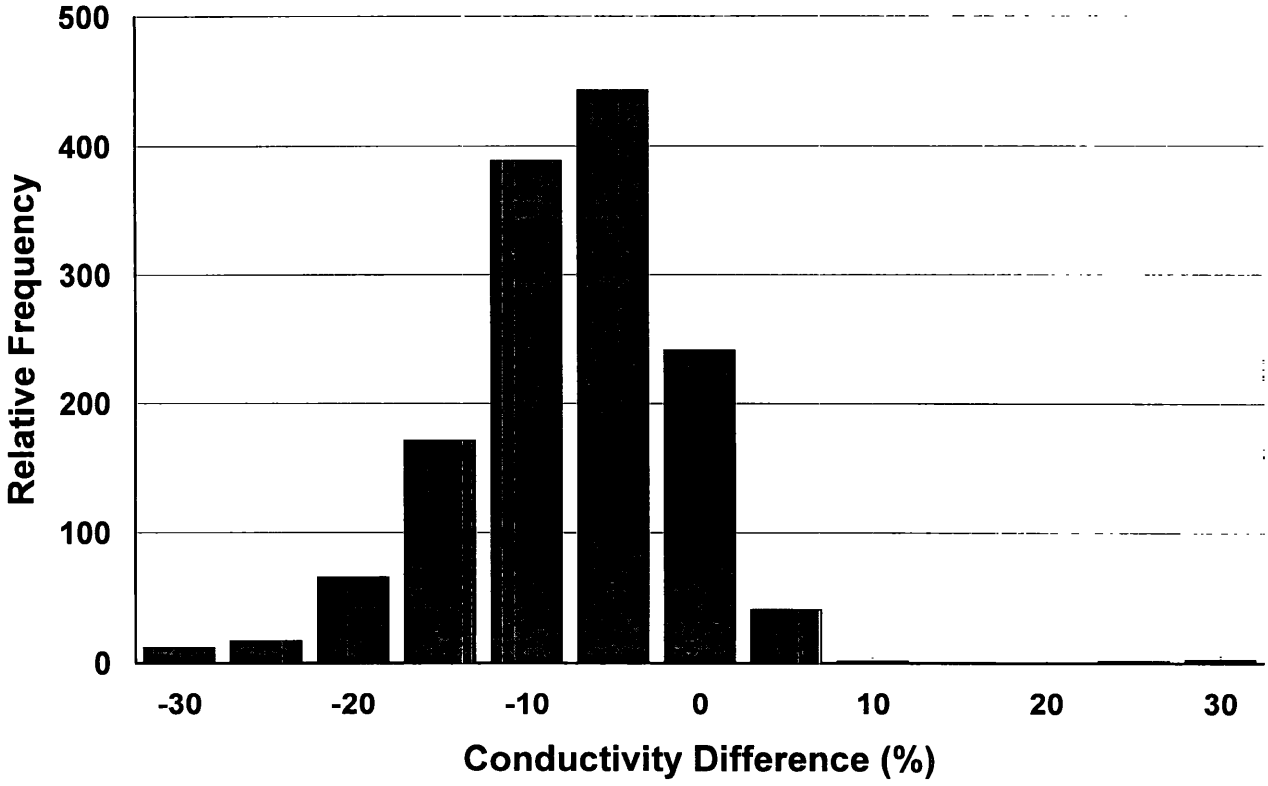

Figure B.4. Relative frequency distribution of the computed conductivity difference for all streamwater samples.